Implementation of Bacteriogenic Manganese Oxide Nanoparticles to Manage Biotic and Abiotic Stresses

BY

Maryam Anar

Department of Plant Sciences

Quaid-i-Azam University Islamabad, Pakistan

2024

Implementation of Bacteriogenic Manganese Oxide Nanoparticles to Manage Biotic and Abiotic Stresses

A THESIS SUBMITTED FOR THE PARTIAL FULFILLMENT OF THE REQUIREMENTS FOR THE DEGREE OF

DOCTOR OF PHILOSOPHY

in

Plant Sciences

By

Maryam Anar

Department of Plant Sciences

Quaid-i-Azam University Islamabad, Pakistan

2024

In the name of Allah, the Entirely Merciful, the Especially Merciful.

All the praise is due to Allah, Lord of worlds. The Entirely Merciful, the Especially Merciful, Sovereign of the Day of Recompense.

It is You we worship, and You we ask for help. Guide us to the straight path. The path of those upon whom You have bestowed favors, not of those who have evoked Your anger or of those who are astray.

Surah Al-Fatiha

DECLARATION OF ORIGINALITY

I hereby declare that the work accomplished in this thesis is the result of my own research carried out in the Molecular Plant Pathology Laboratory, Department of Plant Sciences, Quaid-i-Azam University, Islamabad. This thesis has not been published previously nor it contain material from the published resources that can be considered as violation of international copy right law.

Furthermore, I also declare that I am aware of the terms "copyright" and "plagiarism". If any copyright violation is found in this research work, I will be responsible for the consequences of any such violation.

Maryam Anar

PLAGIARISM CERTIFICATE

It is certified that Ms. Maryam Anar (Registration No. 03042113006) has submitted his PhD dissertation entitled "**Implementation of Bacteriogenic Manganese Oxide Nanoparticles to Manage Biotic and Abiotic Stresses**" and it has been checked on Turnitin for similarity index (plagiarism). Thesis plagiarism has been found to be 15%, which lies in the limit provided by HEC (19%).

Prof. Dr. M. Farooq Hussain Munis

Professor,

Department of Plant Sciences,

Quaid-i-Azam University,

Islamabad

APPROVAL CERTIFICATE

This is to certify that the research work in this thesis, entitled **"Implementation of Bacteriogenic Manganese Oxide Nanoparticles to Manage Biotic and Abiotic Stresses"** was conducted by **Ms. Maryam Anar** under the supervision of **Dr. Muhammad Farooq Hussain Munis**. No part of this thesis has been submitted anywhere else for any other degree. This thesis is submitted to the **Department of Plant Sciences, Faculty of Biological Science, Quaid-i-Azam University, Islamabad** in partial fulfillment of requirements for the degree of **Doctor of Philosophy** in the field of **Plant Science**.

Supervisor

Prof. Dr. Muhammad Farooq Hussain Munis
Department of Plant Sciences,
Quaid-i-Azam University, Islamabad

External Examiner 1

Dr. Qaiser Hussain
Associate Professor,
Institute of Soil and Environmental Sciences,
PMAS-Arid Agriculture University, Rawalpindi

External Examiner 2

Dr. Muhammad Ibrar Shinwari
Associate Professor,
Bioscience, CIRBS, Alfarabi Research Complex,
International Islamic University, Islamabad,
Pakistan

Chairman

Prof. Dr. Hassan Javed Chaudhary
Department of Plant Sciences,
Quaid-i-Azam University, Islamabad

Dated: 20 January, 2025

DEDICATED TO

My Most Loving Parents

Mr. Chaudhry Muhammad Anar & Mrs. Shameem Akhtar

Whose unwavering love, sacrifices, and belief in me have been the foundation of all my achievements. You opened doors for me to learn and grow, and your endless support has empowered me to reach my goals. This achievement is as much yours as it is mine, and I will forever need your love and guidance, and no words can truly express my gratitude.

&

To my loving Siblings,

Anam Anar

Arooj Fatima

Ahmad Hassan

Muhammad Hussnain

Muhammad Qasim

whose care, support, and belief in me have been a beacon of strength – my success is a reflection of all of you. I love you all deeply and endlessly.

ACKNOWLEDGEMENTS

*Begin with **Allah's** name, who is the Most Merciful and the Most Gracious. **"Almighty Allah"** deserves all of the glory. Thank you, Allah, for providing me with the ability to seek knowledge and explore some of the numerous parts of His creation. I am grateful for my abilities and His guidance in completing this thesis. He has always lavished me with more than I deserve.*

*Innumerable salutations to the **Holy Prophet (Peace Be Upon Him)**, wellspring of wisdom and benefits for all of creation, who has directed his Ummah to seek knowledge from cradle to grave and enabled me to gain honor in life.*

*First and foremost, I would like to express my deepest and most heartfelt gratitude to my esteemed supervisor, **Prof. Dr. Muhammad Farooq Hussain Munis**, Department of Plant Sciences, Quaid-i-Azam University, Islamabad. His boundless patience, exceptional wisdom, and steadfast support have been the cornerstone of my PhD journey. His insightful guidance, inspiring mentorship, and unwavering encouragement have shaped not only my research but also my personal and professional growth. No words can fully convey the immense respect and admiration I have for him. He has been more than just a supervisor—he has been a mentor, a guide, and a source of constant inspiration. His faith in my abilities, especially in difficult moments, kept me moving forward. I feel incredibly fortunate and blessed to have had his support. This achievement, from start to finish, was made possible because of him, and I will be forever indebted to him for his kindness. Truly, all credit for this accomplishment belongs to him. My words will never fully express my profound gratitude and feelings for him.*

*I would like to extend my deepest gratitude to my foreign supervisor, the beacon of knowledge, **Professor Dr. Masaaki Morikawa**, at the Faculty of Environmental Earth Science, Hokkaido University-Japan. His unwavering guidance, invaluable encouragement, and insightful suggestions have profoundly enriched my time in Hokkaido, Sapporo, and offered me an incredible opportunity to deepen my expertise in the field. The months spent under his supervision were truly transformative, both academically and personally. I am also sincerely thankful to the members of his lab for their constant support, fruitful collaboration, and warm friendship throughout this journey. Their kindness and expertise made my experience even more rewarding.*

*I express my thanks to **Dr. Hassan Javed Chaudhary** Chairperson, Department of Plant Sciences, Faculty of Biological Sciences, Quaid-i-Azam University, Islamabad, for providing the support and equipment. I would like to special thanks to **Dr. Mushtaq***

Ahmad *and* ***Dr. Umar Masood Quraishi*** *for their guidance and very nice attitude and also thankful to* ***Dr. Imran*** *(Department of Microbiology) for provision of equipment facility.*

Most importantly, this journey would not have been possible without the unwavering love and patience of my family, to whom this dissertation is dedicated. Their constant support, concern, and strength have been my foundation through all these years. Words cannot express the depth of my gratitude to them for their endless love and encouragement. My heartfelt thanks go especially to my beloved ***Ami*** *and* ***Abu****, whose prayers, boundless love, and sincere support—financially, morally, and spiritually—have been a guiding light in every step of this journey. I also extend my deepest appreciation to my elder sister,* ***Anam Anar****, whose love, support, and constant presence have been a source of strength and comfort. I am forever grateful for her encouragement. To my loving sister,* ***Arooj Fatima****, who, despite being younger, has taken on the role of an elder sister, acting as my right hand, roommate, and soulmate throughout my PhD journey. Her unwavering support through every up and down has been invaluable. To my dear brothers,* ***Ahmad Hassan, Muhammad Hussnain,*** *and* ***Muhammad Qasim,*** *your pride in me, your unwavering encouragement, and your unconditional love have been my greatest sources of strength. You are truly the light of my life, and I love you all with all my heart.*

No words can truly capture the depth of my gratitude to my affectionate and dear friends. I am incredibly fortunate to have the unwavering support of some very special individuals. My heartfelt thanks go ***to Kinza Tahir*** *and* ***Mahnoor Akbar****, whose constant care and encouragement have been a source of strength during both joyous and challenging times. You have stood by my side, pushing and motivating me when I needed it most. 'Thank you' hardly seems enough, but it is said with the deepest appreciation and respect for your friendship, understanding, and boundless support. Your friendship is a true treasure, and the memories we've shared will remain etched in my heart forever.*

I am also deeply thankful to my wonderful friends ***Hassen Sarfaraz, Maryana****, and* ***Noor ul-Ain****. The moments we've shared, the laughter, outings and the endless conversations have made this journey an unforgettable experience. You have all added such beauty and warmth to my life, and the memories we've created together will stay with me forever. Your friendship has truly been a blessing, one that I will always hold close to my heart.*

*A very special thanks to **Shazmin**, who has shown me the true meaning of friendship. Though she wasn't directly part of my PhD journey, her unwavering support was always present. I also want to thanks to the wonderful members of **Tabar,** especially **Nimra Yasmeen**, their love, friendship, and presence in my life means alot. I love and cherish them all.*

*I extend my heartfelt gratitude to my wonderful seniors, **Dr. Urooj Haroon, Dr. Asif Kamal**, and my dear colleague **Farhana, Hasna Bibi** and **Hira Saleem** for their unwavering support and the countless moments we shared in the lab, filled with laughter, discussions, and encouragement. From the very first day, they welcomed me with open arms, offering guidance and friendship. Special thanks **to Dr. Urooj Haroon** who helped me to initiate my work and stuck with me till the last part of the experiment. Special prayers for her and I will forever cherish the prayers and positive energy she brought into my life.*

*My deepest and most heartfelt thanks go to my friends and precious members of my MMP Lab—**Rabia Nawab**, **Minhas Elahi**, **Muhammad Anas**, **Abdul Rehman**, **Hassaan Ateeb, Kawal Aftab**, **Sohail Riaz and all members of MMP LAB**. Your unwavering support, motivation, and cooperation have been my pillars during the toughest times. I am truly grateful for each of you and for all the ways you've helped me along the way.*

*A very special thanks to **Bushra Nisar**, whom I had the pleasure of meeting in Sapporo. She is an incredibly kind and amazing person, as well as a wonderful listener. Thank you for your time, encouragement, and unwavering support. I have learned so much from you, and I am truly grateful for the wisdom and kindness you've shared with me.*

*A very special thanks to my beloved Chachu **Mr. Javed Iqbal** for his constant support and encouragement throughout my life. His unwavering belief in me has been a source of strength, and my love and gratitude for him cannot be expressed in words. He has always been there for me, and for that, I am forever thankful.*

In the end I want to present my unbending thanks to all those hands who prayed for my betterment and serenity.

Maryam Anar

Contents

LIST OF TABLES

LIST OF FIGURES

LIST OF ABBREVIATIONS

%	Percentage
°C	Degree Celsius
°E	Degree's east
°N	Degree's north
Ag	Silver
AgNPs	Silver Nanoparticles
Al	Aluminium
As	Arsenic
Au	Gold
AuNPs	Gold Nanoparticles
CAT	Catalase
Cd	Cadmium
Cdse	Cadmium Selenide
Chl	Chlorophyll
CMV	Cucumber Mosaic Virus
Cnts	Carbon Nanotubes
CRD	Completely Randomized Design
Cu	Copper
Cu Nps	Copper Nanoparticles
CVD	Chemical Vapor Deposition
DCPIP	2,6-Dichlorophenol-Indophenol
DHPS	Disodium dihydrogen phosphate solution
DNA	Deoxyribonucleic acid
DNS	Dinitrosalicylic Acid
dNTP	Deoxyribonucleotide triphosphate
DW	Dry Weight
EC	Electrical conductivity
EDTA	Ethylenediaminetetraacetic acid
EDX	Energy-Dispersive X-Ray Spectroscopy
FAO	Food And Agriculture Organization
FCBP	Fungal Culture Bank of Pakistan

FCC	Face-Cantered Cubic
Fe2O3	Iron Oxide
FTIR	Fourier Transform Infrared
FW	Fresh Weight
H_2O_2	Hydrogen peroxide
H_2SO_4	Sulfuric Acid
$Hgcl_2$	Mercuric Chloride
Hsps	Heat Shock Proteins
IPM	Integrated Pest Management
IPM	Integrated Pest Management
K	Potassium
$K_2Cr_2O_7$	Potassium Dichromate
Kbr	Potassium Bromide
LB	Luria Bertani
MDA	Malondialdehyde
Mg	Milligram
mg g^{-1} dw	Milligram per gram dry weight
MHPS	Monosodium dihydrogen phosphate solution
Ml	Microliter
mM	Millimolar
MMT	Million metric tons
Mno Nps	Manganese Oxide Nanoparticles
Mnso4.5H2O	Manganese Penta Sulphate
MRI	Magnetic Resonance Imaging
ms/m	Millisiemens per metre
N	Nitrogen
Na	Sodium
Nacl	Sodium Chloride
NARC	National Agricultural Research Centre
NBT	Nitro Blue Tetrazolium Chloride
Ng	Nanogram
Nm	Nanometer

NPs	Nanoparticles
OD	Optical density
P	Phosphorus
Pb	Lead
Pbs	Lead Sulfide
PCA	Principal Component Analysis
PCR	Polymerase Chain Reaction
PDA	Potato Dextrose Agar
PLGA	Poly(Lactic-Co-Glycolic Acid)
POD	Peroxidase Dismutase
PPD	P-Phenylenediamine
Ppm	Parts per million
PVA	Polyvinyl Alcohol
PVD	Physical Vapor Deposition
PVP	Polyvinylpyrrolidone
ROS	Reactive Oxygen Species
Rubisco	Ribulose 1,5-bisphosphate carboxylase/oxygenase
SEM	Scanning Electron Microscopy
SOD	Superoxide Dismutase
SPR	Surface Plasmon Resonance
TBA	Thio barbituric Acid
TCA	Trichloroacetic Acid
TF	Transcription factor
Tio_2	Titanium Dioxide
TLCV	Tomato Leaf Curl Virus
TMV	Tomato Mosaic Virus
tRNA	Transfer ribonucleic acid
TSS	Total soluble sugar
TSWV	Tomato Spotted Wilt Virus
TW	Turgid Weight
TYLCV	Tomato Yellow Leaf Curl Virus
UV	Ultraviolet

XRD	X-Ray Diffraction
Zn	Zinc
ZnO	Zinc Oxide
μ M/mg	Micro molar per milligram
μg/g	Microgram per gram
μm	Micrometer

Abstract

Post-harvest diseases, metal stresses and fungal infections are significant yield-limiting factors affecting a variety of crops. Various techniques are being employed to address these challenges. The economy of Pakistan heavily relies on crop and fruit production, making it essential to tackle these issues with modern techniques to enhance plant and fruit yield. In the past decade, nanotechnology has been reported to offer innovations in the food and agricultural sectors, offering effective solutions to plant ailments. By harnessing the potential of nanotechnology, we can significantly advance agricultural practices and ensure sustainable growth in this vital industry.

This study has been planned for the biological synthesis and application of manganese oxide nanoparticles (MnO NPs) on tomato to control its fruit rot disease, Pb stress, and fusarium wilt.

For better understanding, this study has been presented in three sections. In the first section, surveys were conducted to collect tomato fruit with usual symptoms of brown rot. Diseased fruit parts were excised and cultured on potato dextrose agar (PDA) media plates. After 3-5 days, mycelial mass could be observed in Petri plates and based on its morphological, microscopic and molecular analyses, it was identified as *Aspergillus nigar*. To control the spread of this disease, manganese oxide nanoparticles (MnO NPs) were prepared in bacterial broth-culture. *Bacillus subtilis* was grown at 45°C, to induce mild stress of high temperature and its filtrate was obtained and mixed with the solution of manganese acetate. Calcination was performed for the synthesis of MnO NPs, which were later characterized. Fourier transform infrared (FTIR) spectrum revealed the presence of few important stabilizing and reducing agents (carboxylic acid, alkenes, and alkyl halides) on the surface of MnO NPs. X-Ray diffraction (XRD) analysis revealed the size (39 nm) and crystal-like nature of synthesized MnO NPs. Energy-dispersive X-ray spectroscopy (EDX) described the mass percentage of manganese (26.4%) and oxygen (23.3%). Scanning electron microscopy (SEM) displayed nearly spherical shape of MnO NPs and confirmed their nano-size. Successfully synthesized MnO NPs exhibited significant mycelial growth inhibition of *A. niger* and notable control of tomato black rot disease. NPs-treated fruit maintained better biochemical composition and greater organoleptic properties than untreated fruit, and sustained higher percentage of soluble solids, total sugars, reducing sugars and fruit firmness. These results not only

proved the usefulness of bacteria supplemented MnO NPs but to our knowledge, this is the first study of tomato black rot, caused by *A. niger* in Pakistan.

In the second part of this study, the effects of nanoparticles were further investigated on tomato plants. This segment focused on assessing the impact of lead stress on plant growth and development. Moreover, this study provided valuable insights into how nanoparticles can mitigate the adverse effects of heavy metal toxicity. Lead (Pb) is a well-recognized toxic trace element that is harmful for both plants and humans. In this study, the nano-priming of tomato seeds was carried out by the fabricated nanoparticles (NPs) to mitigate Pb stress in tomato seedlings. Before sowing under Pb stress conditions, tomato seeds were primed with three different concentrations (0.25 mg/ ml, 2.5 mg/ ml and 5.0 mg/ ml) of MnO-NPs. Synthesized MnO-NPs were characterized. Fourier transform infrared spectrum (FTIR) described the presence of carboxylic acid, alkenes, and alkyl halides on the surface of MnO-NPs, that serve as stabilizing and reducing agents. X-ray diffraction revealed the average size (22 nm) and crystalline structures of MnO NPs while scanning electron microscopy (SEM) also confirmed the nano-flower structure of MnO-NPs. The energy dispersive X-Ray (EDX) analysis determined the mass percentage of manganese (38.27%) and oxygen (36.91%). In comparison to control, application of different concentrations of MnO-NPs improved growth attributes of tomato seedlings including shoot and root lengths, plants fresh and dry weights, chlorophyll and carotenoid contents, relative water content, and proline and sugar accumulation. Nano-priming also decreased relative electrolyte leakage and the production of malondialdehyde and hydrogen peroxide. Seed priming positively influenced tomato seedling and enhanced the gene expression of chalcone synthase and phenylalanine ammonia lyase enzymes, while the expression of chlorophyllase was reduced. These findings suggested that MnO-NPs help tomato seedlings to resist the absorption and accumulation of Pb in roots and leaves.

In the third and last section of this study, MnO NPs were applied to control the fusarium wilt of tomato. *Fusarium oxysporum* f. sp. *Lycopersici* is the most demolishing myco-pathogen of tomato plant. In this study, MnO NPs were again synthesized using *Bacillus subtilis* and applied to control Fusarium wilt of tomato. Fourier transform infrared (FTIR) spectroscopy of MnO NPs showed the presence of carboxylic acid, alkenes, alcohols, esters, ethers and alkyl halides on their surface, that serve as stabilizing and reducing agents. UV–vis spectroscopy at 420 nm indicated the synthesis of NPs. X-ray diffraction (XRD) determined their average size (28 nm) while scanning electron

microscopy (SEM) displayed spherical structure of MnO NPs. The energy dispersive X-ray (EDX) analysis revelaed the highest presence of manganese and oxygen. For mycelial growth inhibition of *F. oxysporum*, three different concentrations of MnO NPs (0.5 mg/mL, 2.5 mg/mL, and 5.0 mg/ mL) were tested, *in vitro*. Among these, 2.5 mg/mL concentration exhibited best results, and it was used further for the priming of tomato seeds in pot experiment (*in vivo*). Findings of pot experiment revealed significant control of Fusarium wilt of tomato by the application of MnO NPs (88%), in comparison to control. These plants also displayed notable improvement in growth attributes like shoot and root lengths, plant fresh and dry weights, chlorophyll, carotenoid and relative water content, and proline and sugar accumulation. Nano-priming also improved antioxidant enzymatic activities of superoxide dismutase (SOD) and peroxidase (POD) and decreased relative electrolyte leakage and the production of malondialdehyde and hydrogen peroxide. A histopathological assay revealed severe damage of root and shoot tissues by the application of *F. oxysporum*. Contrarily, the application of MnO NPs rescued the plant vascular system. These findings suggest a strong role of MnO NPs in controlling the most devastating wilting disease of tomato.

Conclusive findings of this study elaborated the successful deployment of Bacillus-MnO nanocomposites for controlling different biotic and abiotic stress conditions. These MnO NPs proved very effective in mitigating fruit rot, Fusarium wilt and Pb stress. These outcomes mark a significant step toward sustainable agriculture, reducing dependence on chemical fungicides and minimizing environmental risks.

1. INTRODUCTION

1.1 TOMATO (*Solanum lycopersicum*)

Tomato (*S. lycopersicum*), belongs to Solanaceae family and ranks among the most consumed vegetables, globally. Originating from western South America, tomatoes were first cultivated in Mexico, and their cultivation expanded to Europe and the other parts of the world after the Spanish conquest (Knapp & Peralta, 2016). The tomato is not only a staple in numerous culinary traditions but also it also contains essential nutrients and bioactive compounds. It is regarded as the second notable vegetable crop, following potatoes (FAO, 2022). Tomatoes are cultivated in a variety of climates, from temperate to tropical, and are grown year-round in many regions (Coelho et al., 2023).

1.2 ECONOMIC IMPORTANCE OF TOMATOES

Tomatoes hold substantial economic value as both a fresh and processed product. They are a major agricultural commodity, contributing significantly to the global economy. In 2022, 192 million metric tons global production of tomato has been reported, with major producers including China, India, and the US (Ma et al., 2023). Various processed products including sauces, juices, and canned tomatoes are also sold. In the United States alone, the tomato processing industry contributes over $1 billion annually to the economy, providing jobs and supporting rural communities (Chanda et al, 2021).

In Pakistan, tomatoes are a crucial component of the agricultural sector, with the country being a major tomato producer. In 2022, Pakistan produced around 3.5 million metric tons of tomatoes, making it one of the leading producers in South Asia (Ndondo, 2023). The domestic market heavily relies on tomatoes for daily consumption, and they are a key ingredient in traditional Pakistani cuisine. However, the marketing of tomato is challenging due to its perishable nature and fluctuating market prices, which impact both producers and consumers (Ahmed, 2022).

1.3 MEDICINAL IMPORTANCE OF TOMATOES

Tomatoes are highly regarded for their significant medicinal attributes. The health advantages of tomatoes are primarily credited to their rich content of essential vitamins, minerals, and phytochemicals. Here’s a more detailed look at the various medicinal uses of tomatoes (Kumar et al., 2012):

1.3.1 Cardiovascular Health

Tomatoes are known for their cardiovascular benefits, largely due to their high lycopene content. Lycopene, a carotenoid pigment, has been reported for reducing cardiovascular risk. Several studies have shown that lycopene can lower levels of cholesterol and triglycerides, reduce blood pressure, and improve overall heart health (Przybylska et al., 2022). Additionally, the high vitamin C content in tomatoes acts as an antioxidant, protecting blood vessels from oxidative damage and dipping the risk of atherosclerosis (Mordente et al., 2011).

1.3.2 Cancer Prevention

The anti-cancer properties of tomatoes are well-documented, particularly due to their lycopene content. The antioxidant activities of Lycopene's protect body from cancer development (Atasoy, 2012). The polyphenols in tomatoes, such as flavonoids and phenolic acids, also contribute to their anti-cancer effects (Martí et al., 2016).

1.3.3 Digestive Health

Tomatoes are a rich in fibre, which regulates bowel movements. The soluble fibre in tomatoes, such as pectin, act as a prebiotic, fostering the growth of beneficial gut bacteria (Borguini & Ferraz Da Silva Torres, 2009). Additionally, tomato contains high-water content which helps in hydration and digestion and supports gastrointestinal function.

1.3.4 Skin Health

Tomatoes offer numerous benefits for skin health, thanks to their antioxidant content. Lycopene and vitamin C in tomatoes protect skin from ultraviolet (UV) radiations. Tomato extracts are often used in topical skincare products to improve skin texture, reduce acne, and diminish dark spots. The antioxidants in tomatoes also help in collagen synthesis, enhancing skin elasticity and reducing wrinkles (Kontaxi et al., 2024).

1.3.5 Diabetes Management

Tomatoes has low glycemic index and high fibre which are important to manage diabetes. The fibre in tomatoes slows down the absorption of sugar and regulates blood

sugar levels. Additionally, the antioxidants in tomatoes improve the sensitivity of insulin (Perveen et al., 2015).

1.3.6 Bone Health

Tomatoes contribute to bone health through their high vitamin K and calcium content. Vitamin K is essential for bone mineralization and maintaining bone density, while calcium is a crucial component of bone structure. Regular consumption of tomatoes can support bone health and potentially reduce the risk of osteoporosis (Lanham-New, 2008).

1.3.7 Immune System Support

Tomato confines a variety of vitamins (vitamin C, vitamin A) and minerals (Zinc), which boosts the immune system. Vitamin C is helpful in the fabrication of white blood cells and supports overall immune function, while vitamin A helps maintain the integrity of mucosal surfaces and skin (Baidya & Sethy, 2020).

1.3.8 Anti-Inflammatory Effects

Due to the presence of antioxidants, tomatoes possess anti-inflammatory properties. Lycopene and vitamin C help reduce inflammation in the body by neutralizing free radicals and inhibiting inflammatory pathways. Regular consumption of tomatoes may be beneficial for managing chronic inflammatory conditions such as arthritis (Salehi et al., 2019).

1.3.9 Weight Management

Tomato is low-calorie vegetable and helps in weight management. It also contains high-water content. Eating tomatoes gives a feeling of fullness and reduces food intake. Including tomatoes in a balanced diet may support weight loss and maintenance (Tohill & Joint, 2005).

1.3.10 Neurological Health

Emerging research suggests that the antioxidants in tomatoes, particularly lycopene may reduce oxidative stress and brain inflammation (Rao & Balachandran, 2002).

1.4 NUTRITIONAL IMPORTANCE OF TOMATOES

Tomatoes are a nutrient-dense food, providing essential vitamins, minerals, and antioxidants. Vitamin C improves immune function and skin health. Additionally, tomatoes provide significant amounts of potassium, which is important in regulating fluid balance and blood pressure. Lycopene and other phytonutrients in tomatoes contribute to reducing oxidative stress and inflammation (Collins et al., 2022).

1.5 ENVIRONMENTAL STRESSES IN TOMATOES

Tomatoes are susceptible to various abiotic pressures. These stresses include heavy metal stress, alkalinity, high temperature, drought and salinity can severely impact tomato production. These stresses lead to reduced fruit quality and yield, affecting both the economic viability and nutritional value (Singh et al., 2018). Advances in genetic research and breeding strategies are aimed at enhancing tomato resilience to these environmental stresses, ensuring stable production and quality (Tohill & Joint, 2005).

1.5.1 Biotic Stresses

Tomatoes, being a widely cultivated and economically important crop, are prone to a range of biotic stresses. These stresses include pests, fungi and bacteria, which pose significant challenges to tomato cultivation. These stresses can significantly impact tomato growth, yield, and quality. Biotic stresses in tomatoes are categorized into several classes (Panno et al., 2021):

1.5.1.1 Parasitic Diseases

Fungi, bacteria, viruses, and nematodes are the notable parasites of tomato. These pathogens infect tomatoes and cause various disorders, leading to reduced plant health and productivity. Key parasitic diseases affecting tomatoes include (Singh et al., 2014):

Fungal Diseases:

- **Fusarium Wilt (*Fusarium oxysporum* f. sp. lycopersici):** In Fusarium wilt, tomato plants exhibit vascular discoloration and wilting. The fungus attacks the vascular system, restricting water and nutrient transport, leading to wilting and eventually plant death. Lower leaves get yellow and lead to the necrosis and

collapse of the entire plant. Fusarium wilt is particularly challenging to manage due to the incidence of pathogen in the soil (Srinivas et al., 2019).

- **Early Blight (*Alternaria solani*):** It is fungal disease in which symptoms are observed in the form of dark and concentric lesions on all sections of the plant (leaves, stems, fruits). These lesions expand and coalesce later, leading to premature leaf drop and reduced photosynthetic capacity (Chaudhary et al., 2021).
- **Late Blight (*Phytophthora infestans*):** This disease also affects all plant parts. Symptoms of this disease include large, water-soaked lesions that rapidly decay. It can lead to substantial yield losses and is particularly problematic in humid conditions (Tsedaley, 2014).
- **Powdery Mildew (*Leveillula taurica*):** In this disease, the fungus can be observed on the undersides of leaves as a white-powdery substance. It can cause leaf curling and reduced fruit set (Sudha & Lakshmanan, P2009).

Bacterial Diseases:

- **Bacterial Spot (*Xanthomonas perforans*):** In this disease, the causal bacterial pathogen infects, and typical dark, sunken lesions appear on all plant parts. It can lead to significant defoliation and fruit drop (Abrahamian et al., 2021).
- **Bacterial Canker (*Clavibacter michiganensis* subsp. michiganensis):** In this disease, water-soaked lesions appear on leaves and soft-parts of stems and cause plant wilting and death. It also affects fruit quality, leading to severe economic losses (Myung et al., 2008).

Viral Diseases:

- **Tomato Mosaic Virus (ToMV):** ToMV disease reduces fruit quality and yield by causing mottling and distortion. Tomato plants also show stunted growth (Ambros et al., 2017).
- **Tomato Yellow Leaf Curl Virus (TYLCV):** TYLCV disease tomato plants exhibit stunted growth. It is transmitted by whiteflies and typical viral symptoms including leaf curling and yellowing are observed (Zhang et al., 2009).

Nematode Diseases:

- **Root-Knot Nematodes (Meloidogyne spp.):** The infection of nematodes exhibits typical root-knot symptoms in tomato. Plants show poor growth due to reduced water and nutrient uptake. Infested tomato plants also exhibit poor fruit development (Wesemael et al., 2011).

1.5.1.2 Non-Parasitic Diseases

Non-parasitic diseases in tomatoes are primarily caused by environmental factors and are not attributable to pathogens. These include:

Physiological Disorders:

- **Blossom End Rot:** The deficiency of calcium results in the bud end of the tomato plant. It is exacerbated by inconsistent watering practices (Taylor & Locascio, 2004).
- **Catfacing:** It is a deformity of tomato fruits caused by environmental stressors such as cool temperatures during flowering. The affected fruits have malformed and scarred surfaces (Rot, 2021).

Nutrient Deficiencies:

- **Nitrogen Deficiency:** Tomatoes suffering from nitrogen deficiency exhibit yellowing of older leaves and reduced growth. Nitrogen is crucial for healthy foliage and fruit development (Pretorius, 2009).
- **Potassium Deficiency:** Potassium deficiency leads to marginal leaf scorch and poor fruit quality. Potassium is essential for regulating various physiological processes in tomatoes (Alva et al., 2006).

1.5.2 Abiotic Stresses

Soil and water resources are increasingly under strain due to growing populations and climate change, posing a significant challenge for tomato cultivation. Sustainable farming practices are essential for addressing these challenges (Spaldon et al., 2015). Abiotic stresses, which restrict tomato growth and yield, are a primary concern for modern agriculture. The goal of contemporary research is to improve crop production in unstable climate conditions, which are major obstacles to effective farming systems

(Gora et al., 2019). Research should focus on improving understanding of climate factors, developing innovative selection and screening methods, and adopting sustainable agricultural practices (Press La Pena & Hughes, 2007).

1.5.2.1 *Temperature Extremes*:

High temperatures adversely affect tomato production and yield, leading to several physiological and morphological changes. Exposure to temperatures above 30°C can impair fruit quality. Heat stress (exceeding 35°C) can cause significant flower drop and a decrease in fruit set (Zhu et al., 2021). Elevated temperatures compromise photosynthetic efficiency by inhibiting key enzymes such as RuBisCO, which leads to reduced carbon fixation and overall plant growth (Wijewardene et al., 2021). Additionally, heat stress accelerates respiration rates, increasing energy expenditure and reducing the energy available for fruit development (Ul Hassan et al., 2021).

At genetic and molecular levels, high temperatures induce the demonstration of heat shock proteins (HSPs). These proteins protect the denaturation of other proteins (Tutar & Tutar, 2010). Transcription factors such as HsfA1 and HsfB1 are upregulated under heat stress, initiating heat-responsive gene expression pathways that facilitate acclimation (Haider et al., 2021). Morphologically, heat stress influences the size and colour of tomato fruit due to the disruptions in carotenoid synthesis. Additionally, leaves may exhibit chlorosis and reduced size, which impairs photosynthesis and whole plant condition (Haider et al., 2022).

Low temperatures, particularly those below 10°C, also negatively impact tomato plants. Cold stress can delay germination and seedling emergence, with seeds taking longer to sprout and seedlings showing stunted growth (Bhattacharya, 2022). Decreased metabolic activity and enzyme function also reduce plant growth (Armstrong & Drew, 2002).). Tomato plants also upregulate genes involved in cold acclimation, such as CBF/DREB, which promote the synthesis of cryoprotectants like proline and antifreeze proteins (Jan et al., 2017). In cold stress, SOD and catalase are also upregulated (Al-Issawi et al., 2016).

Morphologically, cold temperatures can cause reduced root growth, smaller shoot size, and leaf curling with necrosis. Increased anthocyanin levels often result in darker leaf pigmentation, serving as a protective response (Rao et al., 2016). Addressing

temperature-related stresses requires the development of heat and cold-resistant tomato varieties, optimizing environmental conditions, and employing effective agronomic practices to mitigate these adverse impacts on production.

1.5.2.2 *Drought Stress*:

Drought is an crucial abiotic constraint of tomato. Drought conditions impact approximately 40% of global tomato production (Fahad et al., 2017). Due to the unavailability of water, tomato plants exhibit numerous physiological and morphological changes. Drought stress leads to stunted growth, reduced leaf area, and poor fruit development. Roots become shorter and less dense, compromising water and nutrient uptake. The reduction in leaf area also limits photosynthetic capacity, which directly affects fruit yield and quality (Carranca et al., 2018).

In regions with limited water resources, such as parts of South Asia, inadequate irrigation infrastructure exacerbates the impact of drought on tomato cultivation. For instance, in some areas, only a fraction of the available land is irrigated effectively, leading to severe water shortages that affect crop yields. The efficiency of irrigation systems and the availability of water resources are critical factors influencing the resilience of tomato crops to drought conditions (Aryal et al., 2020). Waterlogging stress, although less common than drought, also impacts tomato production. Excessive water in the soil can lead to reduced oxygen availability, causing root dysfunction and a decrease in nutrient uptake. This stress can lead to poor fruit set and reduced overall yield (Shao et al., 2016). In waterlogged conditions, susceptible tomato varieties show a noteworthy decrease in plant biomass and gas exchange through stomata. Conversely, varieties with better vascular tissues and enhanced water transport mechanisms tend to exhibit higher resilience to such stress (Sharma et al., 2021).

Genetic studies indicate significant variations in drought resistance among tomato cultivars, with some varieties showing enhanced physiological and molecular responses in drought restrictions (Ye et al., 2018). Key characters linked with drought tolerance include the ability to maintain turgor pressure, enhanced root growth, and efficient water use. Molecular mechanisms include the upregulation of genes like dehydrins, osmotin, and other protective proteins (Parveen, et al., 2019).

1.5.2.3 *Mineral stress*:

Mineral stress is a significant constraint on tomato growth, resulting from nutrient deficiencies. Essential nutrients (N, P, K) are critical for tomato development. Toxicities of non-essential elements like aluminum (Al), sodium (Na), and heavy metals also severely impact plant health. For instance, high concentrations of sodium and chloride can lead to salt stress, which hampers plant development and productivity (Pandey, 2015).

Globally, mineral stress affects approximately 30 million hectares of tomato-growing areas, primarily due to issues such as soil acidity or alkalinity. Inadequate nutrient availability or toxicity is often exacerbated using inappropriate fertilization practices, contamination from industrial discharges, and improper waste management. For tomatoes, mineral imbalances can cause symptoms like chlorosis, reduced fruit size, and poor fruit quality, ultimately leading to decreased yields (Wolf, 2024).

1.5.2.4 *Salt stress*:

Salt stress is particularly prevalent in areas with saline or sodic soils. In saline soils, high concentrations of soluble salts, especially sodium chloride (NaCl) disturb water uptake. These conditions are often intensified by human caused activities, like the irrigation with saline water or inadequate drainage systems (Yadav et al., 2011).

The mineral stress on tomatoes is multifaceted. Nutrient deficiencies and toxicities can affect the key processes of photosynthesis and respiration. For example, high soil salinity reduces osmotic potential, causing dehydration and reduced cell turgor pressure. This stress affects nutrient uptake and disrupts cellular metabolism, resulting in poor plant performance (Roșca et al., 2023). Salinity stress poses a severe threat to tomato cultivation. The impact of salinity on tomatoes includes reduced photosynthetic rates, impaired nutrient uptake, and decreased fruit quality. Salinity affects tomatoes by causing ionic imbalances and oxidative stress, which further disrupt physiological functions and reduce overall plant productivity (Majeed & Muhammad, 2019).

1.5.2.5 *Metal Stress*:

Toxic heavy metals seriously impact the growing and development of tomato plants. A variety of heavy metals containing cadmium (Cd), lead (Pb), zinc (Zn), copper

(Cu), and arsenic (As) can become concentrate in the soil and contaminate irrigation water (Ghori et al., 2019).

Cadmium (Cd): Cadmium is particularly toxic even at relatively low concentrations. Cadmium accumulation in tomato plants leads to reduced chlorophyll content, impaired photosynthetic activity, and stunted growth. Additionally, Cd disrupts enzyme activities, including those involved in nitrogen metabolism (Hernández-Baranda et al., 2019).

Lead (Pb): Lead affects tomato growth by inhibiting seed germination, reducing root and shoot biomass, and impairing nutrient uptake. Lead accumulates in plant tissues, affecting cellular processes and causing physiological disorders. It also disrupts the balance of essential nutrients, leading to deficiencies that further impair plant growth (Zulfiqar et al., 2019).

Zinc (Zn): Excessive levels of Zinc can lead to toxicity. It can inhibit root growth, reduce biomass accumulation, and cause leaf chlorosis. Zn toxicity affects the synthesis of chlorophyll and enzymes, leading to impaired photosynthesis and overall plant growth (Kaur & Garg, 2021).

Copper (Cu): Copper is another essential element, but excessive copper levels can be toxic to tomatoes. Cu toxicity leads to symptoms such as leaf curling, necrosis, and reduced fruit yield. It also affects the function of various enzymes and interferes with photosynthesis and respiration (La Torre et al., 2018).

Arsenic (As): Arsenic contamination in soil is harmful to tomatoes. It interferes the uptake of essential nutrients and further utilization and causes damage to plant tissues by altering physiological processes (Madeira et al., 2012).

Physiological and Molecular Responses: Metal stress activates stress-related genes, synthesizes important metal-binding proteins like metallothionein and phytochelatin and upregulates antioxidants to mitigate oxidative damage (Madeira et al., 2012). Plants also adopt other mechanisms to sequester or detoxify heavy metals, such as vacuole compartmentalization and metal transport proteins (Ghori et al., 2019).

Impact on Yield and Quality: Metal stress can significantly impact tomato yield and quality. High levels of metal contamination lead to reduced fruit size, altered fruit color,

and lower nutritional quality. Additionally, metal stress can affect plant productivity (Carvalho et al., 2018).

1.6 BOTANICAL DESCRIPTION OF TOMATO

Tomato is an annual, herbaceous plant characterized by a bushy and sprawling growth habit. It typically reaches a height of 0.5 to 2 meters. It exhibits a sprawling, often vine-like appearance with compound, alternate leaves that are arranged along the stem. Tomato plants are covered with glandular and non-glandular hairs, which secrete compounds that can deter pests and pathogens (Yousaf, 2007).

Tomato seedlings are hypogeal, meaning that the cotyledons remain under the surface of soil while the true leaves emerge above ground. The initial true leaves are simple, ovate to pinnate, and possess serrated margins. Mature tomato leaves are compound, typically with 5 to 9 leaflets arranged on a central rachis. The leaflets are usually dark green and have a slightly wrinkled surface (Vági et al., 2013).

It has a fibrous root system, which can extend deeper than 60 cm and spread horizontally. This root system supports the plant's growth, absorbs water and nutrients and helps it adapt to varying soil conditions (Yousaf, 2007). Tomato stems are usually green and can be either determinate (bushy) or indeterminate (vining). The stems are herbaceous, solid, and may have a slightly hairy texture. In determinate varieties, the plant grows to a compact size and flowers set fruit simultaneously, leading to a uniform harvest (Hanson, 1996).

Tomato flowers are typically small, with a yellow corolla, and are arranged in clusters or inflorescences. Each flower has five petals, five stamens (with fused filaments), and a single, superior ovary with a single carpel. Tomatoes are mostly self-pollinating, but cross-pollination can occur with the help of insects. After pollination, the flowers develop into fruit, which is a berry-like structure containing multiple seeds. The fruit's size, shape, and color can vary widely among different tomato varieties, including round, plum, and cherry types, and colors ranging from red to yellow, orange, and even purple (Pucci 2015).

Tomato pods are actually berries, and they develop from the ovary of the flower. The fruit is typically round to oval and it varies in size (5 to 10 cm). Tomato fruit development

involves a continuous growth period, where the fruit enlarges and matures. Ripening of tomatoes changes the fruit color (from green to red) and enhances the flavour profile (Bareham, 2012).

Tomatoes are usually grown in warm weather conditions and crop is frost sensitive. They are commonly cultivated in well-drained, loamy soils and have a growing period of approximately 60 to 90 days (Singh, 2018).

1.7 DISTRIBUTION OF TOMATO

The cultivated tomato (*S. lycopersicum L.*) is intuitive to western South America, particularly the Andean region encompassing modern-day Peru, Ecuador, and northern Chile, the tomato has been cultivated for thousands of years (Knapp & Peralta, 2016). The initial adoption of tomato was limited, with the fruit often grown ornamentally rather than for consumption due to its perceived toxicity (Van Andel et al., 2022). However, by the 18th century, tomatoes had become widely accepted in European cuisine, leading to their spread across the continent.

The distribution of tomato was further expanded with European colonization and exploration, reaching regions such as Africa, Asia, and Oceania. It was introduced to Africa in the late 19th century and to parts of Asia and Oceania throughout the 20th century, adapting to a variety of climates and soil types along the way (Flores et al., 2023).

Today, tomatoes are grown in diverse climatic conditions across the globe, with major production in India, China, the United States, Turkey, and Italy. These countries are significant contributors to both fresh tomato markets and processed tomato products, including sauces, paste, and juices. The crop's adaptability and extensive cultivation are supported by the development of numerous varieties suited to different climates, soil conditions, and cultivation practices (Nicola et al., 2009).

Tomatoes are referred to by various names in different languages and regions: "Tomate" in Spanish, "Tomate" in French, "Pomodoro" in Italian, "Tomat" in German, and "Tomato" in English-speaking countries. In Africa and Asia, local names and varieties further reflect crop's global spread and cultural significance (Robertson & Labate, 2007).

1.8 CHEMICAL CONSTITUENTS OF TOMATO

Tomato is rich in nutrients, making it an important part of human diets worldwide. The chemical composition of tomatoes includes approximately 95% water, which contributes to their low caloric content and hydrating properties (Nicola et al., 2009). Carbohydrates make up around 3-4% of the fruit, which provide sweetness and energy. The protein content is relatively low, at about 1%, but consist of all the essential amino acids necessary for human nutrition (Sadiq & Aliyu, 2018).

Tomatoes are particularly notable for their high concentration of vitamin C and antioxidants. Every 100 grams of tomato contains 20-30 mg of Vitamin C, which is vital for collagen synthesis (Frusciante et al., 2007). They also contain significant amounts of vitamin A, which is important for vision, skin health, and immune function. The color of tomatoes is attributed to an oxidant naming lycopene, which resists cancer and cardiovascular diseases (Borguini & Ferraz Da Silva Torres, 2009). In addition to vitamins, tomatoes contain a variety of minerals essential for health, including potassium, phosphorus, magnesium, and calcium, which are involved in bone health and metabolic functions (Frusciante et al., 2007). Tomatoes also provide dietary fibre, particularly in the form of pectin (Collins et al., 2022). Tomatoes also contain flavonoids and phenolic acids, which reduce inflammation. Furthermore, tomatoes have small amounts of B vitamins, including folate, which is essential for DNA synthesis (Slimestad & Verheul, 2009).

The composition of tomatoes can vary, and fully ripened tomatoes typically have higher levels of lycopene and vitamin C compared to less mature fruits (Bertin & Génard, 2018). Additionally, processed tomato products such as sauces and pastes may contain concentrated levels of certain nutrients, particularly lycopene, making them a valuable component of diet (Wu et al., 2022).

Tomatoes also have trace amounts of citric and malic acids, which contribute to their characteristic tangy flavour and help enhance the absorption of certain minerals like iron (Petro-Turza, 1986). The presence of chlorogenic acid, a polyphenol compound, further adds to the antioxidant capacity of tomatoes and may contribute to health benefits such as improved cardiovascular health and reduced risk of neurodegenerative diseases (Wu et al., 2022).

1.9 ECONOMIC IMPORTANCE OF TOMATO

Tomatoes have a crucial economic role globally, due to their versatility, high nutritional value, and extensive use in both fresh and processed forms. The economic significance of tomatoes extends across various sectors, including food production, industry, pharmaceuticals, and agriculture.

1.9.1 Source of Food and Nutritional Value

Tomatoes are available in diverse forms like fresh, canned, dried, and treated into results such as sauces, pastes, ketchups, juices, and soups (Yadav et al., 2022). This widespread use makes them a staple in diets globally, contributing to food security and nutrition. The high vitamin C content, along with lycopene and other antioxidants, enhances their role in preventing chronic diseases, thereby contributing to human health (Panno et al., 2021). Tomatoes has been reported good in prostate cancer (Weisburger, 1998). Tomato production has been reported as $190 billion as of 2022 (FAO, 2022). In many developing countries, tomatoes contribute in rural development (Sánchez-Sánchez et al., 2024).

1.9.2 Industrial Uses

The tomato processing industry is a major economic sector in many countries, particularly in regions like Southern Europe, North America, and parts of Asia. The global processing tomato industry produces over 38 million tonnes annually, involving a complex value chain that includes farming, transportation, processing, packaging, and marketing (Costa & Heuvelink, 2005). Tomatoes are processed into tomato paste, canned tomatoes, and sauces. These products are in high demand in both domestic and international markets, making the tomato processing industry a key contributor to the economies of producing countries (Geoffrey et al., 2014).

Tomato by-products, like seeds and skins, are also being used. For instance, tomato seeds are rich in oil, while skins are used to extract lycopene. Additionally, tomato pomace is used in animal feed, reducing waste and adding economic value (Szabo et al., 2021).

1.9.3 Use in Pharmaceuticals and Nutraceuticals

Tomatoes are valued in the pharmaceutical and nutraceutical industries for their bioactive compounds, especially lycopene, flavonoids, and polyphenols. The demand for lycopene supplements and products is increasing, driven by consumer awareness of its health benefits, making tomatoes a significant raw material for nutraceutical production (López-Yerena et al., 2023).

Furthermore, tomato extracts are used in skin-care products due to their antioxidant properties, which resist UV radiation (Kontaxi et al., 2024). This broad range of applications supports a thriving market for tomatoes in health and wellness industries.

1.9.4 Role in Sustainable Agriculture and Environmental Impact

Tomato cultivation is essential in sustainable agricultural practices. The roots of tomato plants contribute to soil structure by improving soil aeration and water retention capacity. Additionally, tomato plants support beneficial soil microorganisms, contributing to healthier soils (Gatahi, 2020). Tomatoes are also used in rotation with other crops to reduce pest and disease pressures (Ramasamy & Ravishankar, 2018).

1.9.5 Socioeconomic Contributions

Tomatoes contribute significantly to the socioeconomic development of producing regions. In countries like India, China, and the United States, tomato production provides substantial employment opportunities, particularly for women and marginalized communities. Small-scale tomato farming is a source of livelihood for millions of families in developing countries, where it plays a role in poverty reduction. The crop's high market value and relatively short growth cycle allow for multiple harvests per year, offering steady income to farmers (Colvin et al., 2012).

Tomato farming also enhances rural development by promoting local business opportunities in seed production, input supply, and marketing. The presence of a robust tomato industry can spur the growth of related sectors such as packaging, transportation, and retail, fostering overall economic development in rural areas (Geoffrey et al., 2014).

1.10 TOMATO CULTIVATION IN PAKISTAN:

In Pakistan, major tomato-growing regions include Punjab, Sindh, Baluchistan, and Khyber Pakhtunkhwa, which offer diverse climatic conditions suitable for tomato

production (Bashir et al., 2021). The crop is grown on approximately 59,000 hectares, yielding around 529,600 tonnes annually (Bashir et al., 2021). In Pakistan, tomatoes are cultivated primarily in two major growing seasons: autumn (rabi) and spring (kharif). In Sindh and Punjab, planting typically occurs in February and July, respectively, to ensure year-round availability (Bashir et al., 2022).

1.10.1 Climatic and Soil Requirements

Tomatoes thrive in a variety of soil types (Singh, 2018). They grow at moderate temperatures, ideally between 20-25°C. In Pakistan, the diverse climatic conditions across different regions allow for flexible cultivation practices, though high temperatures in summer can stress the plants and affect yield (Singh, 2018).

1.10.2 Major Challenges

Tomato cultivation in Pakistan faces several challenges, including water scarcity, pest infestations, and diseases. Water scarcity is a critical issue due to the irregular availability of irrigation resources, which impacts tomato yields significantly. Efficient water management practices such as drip irrigation are increasingly adopted to conserve water and improve productivity (Qadir et al., 2007). Pest infestations, particularly from *Helicoverpa armigera* and whiteflies, pose substantial risks to tomato crops. IPM are employed to mitigate these problems (Islam, 2016).

Disease management is another crucial aspect of tomato cultivation. Tomato leaf curl virus (TLCV) and late blight (*P. infestans*) are common diseases that significantly affect crop yield and quality. The application of appropriate fungicides and insecticides help control these diseases (Dhaliwal et al., 2020).

1.11 POST HARVEST DISEASE

The pathogens of tomato often remain in or on the produce, leading to spoilage and reduced market value (Qadri et al., 2020). Fungal pathogens like *Botrytis cinerea*, *Penicillium* spp., *Aspergillus* spp., and *Fusarium* spp. are notorious for causing rot and decay. *Botrytis cinerea* causes soft rot and significant post-harvest losses. *Penicillium* spp. are known for blue mold rot, particularly in fruits like apples and citrus, and can produce harmful mycotoxins that contaminate produce. *Aspergillus* spp. can cause

Aspergillus rot and is also associated with mycotoxin production, which poses health risks to consumers (Ezzouggari et al., 2024).

Bacterial pathogens contribute to post-harvest diseases as well. *Pseudomonas* spp., *Erwinia* spp., and *Xanthomonas* spp. cause soft rot and other bacterial infections. These bacteria degrade plant tissues, resulting in mushy, decayed produce with unpleasant odours. Soft rot bacteria thrive in high moisture conditions and can quickly lead to significant spoilage (Fenta et al., 2023).

Viral infections, while less common, can also be problematic. Cucumber Mosaic Virus (CMV) and Tomato Spotted Wilt Virus (TSWV) can persist in plant tissues and affect the quality of produce post-harvest. These viruses often lead to symptoms like mottling, stunting, and reduced marketability of the crops (Qi et al., 2021).

Infected fruits often exhibit a range of quality issues, including:

- **Soluble Solids:** The soluble solids content, which is a critical indicator of fruit sweetness and flavour, can be adversely affected by postharvest diseases. The enzymatic activity associated with fungal infections can lead to a reduction in soluble solids, impacting the sensory attributes of the fruit (Ansari & Tuteja, 2015).
- **Firmness:** Disease progression typically leads to a damage of fruit firmness by enzymatic breakdown of cell wall components. For instance, pathogens like *Botrytis cinerea* can cause soft rot, significantly diminishing the textural quality of fruits and rendering them unsuitable for fresh consumption (Zhang et al., 2021).
- **Reducing Sugars:** The degradation of reducing sugars is another notable effect of postharvest diseases. The pathogens' metabolic activities can alternate carbohydrate profile of fruits, affecting their sweetness and overall flavour (Ansari & Tuteja, 2015).
- **Ascorbic Acid (Vitamin C):** It is vital for fruit nutritional value. Postharvest diseases can lead to a reduction in ascorbic acid amount and enzymatic degradation. This reduction impacts the nutritional quality of the fruit (Zhang et al., 2021).

Economic impact of postharvest diseases is staggering, with worldwide losses estimated at around $150 billion, representing roughly one-third of global food production. For individual growers, losses can reach 25% to 50% of their fruit and vegetable crops. This economic toll is not only due to the direct loss of produce but also the reduced market value and increased processing costs associated with infected fruits (Moradinezhad & Ranjbar, 2023).

Quality degradation is another critical issue. Infected fruits typically exhibit visible symptoms such as molds, rots, and decay, which drastically reduce their market value and suitability for fresh consumption. Blemishes, discoloration, and abnormal ripening further diminish the appeal of the produce. While some infected fruits may still be processed, they fetch a lower price and may be deemed unsuitable for fresh sale (Moradinezhad & Ranjbar, 2023).

1.12 POST-HARVST DISEASE ON TOMATO

1.12.1 Gray Mold:

This disease is caused by *Botrytis cinerea*, and it is one of the most common post-harvest diseases in tomatoes. This fungal pathogen thrives in humid environments and can cause extensive fruit decay. The disease typically starts as small, water-soaked lesions that quickly develop into a gray, fuzzy mold covering the fruit. Gray mold can be particularly problematic in storage and transportation due to high moisture levels and inadequate ventilation. Management strategies for gray mold include controlling humidity, improving air circulation, and applying fungicides. Regular inspection and removal of affected fruits are also critical (Dik & Wubben, 2007).

1.12.2 Bacterial Soft Rot:

Erwinia carotovora causes bacterial soft rot. The fruit become soft, mushy, and water-soaked, with a distinct foul odor. The disease is often associated with mechanical injuries to the fruit, which provide entry points for the bacteria. High moisture levels during handling and storage exacerbate the problem. Management involves improving handling practices to reduce injuries, using antimicrobial treatments, and maintaining optimal storage conditions. Avoiding overwatering and ensuring proper drainage can also help mitigate the risk of bacterial soft rot (Osdaghi, 2023).

1.12.3 Alternaria and Cladosporium Rots:

Fungal pathogens cause various forms of rot and discoloration in tomatoes. *Alternaria* spp. often lead to dark, sunken lesions with concentric rings, while *Cladosporium* spp. may cause small, dark spots that can coalesce into larger areas of decay. Both types of fungi cause diseases at high humidity and warmth. Ensuring proper ventilation and avoiding excessive moisture during storage can also help reduce the incidence of these fungal rots (Animashaun, 2015).

1.12.4 Aspergillus Rot:

The genus *Aspergillus*, particularly *Aspergillus niger* and *Aspergillus flavus*, can lead to substantial post-harvest issues in tomatoes. These fungi are prevalent in environments with high humidity and inadequate ventilation, conditions that favour their growth. *Aspergillus* rot typically presents as dark and sunken lesions, which rapidly expand and result in significant decay. Infected tomatoes may also develop a characteristic black mold, especially in the case of *A. niger*. *Aspergillus* spp. are capable of producing mycotoxins, such as ochratoxin A and aflatoxins, which pose health risks to consumers and can render the produce unsafe for consumption (Rodrigues & Kakde, 2019).

1.12.5 Fusarium Wilt:

Although more common in the field, Fusarium wilt can also affect tomatoes post-harvest. This disease results in vascular discoloration and wilting symptoms. During post-harvest, infected fruits may show signs of vascular discoloration and reduced shelf life. Management involves using resistant cultivars, maintaining good field hygiene, and avoiding the use of contaminated soil or plant material (Nasrin et al., 2018).

1.12.6 Phytophthora Rot:

Phytophthora spp. can cause severe rot in tomatoes, particularly in conditions of high moisture. This pathogen leads to the rapid decay of fruit and can spread quickly through water or contaminated soil. Managing *Phytophthora* rot involves improving drainage, avoiding overhead irrigation, and applying appropriate fungicides (Kumar et al., 2018).

1.13 TECHNOLOGICL ADVANCEMENT:

Recent advancements in agricultural technology, including the application of nanotechnology, have shown promising results in enhancing crop management and disease control. Nanotechnology involves the use of nanoparticles to improve agricultural practices. In crop protection, nanoparticles can deliver pesticides and fertilizers more efficiently, target specific pathogens with higher precision, and reduce the overall chemical usage. For instance, nano-silver and nano-copper have demonstrated antimicrobial properties that can help in controlling plant diseases. Additionally, these innovations aim to increase crop yield, reduce resource usage, and improve sustainability in agriculture (Usman et al., 2020).

1.14 NANOTECHNOLOGY

Nanotechnology involves the use of nanoparticles, typically between 1 and 100 nanometres (nm) (Shang et al., 2019).

1.14.1 NANOPARTICLES

Nanoparticles, with 1-100 nm size, are tiny entities that possess unique features. The distinct behaviors of nanoparticles arise from quantum effects and size-dependent properties. This introduction will explore the fundamental characteristics of nanoparticles, including their types, properties, and applications, providing a comprehensive understanding of their significance in various fields (Fu et al., 2020).

1.15 APPROACHES TO SYNTHESISE NANOPARTICLES

1.15.1 Top-Down Approach

The top-down approach is often used when starting with a solid bulk material and requires several techniques to achieve the desired nanoscale dimensions. Key techniques within the top-down approach include (Yadav et al., 2012):

- **Mechanical Milling/Grinding**: This technique involves physically breaking down bulk materials into nanoscale particles using grinding mills or ball mills. The process includes grinding the material under controlled conditions to reduce the particle size. Mechanical milling is effective for producing nanoparticles of various materials, including metals and ceramics (Yadav et al., 2012).

- **Laser Ablation**: The target material, typically a metal or semiconductor, is vaporized into a plasma, . As the plasma cools, nanoparticles condense and form. Laser ablation allows to produce nanoparticles with controlled sizes and is useful for creating particles in a clean environment (Abid et al., 2022).
- **Spark Ablation**: Like laser ablation, spark ablation uses electrical discharges to vaporize the target material. The generated vapor then condenses into nanoparticles. Spark ablation is advantageous for producing nanoparticles from a wide range of materials and is particularly noted for its simplicity and scalability (Abid et al., 2022).
- **Lithography Methods**: Lithography techniques, including photolithography and electron beam lithography, involve creating nanoscale patterns on a substrate using light or electron beams. These methods are commonly used in semiconductor manufacturing to produce precise nanoparticle patterns and structures (Yadav et al., 2012).

1.15.2 Bottom-Up Approach

In this method, nanoparticles are produced from atomic or molecular precursors. These NPs are synthesized with better particle size, shape, and composition. It is widely used for producing uniform nanoparticles and includes several key techniques (Arole et al., 2014):

- **Chemical Reduction**: Chemical reduction is commonly used for synthesizing metallic nanoparticles with better supervise over particle size and scattering (Biswas et al., 2012).
- **Sol-Gel Synthesis**: The sol-gel transition is involved in these techniques (Arole et al., 2014).
- **Coprecipitation**: In coprecipitation, multiple metal salts are precipitated together in a solution, forming nanoparticles (Biswas et al., 2012).
- **Microemulsion**: This technique involves the formation of a microemulsion, a stable dispersion of water in oil or vice versa, to produce nanoparticles.

Microemulsion synthesis is useful for creating nanoparticles with narrow size distributions (Ortega et al., 2017).

- **Hydrothermal/Solvothermal Synthesis**: It involve the use of intense-pressure and great-temperature conditions to produce nanoparticles from precursor solutions. These methods offer high control over particle size and crystallinity and are commonly used for synthesizing metal oxides and other materials (Feng et al., 2017).
- **Sono-chemical Synthesis**: This synthesis uses ultrasound waves for to the formation of nanoparticles (Xu et al., 2013).
- **Electrochemical Synthesis**: Electrochemical methods involve electrodes to produce nanoparticles. In this technique voltage and other electrochemical parameters are applied (Sáez & Mason, 2009).
- **Gas Phase Synthesis**: In gas phase synthesis, metal vapours are chemically or physically transformed into nanoparticle (Kruis et al., 1998).
- **Biological/Green Synthesis**: This environmentally friendly approach uses biological agents, leading to nanoparticles that are potentially less toxic and more sustainable (Alsaiari et al., 2023).

1.16 TYPES OF NANOPARTICLES

For of their tiny size, nanoparticles have exceptional chemical and physical properties. These NPs maintain a high area-to-volume ratio, which makes them highly effective. The following categories can be used to categorize nanoparticles (Khan & Hossain, 2022):

1. **Metallic Nanoparticles:** Gold, silver, platinum, and copper are commonly used metals for the synthesis of nanomaterials. Au NPs are identified for their distinct optical traits and are used for sensing and therapeutic delivery. Silver nanoparticles (Ag NPs) possess antimicrobial properties and are employed in wound dressings and disinfectants. Platinum and copper nanoparticles are used in catalysis and environmental remediation Amendola et al., 2017).

2. **Semiconductor Nanoparticles:** These NPs are synthesized from materials with semiconductor properties that exhibit size-dependent optical traits. Quantum dots emit specific wavelengths of light. Materials like cadmium selenide (CdSe) and lead sulfide (PbS) are used to synthesize quantum dots (Ishfaq et al., 2023).
3. **Metal Oxide Nanoparticles:** These types of NPs include Titanium dioxide (TiO_2), zinc oxide (ZnO), and iron oxide (Fe_2O_3), with diverse photocatalytic and antibacterial properties. TiO_2 nanopartiles are used for photocatalysis and self-cleaning surfaces, while ZnO nanoparticles are employed in sunscreens and as antibacterial agents. Iron oxide nanoparticles are utilized in MRI imaging and environmental cleanup (Biju et al., 2008).
4. **Carbon-Based Nanoparticles:** This type of NPs include carbon nanotubes (CNTs), graphene, and fullerenes, These NPs possess exceptional mechanical and thermal properties (Díez-Pascual, 2021).
5. **Polymeric Nanoparticles:** These NPs are composed of organic polymers which are biocompatible and degradable (Elsabahy & Wooley, 2012).

1.16.1 Fundamental Properties of Nanoparticles

1. **Size and Surface Area:** Most significant feature of nanoparticles is their minor size, which provides high surface-in the direction of volume ratio, which improves their reactivity and dealings with surrounding environments. For instance, nanoparticles with diameters in the nanometer range exhibit significantly greater surface energy and surface reactivity, which is important in catalysis and drug delivery, where enhanced surface interaction can lead to improved performance (Ghosh & Pal, 2007).

2. **Quantum Effects:** These effects become important at the nanoscale. These effects arise due to the confinement of electrons within the nanoparticle, leading to unique optical, electronic, and magnetic properties. (Elsabahy & Wooley, 2012).

3. **Optical Properties:** Nanoparticles interact with light and consequently exhibit unique optical properties. The phenomenon of surface plasmon resonance (SPR) is particularly notable in metallic nanoparticles. SPR occurs when transmission

electrons in the nanoparticle resonate with confrontation light, leading to intense absorption and scattering. This property is utilized in various applications, including biosensing and imaging (Ishfaq et al., 2023).

4. **Magnetic Properties:** Nanoparticles of magnetic materials, such as iron oxide, exhibit size-dependent magnetic properties. Superparamagnetic is a prominent feature of magnetic nanoparticles, where they exhibit strong magnetic response in a magnetic field. This property is advantageous in in MRI and drug delivery (Patsula et al., 2016).

5. **Chemical Reactivity:** Due to their unique surface chemistry, the chemical reactivity of nanoparticles is significantly enhanced. Surface functionalization of nanoparticles attaches different chemical groups, which can be used to achieve interactions with target materials. This property is useful in catalysis, where nanoparticles serve as efficient catalysts due to their increased surface reactivity (Paladini & Pollini, 2019).

1.16.2 Characteristics of Nanoparticles

1. **Surface Modifications:** Surface modification of nanoparticles is crucial for enhancing their stability, functionality, and biocompatibility. Various methods, such as dipping with surfactants, ligands, or polymers, can be employed to modify the outside of nanoparticles. These modifications can improve their solubility and reduce agglomeration (Ghosh & Pal, 2007).

2. **Size Distribution and Shape:** These are the most important characteristics of synthesized nanoparticles. Spherical nanoparticles are often used in imaging and sensing, while rod-shaped nanoparticles exhibit anisotropic optical properties that can be utilized in therapeutic applications (Elsabahy & Wooley, 2012).

3. **Toxicity and Environmental Impact:** It is critical to understand the potential toxicity of nanoparticles before their application in the field. While nanoparticles offer numerous advantages, their small size and reactivity can affect health and environment. Studies on nanoparticle toxicity are essential for ensuring their safe use and minimizing potential adverse effects (Elsabahy & Wooley, 2012).

4. **Synthesis and Fabrication:** The synthesis and fabrication of nanoparticles involve different methods. Physical techniques, such as sputtering and laser ablation, involve the direct material manipulation to produce nanoparticles. Chemical approaches, like sol-gel processes and vapor accumulation, entail chemical processes to produce nanoparticles. In biological systems, microorganisms (like fungi plus bacteria) and plant extracts, offer suitable and environmentally friendly alternatives for nanoparticle synthesis (Ishfaq et al., 2023).

1.17 KINDS OF NANOPARTICLES USED IN AGRICULTURE

Nanoparticles have been reported to play important roles to enhance crop production, pest management, and soil health. This section has been written for describing their types, applications, and benefits in the field of agriculture (Paladini & Pollini, 2019).

1.17.1 Metallic Nanoparticles

Metallic nanoparticles, including those made from Ag, Au and Cu, are extensively being used in agricultural practices due to their antimicrobial properties and potential to improve crop yield (Hyder et al., 2022).

- **Silver Nanoparticles (Ag NPs):** These nanoparticles are utilized in controlling plant diseases and inhibiting microbial growth in soil. They can effectively target a variety of pathogens. Ag NPs are used in seed treatments to promote germination and protect seedlings from soil-borne diseases previously, Ag NPs have been exposed to progress plant development and lower the incidence of plant illnesses by halting the spread of pathogens (Sharma et al., 2018).

- **Gold Nanoparticles (Au NPs):** Gold nanoparticles are primarily known for their role in plant disease detection and monitoring. Their exceptional optical traits like surface plasmon resonance (SPR), enable them to be used in sensitive and sophisticated biosensors for recognition of different pathogens of plants (Kulabhusan et al., 2022).

- **Copper Nanoparticles (Cu NPs):** Cu NPs are effective in limiting fungal infections in yields and they are quickly replacing traditional copper-based fungicides. Due to their greater surface reactivity, they exhibit enhanced efficacy, which improves their interaction with fungal cells (Pariona et al., 2019).

1.17.2 Metal Oxide Nanoparticles

This type of NPs includes titanium dioxide (TiO2), zinc oxide (ZnO), manganese oxide (MnO) and iron oxide (Fe_2O_3). Directly to their photocatalytic, antibacterial, and magnetic assets, these nanoparticles have diverse applications in agriculture industry (Maity et al., 2022).

- **Titanium Dioxide Nanoparticles (TiO2 NPs**): TiO2 nanoparticles are extensively employed for their photocatalytic properties, which assist the breakdown of pollutants, particularly organic pollutants in soil and water. TiO2 NPs can enhance soil health by degrading harmful chemicals and improving nutrient availability. Additionally, they are used in developing smart fertilizers and pesticide delivery systems, where their photocatalytic activity ensures their controlled release (Mahlambi et al., 2015).

- **Zinc Oxide Nanoparticles (ZnO NPs):** These NPs have exceptional antimicrobial and UV-blocking assets. ZnO NPs are used to improve plant health by acting as antifungal agents and protecting plants from harmful UV radiation. They also serve as micronutrient sources, promoting the growth and maturity of plants (Irede et al., 2024). They are widely used in agriculture.

- **Manganese Oxide Nanoparticles (MnO NPs)**: MnO NPs exhibit several unique properties, including high surface reactivity and catalytic activity. They are utilized in various applications due to their ability to enhance the oxidation of organic contaminants, making them useful in environmental cleanup and water treatment (Yadav et al., 2023). MnO NPs also act as a source of manganese, an essential micronutrient. Their catalytic properties contribute to the breakdown of pollutants and the enhancement of nutrient availability in the soil.

- **Iron Oxide Nanoparticles (Fe2O3 NPs):** These NPs are utilized for their magnetic properties, which enable them to remediate contaminated soil and water. Fe_2O_3 NPs remove soil and water contamination through magnetic separation. They also serve as carriers for delivering fertilizers and pesticides, providing controlled release and targeted application (Jabbar et al., 2022).

1.17.3 Carbon-Based Nanoparticles

In the synthesis of these NPs, carbon nanotubes (CNTs) and graphene are used. These NPs have more mechanically strength, greater electrical conductivity, and versatility in agricultural applications.

- Carbon Nanotubes (CNTs): They have greater mechanical strength and ability to improve soil structure. They are incorporated into soil to enhance its physical properties, leading to better aeration and water retention. CNTs are also used in developing advanced sensors for plants and soil (Sanjinés et al., 2011).

- Graphene: Graphene nanoparticles are used in developing sensors for detecting plant diseases and monitoring soil nutrients. Additionally, graphene-based materials are incorporated into fertilizers and pesticides to enhance their effectiveness and reduce environmental impact (Sanjinés et al., 2011).

1.17.4 Polymeric Nanoparticles

Polymeric nanoparticles are composed of organic polymers and are very effective in controlled release of nutrients and pesticides and their targeted delivery.

- Poly(lactic-co-glycolic acid) (PLGA) Nanoparticles: These are newly used NPs and they are employed for their biodegradability and ability to encapsulate various agricultural chemicals. They are used to create smart fertilizers and pesticide formulations for enhancing their efficiency and reducing the frequency of application (Schnoor et al., 2018).

- Polyvinyl Alcohol (PVA) Nanoparticles: PVA nanoparticles are utilized for their water solubility and biocompatibility. They are used for the coating of seeds with biodegradable films and for the controlled release of nutrients (Yin et al., 2018).

1.18 MnO NANOPARTICLES: SYNTHESIS, PROPERTIES, AND BENEFITS

Manganese oxide nanoparticles (MnO NPs) are of considerable interest in agriculture, environmental remediation, and medical fields. The following section will provide an in-depth look at these synthesis techniques, including traditional chemical methods and emerging green synthesis approaches (Perfileva & Krutovsky, 2024).

1.18.1 Chemical Synthesis Methods

- **Sol-Gel Method:** This method is frequently employed for synthesizing MnO NPs. This technique involves dissolving manganese salts, such as manganese chloride or manganese nitrate, in a solvent to form a sol. The sol is then gelled with a gelling agent and heat-treated to produce MnO nanoparticles (Kistan et al., 2024).

- **Hydrothermal Synthesis:** Hydrothermal synthesis utilizes high-pressure and high-temperature conditions to produce MnO NPs. Manganese precursors are dissolved in an aqueous solution and subjected to hydrothermal conditions in a sealed autoclave. This method results in nanoparticles with uniform size and high crystallinity, enhancing their stability and reactivity (Yadav et al., 2023).

- **Chemical Vapor Deposition (CVD):** CVD is used to produce high-quality MnO NPs with controlled size and shape. In this process, manganese-containing gases are decomposed. CVD is advantageous for synthesizing NPs with specific surface characteristics and is suitable for applications requiring high-purity materials (Bigiani, 2020).

1.18.2 Biological Synthesis Methods

- **Bacterial Synthesis:** The use of bacteria for synthesizing MnO NPs has gained popularity due to its environmentally friendly nature. Certain bacteria can produce MnO NPs by reducing manganese ions. These bacteria secrete extracellular enzymes that facilitate the conversion of manganese salts into MnO nanoparticles (Zhang et al., 2023).

- **Fungal Synthesis:** A variety of fungi (*A. niger, F. oxysporum*) are utilized to synthesize MnO NPs. These fungi produce MnO nanoparticles through bioreduction processes where fungal cells secrete metabolites and enzymes that reduce manganese ions (Mohiudden et al., 2023).

- **Viral Synthesis:** The use of viruses for MnO NP synthesis is a novel approach. Certain bacteriophages and other viruses serve as templates for nanoparticle formation. The viral proteins interact with manganese ions, facilitating the fabrication of MnO nanoparticles. This method leverages the unique properties of viral capsids (Choi & Lee, 2020).

1.18.3 Green Synthesis Methods

- **Plant-Based Synthesis:** In green synthesis, plant extracts, rich in phytochemicals such as polyphenols, act as reducing agents that convert manganese salts into MnO nanoparticles. This method is sustainable, avoids hazardous chemicals, and often results in nanoparticles with beneficial surface properties (Hano & Abbasi, 2021).

- **Algal Synthesis:** Algae are another biological source for the synthesis of MnO NPs. Algal biomass, particularly from species like *Chlorella* and *Spirulina*, can be used to produce MnO nanoparticles. Algae contain various biomolecules that facilitate the capping of nanoparticles. Algal synthesis is considered an environmentally friendly method that also supports waste recycling (Khan et al., 202).

1.18.4 Properties of MnO Nanoparticles

Manganese oxide nanoparticles (MnO NPs) are being applied for catalysis, environmental remediation, and agriculture. In this section, the fundamental properties of MnO NPs, including their structural characteristics, magnetic behaviour, catalytic activity, and interactions with biological systems have been described in detail (Bigiani, 2020).

1.18.5 Structural Characteristics

MnO NPs possess a range of structural characteristics that influence their properties and applications. MnO NPs are synthesized in varying shapes such as spheres, cubes, and rods. The crystal structure of MnO is typically face-centered cubic (FCC) or rock-salt type, which impacts its stability and reactivity. Studies have shown that the synthesis method, including sol-gel, hydrothermal, and biological approaches, significantly affects the size and shape of MnO NPs (Dawadi et al., 2021).

1.18.6 Magnetic Properties

One of the notable properties of MnO NPs is their magnetic behavior. MnO exhibits ferromagnetic and antiferromagnetic properties. The magnetic traits of MnO NPs are attributed to the presence of manganese ions with unpaired electrons. These magnetic properties make MnO NPs suitable for applications in magnetic separation, data storage, and targeted drug delivery. Research has demonstrated that the magnetic behaviour of MnO NPs changes with their size and morphology (Yadav et al., 2023).

1.18.7 Catalytic Activity

MnO NPs exhibit significant catalytic activity in various chemical reactions, including oxidation and reduction processes. Studies have also highlighted their effectiveness in the degradation of dyes, pesticides, and other hazardous substances (Kuo et al., 2015).

1.18.8 Biological Interactions

MnO NPs interact with biological systems and study of this interaction is a crucial area of research, particularly for their applications in medicine and agriculture. MnO NPs show antibacterial and antifungal properties for disease management and plant protection. Their interaction with biological cells can affect cellular processes, including oxidative stress and apoptosis (Zhang et al., 2023).

1.18.9 Optical Properties

Due to their optical behaviour, MnO NPs enhance signal intensity and provide high-resolution images (Alsaif et al., 2024).

1.19 BENEFITS OS NANOPARTICLES IN AGRICULTURE

Manganese oxide nanoparticles (MnO NPs) offer substantial advantages in agriculture which are particularly notable in managing post-harvest diseases, metal stress, and biotic stress, among other aspects of agriculture (Perfileva & Krutovsky, 2024).

1. **Soil Health and Improvement** High surface area and reactivity of NPs enable their effective interaction with soil components, leading to improved soil fertility and structure. MnO NPs contribute to better soil aeration and water retention, which supports optimal root growth and nutrient uptake. They also remediate contaminated soils by catalyzing pollutant's breakdown and removing heavy metals through their catalytic and magnetic properties (Perfileva & Krutovsky, 2024).

2. **Enhancing Plant Growth** MnO NPs positively impact plant growth and development. MnO NPs supply essential manganese, a critical micronutrient involved in photosynthesis and respiration. By providing manganese in a bioavailable form, MnO NPs help overcome deficiencies and boost crop yields (Dawadi et al., 2021).

3. **Disease Management** The antimicrobial and antifungal properties of MnO NPs make them effective in managing plant diseases, including post-harvest diseases. MnO NPs can restrain pathogenic microorganisms, such as fungi and bacteria, that source various plant illnesses. Their application can reduce disease incidence and severity, leading to healthier plants and improved crop quality. MnO NPs can lessen the reliance on chemical pesticides (Shah et al., 2022).

4. **Control of Metal Stress** MnO NPs are valuable in mitigating metal stress in plants. They can interact with soil components to enhance metal bioavailability and promoting metal uptake in a controlled manner. This function ensures better plant growth and development (Zhou et al., 2020).

5. **Biotic Stress Control** MnO NPs offer potential in controlling biotic stress caused by pathogens and pests. Their antimicrobial properties can effectively manage

fungal and bacterial infections, while their toxic effects on pests can repel or kill harmful insects. Incorporating MnO NPs into integrated pest management (IPM) systems supports sustainable farming practices (Cao & Wang, 2022).

6. **Environmental Sustainability** The application of MnO NPs supports environmental sustainability. Their role in enhancing soil health, improving nutrient availability, and managing plant diseases minimizes reliance on synthetic chemicals. Additionally, MnO NPs contribute to soil and water remediation, helping to mitigate environmental pollution and promote healthier ecosystems (Babu et al., 2022).

1.20 POSTHARVEST DISEASE CONTROL THROUGH NANOPARTICLES

The application of nanoparticles in controlling postharvest diseases in plants represents a promising advancement in agricultural technology. NPs are very effective in controlling postharvest illnesses brought on by bacteria, fungus, and other pathogens (González-Estrada et al., 2019).

1.20.1 Effectiveness of NPs in Controlling Postharvest Diseases:

Numerous studies have revealed that using nanoparticles in controlling postharvest diseases (González-Estrada et al., 2019). This section will describe disease-controlling abilities of NPs, in detail.

1. **Fungal Diseases:** Diseases caused by different fungi have been reported to be controlled by a variety of nanoparticles. For instance, silver nanoparticles (Ag NPs) are effective in dominating the growth of *B. cinerea*, which are known to cause significant postharvest decay (Amiri et al., 2022).

2. **Bacterial Diseases:** Nanoparticles also show promise in managing bacterial postharvest diseases. ZnO NPs have been effective against *Erwinia carotovora* and *Xanthomonas campestris*. ZnO NPs can disrupt cell membranes of bacteria and disturb their cellular processes, reducing bacterial growth and proliferation (Raza et al., 2024).

3. **Mode of Action:** Nanoparticles are very efficient in disease control as they can penetrate plant tissues and interact directly with pathogens. Nanoparticles can disrupt microbial cell walls, induce oxidative stress, and interfere with pathogen metabolism. Their small size allows for enhanced penetration and more efficient delivery of antimicrobial agents compared to traditional methods (Amiri et al., 2022). Many scientists are working in this area.

4. **Impact on Fruit Quality:** The use of nanoparticles for controlling postharvest diseases not only helps in reducing pathogen load but also contributes to maintaining fruit quality. By preventing disease progression, nanoparticles help preserve key quality properties of produce fruit (González-Estrada et al., 2019).

5. **Sustainability and Safety:** Nanoparticle-based treatments have potential to replace conventional chemical fungicides and bactericides. They reduce the need for toxic chemicals and minimize environmental contamination. However, the assessment of potential risks linked with nanoparticle accumulation in the environment and their safe application in agriculture is also very important (Shah et al., 2022).

1.21 EFFECT OF NPs TO CONTROL METAL STRESS IN PLANTS

Nanoparticles (NPs) have acquired considerable attention for their potential use to mitigate stress of heavy metal in plants. This section will provide insight on how nanoparticles help alleviate metal stress, focusing on their mechanisms of action, specific examples, and potential synergistic effects (Kuo et al., 2015).

1.21.1 Reduction of Metal Bioavailability

Nanoparticles can significantly influence the acceptance of heavy metals by plants. NPs have the ability to adsorb heavy metals like cadmium (Cd) and lead (Pb), and reduce their mobility and bioavailability. This adsorption process helps to sequester the metals in the soil, making them less accessible to plant roots (Shah et al., 2022).

1.21.2 Enhancement of Plant Defence Systems

Nanoparticles can boost the defence mechanisms of plants by lowering the oxidative stress induced by heavy metals. For instance, nanoparticles can enhance enzymatic activities of SOD, and CAT also POD, which can mitigate oxidative damage (Dawadi et al., 2021).

1.21.3 Regulation of Metal Transport

Nanoparticles affect the demonstration of metal transport and homeostasis shared genes. For example, ZnO NPs can improve the expression of metal transporter genes in plants (Jośko et al., 2021).

1.21.4 Improvement of Plant Growth and Physiology

NPs can increase plant growth and physiological functions underneath metal stress. Nanoparticles like SiO_2 and TiO_2 have been shown to increase plant growth parameters and overall biomass in plants exposed to metal stress (Ullah & Ullah, 2019).

1.21.4.1 Specific Examples

Several studies highlight the effectiveness of nanoparticles in reducing metal stress:

- **Silicon Dioxide Nanoparticles**: These NPs alleviate aluminium toxicity in maize, grown on acidic soils, and enhance root and shoot growth (Jośko et al., 2021). These are also being applied on other crops.
- **Zinc Oxide Nanoparticles**: These NPs have been reported to regulate ROS scavenging mechanisms and reduce cadmium toxicity in tomato plants (Ullah & Ullah, 2019).
- **Iron Oxide Nanoparticles**: These NPs stimulate root growth and reduce cadmium-induced stress (Shah et al., 2022).

1.21.4.2 Synergistic Effects

Combining nanoparticles with other compounds, such as plant hormones or antioxidants, can enhance their protective effects against metal stress. For instance, the

co-application of nanoparticles with exogenous plant growth regulators has shown synergistic benefits in improving stress tolerance and growth under metal stress (Jampílek & Kráľová, 2019).

1.21.5 Overall Impact on Gene Expression

Nanoparticle exposure generally induces notable changes in the plant transcriptome, although these effects are often less pronounced than biotic stress, salinity, or drought. Despite this, nanoparticles still affect gene expression significantly and can lead to measurable phenotypic differences in plants (Tumburu et al., 2017).

1.21.5.1 Down-regulation of Genes

A common effect of nanoparticle exposure is the downregulation of gene expression across various gene subsets involved in disease responses, cellular processes, and metabolic functions (Husain et al., 2013).

1.21.5.2 Delivery Mechanisms

Nanoparticles can be applied through various delivery mechanisms, including soil amendments, hydroponic systems, and foliar sprays. Foliar application has often shown superior results in terms of nanoparticle uptake and stress alleviation compared to soil application (Tumburu et al., 2017).

1.22 NANOPARTICLES FOR CONTROLLING BIOTIC STRESS IN PLANTS

Nanoparticles (NPs) have gained significant attention as a novel approach to managing biotic stress in plants, particularly in controlling fungal infections. The following review explores the effectiveness of nanoparticles in mitigating fungal stress in sustainable agriculture (Ali et al., 2024).

1.22.1 Antimicrobial Properties

Nanoparticles, especially those composed of metals and metal oxides interact with fungal cells in various ways, disrupting their growth and replication (Mohamed et al., 2021).

1.22.2 Enhanced Plant Défense

Nanoparticles not only possess inherent antimicrobial properties but also enhance plant defence mechanisms. They stimulate the plant's own defence responses, leading to improved resistance to fungal attacks. This is achieved through the induction of defence-related enzymes and compounds (Ali et al., 2024).

1.22.3 Improved Delivery of Antifungal Agents

Nanoparticles can serve as carriers for antifungal compounds, improving their delivery and effectiveness. This targeted delivery system allows for the use of lower doses of antifungal agents, reducing the environmental impact and potential for chemical resistance (Soliman, 2017).

- **Nanoparticle-Loaded Antifungal Agents**: Incorporating antifungal compounds into nanoparticles enhances their stability and controlled release. This approach ensures a more efficient and targeted application, improving the efficacy of antifungal treatments (Soliman, 2017).

1.22.4 Specific Examples and Mechanisms

The effectiveness of NPs against fungal pathogens is evident through various studies:

- **Silver Nanoparticles**: Ag NPs disrupt fungal cell membranes and interfere with enzyme function, leading to cell death. They also generate ROS, which further damages fungal cells and inhibits mycelial growth (Yetisgin et al., 2020).

- **Copper Nanoparticles**: Cu NPs inhibit fungal spore germination and mycelial growth by causing structural damage to fungal cells and disrupting essential cellular processes (Sousa et al., 2020).

1.22.5 Synergistic Effects

Combining nanoparticles with other control methods or plant growth-promoting microorganisms can enhance their effectiveness against fungal pathogens. For example, integrating nanoparticle treatments with beneficial microbes can provide a more robust defence mechanism and improve overall plant health (Ali et al., 2024).

1.22.6 Potential for Sustainable Agriculture

Nanoparticle-based treatments offer a promising substitute to mainstream fungicides, with the potential to decrease chemical inputs in agriculture. By improving disease control and increasing plant resistance, nanoparticles contribute to more sustainable agricultural practices. Ongoing research aim to optimize nanoparticle use and assess their broader environmental impact (Shah et al., 2022).

1.23 AIMS AND OBJECTIVES

This study was aimed to synthesize and characterize nanoparticles for the effective command of post-harvest fruit diseases, mitigation of metal stress, and the controlling of Fusarium wilt of tomato.

Specifically, the objectives were to:

1. Synthesize MnO nanoparticles in the extract of beneficial bacteria (*Bacillus subtilis*), using environmentally friendly methods.
2. Characterize their physiology and chemical attributes through advanced techniques such as scanning electron microscopy (SEM), energy-dispersive X-ray diffraction spectroscopy (XRD), Energy Dispersive X-ray (EDX) analysis and Fourier Transformed Infrared (FTIR) Spectroscopy.
3. Evaluate antifungal efficacy of the synthesized MnO NPs against common pathogens responsible for post-harvest fruit diseases in tomatoes.
4. Assess their potential to improve the harmful consequences of heavy metals on plants.
5. Investigate the effectiveness of NPs in controlling Fusarium wilt, focusing on disease progression and overall plant health indicators.
6. Examine the impact of nanoparticle treatments on key post-harvest quality parameters, including shelf life, nutritional content, and sensory attributes of tomatoes.
7. Analyse the sustainability and economic viability of integrating NPs into tomato cultivation practices.

2. MATERIALS AND METHODS

2.1 EXPERIMENT 1: BIOSYNTHESIZED MANGANESE OXIDE NANOPARTICLES MAINTAIN FIRMNESS OF TOMATO FRUIT BY MODULATING SOLUBLE SOLIDS AND REDUCING SUGARS UNDER BIOTIC STRESS

2.1.1 Collection of Unhealthy Fruit Models

Tomato fruit having distinct black rot symptoms were gathered from regional fruit and vegetable market of Islamabad. These collected samples were brought to the Molecular Plant Pathology laboratory in sterilized bags for further analyses.

2.1.2 Isolation and Identification of Pathogen

Collected fruit samples by using 70% ethanol were surface sterilized with and a small section (3–4 mm) of diseased area was erased and kept in sterile Petri plates, owning potato dextrose agar (PDA) medium. These Petri plates placed for 4–6 days in an incubator at 25 ± 2 °C. After the appearance of mycelial colonies, the mycelial threads were sub-cultured on PDA medium. Based on characteristic morphological feature of colonies (color, growth pattern etc.), the isolated pathogen was identified (Donsch et al., 1980, Barnett and Hunter, 1998).

For microscopic observation, on glass slide mycelia were placed, dyed with lactophenol cotton blue, under light microscope observed at 100 × magnification.

2.1.2.1 Pathogenicity Test

For separated pathogen the pathogenicity test was proven, following Koch's postulates (Ali et al., 2020). A desired concentration of conidial suspension (106 conidia/mL) was achieved by shaking the mycelia of seven days old fungus in Czapek-Dox broth media at 25 ± 2°C. Sterile needle was utilized to make a small hole in healthy tomato fruit and 5 µL of conidial suspension was inserted. Normal fruits were injected with sterile distilled water. All fruits sample covered with muslin cloth and incubated at 25 ±2 °C. After one week, infection symptoms were recorded. From this symptomatic diseased fruit, the pathogen was again re-isolated and cultured on PDA media for 5–7

days at 25 ± 2 °C. The colony morphology was compared with that of originally isolated pathogen.

2.1.2.2 Molecular Identification of Isolated Fungus

The nominated fungal strains were molecularly characterized by isolating DNA using the CTAB method, which effectively extracted high-quality genomic DNA suitable for downstream applications. Following extraction, the 16S rRNA gene, a widely used marker for bacterial identification and phylogenetic studies, was successfully amplified through polymerase chain reaction (PCR) using a Bio-Rad T100 PCR thermal cycler. The amplification process employed Universal primers (27F and 1492R), which are highly conserved regions flanking the 16S rRNA gene across a broad range of bacterial species. The PCR reaction mixture included 20-30 ng of extracted genomic DNA and 10 mM of each primer in the PCR master mix. The thermal cycling protocol began with an early denaturation at 94°C for 4 minutes, tracked by 34 cycles of denaturation at 94°C for 40 seconds, annealing at 55°C for 50 seconds, and extension at 72°C for 45 seconds, ending with a final extension at 72°C for 4 minutes to ensure complete DNA synthesis. The resulting PCR products, which represented amplified fragments of the 16S rRNA gene, were then sequenced to obtain their nucleotide sequences. These sequences were exposed to BLAST analysis (http://www.ncbi.nlm.nih.gov) to compare them against known sequences in community databases, allowing for the determination of sequence similarities and the identification of the bacterial strains at the species level, thus providing insights into their genetic relationships and potential functional roles (White et al., 1990).

2.1.2.3 Phylogenetic Analysis Using Mega 7.0

To explore evolutionary relationships, the subsequent sequence was aligned with 15 related sequences using the MUSCLE program. Following this alignment, a phylogenetic tree was assembled using MEGA 7 software (Kumar et al., 2016). This learning equipped insights into the evolutionary lineage and relatedness of the isolated pathogen to other known species.

This comprehensive characterization, combining microscopic and molecular techniques, ensured a precise identification and understanding of the isolated pathogen, contributing valuable information for further studies and management strategies.

2.1.3 Synthesis of Manganese Oxide Nanoparticles (MnO NPs)

To produce NPs, a standard procedure was followed (Singh et al., 2011), with little modifications. *Bacillus subtilis* was cultured in broth Luria Bertani (LB) media at 35–37 °C, for three days. The culture was then centrifuged, and clean bacterial biomass (10 g) was transferred to 100 mL filtered water and again put cultured for a week at 45 °C in an orbital shaking incubator at 20 rpm. The bacterial biomass was then sonicated for 40 min at normal room temperature, and the pH of filtrate was determined. A stock solution of 1000 mg L^{-1} manganese acetate was prepared in Milli Q water and filter sterilized. To synthesize MnO NPs, bacterial filtrate and manganese acetate solution were added in 1:1 ratio, in a beaker and agitated for 24–48 h. The synthesis of NPs was anticipated by observing the difference in colour of the solution. After the change of colour, the samples were centrifuged, and the pellet was washed and stayed overnight at 40 °C. For calcination, the nanoparticles were placed for 2 h at 500 °C, in a furnace.

2.1.3.1 Characterization of Nanoparticles

Following techniques were used to see the size, shape and other characteristics of synthesized MnO NPs.

2.1.3.2 Fourier Transformed Infrared (FTIR) Spectroscopy

FTIR spectroscopy was done to see the nature and also types of functional groups related with MnO NPs. To perform FTIR analysis, a small amount of nanoparticle powder was mixed with potassium bromide (KBr) (kamal et al., 2022). In the FTIR spectrometer, and the spectrum was recorded over a range of wavelengths (typically 400 to 4000 cm^{-1}). The resulting FTIR spectrum provided information about the characteristic absorption peaks corresponding to different functional groups and molecular vibrations within the nanoparticles. This helps in understanding the chemical composition and confirming the presence of certain functional groups associated with the nanoparticles.

2.1.3.3 X-ray Diffraction (XRD) Analysis of MnO NPs

To find out the nature and size of MnO NPs, XRD spectroscopy was performed (Akbar et al., 2022). For XRD analysis, a fine powder of the nanoparticles was prepared and placed in an X-ray diffractometer. The sample was exposed to X-rays, and the diffraction pattern was recorded as a job of the diffraction angle (2θ). The XRD pattern was analysed to identify the distinct peaks corresponding to specific crystal planes. By comparing the observed peaks with standard reference patterns, the phase composition and crystalline structure of the nanoparticles was determined. This method provides insights into the particle size, lattice parameters, and phase identification. Following Scherrer equation for size purpose was used of synthesized MnO NPs:

$$D = \frac{K\lambda}{ß\cos\theta}$$

Where, D = size (diameter), k = shape factor, λ = wavelength of x-ray, ß = full thickness at half-maximum of radians, θ = angle of diffraction.

2.1.3.4 Scanning Electron Microscopy (SEM) and Energy Dispersive X-ray (EDX) Analysis

A sonicated double-distilled water solution of MnO NPs was used for SEM which used to see the apparent morphology and size distribution of nanoparticles. The nanoparticles were first dispersed on a conductive substrate and then coated with a very thin layer of carbon to prevent charging effects. The sample was then examined using an SEM, which scanned the surface with an electron beam and generates images of the nanoparticles. SEM images reveal details about the shape, of the nanoparticles. This technique provides valuable info on particle size spreading and morphology at the nanometer scale (Kamal et al., 2022). EDX is used in conjunction with SEM to analyse the elemental composition of nanoparticles (VEGA3 TESCAN).

2.1.4 Mycelial growth inhibition analysis of MnO NPs, *in vitro*

Mycelial growth inhibition potential of MnO NPs was observed in Petri plates. PDA medium was supplemented with MnO NPs in varying doses (0.25 mg/mL, 2.5 mg/mL and 5.0 mg/mL) and solidified in Petri plates. Using a cork-borer, inoculum discs

(4 mm) of separated fungus were placed in the centre of each plate. As a positive control, culture media devoid of MnO NPs was used. All inoculated dishes were placed in an incubator at 25 ± 2 °C and after one-week, growing inhibition was assessed as under:

$$\text{Fungus growth inhibition \%} = (C\text{-}T) / C \times 100$$

Where: C = Standard mycelial growth on PDA media, T = Mycelial growth on treated (NP amended) media.

2.1.5 Antifungal activity analysis of MnO NPs, *in vivo*

To investigate the effect of MnO NPs on tomato black rot control, a "wound inoculation method" was adopted. To conduct this experiment, 12 fruits were surface sterilized before injecting 5 µL of a fungal conidial solution (106 conidia/mL). Two days after inoculation, MnO NPs were sprayed on the fruits in three concentrations (0.25 mg/mL, 2.5 mg/mL, and 5.0 mg/mL). Control fruits were infected with distilled water and incubated at 25 °C. The infected area on each fruit was determined after 72 hours of therapy.

2.1.6 Organoleptic and Biochemical Properties

Organoleptic and biochemical properties of control and treated tomatoes, several measurements were taken 10 days after fungal inoculation. These measurements include reducing sugars, soluble solids, firmness, total sugars, and ascorbic acid concentration. The detailed methodologies for each parameter are described below:

1. **Reducing Sugars (%)** Reducing sugars in the tomato samples were quantified using the dinitro-salicylic acid (DNS) method. In this method, a known volume of tomato juice was mixed with DNS reagent. The combination was then warmed in a boiling water bath for approximately 5–10 minutes until a red-brown color developed, indicating the presence of reducing sugars. After cooling, the absorbance of the liquid was determined at 540 nm using a spectrophotometer. The concentration of reducing sugars was concluded using a standard curve prepared with known concentrations of glucose. The end result was conveyed as a percentage of reducing sugars in the sample (de Jesús Ornelas-Paz et al., 2018).

2. **Soluble Solids (% Brix)** This primarily representing the sugars and acids in tomato juice, was measured using a digital refractometer (Pam Abbe, model PA203×, MISCO Refractometer, Solon, OH). A few drops of tomato juice were placed on the refractometer's prism surface, and the instrument was calibrated to measure the refractive index, which directly provides the soluble solids content in percentage Brix (% Brix). The measurement was taken at normal temperature, and the results were recorded to represent the concentration of dissolved solids in the tomato juice (de Jesús Ornelas-Paz et al., 2018).

3. **Firmness (N)** The firmness of the tomato fruit was assessed using a TA.XTplus Texture Analyzer (Stable Micro Systems Ltd., Godalming, Surrey, UK). The sample of experiment was placed on the platform of the texture analyser, and a cylindrical probe was inserted into the tomato to a intensity of 10 mm with a constant force of 2 grams. The force required to penetrate the fruit was measured in Newtons (N). This value was used to indicate the firmness of the tomatoes, where a higher force represents firmer fruit. The firmness test was repeated on different sections of each tomato to ensure uniformity and reliability of the measurements (de Jesús Ornelas-Paz et al., 2018).

4. **Total Sugars (%)** Total sugars in the tomato experiments sample were revealed using the anthrone method. A known volume of tomato juice was mixed with anthrone reagent and then heated in a boiling water bath for 8–10 minutes. The reaction between the anthrone reagent and sugars produced a green-blue color, which was determined at 620 nm with help of spectrophotometer. The total sugar content was finalized by evaluating the absorbance of sample's to a standard curve containing known glucose values. The findings were represented as a percentage of total sugars in tomato juice (Meena et al., 2022).

5. **Ascorbic Acid (mol/kg)** Ascorbic acid (Vitamin C) amount in the tomato samples was evaluated by titration against 2,6-dichlorophenol-indophenol (DCPIP) dye. A known level of filtered tomato juice was then reduced with 3% metaphosphoric acid to stabilize the ascorbic acid. This mixture was titrated with DCPIP solution until a lasting light pink color developed, indicating the endpoint of the titration. The amount of ascorbic acid was established using a standard curve of ascorbic

acid absorptions. The concentration of ascorbic acid in the tomato samples was expressed in mol/kg (Meena et al., 2022).

2.1.7 Statistical Analysis

All the investigates were completed in three replicates, unless otherwise stated. MS-Excel 2016 (Microsoft Inc., Redmond, Washington, USA) was used to calculate the mean and standard deviation. The acquired data were subjected to an analysis of variance (ANOVA) using Statistix 8.1. Using the HSD value of p0.05, the significant differences between treatment mean values were calculated.

2.2 EXPERIMENT 2: BACTERIA-BASED MNO NANOPARTICLES ALLEVIATE LEAD TOXICITY IN TOMATO SEEDLING THROUGH IMPROVING GROWTH ATTRIBUTES AND ENHANCED GENE EXPRESSION OF CANDIDATE GENES

2.2.1 Synthesis of MnO-NPs

Mn NPs were synthesized according to the methodology described in section 2.1.3 of this thesis.

2.2.2 Characterization of Nanoparticles

Following procedures were used to see the size, shape and other characteristics of synthesized MnO NPs.

2.2.2.1 Fourier Transformed Infrared (FTIR) Spectroscopy

FTIR spectroscopy was performed according to the process described in section 2.1.3.2 of this thesis.

2.2.2.2 X-ray Diffraction (XRD) Analysis of MnO NPs

XRD analysis was performed according to the process described in section 2.1.3.3 of this thesis.

2.2.2.3 Scanning Electron Microscopy (SEM) and Energy Dispersive X-ray (EDX) Analysis

SEM and EDX analysis were executed according to the details described in section 2.1.3.4 of this thesis.

2.2.3 POT EXPERIMENT

2.2.3.1 Soil Preparation

Uncontaminated soil samples were obtained from Quaid-i-Azam University-Islamabad, (33° 44′ N, 73° 09′ E) Pakistan, at a depth of 5–25 cm. To remove gravel and larger debris, the collected soil was filtered through a 2-mm mesh and subsequently air-

dried for a period of 1 week at a temperature of 22–24 °C. Following properties of collected soil samples were examined

2.2.3.2 Soil Texture

Air-dried samples of soil were filtered to remove particles bigger than 2 mm. A 50 g soil sample was dispersed in 100 mL of sodium hexametaphosphate solution to separate the soil particles. The dispersion was stirred thoroughly and allowed to settle. Soil particle size distribution was measured by recording the suspension density at specific time spaces using a hydrometer. The proportions of sand, silt, and clay were determined based on the sedimentation rates and compared with standard textural classification.

2.2.3.3 Soil Organic Matter

A 1 g air-dried soil sample was mixed with 10 mL of 1 N potassium dichromate ($K_2Cr_2O_7$) and 20 mL of sulfuric acid (H_2SO_4) in concentrated form in a flask. After digestion, the combination was cool down and 100 mL of filtered water was included, followed by 10 mL of orthophosphoric acid. The organic matter was then titrated with 0.5 N ferrous sulphate solution. The percentage of organic matter was determined from the amount of dichromate reduced during the titration.

2.2.3.4 Soil Organic Carbon

The method involved calculating the organic carbon matter from the total soil organic matter measured. The percentage of organic carbon was obtained by multiplying the percentage of organic matter by a factor (usually 0.58), established on the statement that organic carbon constitutes about 58% of the organic matter.

2.2.3.5 Total Nitrogen

A 1 g soil sample was processed with concentrated sulfuric acid and a catalyst (selenium or copper) to convert nitrogen into ammonia. The ammonia was first distilled, and absorbed in a boric acid solution, and quantified with help titration as standard acid. The nitrogen content was determined based on the amount of ammonia distilled and titrated.

2.2.3.6 Phosphorus

A 10 g soil section was combined with 100 mL of Bray-1 solution (0.03 N HCl and 0.1 N NaHCO3). After shaking the mixture for 5 minutes, it was filtered. The phosphorus content in the filtrate was measured using the methodology of ascorbic acid, where phosphorus reacts with a reagent to form a blue-coloured complex, which was measured spectrophotometrically.

2.2.3.7 Electrical Conductivity (EC)

A 1:1 soil-to-water ratio was prepared by mixing soil with deionized water. The mixture was stirred and authorized to equilibrate for time of 30 minutes. The electrical conductivity of the soil suspension was assessed using a conductivity meter (DOS-11 AW), and results were reported in deciSiemens per meter (dS/m).

2.2.3.8 Soil pH

A 1:1 soil-to-water ratio was prepared, and the soil was blended thoroughly with refined water. After allowing the combination to settle for 30 minutes, the pH was assessed using a pH meter (Russell RL060P), providing an accurate reading of soil acidity or alkalinity as shown in (Table 1).

Table 1 *Key properties of the soil used in experiments*

PARAMETER	VALUE
TEXTURE	Clay loam
SAND (%)	35
SILT (%)	36
CLAY (%)	29
ORGANIC MATTER (%)	1.42
ORGANIC C (%)	0.55
TOTAL N (% WT)	0.51
PHOSPHORUS (MG/KG)	8.2
ELECTRICAL CONDUCTIVITY (DS/M)	1.85
PH	7.7

2.2.4 Pb Stress in Soil

Then the soil completely mixed in 2:1 ratio with peat moss, before adding Pb to soil. In a container, soil of 50 ppm concentration was prepared by adding 50 mg Pb in one kg soil, mixed and kept for 2 weeks. Soil was combined carefully at consistent intervals for correct metal stabilization. After 2 weeks, each pot was soaked with this soil and Pb mixture. The concentration of Pb concerned was more than the adequate limit for heavy metal in land, as stipulated by WHO (1996). Before planting, the containers were stored in a compartment at a temperature range of 18–22°C for 2 weeks, and they were moisturized to 70% of their maximum water-holding capacity, using tap water.

2.2.5 Seed Sterilization and Nano-priming

Seed sterilization is a crucial pre-treatment step to eliminate surface contaminants and pathogens that could affect seed germination and plant health. In this study, tomato seeds were taken from National Agricultural Research Centre (NARC) Islamabad and carefully sanitized.

Initially, the seeds were treated with 70% ethanol for 5 minutes. Ethanol acts as a disinfectant, effectively destroying most bacteria and fungi on the seed surface. This step helps to reduce the microbial load and prevent contamination during subsequent treatments. Following ethanol treatment, the seeds were further sterilized by immersing them in a 0.1% mercuric chloride ($HgCl_2$) solution for 1 minute. Mercuric chloride is a strong antimicrobial agent that ensures the elimination of any remaining pathogens on the seeds. The short exposure time is sufficient to disinfect the seed surface without causing significant damage to the seeds themselves. To remove any residual chemicals from the seed surface and prevent potential toxicity during germination, the seeds were completely cleaned with autoclaved water. This washing process was repeated 5 to 6 times, ensuring that all traces of ethanol and mercuric chloride were completely washed away.

Nano-priming is an advanced technique that involves the application of nanoparticles to seeds to enhance their stress tolerance and improve germination and seedling growth.

The preparation of MnO-NP solutions began with dispersing the nanoparticles in deionized water using ultra-sonication. This process involved sonicating the MnO-NPs in water for approximately 30 minutes to achieve a uniform dispersion of nanoparticles. Ultra-sonication ensures that the nanoparticles are well-distributed in the solution, preventing agglomeration and enhancing their effectiveness.

Tomato seeds were then soaked in the MnO-NP solutions at three different concentrations: 0.25 mg/mL, 2.5 mg/mL, and 5.0 mg/mL. The seeds were immersed in these solutions for 20 hours at room temperature, with the soaking process conducted in darkness and continuous aeration. This environment supports optimal seed imbibition while minimizing the risk of fungal growth. After soaking, the seeds were imbibed until they reached phase II of seed imbibition, characterized by full hydration and swelling. The seeds were then dried back to their original moisture content to prepare them for sowing. Control seeds were soaking wet in filtered water for the same duration to compare the effects of nano-priming.

The nano-priming process aims to enhance the seeds' resilience to stress conditions and improve their overall germination performance. By subjecting the seeds to different concentrations of MnO-NPs, the study evaluates the efficacy of these nanoparticles in promoting seed health and growth under various environmental conditions.

2.2.6 Experimental Setup

The experiment was completed to review the effects of nano-priming on tomato seeds under different concentration of Mn NPs and to evaluate the impact of MnO-NPs and lead (Pb) stress on seed germination and growth.

2.2.7 Seed Preparation and Control Treatment

Initially, tomato seeds were treated with MnO NPs at varying concentrations or soaked in deionized water as a control. Seeds that were not primed with nanoparticles were used as control seeds. These control seeds were water-logged in filtered water for the unchanged duration as the MnO NPs-treated seeds, to ensure that any observed effects were due to the nanoparticles and not differences in soaking time or method. After

soaking, all seeds were dried back to their original moisture content, as described by Rizwan et al. (2017), to standardize the seed condition before sowing. To simulate metal stress conditions, a soil mixture was prepared according to the protocol of Fatemi et al. (2021). Specifically, 500 mg of lead (Pb) was added to 1 kg of soil, resulting in a final Pb concentration of 500 ppm. This Pb-enriched soil was used to create a metal stress environment for evaluating the seeds' performance under adverse conditions.

2.2.8 Sowing and Treatment Application

Seeds were sown in eight distinct treatment groups to assess the influence of MnO-NP priming and Pb stress on seed performance. The treatments were as follows:

- **C (Control):** Un-primed seeds sown in control soil. This treatment served as a baseline for evaluating the effect of the soil without any nanoparticle treatment.
- **N1:** Seeds primed with a 0.25 mg/mL concentration of MnO-NPs and sown in control soil. This treatment assessed the impact of the lowest concentration of MnO-NPs on seed performance in the absence of Pb stress.
- **N2:** Seeds primed with a 2.5 mg/mL concentration of MnO-NPs and sown in control soil. This treatment evaluated the effects of a moderate concentration of MnO-NPs.
- **N3:** Seeds primed with a 5.0 mg/mL concentration of MnO-NPs and sown in control soil. This treatment examined the influence of the highest concentration of MnO-NPs.
- **Pb:** Un-primed seeds sown in Pb-stressed soil. This treatment served as a control for evaluating the effects of Pb stress without nanoparticle priming.
- **Pb + N1:** Seeds primed with 0.25 mg/mL MnO-NPs and sown in Pb-stressed soil. This treatment assessed the potential mitigation of Pb stress by the lowest concentration of MnO-NPs.

- **Pb + N2:** Seeds primed with 2.5 mg/mL MnO-NPs and sown in Pb-stressed soil. This treatment evaluated the effectiveness of a moderate concentration of MnO-NPs in alleviating Pb stress.

- **Pb + N3:** Seeds primed with 5.0 mg/mL MnO-NPs and sown in Pb-stressed soil. This treatment considered the effect of the highest concentration of MnO-NPs on seeds subjected to Pb stress.

The experimental treatments were ordered in a entirely randomized design (CRD) with three duplicates per treatment. This design was chosen to ensure the validity and reliability of the results by minimizing bias and randomizing the experimental conditions. Each treatment group was replicated three times to allow for statistical analysis and to account for variability within the experimental setup.

2.2.9 Experimental Analysis of Plants

All cultivated tomato seedlings were collected after 21 days of planting and following physiological, biochemical and antioxidant constraints were measured.

2.2.9.1 Measurement of Growth Features of Plants

The growth qualities of all the collected experimental plants such as shoot length, root length, dry weight and fresh weight of plants were noted, carefully. These plant parts were determined using a regular scale while fresh and dry weights were assessed using electrical weighing balance (Haroon et al. 2021).

2.2.9.2 Measurement Of Osmolytes

To measure osmo-protectants in wheat leaves, two primary methods were employed.

2.2.9.2.1 Proline Content Measurement

The proline content in tomato leaves was calculated using the protocol outlined by Bates et al. (1973). Initially, 0.1 grams of leaf tissue was beaten in 4 mL of a 3% sulfosalicylic acid solution. This combination was then centrifugated at 3000 rpm for 5 minutes to separate the soluble proline from the leaf debris. Following centrifugation, 2

mL of the supernatant was combined with 2 mL solution of an acidic ninhydrin. The acidic ninhydrin solution was made by dissolving 1.25 g of ninhydrin in 30 mL of glacial acetic acid and 20 mL of 6 M phosphoric acid. The resultant mixture was incubated in a water bath at 100 °C for 1 hour to speed up the interaction between ninhydrin and proline. The absorbance was determined at 520 nm with a spectrophotometer.

2.2.9.2.2 Total Soluble Sugar Measurement

The quantification of soluble sugars was accomplished using "phenol sulfuric acid method". Specifically, 0.01 g of dried leaves was completely mixed with water. The resulting isolate was filtered and subsequently treated with a solution of 5% phenol and 98% sulfuric acid. After letting the mixture to stand for 1 h, the absorbance was considered at 485 nm, using a spectrophotometer (Abbasi et al. 2020).

2.2.9.3 Measurement of Physiological Traits of Plant

Freshly picked leaves (0.1 g) were crushed in 80% acetone and stored in the dark for 24 hours. The absorbance of extracts was tested at various pH levels to determine their carotenoid and chlorophyll concentrations. Photosynthetic pigments were estimated using the following formulae:

$$\text{Chl a} = [12.7\ (663\text{ nm OD}) - 2.69\ (645\text{ nm OD})] \times V \div 1000 \times W$$

$$\text{Chl b} = [22.9\ (645\text{ nm OD}) - 4.68\ (663\text{ nm OD})] \times V \div 1000 \times W$$

$$\text{Carotenoids} = (\text{OD at } 480\text{ nm}) \times 4$$

2.2.9.4 Relative Water Content

RWC was assessed using Whetherley's (1950) technique. A fresh leaf was collected and weighed measured as fresh weight (FW). Then this leaf was placed on a petri dish filled with filtered water overnight, in the dark. After 24 hours, the leaf turgid weight (TW) was measured using a sensitive weighing scale. The leaf was heated in an oven at 72 °C overnight to calculate its dry weight (DW). The relative water content of leaves was determined using the following formula:

$$\text{RWC (\%)} = (FW - DW) / (TW - DW) \times 100$$

2.2.9.5 Oxidative Stress Biomarkers Determination

2.2.9.5.1 Relative electrolytic leakage

The leaf part was chopped into very small pieces (0.5 g) and put in a test tube having 10 mL of cleaned water. After leaving the test tubes at 4 °C for whole night, the electric conductivity (R1) was assessed with an electrical conductivity meter. The test tubes with leaves were autoclaved for 30 minutes, and the contents were allowed to cool off (Lutts et al., 1996). The electric conductivity was again determined (R2) using EC meter and the Relative electrolytic leakage was determined by the following formula.

$$\text{Relative Electrolytic leakage (\%)} = R1 \div R2 \times 100$$

2.2.9.5.2 Malondialdehyde (MDA)

The quantification of malondialdehyde (MDA) was conducted using, 0.2 grams of fresh leaf tissue were properly homogenized in 5 mL of thiobarbituric acid (TBA) solution. The homogenized combination was then at 12,000 rpm centrifuged for 10 minutes to split the supernatant from the cellular debris. A 1 mL aliquot of the supernatant was mixed with 20% trichloroacetic acid (TCA) to precipitate proteins and isolate the MDA-TBA complex. This fusion was subsequently boiled to 90°C and boiled for 30 minutes to facilitate the formation of the MDA-TBA complex. After boiling, the mixture was chilled in an ice. The absorbance measurement of the chilled mixture was dignified at 450 nm wavelengths, 532 nm, and also 600 nm using a spectrophotometer (AA240FS, USA). The absorbance readings at these wavelengths were used to calculate the MDA content, which serves as an marker of lipid peroxidation and oxidative stress within the plant tissues.

2.2.9.5.3 Hydrogen Peroxide (H_2O_2)

The hydrogen peroxide (H_2O_2) amount was told using the methodology described by Jana and Choudhuri (1981). An extract of the plant tissue (3 mL) was prepared and agreed with 1 mL of 0.1% titanium sulphate, which had been dissolved in 20% sulfuric acid (H_2SO_4). This reaction forms a coloured complex with H_2O_2. The absorbance of the following result was then considered at a wavelength of 410 nm with a spectrophotometer (AA240FS, USA). The shade intensity at this wavelength is immediately proportional to

the concentration of H_2O_2 in the sample, allowing for accurate quantification of this reactive oxygen species.

2.2.9.6 Appraisal Of Antioxidant Enzymes Activities

2.2.9.6.1 Superoxide Dismutase (SOD) Assay

The superoxide dismutase (SOD) action in plant tissues was calculated with the technique described by Beauchamp and Fridovich (1971). This assay involves preparing various phosphate buffers, homogenizing plant tissues, and measuring SOD activity by comparing absorbance amendments in the presence and absence of the enzyme.

1. Preparation of Phosphate Buffers

Two phosphate buffers were prepared to maintain the appropriate pH for the assay:

- **Monosodium Dihydrogen Phosphate Solution:** 15.6 g of monosodium dihydrogen phosphate was dissolved in 500 ml of water.
- **Disodium Hydrogen Phosphate Solution:** 53.65 g of disodium hydrogen phosphate was dissolved in 600 ml of distilled water.

To prepare the pH 7 phosphate buffer, monosodium dihydrogen phosphate solution of 97 mL was mingled with 183 mL of disodium hydrogen phosphate, and the complete level was high to 600 mL with refined water. Similarly, for the pH 7.8 buffer, 25.5 mL of MDPS was mixed with 275.5 mL of DHPS, and the total volume was changed to 600 mL with distilled water.

2. Sample Preparation

- **Buffer Preparation for Homogenization:** A solution having 1 g of polyvinylpyrrolidone (PVP) and also 0.0278 g of Na2EDTA was prepared in 100 mL of pH 7 phosphate buffer.
- **Homogenization:** About 0.2 g of plant tissue crushed with 4 mL of the above buffer using an ice-cold pestle and mortar. The resulting homogenate monosodium dihydrogen phosphate solution was centrifuged at 4°C for 10

minutes, and the supernatant was taken. The volume of the supernatant was then altered to 8 mL with pH 7 phosphate buffer.

3. Reaction Mixture Preparation

- **Preparation of Reaction Solution:** A reaction solution was planned by merging 100 mL of pH 7.8 phosphate buffer with 0.0278 g of Na2EDTA, 1.5 g of methionine, and 0.04 g of Nitro Blue Tetrazolium Chloride (NBT). This solution was then diluted to 50 mL with pH 7.8 phosphate buffer.

- **Preparation of Riboflavin Solution:** A solution of riboflavin (0.0093 g) was prepared by dissolving it in 100 mL of phosphate buffer at pH 7.8, and then the final volume was got up to 50 mL using water.

4. Assay Procedure

- **Reference, Blank, and Reaction Mixture Preparation:** The assay setup included three types of samples:

    - **Reference:** 2 mL of the solution of reaction (from step 3) and 0.5 mL of riboflavin solution (from step 4).

    - **Blank:** 2 mL of the reaction solution and 0.5 mL of pH 7 buffer.

    - **Reaction Mixture:** 2 mL of the reaction solution, 0.5 mL of riboflavin solution, and 0.5 mL of the enzyme extract (from step 2).

The samples of reference were kept in full darkness, while the reaction mixtures were exposed to a light chamber for 20 minutes to initiate the reaction.

5. Measurement and Calculation

- **Absorbance Measurement:** After the reaction period, the absorbance at 560 nm was determined using a spectrophotometer. The SOD activity was checked by comparing the absorbance of the reaction mixture to that of the reference and blank samples.

The activity was calculated using the following procedure:

$$R4 = R3 - R2$$

$$A = R1\ (50/100)$$

$$Final = R4/A$$

where:

- R1 = Absorbance of Reference
- R2 = Absorbance of Blank
- R3 = Absorbance of Sample
- R4 = Difference between Sample and Blank Absorbance
- A= Adjusted Absorbance of Reference

To assess peroxidase (POD) activity in plants, the technique adapted from Reddy et al. (1985) was employed, with slight modifications to suit the experimental requirements.

2.2.9.6.2 Peroxidase (POD) Activity

1. Calcium Chloride Solution: A 0.5 M solution of calcium chloride was ready by dissolving 5.55 grams of the compound in filtered water, and then volume was corrected to 100 ml. This mixture was stored in a refrigerator and kept on ice before use to maintain its efficacy.

2. MES Buffer Solution: A 0.02 M MES buffer was created by mixing 293 mg of MES in 75 mL of purified water. Sodium hydroxide was used to modify the pH to 6.0, ensuring conditions favorable for enzyme functionality.

3. p-Phenylenediamine (PPD) Solution: A 0.1% p-Phenylenediamine (PPD) solution was prepared by mixing 0.1 grams of PPD in 100 mL of MES buffer, providing the substrate necessary for the peroxidase reaction.

Crude Enzyme Extract Preparation

1. Tissue Homogenization: New or cold plant material (1 gram) was put in an ice-cold mortar, and the tissue was homogenized with 5 mL of chilled 0.5 M calcium chloride solution using a cool pestle. This step helps to extract the enzymes while maintaining their activity.

2. Centrifugation: The homogenate was centrifuged at 1,000 rpm for 8 minutes. The supernatant was carefully collected and transferred to a clean test tube, which was then kept on ice to preserve enzyme activity.

3. Re-extraction: The remaining pellet was resuspended in an additional 2.5 mL of ice-cold calcium chloride solution and centrifuged again. The new supernatant was combined with the previously collected supernatant to ensure complete enzyme extraction.

Reaction Mixture and Measurement

1. Reaction Mixture Preparation: The mixture was made by combining 0.1 mL of enzyme separate, 1.5 mL of MES buffer, 0.5 mL of p-Phenylenediamine (PPD) solution, and 0.45 mL of hydrogen peroxide (H_2O_2), making up a total volume of approximately 2.55 mL.

2. Measurement: To measure the peroxidase activity, MES buffer was consumed as a blank. The initial absorbance was noted immediately (zero-minute reading), and the final absorbance was recorded after 3 minutes of incubation. The hydrogen peroxide was inserted to the reaction mixture right beforehand putting the cuvette into the spectrophotometer to begin the reaction.

3. Calculations: The difference in absorbance (ΔA510) was determined using the formula:

Change in A510: Af - Ai

Af = Final reading (after 3 minutes) Ai = Initial reading (zero minute)

where Af signifies the final absorbance reading after 3 minutes, and Ai correspond to the initial absorbance reading at zero minutes. This calculation reflects the peroxidase activity grounded on the change in absorbance at 510 nm.

2.2.10 Lead Measurements in Plant Tissues

To determine Lead (Pb) concentrations in plant tissues, a systematic approach was employed, adhering to the methodology of Irshad et al. (2020). Initially, plant models were meticulously split into roots and leaves. Each section underwent thorough washing

with simple water to remove any surface contaminants, then by rinsing with deionized (DI) water to ensure complete removal of any residual impurities. Once cleaned, the plant parts were subjected to drying in an oven set to 65°C. This temperature was maintained to effectively dry the samples while preventing the degradation of the plant material. Following the drying process, a precise quantity of 0.5 grams of the dried plant tissue was weighed and prepared for digestion.

The digestion process involved the use of concentrated nitric acid (HNO_3), which was additional to the plant samples to break down the organic matrix and release the lead into a solution. This step is crucial for accurate quantification, as it converts the solid plant material into a digestible liquid form suitable for analysis. After digestion, the lead content in the plant samples was quantified using an atomic absorption spectrophotometer (Varian FAAS-240, Triad Scientific, USA). This analytical technique is highly sensitive and precise, allowing for the detection and measurement of trace levels of lead in the plant tissues. The atomic absorption spectrophotometer works by measuring the absorption at specific wavelengths of light by the lead atoms, providing an accurate assessment of the lead concentration in the plant samples.

2.2.11 Gene Expression Analysis of Stress-Related Enzymes

Appearance of defence-linked genes was observed in four dealings viz. C (un-primed seeds sown in control soil), N2 (seeds primed with 2.5 mg/mL concentration of MnO-NPs and sown in control soil), Pb (Un-primed seeds sown in metal stressed soil), Pb + N2 (seeds prepared with 2.5 mg/mL concentration of MnO-NPs and sown in metal stressed soil) For the separation of total RNA and synthesis of cDNA from tomato seedlings of these treatments, the procedure of Goupil et al. (2009) was ensued. For quantitative real-time PCR (qPCR), Primer3 software was used to design primers (Thornton and Basu 2011) from the partial gene sequences of three defence-related genes (Table 2) available on NCBI database. In this analysis, Ubiquitin was used as housekeeping (internal control) gene for normalization. Complete information of studied genes has been provided in Table. 2

Table 2 Primers used for qRT-PCR

GENE NAME	NCBI	PRIMER SEQUENCE

	GENBANK ID	
CHLOROPHYLLASE	XM_010328388	Forward primer 5′ GGGGTAAGAGGAAAGGCAAC 3′ Reverse primer 5′ CCACATCTCGAAGCTCAACA 3′
CHALCONE SYNTHASE	HQ008773	Forward primer 5′ GCCAAAACTTGGCAAAGAAG 3′ Reverse primer 5′ CAGCAAAGCAACCTTGTTGA 3′
PHENYLALANINE AMMONIA LYASE	M90692	Forward primer 5′ CTCACTGGCAGGCCTAACTC 3′ Reverse primer 5′ CGTTCATCACTTCAGCGAAA 3′
UBIQUITIN	NM_001366381	Forward primer 5′ GGAGGACGGACGTACTCTAGC 3′ Reverse primer 5′ TTCGACCTCAAGGGTAATCG 3′

2.2.12 Data Analysis

The data were exposed to one-way analysis of variance (ANOVA). Fisher's LSD (least significant difference) experiment was used to calculate errors of means with a significance level of 5%. Correlation analysis and principal component analysis (PCA) were perfprmed using R-studio.

2.3 EXPERIMENT 3: *BACILLUS*-MEDIATED MANGANESE OXIDE NANOPARTICLES AMELIORATE FUSARIUM WILT OF TOMATO BY PROTECTING ITS VASCULAR SYSTEM AND IMPROVING ANTIOXIDATIVE ENZYMATIC ACTIVITIES

2.3.1 Synthesis of MnO NPs

Bacteria-based nanoparticles were synthesized according to the methodology described in section 2.1.3 of this thesis.

2.3.2 Characterization of Nanoparticles

Synthesized Mn-O-NPs were assessed for size determination and analyses of other characteristic features using the following techniques.

2.3.2.1 Fourier Transformed Infrared (FTIR) Spectroscopy

FTIR spectroscopy was done according to the process described in section 2.1.3.2 of this thesis.

2.3.2.2 X-ray Diffraction (XRD) Analysis of Mn-O-NPs

XRD analysis was done according to the process described in section 2.1.3.3 of this thesis.

2.3.2.3 SEM and EDX Analysis

SEM and EDX analysis were executed according to the details described in section 2.1.3.4 of this thesis.

2.3.3 Collection and purification of microbes

Pathogenic fungus (*F. oxysporum*) was acquired from First Fungal Culture Bank of Pakistan (FCBP), Punjab University, Lahore, Pakistan. Fungus was flourished on autoclaved SDA media which was prepared by dissolving 40 g of dextrose, 10 g of peptone, and 15 g of agar in 1,000 mL of water (Esmaeili et al., 2009). Fungal mycelia were inoculated in the center of solidified sabouraud dextrose agar (SDA) media surrounding petri plates and placed at 27 °C for a week.

2.3.4 Mycelial growth inhibition analysis of Mn-O NPs, *in vitro*

To inhibit mycelial growth by checking the potential of Mn-O NPs was observed in petri plates having solidified Potato dextrose agar (PDA) medium. PDA medium was supplemented with Mn-O NPs in varying doses (0 mg/mL, 0.5 mg/mL, 2.5 mg/mL and 5 mg/mL) and solidified in petri plates. Using a cork-borer, 4mm of inoculum discs of isolated fungus were put in the center of each plate. As a positive control, culture media devoid of Mn-O NPs was used. All plates were rested in an incubator at 25 ± 2 °C and after one week, growth inhibition was assessed as under (Farhana et al., 2024):

$$\text{Mycelial growth inhibition \%} = \text{C-T /C} \times 100$$

Where, C = mycelial growth in control plates, and T = mycelial growth in treated plates.

2.3.5 *In vivo* assay

A pot experiment was conducted for the evaluation of antimycotic properties of *B. subtillus* and MnO-NPs against *Fusarium* wilt of tomato, caused by *F. oxysporum*. The experimentation was conducted in Randomized Complete Block Design (RCBD) by using three replicates of each treatment. Experiment was performed in following steps:

2.3.6 Formulation of fungal inoculum

To prepare fungal inoculum, sorghum seeds were added in sterilized Erlenmeyer flasks having 200 gm seeds. The flask was autoclaved and a mycelial plug of *F. oxysporum,* taken from fresh fungal culture (5 days old) was added in flask. Then the flask was tightly taped up with aluminum foil and also incubated at 30 °C in a shaking incubator at 120 rpm for 4 days to achieve maximum growth of fungal inoculum (Khan & Khan, 2001).

For the preparation of bacterial inoculum, 250 mL of LB broth was prepared by dissolving tryptone (2.5 gm), yeast extract (1.5 gm) and sodium chloride (2.5 gm) and autoclaved (Rayner & Sadler, 1990). Bacterial single colony was picked from 24 hours old culture of *P. putida* and streaked on LB broth by using sterilized inoculation loop. After bacterial inoculation, media was incubated at 35 ℃ in a shaking incubator at 120

rpm for 1 day. The cultured bacteria added in the distill water for seed priming of the tomato.

2.3.7 Preparation of soil

Uncontaminated soil samples were obtained from Quaid-i- Azam University-Islamabad, (33° 44′N, 73° 09′E) Pakistan, at a depth of 5–25 cm. To remove gravel and larger debris, the collected soil was filtered through a 2 mm mesh and autoclaved. The sieved soil was analyzed (Table 3) and completely mixed with peat moss in 2:1 ratio. Each pot was filled with 200 gm of that prepared soil.

Table 3 Key properties of the soil used in experiments.

Parameter	**Value**
Texture	Clay loam
Sand (%)	35
Silt (%)	37
Clay (%)	27
Organic matter (%)	1.39
Organic C (%)	0.55
Total N (% wt)	0.53
Phosphorus (mg/kg)	7
Electrical conductivity (dS/m)	1.8
pH	7.6

2.3.8 Seeds priming

Tomato seeds were sourced from the National Agricultural Research Centre (NARC) in Islamabad and sterilized by immersing them in 70% ethanol for 5 minutes, followed by treatment with 0.1% $HgCl_2$ for 1 minute. The seeds were then completely rinsed 5–6 times with autoclaved water. The pot experiment was performed in eight different treatments. In control (C), normal seeds (non-bio primed) were planted and used as control. In solo *Fusarium* treatment (F), non-bio primed seeds were spread in soil, contaminated with *F. oxysporum.* In *Bacillus* treatment (B), bacteriological primed seeds

were sown in soil that was not contaminated with fungus. In Nanoparticle treatment (Np), the best concentrations of Mn-O NPs (2.5 mg/mL) were used for seed priming. In Mn salt treatment (Mn) the same concentration of salt (2.5 mg/mL) is used for seed priming of tomato. For *Bacillus* + Fusarium treatment (B+F), bacteriological primed seeds were sown in *F. oxysporum* contaminated soil. In Nanoparticle + Fusarium treatment (Np+F), MnO Nanoparticle primed seeds were sown in *F. oxysporum* contaminated soil and in *Salt* + *Fusarium* treatment (Mn+F) salt primed seed were sown in *F. oxysporum* contaminated soil by drawing small wells of 10 mm size and covered lightly with soil (Chen et al., 2021).

2.3.9 Harvesting of Plants for Experimental Analysis

All cultivated tomato seedlings were harvested after 21 days of sowing and following physiological, biochemical and antioxidant parameters were measured**.**

2.3.9.1 Determination of disease severity

For the determination of disease severity, a visual estimation of wilting was made by monitoring the wilting of plant in each treatment and visual wilting score was given to each treatment (Tyree & Cochard, 2003). Following the protocol of Cooke (2006), discoloration and yellowing of plants in all treatments was determined.

2.3.9.2 ***Tomato histopathological appraisement.***

Tomato histopathological appraisement was accomplished by employing a valid procedure of Yousaf et al. (2021). Tomato shoot and root samples, in the form of transverse slivers (10 mm) were gathered from each treatment and positioned in fixative acetic acid formalin solution for 36 hours, containing formalin (10%), acetic acid (5%), ethanol (50%) and distilled water (35%) for preservation (Ghazy & El-Nahrawy, 2021). The shoot and root specimens were then kept in finalized fixative ethanol acetic acid solution, prepared by the fusion of ethyl alcohol (75%) and acetic acid (25%) for prolonged stabilization. After fixation, tomato shoot and root specimens were manually sliced into very fine transverse slivers (3 mm). For the preparation of final slides, thin slivers were dehydrated, sequentially diluted by ethyl alcohol and counter stained by safranin. Slide were observed by light microscope at 100× magnification.

2.3.9.3 Measurement of Growth Features of Plants

All harvested experimental plants had their growth data, such as shoot length, root length, fresh weight, and dry weight, meticulously documented. A standardized scale was used to measure the lengths, and an electronic weighing balance was used to calculate the fresh and dry weights (Haroon et al., 2021).

2.3.9.4 Measurement of Osmolytes

2.3.9.4.1 Sugar Content

Soluble sugars were quantified using the phenol-sulfuric acid method. Then, 0.01 g of dried leaf material was thoroughly mixed with water. The extract was then filtered and then treated with 5% phenol and 98% sulfuric acid. After allowing the mixture to sit for 1 hour, its absorbance was measured at 485 nm using a spectrophotometer (Abbasi et al., 2020).

2.3.9.4.2 Proline Contents

Proline content was measured following a standard protocol (Bates et al., 1973). Fresh leaf tissue (1 g) was thoroughly ground in 4 mL of 3% sulfosalicylic acid solution and left at room temperature for 24 hours. After centrifugation, the supernatant was mixed with Ninhydrin and glacial acetic acid were combined and heated in a water bath at 100°C for 1 hour, followed by rapid cooling in an ice bath. Toluene was utilized for extraction, and the absorbance was recorded at 520 nm.

2.3.9.5 Measurement of Physiological Traits of Plants

Chlorophyll level in the given plants was measured using a SPAD-502 meter (Konica-Minolta, Osaka, Japan) (Hassanzadeh et al., 2009). Fresh sample of leaf (0.1 g) were ground in 80% acetone and kept in the dark for 24 hours. The absorbance of carotenoids in the extracts was checked by measuring at 480 nm (Haroon et al., 2021).

Initially, the fresh weight (FW) of the plants was evaluated in order to determine the Relative Water Content (RWC). After that, the leaves were submerged in water for a whole day in order to determine their turgid weight (TW). The leaves were then dry up

in a hot air oven until they reached a consistent dry weight (DW). The RWC was computed utilizing Weatherley's (1950) formula.

$$RWC\ (\%) = (FW - DW) / (TW - DW) \times 100$$

2.3.9.6 Antioxidative enzyme activity

Superoxide dismutase (SOD) antioxidative enzymatic investigation was carried out according to Beauchamp and Fridovich's (1971) published technique. With some slight adjustments based on Gorin and Heidema (1976), the technique described by Vetter et al. (1958) was used to measure the activity of peroxidase (POD) in treated leaves. Furthermore, the method described by Luck (1974) was used to test the concentration of hydrogen peroxide ($H2O_2$) in the leaves in order to determine catalase activity).

2.3.9.7 Oxidative burst assay

The amount of Malondialdehyde (MDA) and Hydrogen Peroxide (H_2O_2) was determined by following the standard protocol of Loreto & Velikova (2001).

2.3.10 Statistical Analyses

Means, standard errors, correlation and regression functions were calculated and analyzed using Microsoft Excel software. Using Statistix version 8.1, the data was treated to one-way ANOVA, followed by Tukey's least significant difference (HSD) test. Correlogram was constructed using RStudio program.

3. RESULTS

3.1 Experiment 1

3.1.1 Microscopic and morphological identification of isolated fungus

Tomato fruit with typical black rot indications were gathered from the market (Fig. 1A) and the disease-triggering pathogen was isolated on PDA media (Fig. 1B-C). The growth of fungus was rapid and fungal mycelia covered the entire petri plate in 5–7 days. The pathogen appeared black from the center and grey whitish from the edges (Fig. 1 B). Mycelia appeared pale yellow and cracked from the back side of Petri plate (Fig. 1C). Microscopic photograph revealed the presence of clear septate hyphae. Long conidiophores were bearing vesicles that were spherical in shape. Conidia were globose and black in color with rough surface (Fig. 1D). All morphological and cultural features revealed this pathogen as *Aspergillus niger* (Ahmed et al., 1993).

3.1.2 Pathogenicity test

A pathogenicity test of isolated fungus was brought out efficiently. After 3 days of injection, the blackish brown spots could be observed, and the surrounding area became soft and pulpy (Fig. 1E). These spots developed quickly after 5 days of inoculation (Fig. 1F). The fungus was seprated on PDA media from this self-inoculated fruit, which displayed similar fungal growth pattern to the previously isolated fungus (Fig 1G, 1H).

3.1.3 Phylogenetic analysis

Obtained 18 S rRNA gene sequence revealed 100% similarity with the strain of *A. niger* (Accession No. MN420840.1). Phylogenetic tree also showed the presence of obtained sequence in the same clade with *A. niger* (Fig. 2).

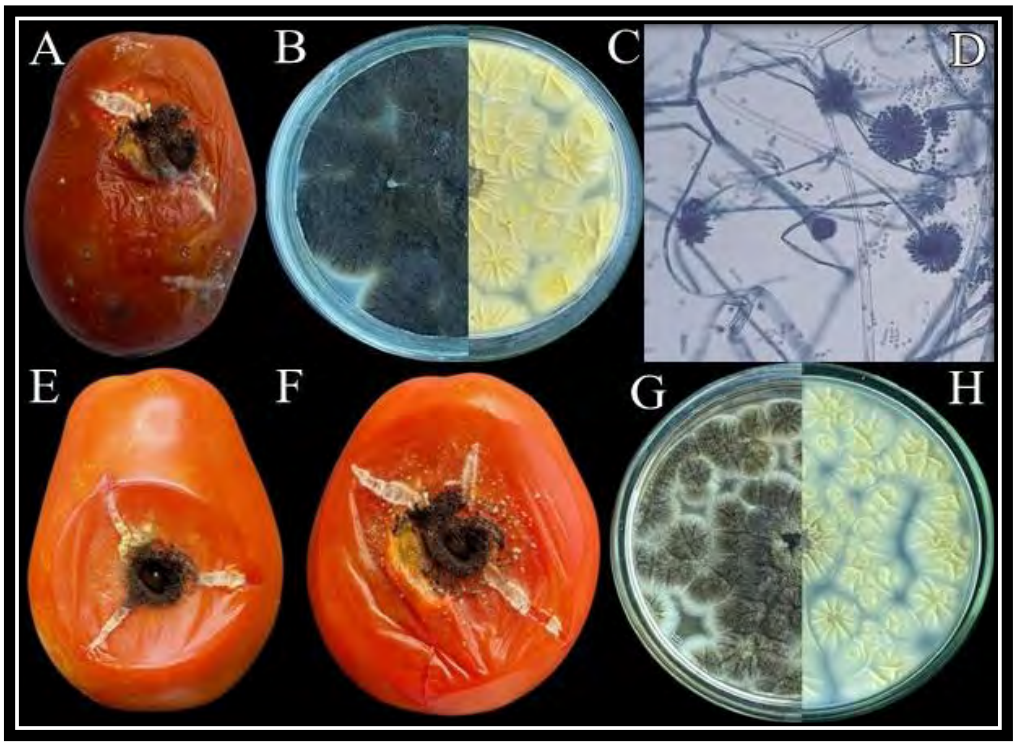

Fig. 1 Black rot symptoms on tomato fruit were assessed in the field (A). The infectious pathogen was isolated and observed from both the front (B) and back (C) sides of Petri plates. Microscopic examination of the isolated fungus was conducted at 100× magnification (D). The fungus was then re-inoculated onto healthy fruit, and disease symptoms were recorded after 3 days (E) and 5 days (F) post-inoculation. The pathogen was subsequently re-isolated on PDA and examined from both the front (G) and back (H) sides.

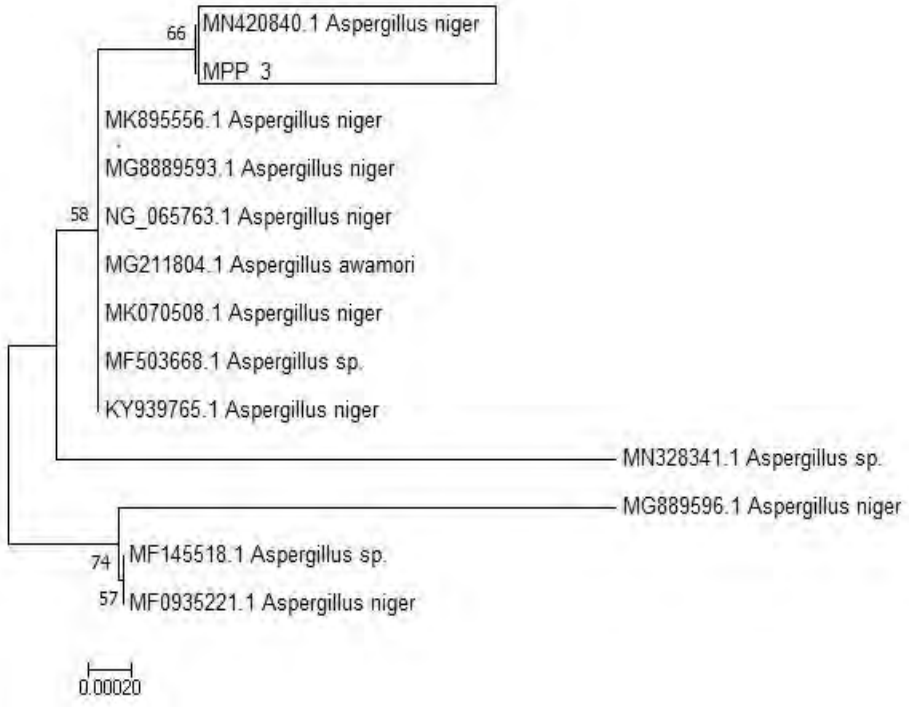

Fig. 2 Phylogenetic tree depicting the evolutionary relationship of 18S sequence of isolated fungus with 12 related sequences on NCBI.

3.1.4 Characterization of Bacteria supplemented MnO NPs *4.*

The following parameters assisted to demonstrate the successful synthesis of MnO NPs.

3.1.4.1 FTIR analysis

FTIR exploration of MnO NPs showed characteristic peaks of different functional groups, accountable for the stability and biosynthesis of synthesized MnO NPs (Fig. 3, Table 4). The spectrum of FTIR was brought in the range of 500–4000 cm^{-1} under infrared radiation. One characteristic peak at 2981.04 cm^{-1}, specified the presence of carboxylic acids (O-H stretch), while other significant peak at 999.76 cm^{-1} (=C-H bend) revealed the presence of alkenes. Three other peaks at 608.58 cm^{-1}, 575.14 cm^{-1}, and 555.91 cm^{-1} indicated C-Cl stretch of alkyl halides, while peaks at 547.21 cm^{-1}, 537.01 cm^{-1}, and 522.83 cm^{-1} displayed C-Br stretch of alkyl halides.

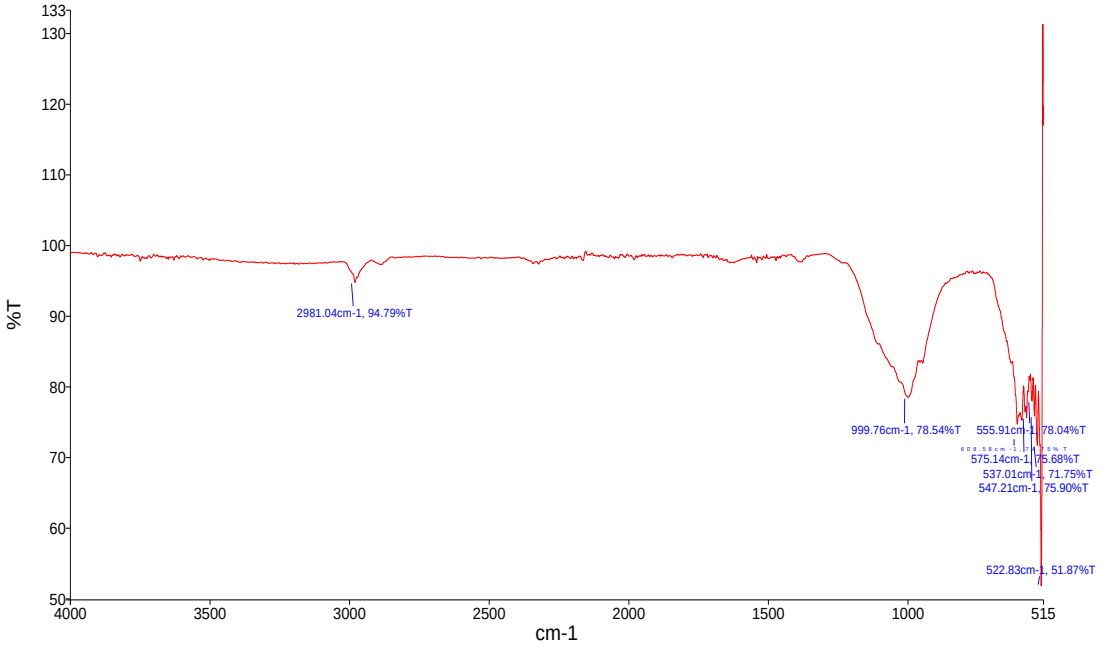

Fig. 3 FTIR spectrum showing standard peaks of important functional groups.

Table 4 FTIR analysis revealing characteristic peak numbers, functional groups, appearance and class of compound on MnO NPs.

Sample No	Sample Peak	Standard Table Absorption (cm^{-1})	Functional group	Bounding	Class Compound
1	2981.04 cm^{-1}	3300–2500 (m)	O-H	O-H stretch	carboxylic acids
2	999.76 cm^{-1}	1000–650 (s)	=C-H	=C-H bend	Alkenes
3	608.58 cm^{-1}	850–550 (m)	C-Cl	C-Cl stretch	alkyl halides
4	575.14 cm^{-1}	850–550 (m)	C-Cl	C-Cl stretch	alkyl halides
5	555.91 cm^{-1}	850–550 (m)	C-Cl	C-Cl stretch	alkyl halides
6	547.21 cm^{-1}	690–515 (m)	C-Br	C-Br stretch	alkyl halides
7	537.01 cm^{-1}	690–515 (m)	C-Br	C-Br stretch	alkyl halides
8	522.83 cm^{-1}	690–515 (m)	C-Br	C-Br stretch	alkyl halides

3.1.4.2 XRD analysis

XRD analysis illustrated visible peaks pattern of MnO NPs at 8.68, 16.24, 32.17, 32.17, 44.86, 61.08 and 82.24 planes, which corresponded to peaks values of (110), (200), (310), (310), (521), (730) and (301), respectively. Clear peaks, displayed by XRD spectra, were comparable to Orthorhombic space group, revealing magnetite manganese oxide (Fig. 4). The patterns plane of XRD was in decent agreement with JSCPD number 01076-0958. The average nanoparticle size was 39 nm (Table 5).

Fig. 4 XRD analysis of MnO NPs.

Table 5 Size of MnO NPs synthesized in *B. subtilis*

Peak Number	2 Theta	FWHM	Crystallite size D (nm)	Average size (nm)
1	8.683	0.416	190.264	39.2008
2	16.241	2.297	34.212	
3	32.170	0.054	1410.67	
4	32.170	0.0689	1106.32	
5	61.028	92.138	0.7425	
6	82.275	223.589	0.2674	
7	44.8519	46.3216	12.5847	

3.1.4.3 SEM and EDX analysis

Surface of MnO NPs was successfully observed by scanning electron microscope (Fig. 5). The uniform spreading of grains was monitored in micrographs. The grains were nearly spherical in structure with uniform size. EDX analysis revealed the elemental makeup of MnO NPs (Fig. 6). Oxygen (23.3%) and manganese (26.4%) were the most dominant elements. Sharp manganese and oxygen peaks proved the synthesis of MnO NPs, in the studied materials.

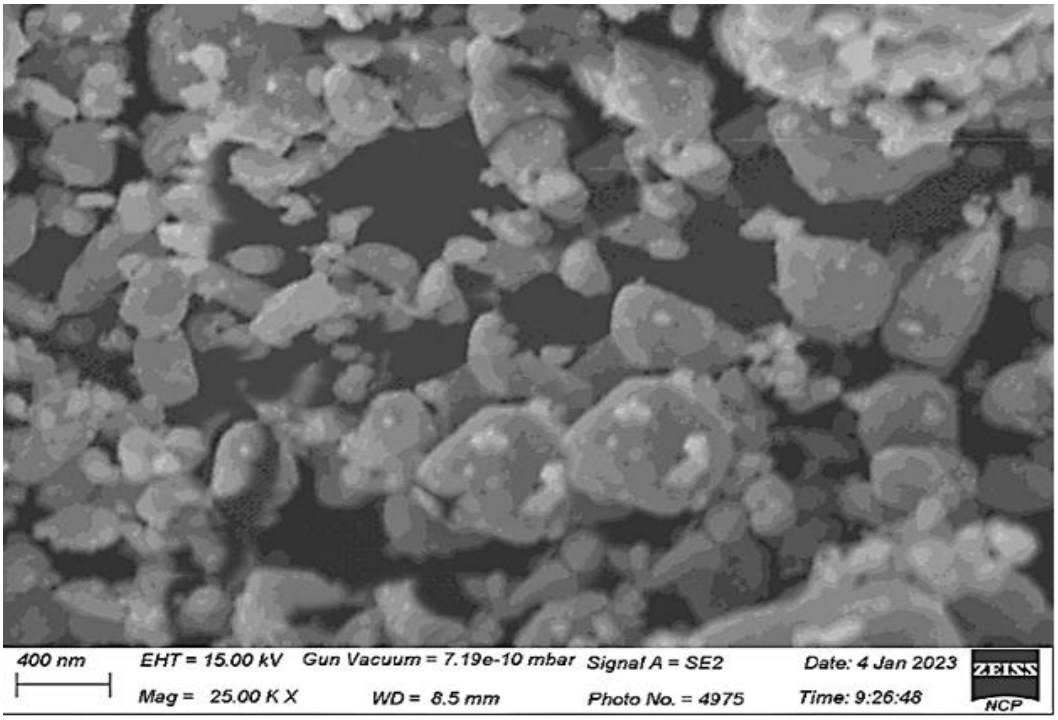

Fig. 5 Scanning electron microscopic photograph of *B. subtilis* supplemented MnO NPs

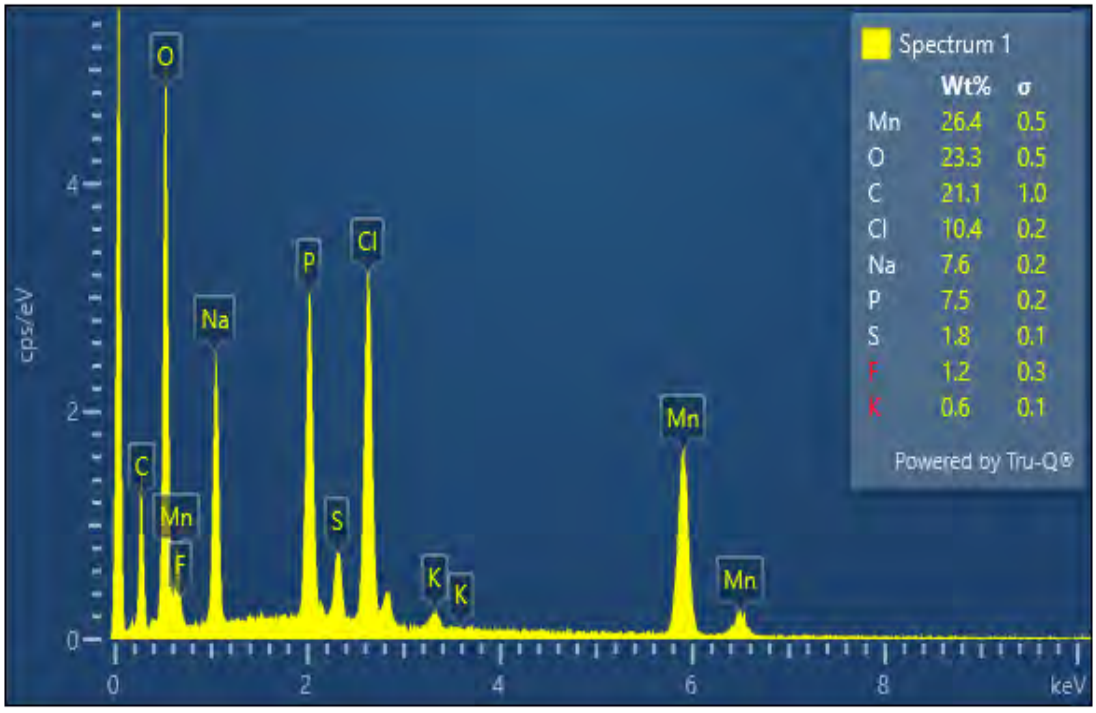

Fig. 5 EDX analysis of *B. subtilis* supplemented MnO NPs.

3.1.5 Fungal growth inhibition assay, *in vitro*

The growth of *A. niger* on PDA media containing MnO NPs was significantly lower than that of control (Fig 7). Even though all concentrations of MnO NPs exhibited mycelial growth inhibition, the greatest development inhibition (86.25%) was displayed by 2.5 mg/mL concentration of MnO NPs (Fig 8.).

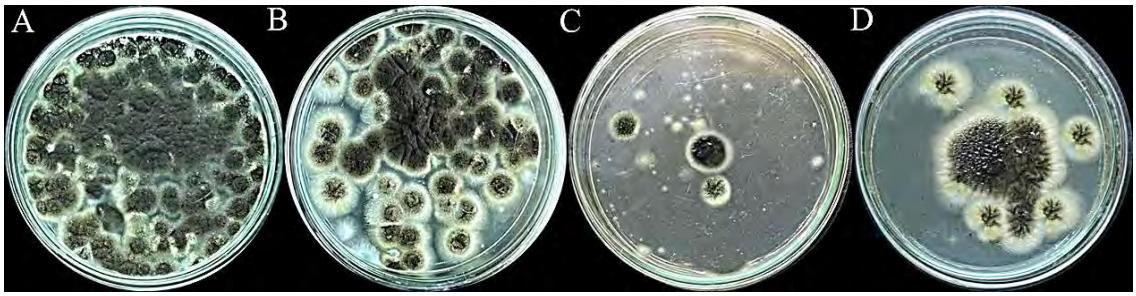

Fig. 6 Mycelial growth inhibition of *A. niger* in control (A), at 0.25 mg/mL concentration (B), at 2.5 mg/mL concentration (C), and at 5.0 mg/mL concentration of MnO NPs (D).

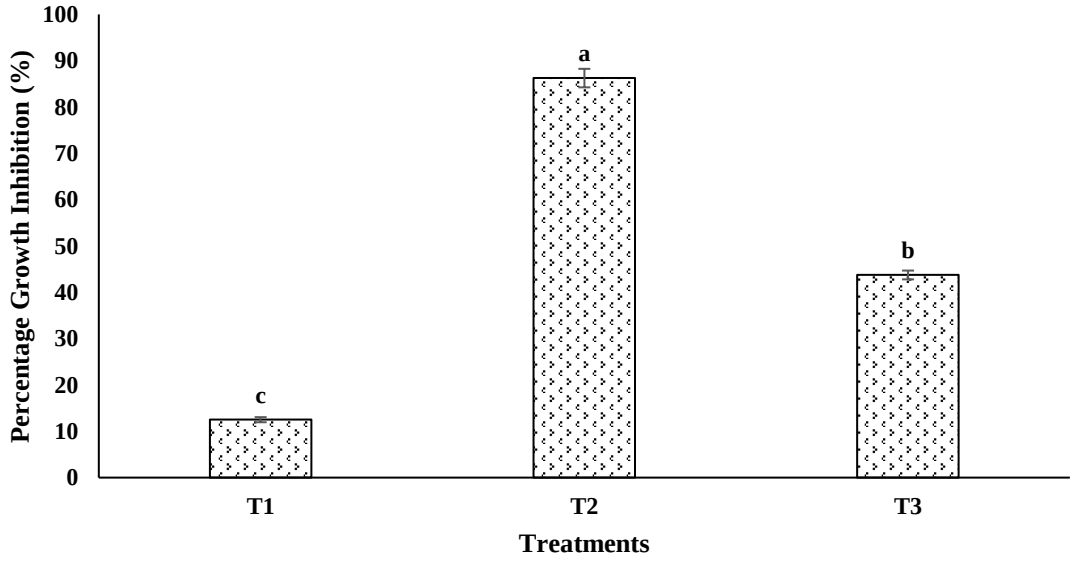

Fig. 7 Growth inhibition of *A. niger* at 0.25 mg/mL concentration (T1), 2.5 mg/mL concentration (T2), and 5.0 mg/mL concentration (T3) of MnO NPs. Capped bars above mean values represent ± SE of three replicates.

3.1.6 Disease control assay of MnO NPs

A variable effect of different treatments on the development of black rot disease was observed (Fig 9, Fig 10). MnO NPs significantly suppressed black rot disease, and the greatest control was displayed by 2.5 mg/mL concentration of MnO.

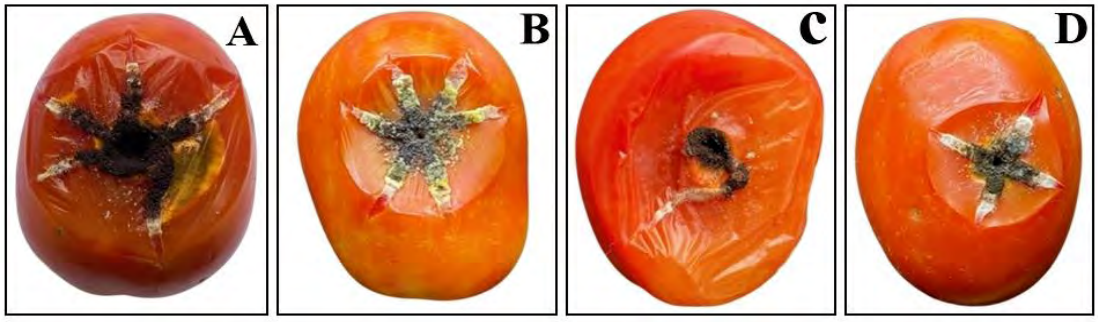

Fig. 8 Disease control assay in tomato fruit. Disease area was observed in control (A), and at different concentrations of MnO NPs including 0.25 mg/mL concentration (B), 2.5 mg/mL concentration (C), and 5.0 mg/mL concentration (D).

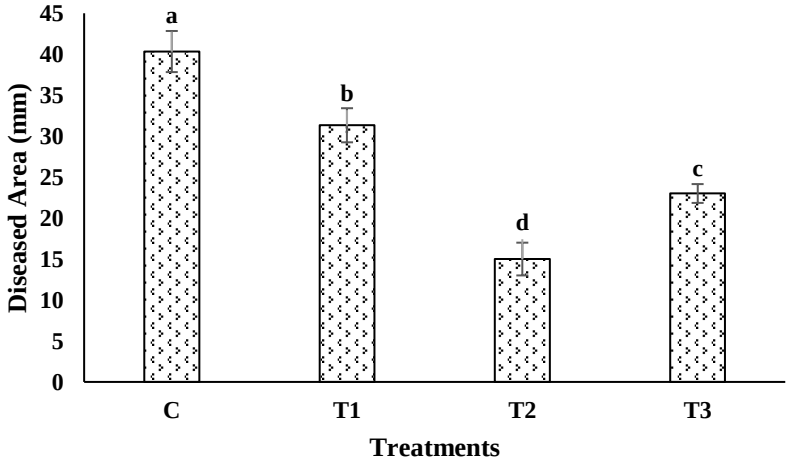

Fig. 9 Effect of different concentrations of MnO NPs on the development of black rot disease in tomato fruit. Control (C), 0.25 mg/mL concentration of MnO NPs (T1), 2.5 mg/mL concentration of MnO NPs (T2), 5.0 mg/mL concentration of MnO NPs (T3). Capped bars above mean values represent ± SE of three replicates.

3.1.7 Biochemical and organoleptic properties.

The quality of tomato fruit was significantly impacted by the fungal inoculation. Therapy of MnO NPs helped tomato fruit to preserve organoleptic and biochemical attributes and resist fruit decay under fungal stress conditions (Table 6). All MnO NPs treated fruit maintained high soluble solids and total sugars than diseased control fruit. The highest soluble solids and total sugar contents were maintained at 2.5 mg/mL concentration of MnO NPs. Diseased fruit also displayed less reducing sugar, ascorbic acid, and total sugar contents in un-treated control fruit. Discoveries of this study proved that the treatment of MnO NPs helps diseased fruit to conserve higher contents of these useful compounds. Fruits treated with MnO NPs were noticeably firmer than control fruits. Tomato fruit exposed to 2.5 mg/mL concentration of NPs had a harder texture than that of other treatments.

Table 6 Biochemical and organoleptic changes in diseased fruit.

Treatments	Soluble solids (%)	Total sugars (%)	Reducing sugars (%)	Ascorbic acid (µmol/ kg)	Firmness (%)
Control	6.0 ± 0.52	7.9 ± 0.9	2.1 ± 0.09	7.5 ± 1.1	14.7 ± 1.5
0.25 mg/ mL NPs	6.5 ± 0.77	8.7 ± 1.2	2.9 ± 0.02	8.1 ± 0.9	20.2 ± 2.1
2.5 mg/ mL NPs	8 ± 0.61	12.5 ± 0.7	4 ± 0.05	14 ± 1	30.5 ± 3.2
5.0 mg/ mL NPs	7.5 ± 0.67	9.8 ± 0.8	3.7 ± 0.01	10.2 ± 1.5	22.4 ± 1.8

Values are described as mean and ± denotes standard error. Dissimilar alphabets represent significantly different values from each other.

3.2 Results of Experiment 2

3.2.1 Characterization of MnO nanoparticles

3.2.1.1 FTIR analysis of synthesized MnO-NPs

FTIR exploration of MnO-NPs revealed characteristic peaks of different functional groups (Fig. 11, Table 7). Several functional groups and proteins immersed in stability and biosynthesis of NPs were identified. The spectrum of FTIR was brought in the range 500–4000 cm^{-1} under infrared radiation. Characteristic peak at 3384.72 cm^{-1}, specified the occurrence of alcohols and phenols (O-H stretch). Another significant peak at 1630.52 cm^{-1} (N–H bend) revealed the presence of 1° amines. Four other peaks at 602.98 cm^{-1}, 590.56 cm^{-1}, 578.87 $cm^{-1}$and 572.31 cm^{-1} indicated C–Cl stretch of alkyl halides, while peaks at 543.32 cm^{-1}, 534.95 cm^{-1}, 527.50 $cm^{-1}$and 517.12 cm^{-1} displayed C-Br stretch of alkyl halides.

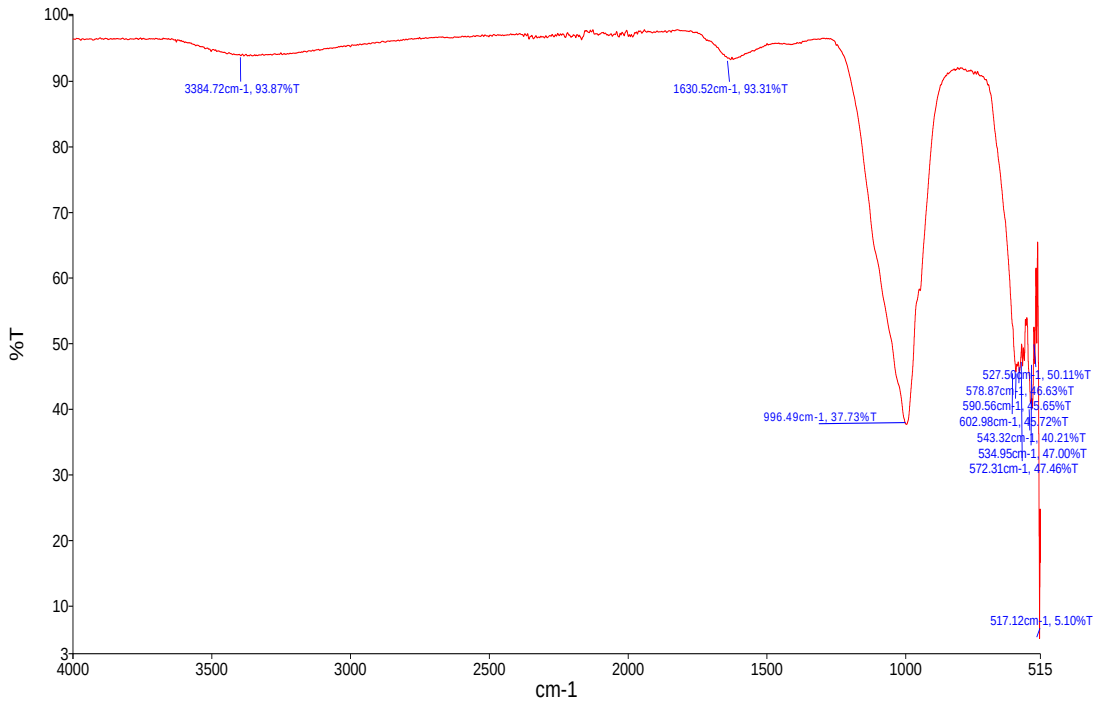

Fig. 10 FTIR spectra of MnO-NPs showing peaks at different wavelengths.

Table 7 FTIR analysis revealed characteristic peak numbers, functional groups, appearance and class of compound on MnO-NPs.

Sample No.	Sample Peak (cm^{-1})	Standard Table Absorption (cm^{-1})	Functional group	Bounding	Class Compound
1	3384.72	3500–3200 (s, b)	O-H	O–H stretch, H–bonded	alcohols, phenols
2	1630.52	1650–1580 (m)	N–H	N–H bend	1° amines
3	996.49	1000–650 (s)	=C–H	=C–H bend	Alkenes
4	602.98	850–550 (m)	C–Cl	C–Cl stretch	alkyl halides
5	590.56	850–550 (m)	C–Cl	C–Cl stretch	alkyl halides
6	578.87	850–550 (m)	C-Cl	C-Cl stretch	alkyl halides
7	572.31	850–550 (m)	C–Cl	C–Cl stretch	alkyl halides
8	543.32	690–515 (m)	C-Br	C-Br stretch	alkyl halides
9	534.95	690–515 (m)	C-Br	C-Br stretch	alkyl halides
10	527.50	690–515 (m)	C-Br	C-Br stretch	alkyl halides
11	517.12	690–515 (m)	C-Br	C-Br stretch	alkyl halides

3.2.1.2 X-ray Diffraction (XRD) analysis of synthesized MnO-NPs

XRD analysis explained visible peaks pattern of MnO-NPs at 8.68, 16.24, 32.17, 44.86, 61.08 and 82.24, which corresponded to peaks values (110), (200), (310), (521), (730) and (301), respectively (Fig. 2). Clear peaks, displayed by XRD spectra, were comparable to Orthorhombic space group, revealing magnetite manganese oxide (Fig 12). The patterns plane of XRD was in decent deal with JSCPD having number 01076-0958. The usual nanoparticle dimension was revealed as 22.2 nm (Table 8).

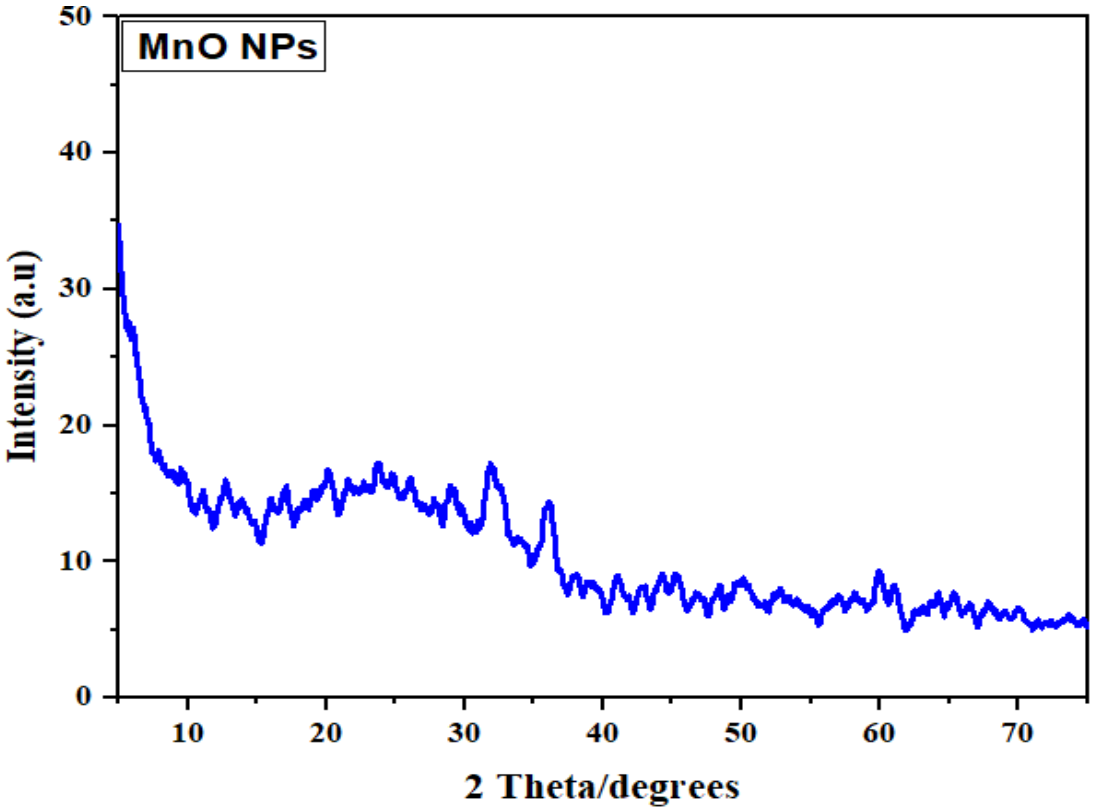

Fig. 11 XRD spectra of MnO-NPs showing peaks at different wavelengths.

Table 8 Size of MnO-NPs synthesized in *B. subtilis.*

Peak Number	2 Theta	FWHM	Crystallite size D (nm)	Average size (nm)
1	8.683	0.416	190.264	22.22319
2	16.241	2.297	34.212	
3	32.170	0.0689	1106.32	
4	61.028	92.138	0.7425	
5	82.275	223.589	0.2674	
6	44.8519	46.3216	12.5847	

3.2.1.3 Scanning electron microscopy and EDX analysis

The superficial morphology of MnO-NPs was learned by scanning electron microscopy which exhibited highly monodispersed flower-like nanostructure (Fig. 13). This nano-flower structure reflected large specific surface area. The elemental makeup of the prepared nanoparticle is displayed in Fig. 14. Manganese and oxygen peaks were detected, confirming the synthesis of MnO-NPs. EDX depicted high weight percentages of oxygen (36.91%) and manganese (38.27%) and low signals for C (20.97%), F (1.23%), Na (2.15%), Mg (0.07%), Al (0.15%), Si (0.11%) and Ca (0.14%).

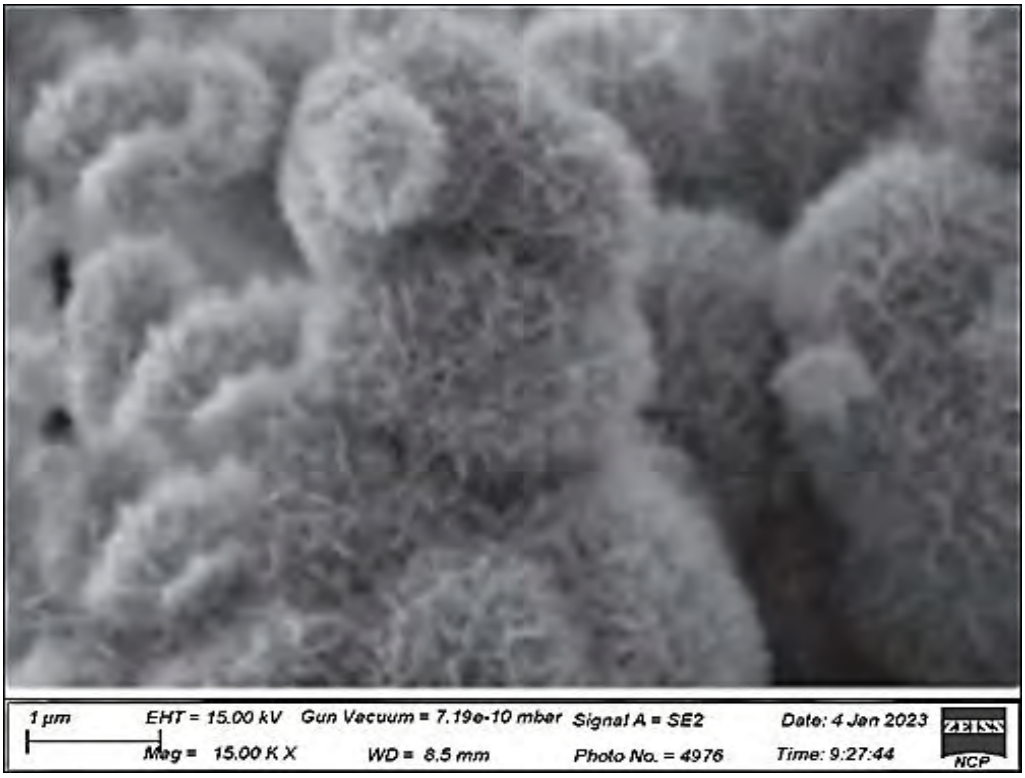

Fig. 12 Scanning electron microscopic photograph of MnO-NPs prepared in *B. subtilis*.

3.2.3. Growth attributes of tomato seedlings

A remarkable decrease in development attributes of tomato seedlings was monitored under Pb stress. Different concentrations of MnO-NPs variably influenced root and shoot lengths (Figure 15 A), and fresh and also dry weights of tomato seedlings (Figure 15 B), in answer to different treatments of MnO-NPs. Interestingly, medium concentration of MnO-NPs (2.5 mg/ ml) performed best under Pb stress conditions.

3.2.3.1. Measurement of osmolytes

Proline and sugar contents were significantly enhanced in the leaves of nano-primed and lead-stressed seedlings of tomato, as compared to control. Various concentrations of MnO-NPs influenced the level of osmolytes in lead-alone treatment. The greatest increase in proline (69%) and sugar content (36%) was observed upon nano-priming with 2.5 mg/ ml concentration of MnO-NPs (Fig. 16).

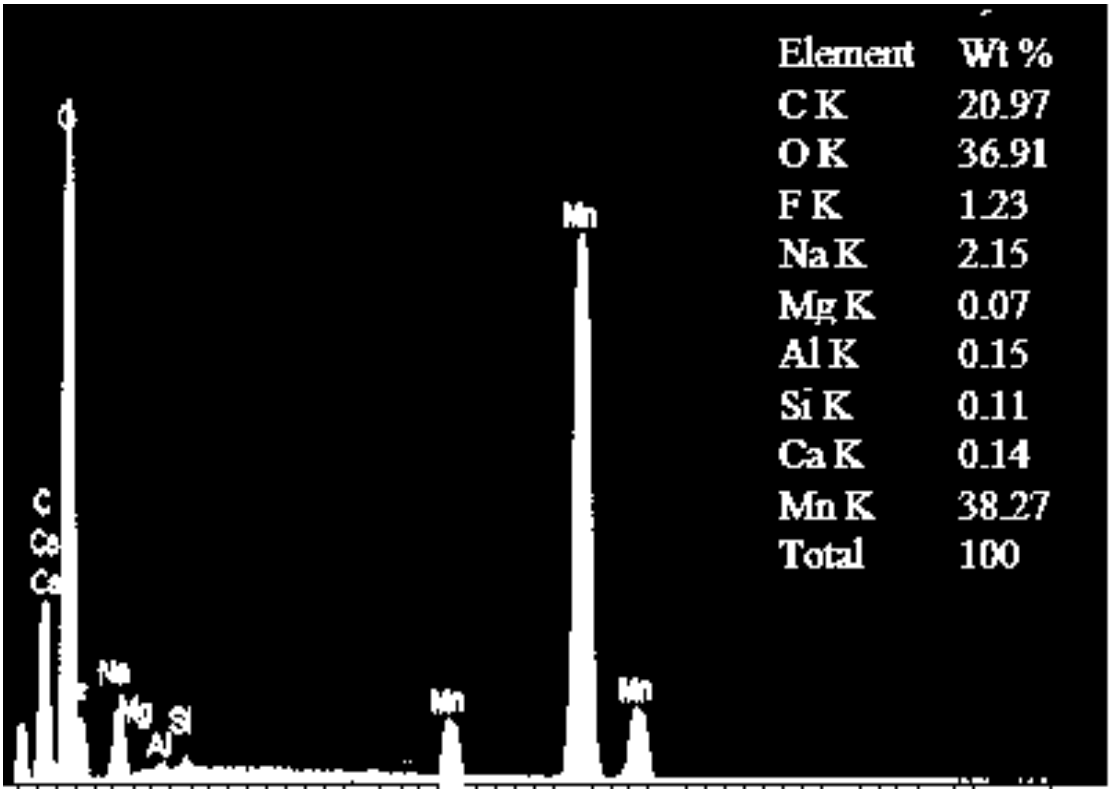

Fig. 13 EDX analysis of MnO-NPs prepared in in *B. subtilis*.

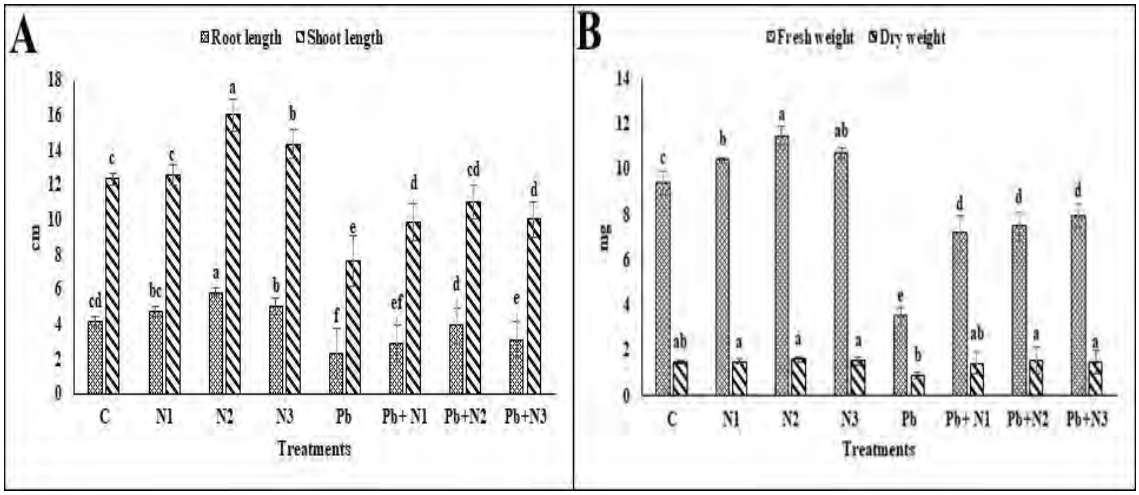

Fig. 14 Influence of seed nano-priming on growth attributes of tomato seedlings, grown in control and lead stressed conditions. The bars with caps above them indicate the standard error (SE) of means. Altered letters indicate significant variation in means.

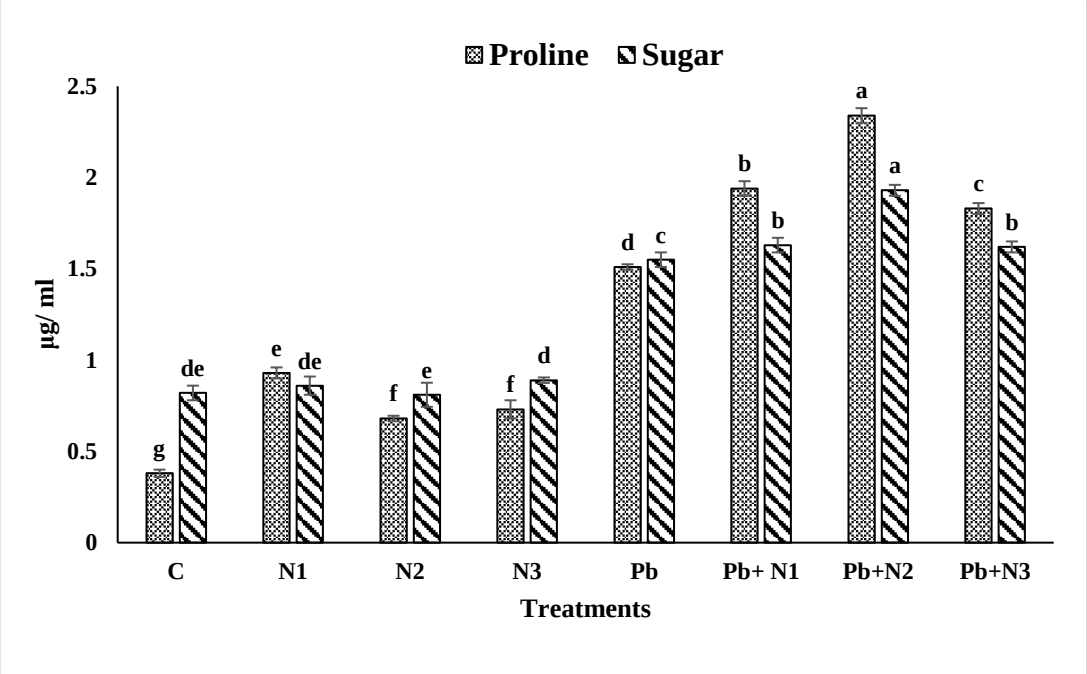

Fig. 15 Effect of seed nano-priming on proline and sugar content of tomato seedlings, grown in control and lead-stressed conditions. The bars with caps above them indicate the standard error (SE) of means. Altered letters indicate significant variation in means.

3.2.3.2.Measurement of physiological traits of plants

Different concentrations of MnO-NPs increased photosynthetic pigments (chlorophyll and also carotenoid) in the seedlings of both control and plants having stress of Pb. In contrast to control seedlings, the presence of Pb lowered the concentrations of chlorophyll and the carotenoid. Though, the nono-priming of MnO-NPs proved effective in mitigating Pb toxicity by maintaining higher levels of chlorophyll and carotenoid. Notably, the highest concentrations of chlorophyll and carotenoid were monitored in plants treated with 2.5 mg/ml concentration of MnO-NPs (Fig. 17).

Leaf RWC was considerably manipulated by MnO-NPs treatments and lead stress conditions. All MnO-NPs treatments increased RWC in tomato seedling under normal as well as Pb stress conditions. Among all treatments of MnO-NPs, the maximum RWC were observed at 2.5 mg/ ml concentration of MnO-NPs (Fig. 8)

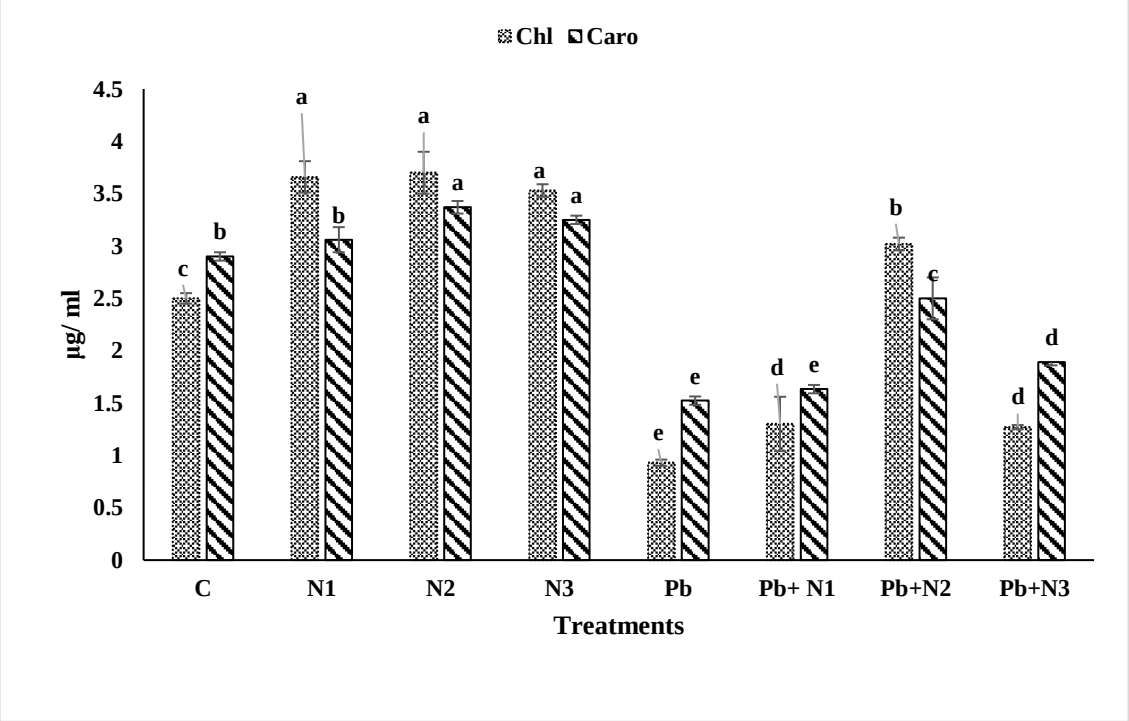

Fig. 16 Effect of seed nano-priming on photosynthetic contents of tomato seedlings, grown in control and lead stressed conditions. The bars with caps above them indicate the standard error (SE) of means. Different letters indicate significant variation in means.

3.2.4. Determination of oxidative stress biomarkers

Seed priming with MnO-NPs significantly impacted the relative electrolytic leakage (REL) in the leaves of tomato seedlings. The above average value for REL was detected in the plants under lead stress, while the minimal value of REL was discovered under the impact of the seed priming with different doses of NPs. The least REL was observed in the plants primed with 2.5 mg/ml concentration of MnO-NPs (Fig. 18).

Current findings revealed that MDA and H_2O_2 insides were enhanced in leaves of lead stressed plants, as related to control (C). Under Pb stress, the MDA contents in leaves were decreased in MnO-NPs treated plants. Variable decrease was observed in MDA content of plants dried with altered concentration of NPs and the maximum decrease in MDA and H_2O_2 content was detected in plants treated with 2.5 mg/ ml concentration of MnO-NPs (Fig. 19).

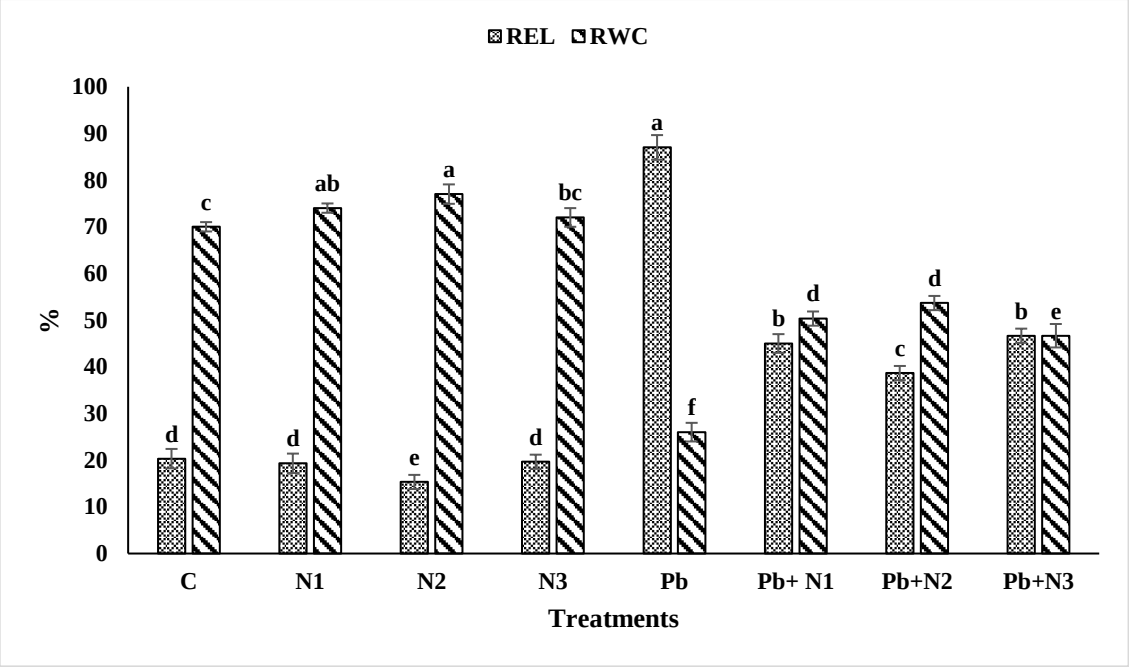

Fig. 17 Consequence of seed nano-priming on relative water content and relative electrolytic leakage of tomato seedlings, grown in control and lead stressed conditions. The bars with caps above them show the standard error (SE) of means. Distinct letters show significant variation in means.

3.2.5. Antioxidant enzymes activities

The presence of lead (Pb) elevated the activities of superoxide dismutase (SOD) and peroxidase (POD) enzymes in tomato seedlings. Notably, the priming of seeds with MnO-NPs further boosted these enzyme activities, with the highest levels of antioxidant enzyme activity recorded in plants treated with a concentration of 2.5 mg/mL of MnO-NPs (Fig. 20)

3.2.6. Pb measurements in plant tissues

Different treatments of NPs decreased the addition of Pb in the roots and leaves of tomato seedlings (Fig. 21). These results indicated the importance of the seed priming of tomato seeds with MnO-NPs. Roots stored more Pb in roots than shoots. Least accumulation of Pb was observed in plants treated 2.5 mg/ ml concentration of MnO-NPs.

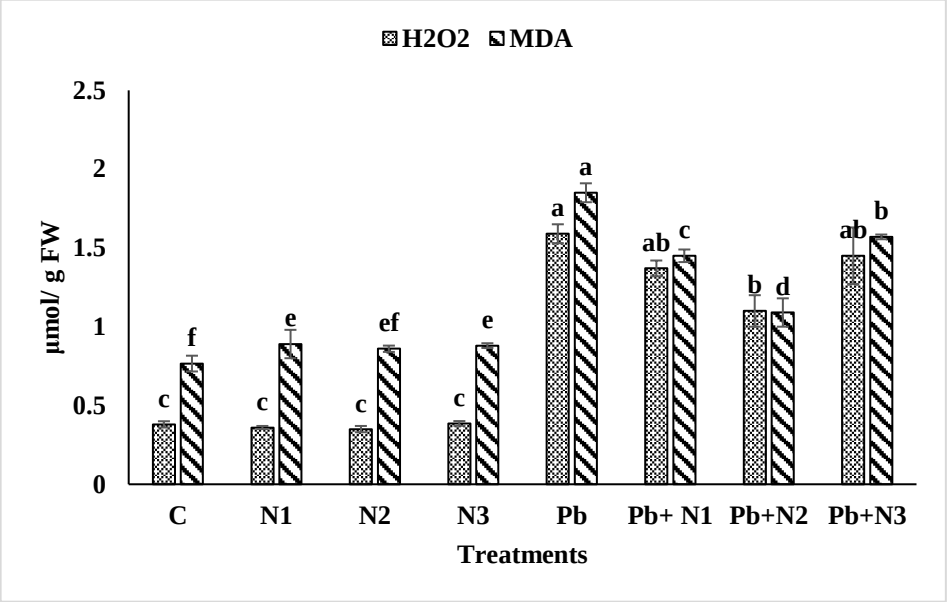

Fig. 18 Outcome of seed nano-priming on MDA and H_2O_2 content of tomato seedlings, grown in control and lead stressed conditions. The bars with caps above them indicate the standard error (SE) of means. Different characters indicate significant variation in means.

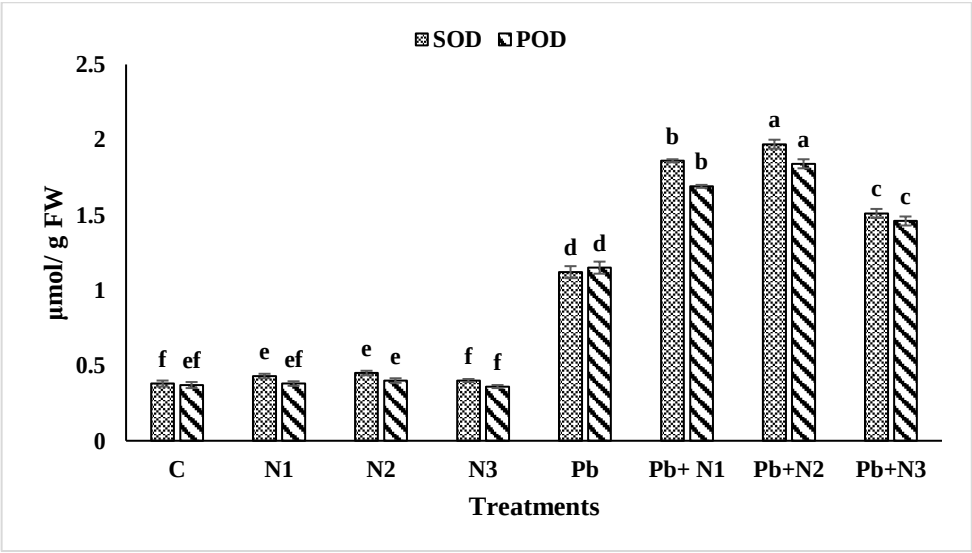

Fig. 19 Effect of seed nano-priming on antioxidant activities of tomato seedlings, grown in control and lead stressed conditions. The bars with caps above them indicate the standard error (SE) of means. Different letters indicate significant variation in means.

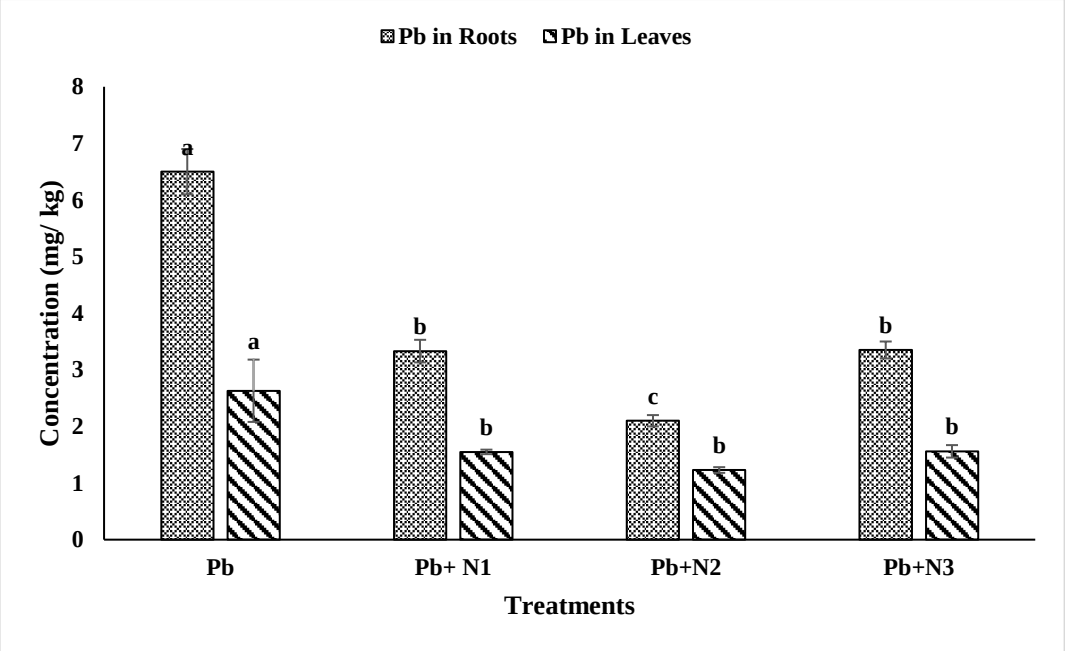

Fig. 20 Effect of seed nano-priming on roots and leaves of tomato seedlings, grown in control and lead stressed conditions. The bars with caps above them indicate the standard error (SE) of means. Different letters indicate significant variation in means.

3.2.7. Principal component analysis and correlation matrix

Principal component analysis (PCA) analyzed the relationship between various attributes in tomato plants, subjected to Pb stress and different concentrations of MnO-NPs (Fig. 22). In PCA, two dimensions (Dim-1 and Dim-2) collectively accounted for approximately 97.4% of the inconsistency in the dataset with 0.6 (r2) value. Dim-1 contributed 88.9% of the total variation, while Dim-2 accounted for 8.5%. Notably, all treatments exhibited distinct and evident impact patterns on tomato seedlings. Specifically, MDA, REL, sugar, H_2O_2, proline, and Pb played a significant role in shaping Dim-1, while other plant traits were more closely associated with Dim-2. To validate the findings of PCA-biplot, a correlation matrix was constructed (Fig. 23). In the correlation matrices, dark red color bars represented strong negative correlations, while dark blue color bars indicated strong positive correlations. The Pearson's correlation matrix showed a compelling positive correlation linking REL, proline, sugar, H_2O_2, MDA and Pb contents. Simultaneously, they showed a robust adverse correlation with growth attributes of plants, photosynthetic attributes and antioxidant enzymatic assay.

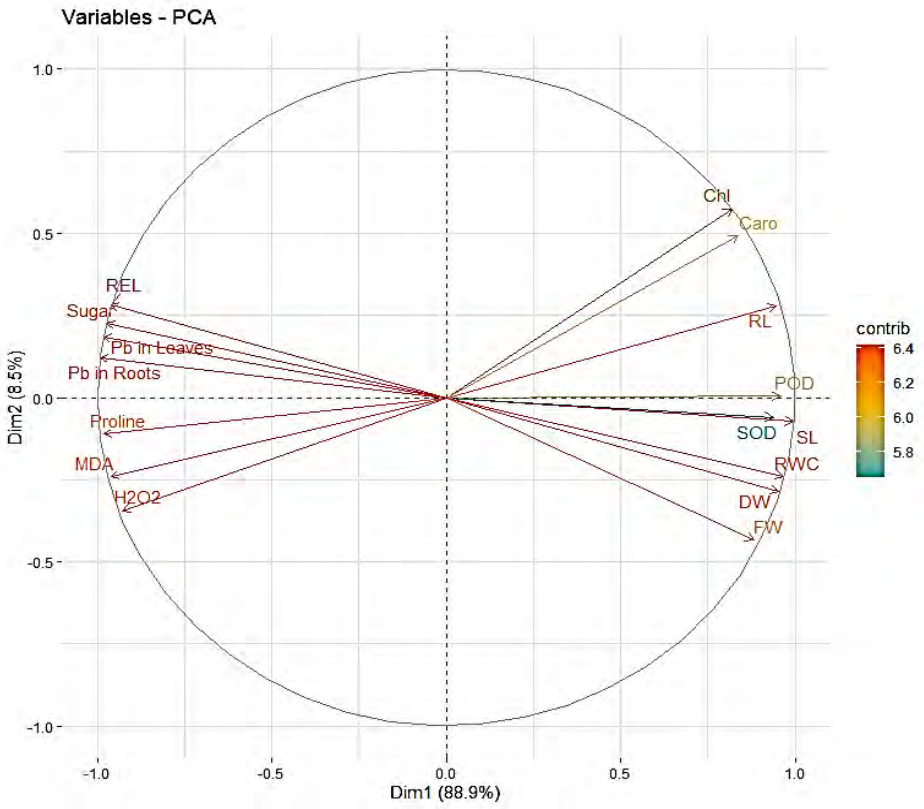

Fig. 21 Principal component analysis expressed the relationship between different studied attributes. Root length (RL); shoot length (SL); fresh weight (FW); dry weight (DW); chlorophyll (Chl); carotenoid (Caro); relative water content (RWC); relative electrolytic leakage (REL); malondialdehyde (MDA); superoxide dismutase (SOD); peroxidase (POD); hydrogen peroxide (H_2O_2).

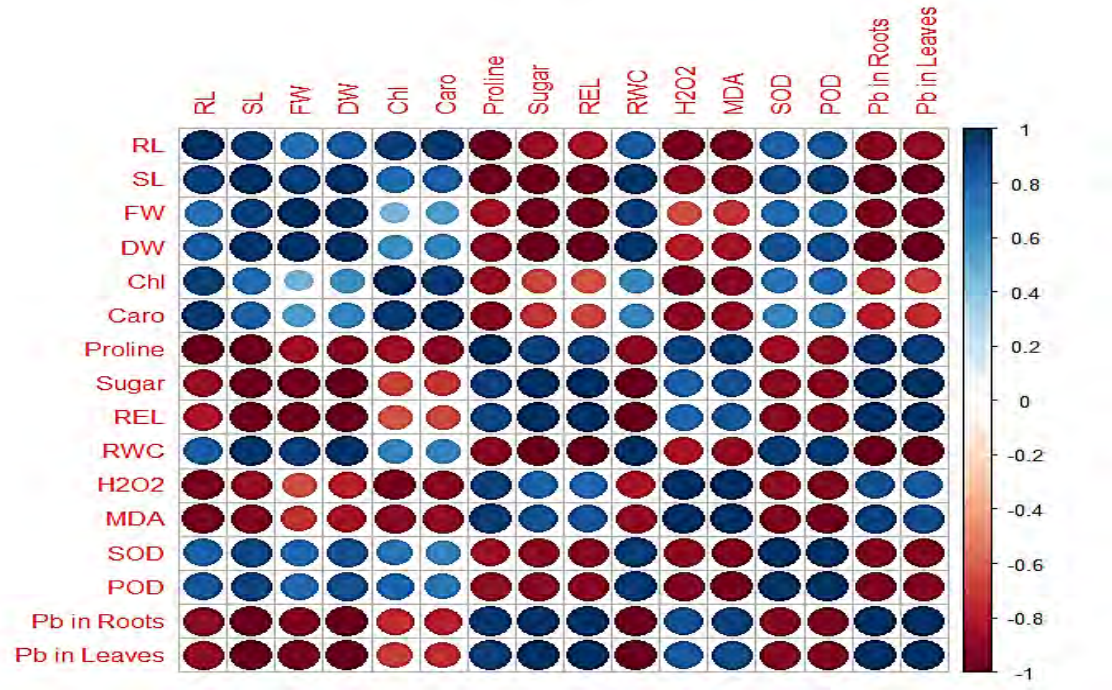

Fig. 22 An analysis of Pearson's correlation was conducted to assess the relationship between various physiological, antioxidant, and biochemical parameters in tomato seedlings subjected to lead (Pb) stress after being treated with manganese oxide nanoparticles (MnO-NPs). The parameters evaluated included root length (RL), shoot length (SL), fresh weight (FW), dry weight (DW), chlorophyll content (Chl), carotenoid levels (Caro), relative water content (RWC), relative electrolyte leakage (REL), malondialdehyde (MDA) concentration, superoxide dismutase (SOD) activity, peroxidase (POD) activity, and hydrogen peroxide (H2O2) levels.

3.2.8. Gene expression analysis of stress related enzymes

Gene expression studies revealed higher expression of chlorophyllase under metal stress environment, indicating the catalysis of chlorophyl to chlorophyllide (Heaton et al. 1996). Application of MnO-NPs reduced the expression of the gene, accountable for the assembly of chlorophyllase and rescued tomato seedlings from stress conditions (Fig. 24A). Expression profiling of chalcone synthase and phenylalanine ammonia lyase genes indicated increased production of these enzymes under stress conditions. Application of MnO-NPs further enriched the appearance of both chalcone synthase (Fig. 24B) and phenylalanine ammonia lyase (Fig. 24C) genes under Pb stress conditions. Chalcone synthase is a basic enzyme of flavonoid biosynthesis pathway. This

enzyme has been reported to be produced under biotic and abiotic stress conditions and it also plays role in salicylic acid defense pathway (Dao et al. 2011). Phenylalanine ammonia lyase is a famous protective plant enzyme that converts L-phenylalanine to the precursors of major defense-related compounds like lignin, flavonoids, and coumarins, under stress conditions (Schuster and Retey 1995). Production of these two enzymes indicates the positive influence of MnO-NPs on tomato.

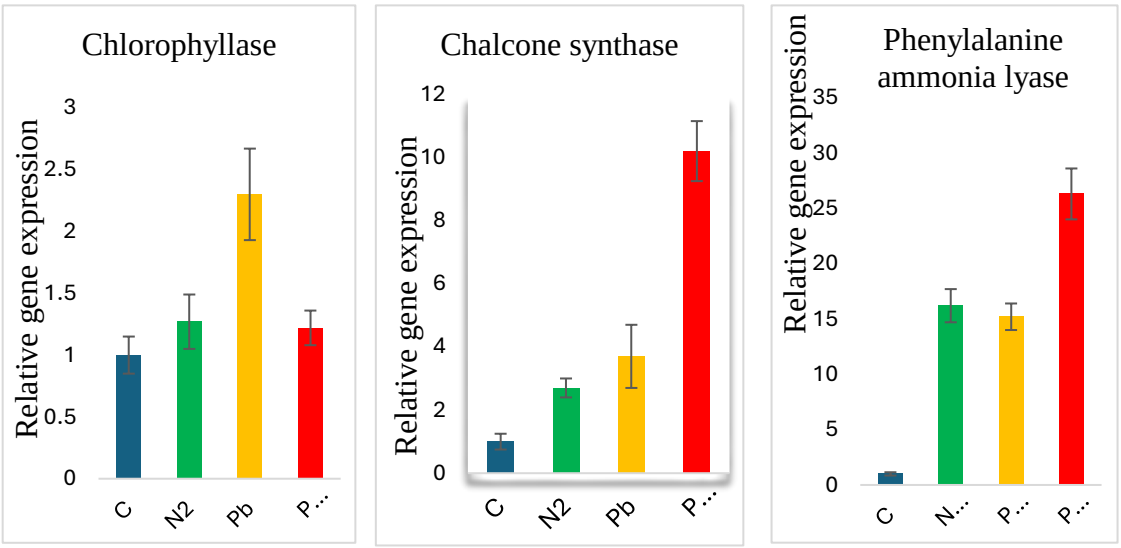

Fig. 23 Effect of seed priming on the appearance of chlorophyllase, chalcone synthase and phenylalanine ammonia lyase in tomato seedling after three weeks of sowing. C = un-primed seeds sown in control soil, N2 = seeds primed with 2.5 mg/ ml concentration of MnO-NPs and sown in control soil, Pb = Un-primed seeds sown in metal stressed soil, Pb+N2 = seeds primed with 2.5 mg/ ml concentration of MnO-NPs and sown in metal stressed soil.

3.3. Results of Experiment 3

3.3.3. Characterization of MnO NPs

The following parameters assisted to demonstrate the successful synthesis of MnO NPs:

3.3.3.1. FTIR analysis

FTIR investigation of MnO NPs revealed characteristic peaks of different functional groups, accountable for the stability and biosynthesis of synthesized MnO NPs (Fig. 25). The spectrum of FTIR was brought in the scope of 500–4000 cm^{-1} under infrared radiation. Characteristic peaks at 3190.60 cm^{-1} (O–H stretch) and 1632.29 (C=O stretch) specified the presence of carboxylic acids while other significant peaks at 1082.91 cm^{-1} (C–O stretch), and 1017.08 cm^{-1} (C–O stretch) revealed the occurrence of alcohols, carboxylic acids, esters, ethers. Peak at 810.10 cm^{-1} (=C–H bend) showed the presence of alkenes. Five other peaks at 646.43 cm^{-1}, 625.89 cm^{-1}, 603.07 cm^{-1}, 579.69 cm^{-1} and 564.17 cm^{-1} indicated C–Cl stretch of alkyl halides, while peaks at 544.45 cm^{-1}, 530.67 cm^{-1}, 523.05 cm^{-1}, and 518.11 cm^{-1} displayed C–Br stretch of alkyl halides (Table 9).

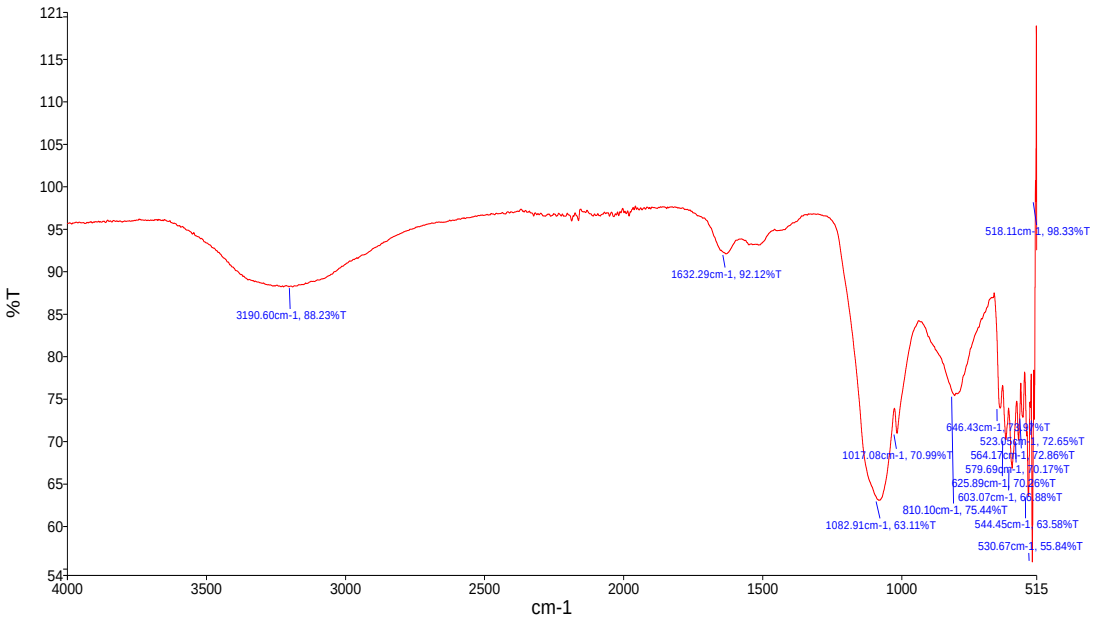

Fig. 24 FTIR spectra of MnO NPs showing peaks at different wavelengths.

Table 9 FTIR analysis with characteristic peak numbers, functional groups, appearance and class of compound on MnO NPs

Sample No	Sample Peak	Standard Table Absorption (cm-1)	Functional group	Bounding	Class Compound
1	3190.60 cm-1	3300–2500 (m)	O-H	O–H stretch	carboxylic acids
2	1632.29 cm-1	1760–1690 (s)	C=O	C=O stretch	carboxylic acids
3	1082.91 cm-1	1320–1000 (s)	C–O	C–O stretch	alcohols, carboxylic acids, esters, ethers
4	1017.08 cm-1	1320–1000 (s)	C–O	C–O stretch	alcohols, carboxylic acids, esters, ethers
5	810.10 cm-1	1000–650 (s)	=C–H	=C–H bend	Alkenes
6	646.43 cm-1	850–550 (m)	C-Cl	C-Cl stretch	alkyl halides
7	625.89 cm-1	850–550 (m)	C–Cl	C–Cl stretch	alkyl halides
8	603.07 cm-1	850–550 (m)	C-Cl	C-Cl stretch	alkyl halides
9	579.69 cm-1	850–550 (m)	C-Cl	C-Cl stretch	alkyl halides
10	564.17 cm-1	850–550 (m)	C-Cl	C-Cl stretch	alkyl halides
11	544.45 cm-1	690–515 (m)	C–Br	C–Br stretch	alkyl halides
12	530.67 cm-1	690–515 (m)	C–Br	C–Br stretch	alkyl halides
13	523.05 cm-1	690–515 (m)	C–Br	C–Br stretch	alkyl halides
14	518.11 cm-1	690–515 (m)	C–Br	C–Br stretch	alkyl halides

3.3.3.2.XRD analysis

XRD analysis described noticeable peaks pattern of MnO NPs at 8.68, 16.24, 32.17, 44.86, 61.08 and 82.24, which corresponded to peaks values (110), (200), (310), (521), (730) and (301), respectively (Fig. 26). Clear peaks, displayed by XRD spectra,

were comparable to Orthorhombic space group, revealing magnetite manganese oxide patterns plane of XRD. It was in decent agreement with JSCPD number 01076–0958. The usual nanoparticle size was determined as 22.2 nm (Table10).

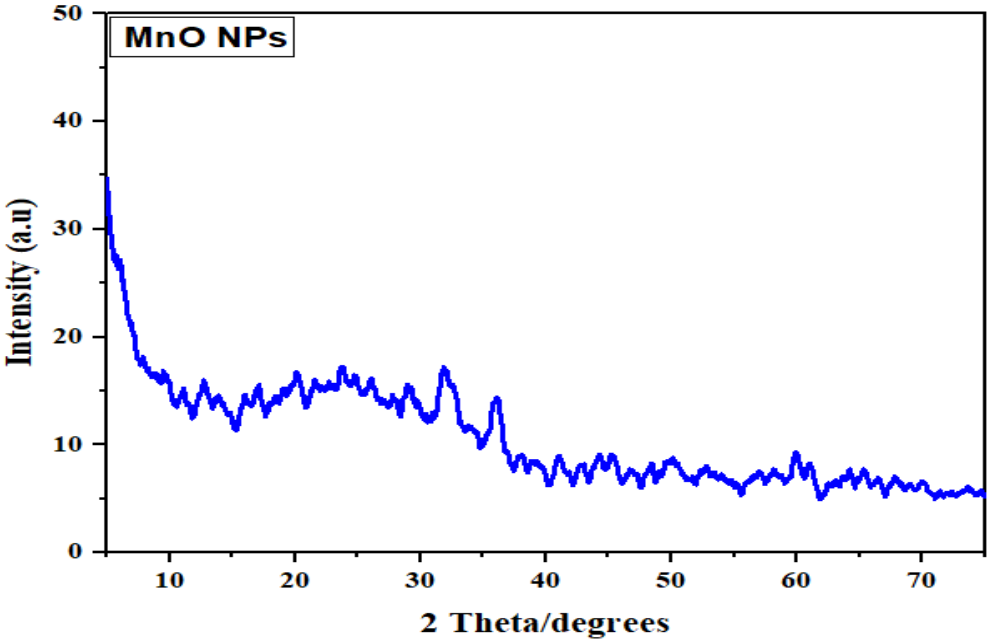

Fig. 25 XRD spectra of MnO NPs showing peaks at different wavelengths.

Table 10 Size of MnO NPs synthesized in *B. subtilis*.

Peak Number	2 Theta	FWHM	Crystallite size D (nm)	Average size (nm)
1	8.683	0.416	190.264	22.22319
2	16.241	2.297	34.212	
3	32.170	0.0689	1106.32	
4	61.028	92.138	0.7425	
5	82.275	223.589	0.2674	
6	44.8519	46.3216	12.5847	

3.3.4. SEM and EDX analysis

Surface of MnO NPs was successfully observed by scanning electron microscope (Fig 27). The uniform spreading of grains was monitored in micrographs. The grains were nearly spherical in appearance with uniform size. EDX analysis uncovered the elemental makeup of MnO NPs. Oxygen (23.3%) and manganese (26.4%) were the most rich elements. Sharp manganese and oxygen peaks proved the synthesis of MnO NPs, in the studied materials (Fig 28).

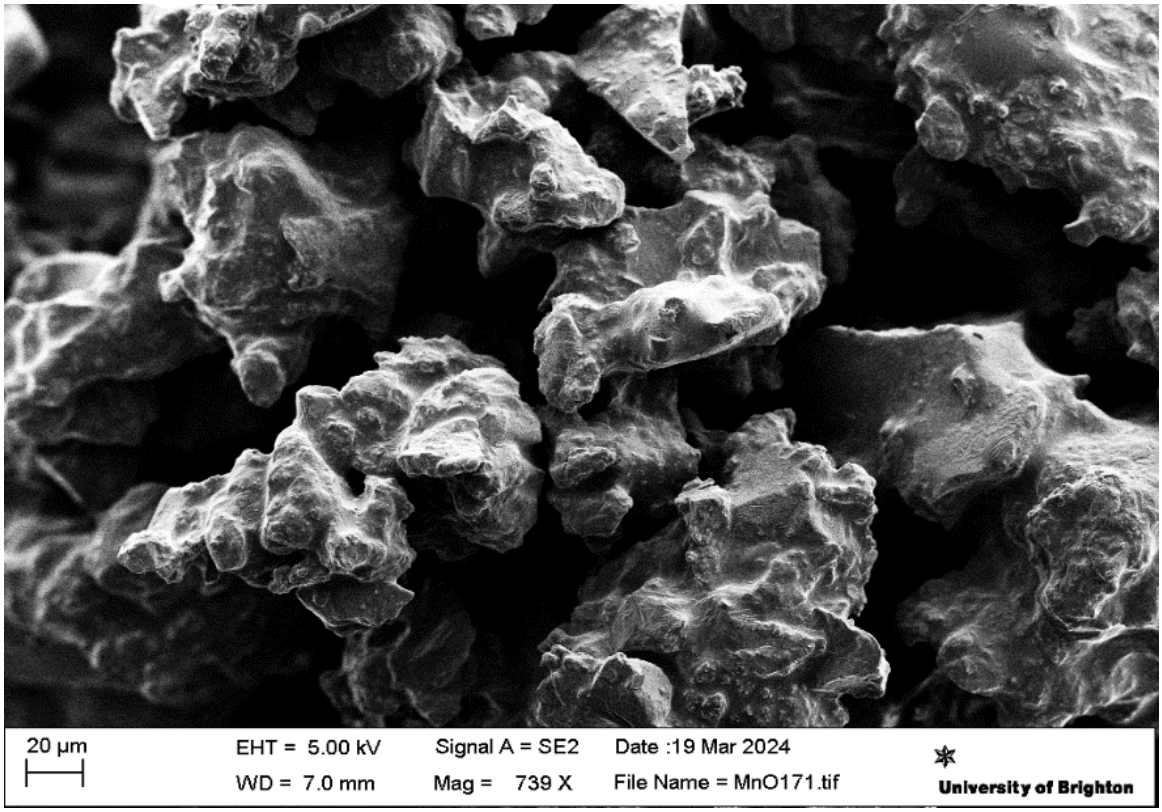

Fig. 26 Scanning electron microscopic photograph of MnO NPs prepared in *B. subtilis*

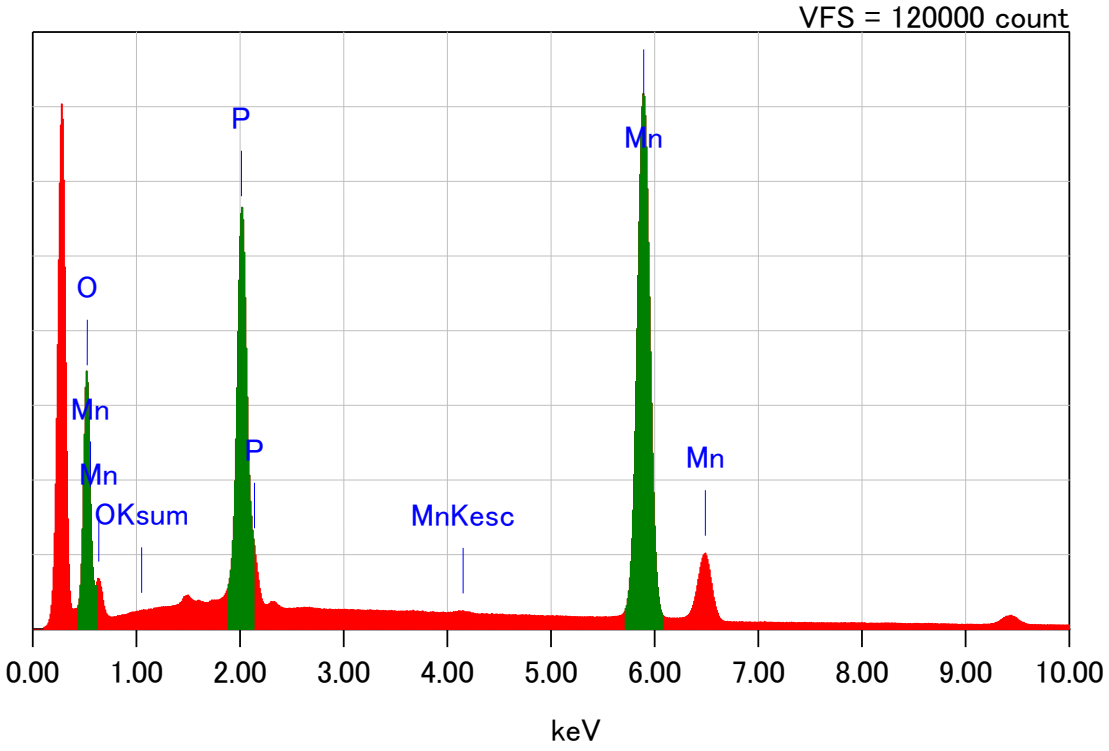

Fig. 27 EDX analysis of MnO NPs prepared in in *B. subtilis*

3.3.2 Growth inhibition assay, *in vitro*

The expansion of *F. oxysporum* on PDA media containing MnO NPs was significantly lower than that of control (Figure 29). While all dilutions of MnO NPs exhibited mycelial growth inhibition, the greatest growth inhibition (86.25%) was displayed by 2.5 mg/mL concentration of MnO NPs (Figure 30).

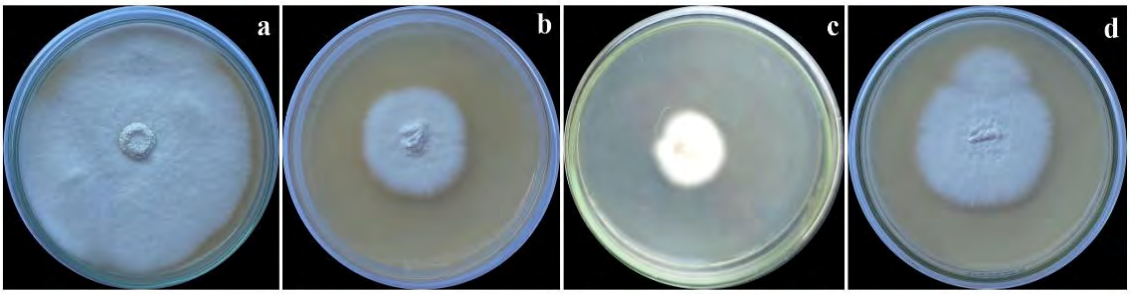

Fig. 28 Mycelial growth reduction of *F. oxysporum* in control (a), at 0.5 mg/mL concentration (b), at 2.5 mg/mL concentration (c), and 5 mg/mL concentration of MnO NPs (d).

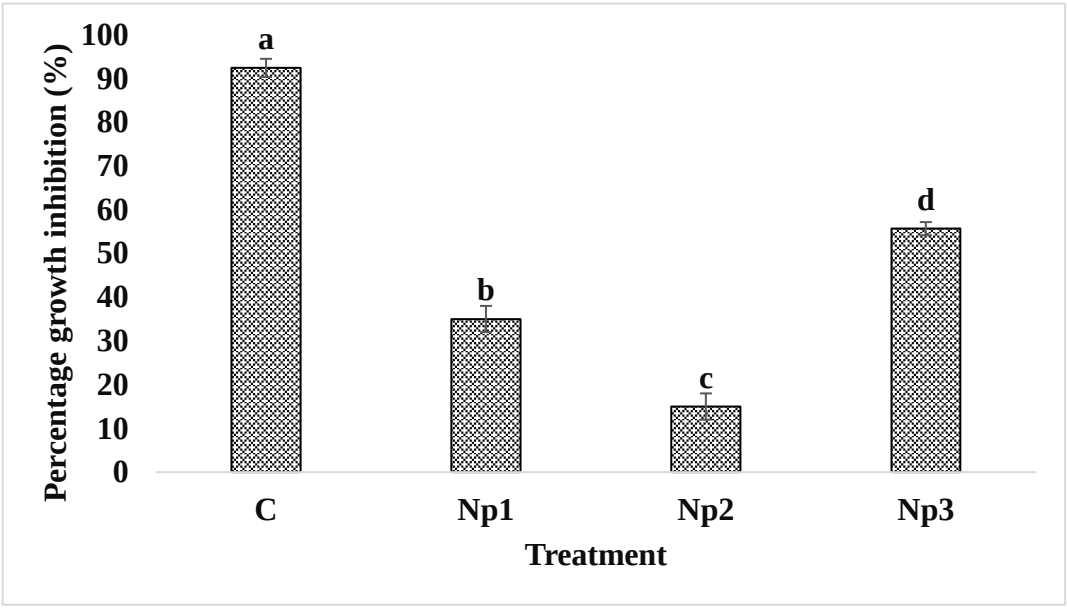

Fig. 29 Mycelial growth inhibition (%) of *F. oxysporum* under the influence of different concentrations of MnO NPs. The bars with caps above them indicate the standard error (SE) of means. Different letters indicate significant variation in means.

3.4. Seed Germination Percentage

Under both normal and pathogen stress conditions, seeds treated with nanoparticles and Bactria used for nanoparticles synthesis enhanced seeds germination (Fig. 31). Treatment NPs displayed the highest germination rate (88%), followed by B treatment (79%). The germination percentages of 64% was observed in F+NP treatment. Variable seed germination percentage was observed in other treatments like Mn salt treatment (57%), F+B (52%) and F+Mn (42%), which were significantly higher than F (*Fusarium*) treatment (32%).

3.3.2 Disease Severity Assay

Infection and disease symptoms were observed in all germinated plants inoculated with *F. oxysporum* (Fig.33). Control plants and plants of treatments Mn, B and NPs did not display wilting symptoms due to the absence of fungal inoculum. *Fusarium* inoculated plants showed severe infection, however plants of F+Mn, F+B and F+NPs treatments exhibited mild wilting.

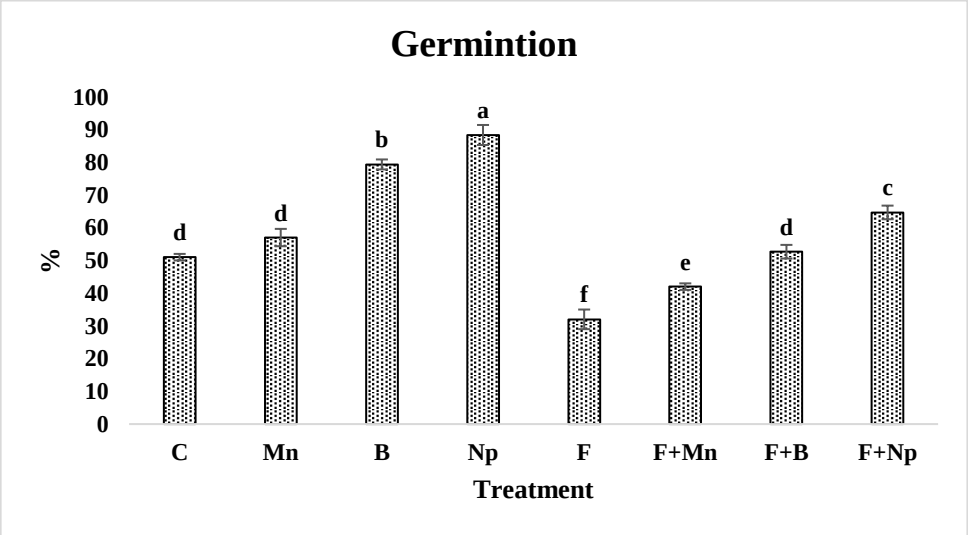

Fig. 30 Germination (%) of tomato seeds under various conditions. Control (C), Mn salt treated plants (Mn), *B. subtilis* primed seeds (B), MnO NPs primed seed (NPs), Seeds sown in *F. oxysporum* contaminated soil (F), Mn salt treated seeds sown in *F. oxysporum* contaminated soil (F+Mn), *B. subtilis* primed seeds sown in soil contaminated with *F. oxysporum* (F+B), MnO NPs primed seeds sown in soil contaminated with *F. oxysporum* (F+NPs).

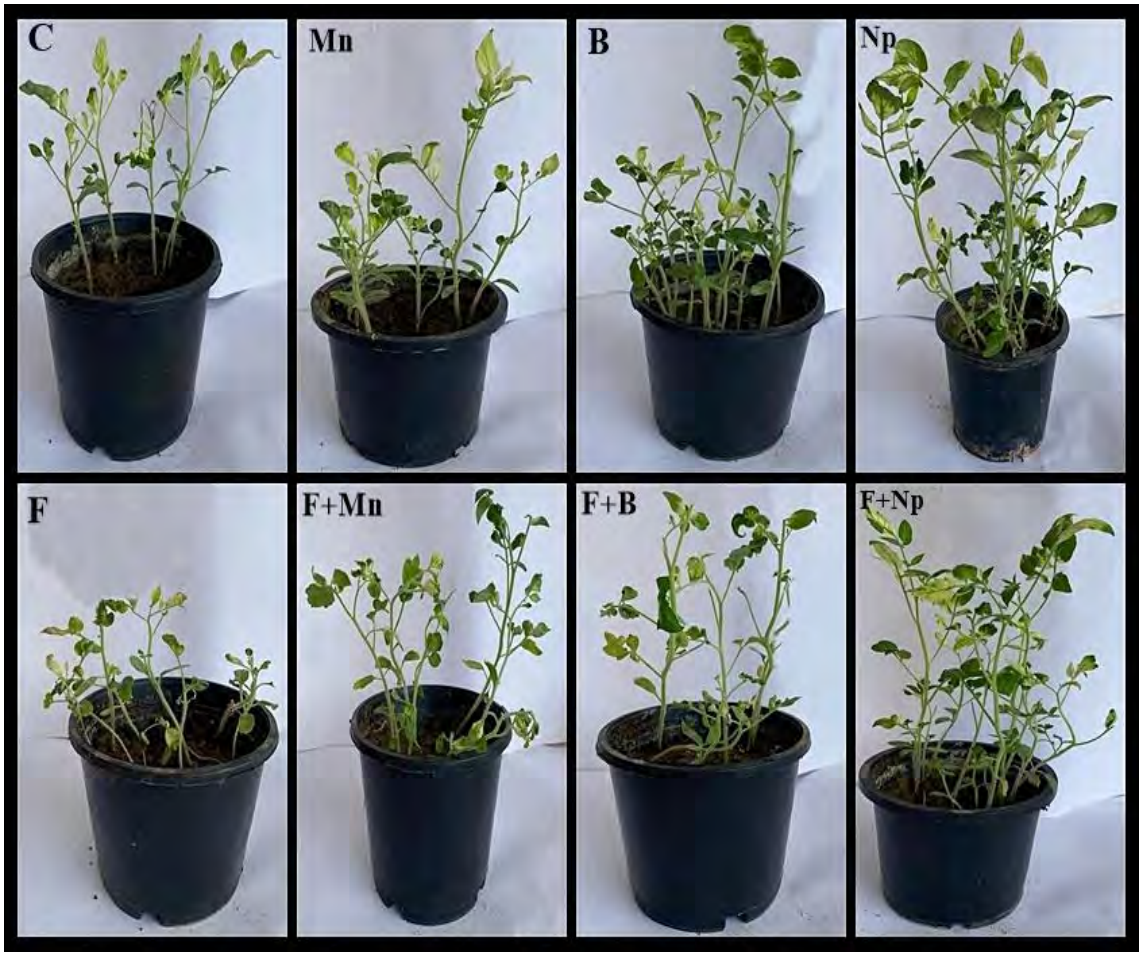

Fig. 31 Assessment of germination after 3 weeks of sowing. Control (C), Mn salt treated soil (Mn), *B. subtilis* primed seeds (B), Mn NPs primed seed (NPs) Seeds sown in *F. oxysporum* contaminated soil (F), seeds sown in *F. oxysporum* contaminated soil with Mn salt treatment (F+Mn), seeds sown in soil contaminated with *F. oxysporum* and *B. subtilis* primed seeds (F+B), seeds sown in soil contaminated with *F. oxysporum* and Mn NPs primed seeds (F+NPs).

Fig. 32 Visual determination of wilting and yellowing. Control (C), Mn salt treated plants (Mn), *B. subtilis* primed seeds (B), MnO NPs primed seed (NPs), Seeds sown in *F. oxysporum* contaminated soil (F), Mn salt treated seeds sown in *F. oxysporum* contaminated soil (F+Mn), *B. subtilis* primed seeds sown in soil contaminated with *F. oxysporum* (F+B), MnO NPs primed seeds sown in soil contaminated with *F. oxysporum* (F+NPs).

3.3.3. Histopathological appraisement

Histopathological study revealed severe damage of root and shoot tissues by the application of *F. oxysporum*. Contrarily, the application of bacterial synthesized MnO NPs and beneficial biocontrol microbe (*B. subtilis)* rescued the vascular system of plants (Fig. 10). In crosswise sectioning of tomato shoots and roots, drastic tissue demolition,

dark necrotic regions, disrupted pith and vascular tissue components could be observed in FC treatment (Figure 34). On the other hand, intactly organized parenchymatous cortical tissue components and vascular components could be observed in B treatment, NPs treatment, and salt treatment. Plants with combined treatments of biotic stress with salt application (F+Mn), beneficial microbe (F+B) and nanoparticles treatment (F+NPs) displayed mild disease symptoms and showed better vascular components than solely *Fusarium* infected plants (F treatment).

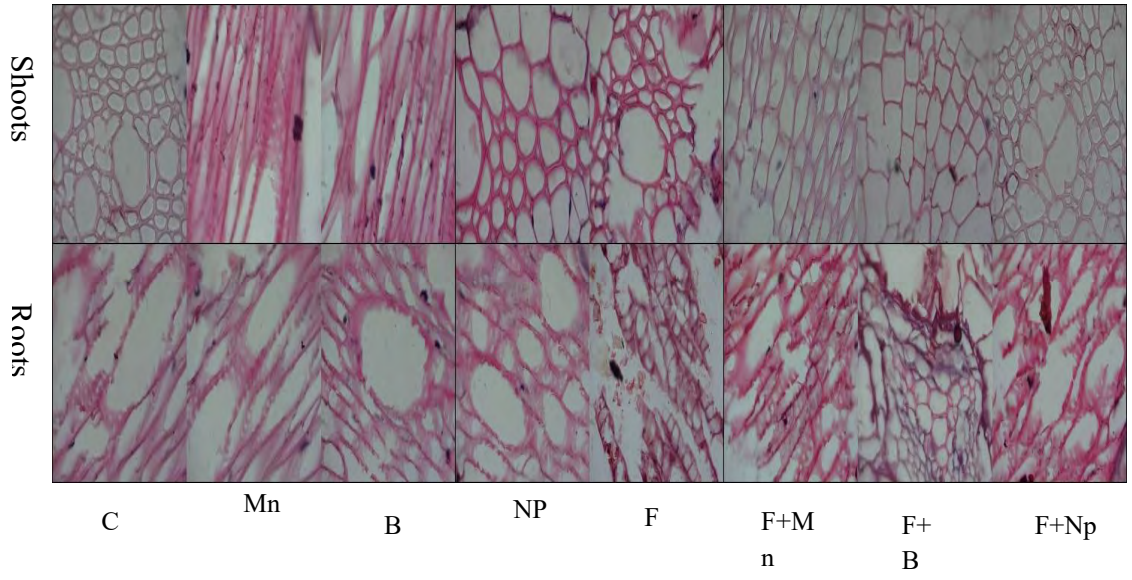

Fig. 33 Tomato histopathological appraisement. Control (C), Mn salt treated plants (Mn), *B. subtilis* primed seeds (B), MnO NPs primed seed (NPs), Seeds sown in *F. oxysporum* contaminated soil (F), Mn salt treated seeds sown in *F. oxysporum* contaminated soil (F+Mn), *B. subtilis* primed seeds sown in soil contaminated with *F. oxysporum* (F+B), MnO NPs primed seeds sown in soil contaminated with *F. oxysporum* (F+NPs).

3.3.4. Measurement of Physiological Traits

The treatment of NPs and *B. subtilis* enhanced the root and shoot lengths of germinated plants (Fig 35). The root and shoot lengths were considerably reduced (44%) in F treatment, as compared to control. F+Mn, F+B and F+NPs treatments had much longer lengths of roots and shoots than F treatment. MnO NPs treated plant seed (NP

treatment) and *B. subtilis* treated plants (B treatment) had the highest lengths of roots and shoots than other treatments (Fig. 35). The fresh root and shoot ratios of infected plants (F treatment) was lowered by 46%, whereas the plants of Mn, B and NP treatments had a higher fresh root shoot ratio respectively, compared to the control (C).

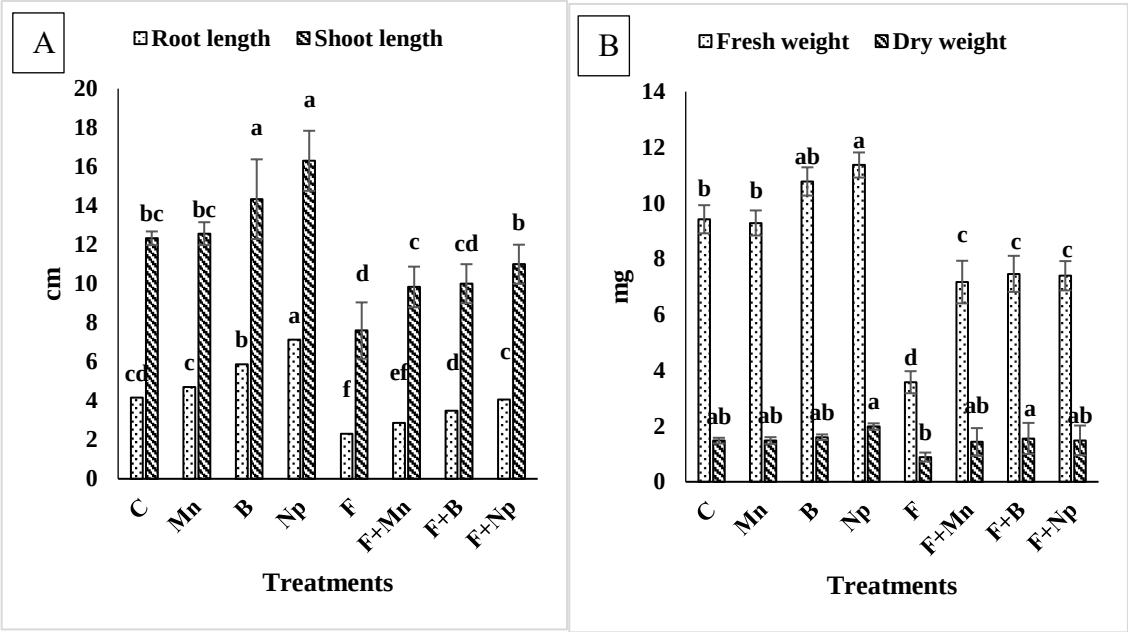

Fig. 34 Root and shoot length (A), Fresh and dry root shoot ratios (B) of tomato plant under various growth conditions**.** Control (C), Mn salt treated plants (Mn), *B. subtilis* primed seeds (B), MnO NPs primed seed (NPs), Seeds sown in *F. oxysporum* contaminated soil (F), Mn salt treated seeds sown in *F. oxysporum* contaminated soil (F+Mn), *B. subtilis* primed seeds sown in soil contaminated with *F. oxysporum* (F+B), MnO NPs primed seeds sown in soil contaminated with *F. oxysporum* (F+NPs).

3.3.5. Osmolytes activity in plant

Proline and sugar contents were significantly increased in the leaves of NPs treated plants, bacterial primed and *F. oxysporum* stressed seedlings of tomato, as compared to control. Treatment of nanoparticles and biocontrol bacteria influenced the levels of osmolytes in stressed treatment. The maximum increase in proline (69%) and sugar content (46%) was observed upon nano-priming with 2.5 mg/mL concentration of MnO NPs (Fig. 36).

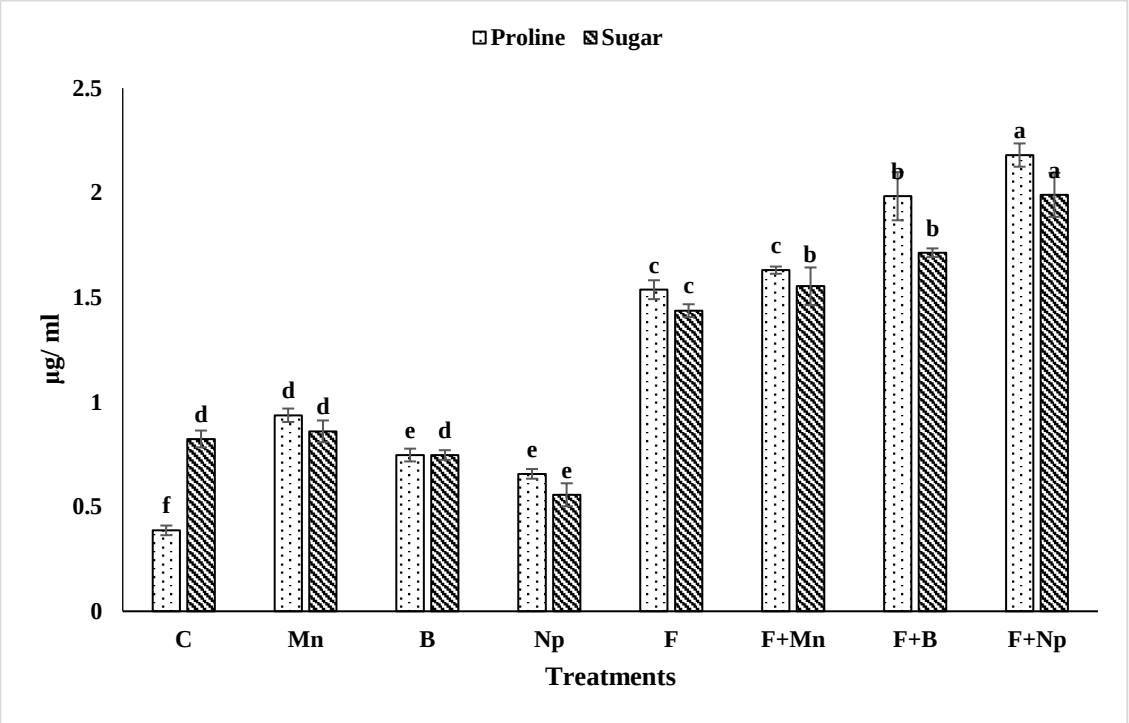

Fig. 35 Sugar and proline contents of tomato plants under various experimental conditions. Control (C), Mn salt treated plants (Mn), *B. subtilis* primed seeds (B), MnO NPs primed seed (NPs), Seeds sown in *F. oxysporum* contaminated soil (F), Mn salt treated seeds sown in *F. oxysporum* contaminated soil (F+Mn), *B. subtilis* primed seeds sown in soil contaminated with *F. oxysporum* (F+B), MnO NPs primed seeds sown in soil contaminated with *F. oxysporum* (F+NPs).

3.3.6. Oxidative burst assay

Application of MnO NPs increased photosynthetic pigments (chlorophyll and carotenoid) in the seedlings of both control and *F. oxysporum* stressed plants. In comparison to control, the presence of *F. oxysporum* lowered the levels of chlorophyll and carotenoid. However, the nono-priming of MnO NPs proved effective in mitigating *F. oxysporum* wilting by maintaining higher levels of chlorophyll and carotenoid. Notably, the highest concentrations of chlorophyll and carotenoid were observed in plants treated with 2.5 mg/mL concentration of MnO NPs (Fig. 37).

Current findings revealed that MDA and H_2O_2 contents were enhanced in the leaves of *F. oxysporum* stressed plants, as compared to control (C). Under *F. oxysporum*

stress, the MDA contents in leaves were decreased in MnO NPs, bacteria and salt treated plants. Variable decrease was observed in MDA content of plants treated with NPs, bacteria and salt and the maximum decrease in MDA and H_2O_2 content was observed in plants treated with 2.5 mg/mL concentration of MnO NPs (fig. 38).

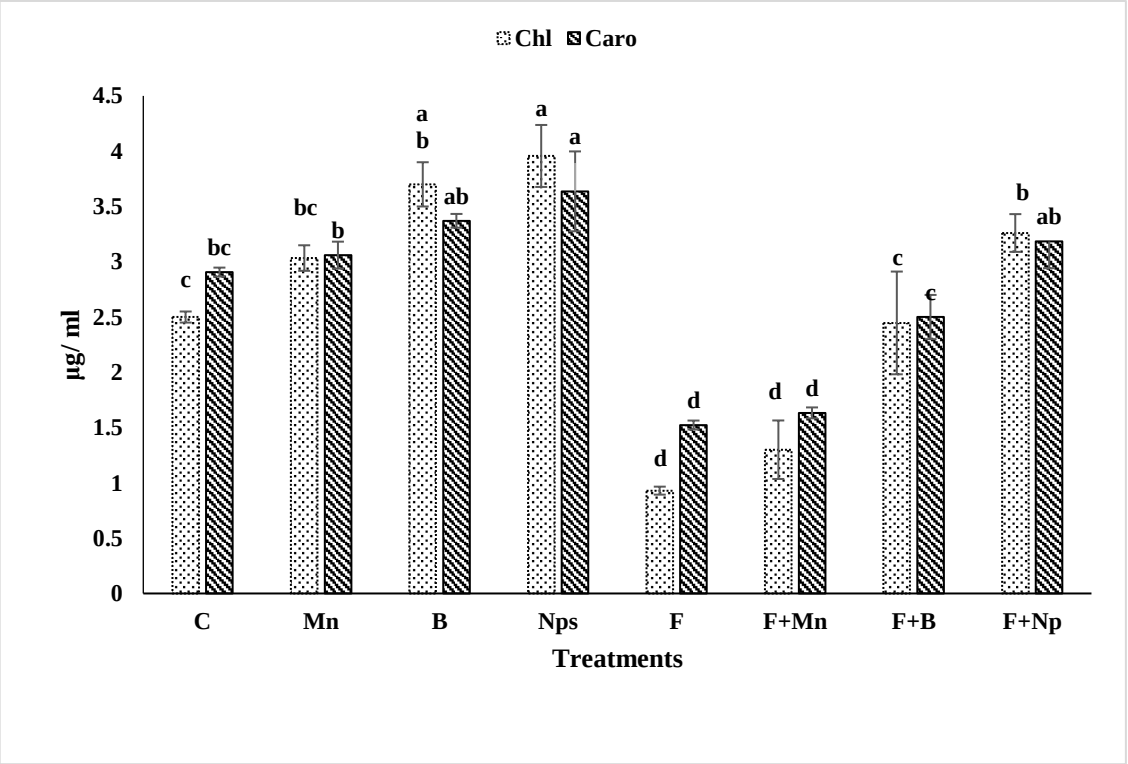

Fig. 36 Appraisal of crucial photosynthetic phytopigments in tomato plants under different growth conditions. Control (C), Mn salt treated plants (Mn), *B. subtilis* primed seeds (B), MnO NPs primed seed (NPs), Seeds sown in *F. oxysporum* contaminated soil (F), Mn salt treated seeds sown in *F. oxysporum* contaminated soil (F+Mn), *B. subtilis* primed seeds sown in soil contaminated with *F. oxysporum* (F+B), MnO NPs primed seeds sown in soil contaminated with *F. oxysporum* (F+NPs).

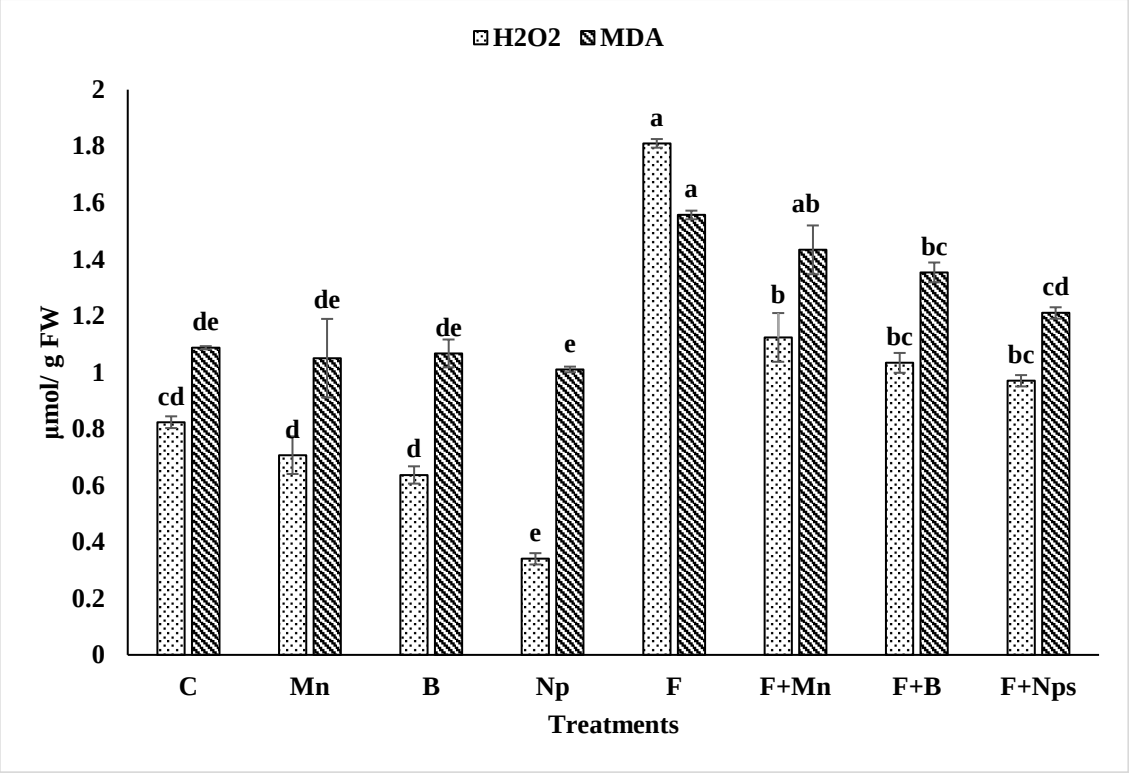

Fig. 37 Oxidative burst assay in tomato plant under various growth states. Control (C), Mn salt treated plants (Mn), *B. subtilis* primed seeds (B), MnO NPs primed seed (NPs), Seeds sown in *F. oxysporum* contaminated soil (F), Mn salt treated seeds sown in *F. oxysporum* contaminated soil (F+Mn), *B. subtilis* primed seeds sown in soil contaminated with *F. oxysporum* (F+B), MnO NPs primed seeds sown in soil contaminated with *F. oxysporum* (F+NPs).

3.3.7. Antioxidant Enzymes Activities

The presence of *F. oxysporum* improved superoxide dismutase (SOD) and peroxidase (POD) enzymes behaviour in tomato seedlings. Interestingly, priming coat of seeds with MnO NPs, bacteria and salt further enhanced this activity and the greatest activity of antioxidant enzymes was monitored in plants treated with 2.5 mg/mL application of MnO NPs (Fig. 39).

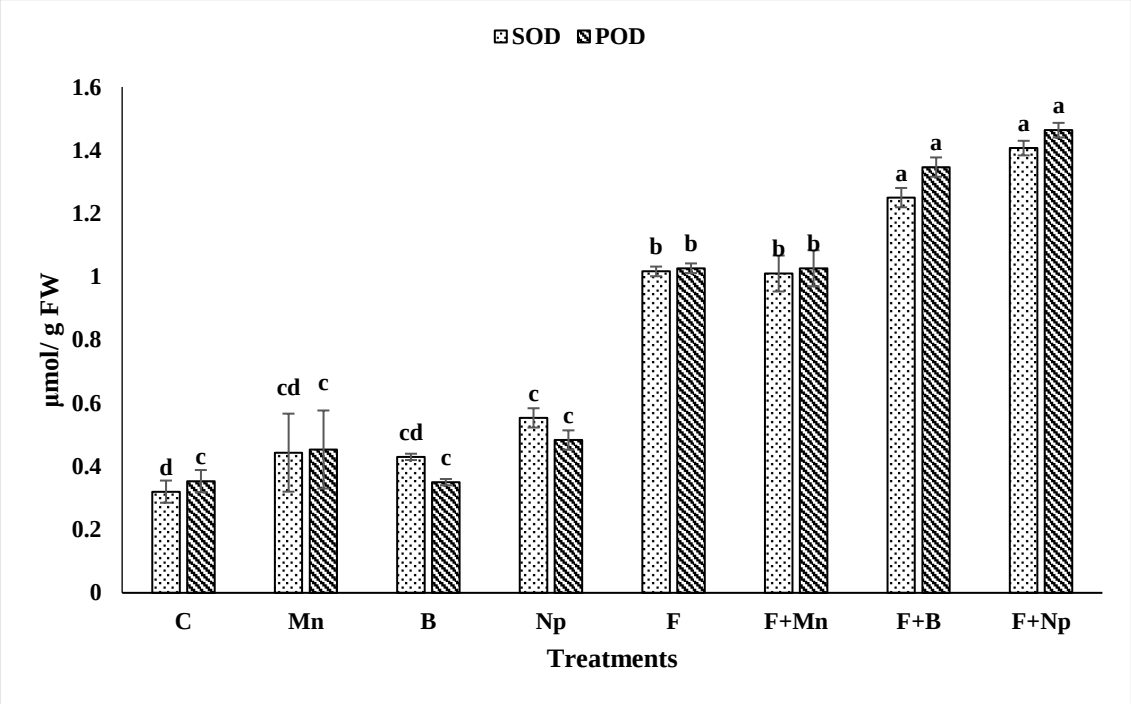

Fig. 38 Oxidative burst assay in tomato plants under various growth states. Control (C), Mn salt treated plants (Mn), *B. subtilis* primed seeds (B), MnO NPs primed seed (NPs), Seeds sown in *F. oxysporum* contaminated soil (F), Mn salt treated seeds sown in *F. oxysporum* contaminated soil (F+Mn), *B. subtilis* primed seeds sown in soil contaminated with *F. oxysporum* (F+B), MnO NPs primed seeds sown in soil contaminated with *F. oxysporum* (F+NPs).

3.3.8. Principal Component Analysis and Correlation Matrix

A correlation matrix illustrates the relationships between various parameters examined in the study (Fig. 40). In this matrix, a dark red color represents strong negative correlations, while dark blue indicates strong positive correlations. The Pearson's correlation matrix showed a fascinating positive correlation among proline, sugar, H_2O_2, MDA, REL, SOD and POD. Simultaneously, they showed a robust negative correlation

with growth attributes of plants, photosynthetic attributes and RWC.

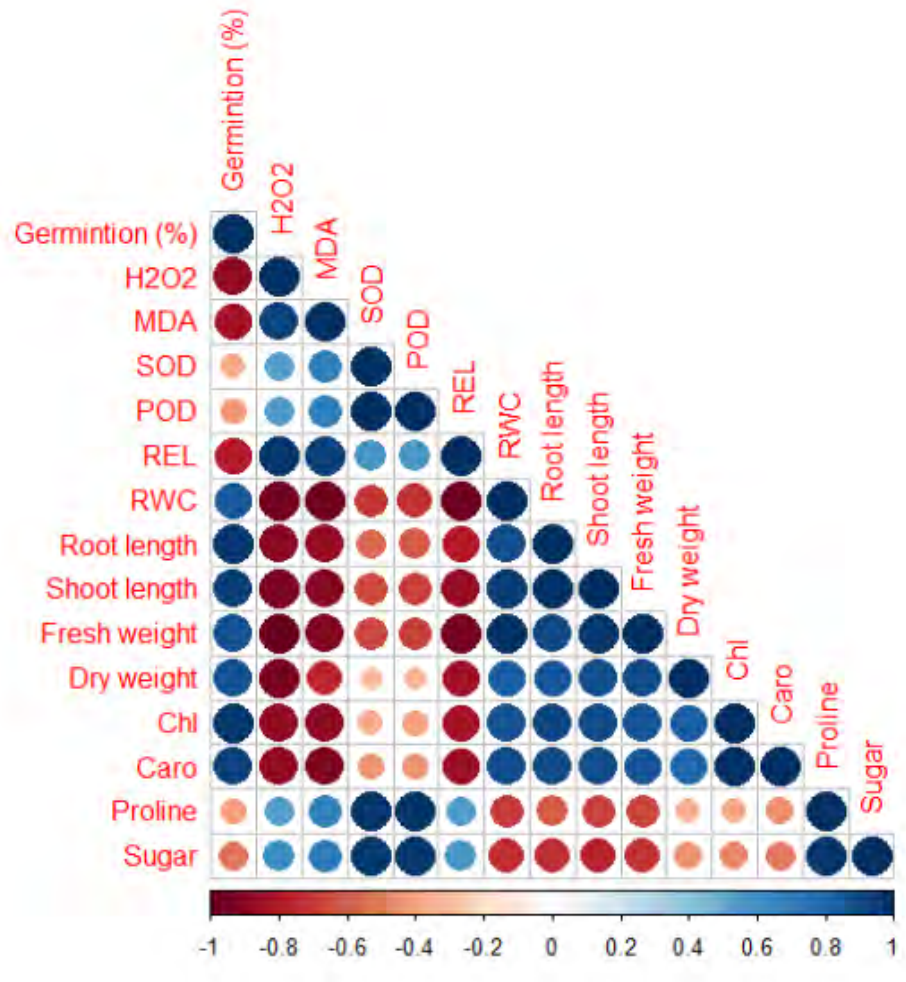

Fig. 39 Pearson's correlation analysis between physiological, antioxidant, and biochemical parameters of tomato seedlings under Fusarium stress after their priming with MnO NPs, *Bacillus subtilis* and Mn Salt. Root length (RL); shoot length (SL); fresh weight (FW); dry weight (DW) chlorophyll (Chl); carotenoid (Caro); relative water content (RWC); relative electrolytic leakage (REL); malondialdehyde (MDA); superoxide dismutase (SOD); peroxidase (POD); hydrogen peroxide (H2O2).

4. DISCUSSION:

Crop yield is notably affected by pathogen attacks, environmental stress, and soil nutrient deficiencies. Traditionally, chemical pesticides are used to mitigate these challenges, but their prolonged cause soil degradation, water contamination, and reduced biodiversity. Moreover, the overuse of chemicals induces resistance in pests and pathogens. In response to these concerns, nanotechnology is being used in the field of in agriculture, for last few decades (Ahmed et al., 2022).

Nanoparticles are target oriented and reduce the harmful effects associated with conventional agrochemicals. Their ability to deliver nutrients and pesticides in controlled doses, improve stress tolerance, and boost plant growth makes nanoparticles an innovative solution for achieving sustainable and higher agricultural productivity (Kumar et al., 2013). Nanoparticles are highly effective delivering nutrients, agrochemicals, and antimicrobial agents directly to plant tissues. This targeted delivery reduces the overall quantity of NPs needed to limit diseases (de França et al., 2020). Nanoparticles have been reported to improve nutrient uptake and promote physiological resilience (Saqib et al. 2019). Additionally, they increase crop yields, reduce chemical dependency, and promote eco-friendly farming practices (Moorthy et al. 2015).

Fruits have long been considered as a commercially and nutritionally important commodity. Postharvest decays of fruit have been a matter of consideration for decades. Even the common consumer is aware of the ongoing issue of postharvest degradation (Janisiewicz and Korsten, 2002). Major factors of post-harvest decays include the infection of microbes and non-technical handling (Droby, 2006).

This analysis has reported the contribution of. *niger* in black rot of tomato fruit. To our information, this is the first details of black rot of tomato, caused by *A. niger*, in Pakistan, Previously, this fungus has been reported to cause black rot of grapes in Pakistan (Ghuffar et al., 2021). In India, *A. niger* has been proved as the causative agent of black rot mold of pear (Parveen et al., 2014). Many other studies have also described the antifungal potential of *B. subtilis* (Zongzheng et al., 2010; Oyedele and Ogunbanwo; Mardanova et al., 2016). Moreover, green MnO NPs have been documented to successfully control the growth of *Candida albicans*, *Curvularia lunata*, *A. niger* and *Trichophyton simii* (Jayandran et al., 2015).

Similar to previous studies, FTIR spectroscopy described the manifestation of various molecules on the surface of MnO NPs (Smuleac et al., 2011; Wang et al., 2014).

Absorbance, in 500 cm^{-1} range is a characteristic attribute of MnO NPs (Kumar et al., 2013). Alkyl halides and other organic compounds are known for their antifungal potential (Ahmed et al., 2022; Khalil et al., 2017). XRD assay verified the crystalline nature of MnO NPs by displaying characteristic diffraction peaks at 2θ degree. These plane dimensions further demonstrate the face-centered cubic crystal structure of MnO NPs (de França et al., 2020). XRD results depicted >100 nm size of synthesized MnO NPs, which recommend their antimicrobial potential (Saqib et al., 2019; Oussou-Azo *et al*., 2020). SEM analysis successfully described the spherical shape of NPs (Ahmed et al., 2022). In this study, different doses of MnO NPs (0.25, 2.5 and 5 mg/mL) successfully inhibited mycelial growth in Petri plates (*in vitro*) and controlled fruit diseases (*in vivo*). The antifungal activities of MnO NPs have been earlier reported against *C. albicans*, *C. lunata* and *T. simii* (Haneefa, 2017). Sugars and soluble solids give better taste to fruits and vegetables (Akbar et al., 2022).

In the second part of the study, the focus was on evaluating the efficacy of NPs in relieving metal stress in plants. Heavy metals (HMs) are known for their high density and high toxicity to humans, plants, and animals, and they pose diverse harmful environmental concerns (Malar et al. 2016). Lead (Pb) is not a necessary element for plant growth or development (Lamhamdi et al. 2013) and its accumulation poses a thoughtful threat to agriculture (Silva et al. 2017). XRD evaluation displayed the stable crystalline nature and smaller size (22.2 nm) of the produced MnO-NPs. These results indicated the antimicrobial potential of MnO-NPs, which is heavily dependent on their size and crystalline nature (Saqib et al. 2019). Like previous findings, SEM micrographs exposed a high monodispersed flower-like nanostructure of MnO-NPs (Cherian et al. (2016). EDX study confirmed the crystalline structure of NPs through the narrow peaks observed in the EDX spectrum (Moorthy et al. 2015).

This study explained the detrimental impacts of Pb on plant biomass. However, the application of MnO-NPs produced in bacterial filtrate exhibited a significant improvement in growth characteristics of Pb-stressed plants. Earlier research has reported the enhanced biomass of Pb-stressed *Coriandrum sativum* L. (Fatemi et al. 2021). Pb stress lowered the levels of proline and sugar, while the supplementation of MnO-NPs to Pb-stressed seedlings increased proline and sugar contents. These conclusions align with the results presented by Ramzan et al. (2022). Proline is an osmolyte which helps plants to bear stress conditions. Additionally, the accumulation of

sugar content regulates osmotic balance between the cytosol and vacuole (El-Saadony et al. 2021). Metal toxicity in plants can also substantially affect the levels of chlorophyll in leaves (Rizwan et al. 2017). Consequently, changes in chlorophyll content directly reflect the health of plants and their response to environmental variations. Our study revealed an enhancement in chlorophyll content which may be linked to the beneficial effects of NPs on chlorophyll fluorescence parameters (Fatemi et al. 2021). Abundance of carotenoids is also useful for plants (El-Saadony et al. 2021). This study described a noticeable increase in carotenoid content, due to the application of NPs. Conversely, high concentrations of Pb stress reduced chlorophyll and carotenoid content in seedlings, indicating a specific response to metal stress (Gajewska et al. 2006).

Furthermore, our research demonstrated a reduction in relative electrolyte leakage (REL) and an improvement in leaf water content in Pb-stressed plants. This response indicates better absorption of water and minerals, facilitated by MnO-NPs (Kumar et al. 2013). In this study, nano-priming with MnO-NPs, successfully decreased the accumulation of MDA and H_2O_2, which aligns with the findings of prior studies (Venkatachalam et al. 2017; Nair et al. 2014; Haroon et al. 2023).

MnO-NPs lowered the uptake of Pb in tomato plants grown in Pb-stressed soil. The reduced bioaccumulation of Pb in tomato tissues can be credited to the alterations in the mobile fractions of Pb in the contaminated soil, caused by NPs. This observation is uniform with previous study that also informed higher Pb deposit in the roots (Malar et al. 2016). This accumulation in roots is influenced by genotypic and environmental factors (Fatemi et al. 2021). Principal component analysis evaluated the relationship between treatments and plant traits under Pb stress conditions and under different concentrations of MnO-NPs. These PCA results are like the results of Chen et al. (2022), who reported severe impacts of Pb application on plant growth and antioxidant contents. Previous studies describe that the metal substances expose a strong positive collaboration with MDA (Venkatachalam et al. 2017).

In the third part of the study, the nanoparticles were applied to manage Fusarium wilt of tomato seedlings. Additionally, the role of bacteria used in synthesizing these nanoparticles and the effects of salts employed during nanoparticle preparation were examined. This section aims to discuss how these biogenic nanoparticles, synthesized through bacterial processes, contribute to manage Fusarium wilt, offering an eco-friendly alternative to conventional treatments. *F. oxysporum* f.sp.*lycopersici* is an extremely

demolishing myco-pathogen of tomato plant (Sachdev et al., 2022). This soil borne fungus induces wilting by extensive demolition and browning of vascular elements, retarded growth and ultimate death of plant (Herrera-Téllez et al., 2019). *Fusarium* wilt is controlled by the employment of myco-suppressive fungicidal chemicals and competitive cultivars (Natsiopoulos et al., 2022). Excessive usage of myco-suppressive fungicidal chemicals provokes the emergence of resistant strains of pathogens and eventual establishment of secondary myco-pathogens of plants (Babu et al., 2015). It is the need of time to replace chemical fungicides with health-friendly disease-control approaches.

In this search, great antimicrobial ability of synthesized MnO NPs was observed. These results indicated the antimicrobial potential of MnO NPs, which is heavily dependent on their size and crystalline nature (Saqib et al. 2019). Like previous findings, SEM micrographs exposed a spherical shape and nanostructure of MnO NPs, which give them antifungal properties (Cherian et al. 2016; Anar et al., 2023). EDX exploration described the elemental composition of the MnO NPs, confirming their crystalline structure through the narrow peaks observed in the EDX spectrum (Moorthy et al. 2015).

In vitro antagonistic properties of MnO NPs and *B. subtilis* have been described earlier (Saritha et al., 2015; Pacios-Michelena et al., 2023; Jabeen et al., 2023). Disease infestations affect germination percentage, growth, and emergence of infection signs (Murali et al., 2013; Hussain et al., 2016; Kejela et al., 2017;). This study also revealed substantial ruination of tomato anatomical attributes of shoots and the roots. Priming of tomato seeds with MnO NPs and *B. subtilis* inoculums, consequently enriched fiber elements, cambial linings and vascular components (increased xylem and phloem elements) in tomato shoots and roots even under stress conditions. Enrichment in these attributes encourage plants to uptake prime minerals and nutrients to cope with wilting. Both MnO NPs and *B. subtilis* facilitated more leaves number, lengths and weights of newly harvested and dried tomato roots and shoots even under disease conditions, when compared with their pertinent controls (Egamberdieva et al., 2015). Current investigation manifested the improvement in proline and sugar accumulation in treated plants with nanoparticles and *B. subtilis* implemented tomato seedlings under *Fusarium* stress. Nanoparticles and BBMs invigorate plant growth by boosting tomato metabolic-based resistance (MBR) under biotic stress (Khan et al., 2023).

This research also showed rigorous disruption of chlorophyll and carotenoid elements. The applications of MnO NPs and *B. subtilis* tremendously boosted the amount of chlorophyll and carotenoid. The disruption in these photosynthetically crucial phytopigment elements is possibly induced by photo-oxidative mechanism and noxious chemicals secreted by myco-pathogen during infection which consequently degrade them (Bashan et al., 1995). Crucial chlorophyll elements are disrupted when myco-pathogen infection diminishes plant intake of prime mineral elements (e.g. Mg), needed for chlorophyll formation (Dehgahi et al., 2015). Consequences of this research also described that application of MnO NPs, *B subtilis* and Mn salt positively influenced the production of chlorophyll and carotenoid contents, which elucidates its anti-oxidative and single molecular oxygen degradation ability (Mohamed et al., 2022).

Tomato plants primed with MnO NPs, *B subtilis* and Mn salt inoculants exhibited improved activities of peroxidase (POD) and also superoxide-dismutase (SOD) enzymes. These conclusive findings have strong concordance with explored outcomes of previous studies (Dong & Cohen, 2001), which clarified promoted ROS-scrounger enzymes activeness in plants under biotic-stress. This study also showed the variable production of MDA and H_2O_2 under biotic stress conditions. These achieved outcomes have congruity with Radhakrishnan et al. (2013) and Gil et al. (2023) who published the reduction in MDA and H_2O_2 production in plants under biotic-stress. MnO NPs and *B. subtilis* can trigger plant defense strategy by lowering the degree of lipid-peroxidative process (lipids oxidative-degradation) and elucidating negative superoxide ions (O^{-2}) and H-peroxides (H_2O_2) (Radhakrishnan et al., 2013).

5. Conclusion

This study represents the first documentation of black rot in tomatoes in Pakistan, caused by *Aspergillus niger*. It also offers an environmentally sustainable method to manage this disease. The successful synthesis of MnO nanoparticles (NPs) using *Bacillus subtilis* filtrate presents a cost-effective approach to limit fruit rot diseases in perishable fruits and vegetables. The results demonstrated that black rot in tomatoes can be effectively controlled by applying MnO NPs at an optimal concentration of 2.5 mg/mL.

Additionally, this research highlights the importance of seed priming with MnO NPs to reduce lead (Pb) toxicity in tomatoes. The study introduced a method for producing MnO NPs in powder form, facilitating their practical use in the field. Seed priming with MnO NPs significantly enhanced plant growth, promoted photosynthetic pigment synthesis, improved osmoregulation, and mitigated Pb-induced stress. This investigation marks the first exploration of nano-priming with MnO NPs supplemented with *B. subtilis* for enhanced growth and Pb stress reduction in tomato plants. The increased activity of chalcone synthase and phenylalanine ammonia-lyase provided insights into the plant's defence mechanisms.

Furthermore, this study optimized the use of MnO NPs, *B. subtilis*, and manganese salt (Mn) to control Fusarium wilt in tomatoes. The application of MnO NPs, in conjunction with *B. subtilis* and Mn salt, improved physiological and enzymatic responses in tomato plants, aiding in the mitigation of Fusarium-induced wilting. MnO NPs proved more efficient than *B. subtilis* or Mn salt alone in disease suppression and growth promotion. This is the first study to investigate the combined use of MnO NPs, *B. subtilis*, and Mn salt for enhancing plant growth and mitigating Fusarium wilt. These findings present an eco-friendly way to manage biotic stress and underscore the potential for further applications.

The successful deployment of Bacillus-MnO nanocomposites for controlling Fusarium wilt marks a significant step toward sustainable agriculture, reducing dependence on chemical fungicides and minimizing environmental risks. This strategy offers a safer, more effective solution for managing Fusarium wilt, contributing to increased tomato yields and fostering agricultural sustainability.

FUTURE PROSPECTS:

The future perspectives of this research open several promising avenues for advancing sustainable agriculture. The successful use of MnO nanoparticles (NPs), particularly those synthesized using *Bacillus subtilis*, offers a foundation for further exploration of nanotechnology in field of plant disease management. There is a need to work oh optimizing the large-scale production of MnO NPs, testing their efficacy in diverse crops and different environmental conditions. Moreover, there is potential for investigating the long-lasting influences of NPs in soil and environment.

Further research could also explore the development of multifunctional nanoparticles that target a broader range of pathogens. Integrating nanotechnology with other agriculture techniques, such as targeted delivery systems, could enhance the efficiency of nanoparticle application, minimizing waste and maximizing plant health benefits. Additionally, exploring the potential of other metal oxide nanoparticles and microbial-based nanocomposites could expand the range of sustainable solutions for crop protection.

In conclusion, this study offered a solid platform for future innovations in disease management, aiming to reduce dependency on harmful chemical pesticides, ultimately contributing to a more sustainable, productive, and resilient agricultural system.

REFERENCES:

Abbasi S, Sadeghi A, Safaie N (2020) Streptomyces alleviate drought stress in tomato plants and modulate the expression of transcription factors ERF1 and WRKY70 genes. Sci Hortic 265:109206.

Abid, N., Khan, A. M., Shujait, S., Chaudhary, K., Ikram, M., Imran, M., ... & Maqbool, M. (2022). Synthesis of nanomaterials using various top-down and bottom-up approaches, influencing factors, advantages, and disadvantages: A review. *Advances in Colloid and Interface Science*, *300*, 102597.

Abrahamian, P., Klein-Gordon, J. M., Jones, J. B., & Vallad, G. E. (2021). Epidemiology, diversity, and management of bacterial spot of tomato caused by Xanthomonas perforans. *Applied microbiology and biotechnology*, *105*(16), 6143-6158.

Ahmed J, Ali M, Sheikh H M, Al-Kattan M O, Haroon U, Safaeishakib M, Munis MFH (2022) Biocontrol of fruit rot of *Litchi chinensis* using Zinc oxide nanoparticles synthesized in *Azadirachta indica*. Micromachines 13(9):1461.

Ahmed, A. (2022). *Modelling farmer and consumer preferences for cleaner food production* (Doctoral dissertation, Durham University).

Ahmed, K. M., and Ravinder Reddy, C. H. *A Pictorial Guide to the Identification of Seedborne Fungi of Sorghum, Pearl Millet, Finger Millet, Chickpea, Pigeonpea, and Groundnut. Information Bulletin no. 34*. International Crops Research Institute for the Semi-Arid Tropics. (1993).

Ahmed, S. F., Mofijur, M., Rafa, N., Chowdhury, A. T., Chowdhury, S., Nahrin, M., & Ong, H. C. (2022). Green approaches in synthesising nanomaterials for environmental nanobioremediation: Technological advancements, applications, benefits and challenges. *Environmental Research*, *204*, 111967.

Akbar, M., Haroon, U., Ali, M., Tahir, K., Chaudhary, H. J., and Munis, M. F. H. Mycosynthesized Fe_2O_3 nanoparticles diminish brown rot of apple whilst maintaining composition and pertinent organoleptic properties. *Journal of Applied Microbiology*. 5 (2022) 3735-3745.

Ali, M., Haroon, U., Khizar, M., Chaudhary, H. J., and Munis, M. F. HFacile single step preparations of phyto-nanoparticles of iron in *Calotropis procera* leaf extract to evaluate their antifungal potential against *Alternaria alternata*. *Current Plant Biology*. *23* (2020) 100157.

Ali, S., Ulhassan, Z., Shahbaz, H., Kaleem, Z., Yousaf, M. A., Ali, S., ... & Zhou, W. (2024). Magnesium oxide nanoparticles as novel sustainable approach in enhancing crop tolerance to abiotic and biotic stresses. *Environmental Science: Nano*.

Al-Issawi, M., Rihan, H. Z., Al-Shmgani, H., & Fuller, M. P. (2016). Molybdenum application enhances antioxidant enzyme activity and COR15a protein expression under cold stress in wheat. *Journal of Plant Interactions*, *11*(1), 5-10.

Alsaiari, N. S., Alzahrani, F. M., Amari, A., Osman, H., Harharah, H. N., Elboughdiri, N., & Tahoon, M. A. (2023). Plant and microbial approaches as green methods for the synthesis of nanomaterials: synthesis, applications, and future perspectives. *Molecules*, *28*(1), 463.

Alsaif, N. A., Atta, A., Abdeltwab, E., & Abdel-Hamid, M. M. (2024). Synthesis, structural characterization, and optical properties of PVA/MnO2 materials for optoelectronics applications. *Macromolecular Research*, *32*(1), 35-44.

Alva, A. K., Mattos Jr, D., Paramasivam, S., Patil, B., Dou, H., & Sajwan, K. S. (2006). Potassium management for optimizing citrus production and quality. *International journal of fruit science*, *6*(1), 3-43.

Ambros, S., Martinez, F., Ivars, P., Hernandez, C., de la Iglesia, F., & Elena, S. F. (2017). Molecular and biological characterization of an isolate of Tomato mottle mosaic virus (ToMMV) infecting tomato and other experimental hosts in eastern Spain. *European Journal of Plant Pathology*, *149*, 261-268.

Amendola, V., Pilot, R., Frasconi, M., Maragò, O. M., & Iatì, M. A. (2017). Surface plasmon resonance in gold nanoparticles: a review. *Journal of physics: Condensed matter*, *29*(20), 203002.

Amiri, M. R., Alavi, M., Taran, M., & Kahrizi, D. (2022). Antibacterial, antifungal, antiviral, and photocatalytic activities of TiO2 nanoparticles, nanocomposites, and bio-nanocomposites: Recent advances and challenges. *Journal of Public Health Research*, *11*(2), 22799036221104151.

Anar, M., Akbar, M., Tahir, K., Chaudhary, H. J., & Munis, M. F. H. (2023). Biosynthesized manganese oxide nanoparticles maintain firmness of tomato fruit by modulating soluble solids and reducing sugars under biotic stress. *Physiological and Molecular Plant Pathology*, *127*, 102126.

Anar, M., Haroon, U., Kamal, A., Tahir, K., Akbar, M., Farhana, ... & Munis, M. F. H. (2024). Bacteria-Based MnO Nanoparticles Alleviate Lead Toxicity in Tomato Seedling Through

Improving Growth Attributes and Enhanced Gene Expression of Candidate Genes. *Journal of Plant Growth Regulation*, 1-14.

Animashaun, M. O. (2015). *The use of hot water treatment by small holders for the control of alternaria alternata, the cause of black mould disease of tomato* (Doctoral dissertation, University of Essex).

Ansari, M. W., & Tuteja, N. (2015). Post-harvest quality risks by stress/ethylene: management to mitigate. *Protoplasma*, *252*, 21-32.

Armstrong, W., & Drew, M. C. (2002). Root growth and metabolism under oxygen deficiency. In *Plant roots* (pp. 1139-1187). CRC Press.

Arole, V. M., & Munde, S. V. (2014). Fabrication of nanomaterials by top-down and bottom-up approaches-an overview. *J. Mater. Sci*, *1*, 89-93.

Aryal, J. P., Sapkota, T. B., Khurana, R., Khatri-Chhetri, A., Rahut, D. B., & Jat, M. L. (2020). Climate change and agriculture in South Asia: Adaptation options in smallholder production systems. *Environment, Development and Sustainability*, *22*(6), 5045-5075.

Atasoy, N. (2012). Biochemistry of lycopene. *Journal of Animal and Veterinary Advances*, *11*(15), 2605-2610.

Babu, A. N., Jogaiah, S., Ito, S. I., Nagaraj, A. K., & Tran, L. S. P. (2015). Improvement of growth, fruit weight and early blight disease protection of tomato plants by rhizosphere bacteria is correlated with their beneficial traits and induced biosynthesis of antioxidant peroxidase and polyphenol oxidase. *Plant Science*, *231*, 62-73.

Babu, S., Singh, R., Yadav, D., Rathore, S. S., Raj, R., Avasthe, R., ... & Singh, V. K. (2022). Nanofertilizers for agricultural and environmental sustainability. *Chemosp*, *292*, 133451.

Baidya, B. K., & Sethy, P. (2020). Importance of Fruits and Vegetables in Boosting our Immune System amid the COVID19. *Food Sci. Rep*, *1*, 50-55.

Bareham, L. (2012). *The big red book of tomatoes*. Grub Street Publishers.

Barnett, H. L., and Hunter, B. B. Illustrated genera of imperfect fungi 4th Edition. St. Paul, MN. (1998).

Bashan, B., Levy, R. S., Cojocaru, M., & Levy, Y. (1995). Purification and structural determination of a phytotoxic substance from *Exserohilum turcicum*. *Physiological and molecular plant pathology*, *47*(4), 225-235.

Bashir, M. K., Ali, A., Farrukh, M. U., Alam, M., & Sabir, M. (2021). Efficiency analysis of tomato crop in District Sheikhupura, Punjab Pakistan. *Custos E Agronegocio Online*, *17*, 134-

Bashir, M. K., Malik, A. U., Farrukh, M. U., Hameed, S., Kamran, M. A., & Ziaf, K. (2022). Forecasting tomato production under climate variability in Pakistan. *JAPS: Journal of Animal & Plant Sciences*, *32*(1).

Bates LS, Waldren RA, Teare ID (1973) Rapid determination of free proline for water-stress studies. Plant Soil 39:205-207

Beauchamp, C., & Fridovich, I. (1971). Superoxide dismutase: improved assays and an assay applicable to acrylamide gels. *Analytical biochemistry*, *44*(1), 276-287.

Bertin, N., & Génard, M. (2018). Tomato quality as influenced by preharvest factors. *Scientia Horticulturae*, *233*, 264-276.

Bhattacharya, A. (2022). Effect of low-temperature stress on germination, growth, and phenology of plants: A review. *Physiological processes in plants under low temperature stress*, 1-106.

Bibi, H., Haroon, U., Farhana, Kamal, A., Akbar, M., Anar, M., ... & Munis, M. F. H. (2023). Impact of bacterial synthesized nanoparticles on quality attributes and postharvest disease control efficacy of apricot and loquat. *Journal of Food Science*, *88*(9), 3920-3934.

Bigiani, L. (2020). Nanoarchitectonics of Manganese, Cobalt, and Iron Oxides: From Design to Advanced Applications.

Biju, V., Itoh, T., Anas, A., Sujith, A., & Ishikawa, M. (2008). Semiconductor quantum dots and metal nanoparticles: syntheses, optical properties, and biological applications. *Analytical and bioanalytical chemistry*, *391*, 2469-2495.

Biswas, A., Bayer, I. S., Biris, A. S., Wang, T., Dervishi, E., & Faupel, F. (2012). Advances in top–down and bottom–up surface nanofabrication: Techniques, applications & future prospects. *Advances in colloid and interface science*, *170*(1-2), 2-27.

Borguini, R. G., & Ferraz Da Silva Torres, E. A. (2009). Tomatoes and tomato products as dietary sources of antioxidants. *Food Reviews International*, *25*(4), 313-325.

Borguini, R. G., & Ferraz Da Silva Torres, E. A. (2009). Tomatoes and tomato products as dietary sources of antioxidants. *Food Reviews International*, *25*(4), 313-325.

Cao, X., & Wang, Z. (2022). Application of nano-agricultural technology for biotic stress management: mechanisms, optimization, and future perspectives. *Environmental Science: Nano*, *9*(12), 4336-4353.

Carranca, C., Brunetto, G., & Tagliavini, M. (2018). Nitrogen nutrition of fruit trees to reconcile productivity and environmental concerns. *Plants*, *7*(1), 4.

Carvalho, M. E., Piotto, F. A., Gaziola, S. A., Jacomino, A. P., Jozefczak, M., Cuypers, A., & Azevedo, R. A. (2018). New insights about cadmium impacts on tomato: plant acclimation, nutritional changes, fruit quality and yield. *Food and Energy Security*, *7*(2), e00131.

Chanda, S., Bhat, M., Shetty, K. G., & Jayachandran, K. (2021). Technology, policy, and market adaptation mechanisms for sustainable fresh produce industry: The case of tomato production in Florida, USA. *Sustainability*, *13*(11), 5933.

Chaudhary, A. K., Yadavb, J., Guptac, A. K., & Guptad, K. (2021). Integrated disease management of early blight (Alternaria solani) of potato. *Trop. Agrobiodivers*, *2*, 77-81.

Chen F, Aqeel M, Maqsood MF, Khalid N, Irshad MK, Ibrahim M, Akhter N, Afzaal M, Ma J, Hashem M, Almari S, Noman A, Lam SS (2022). Mitigation of lead toxicity in *Vigna radiata* genotypes by silver nanoparticles. Environ Pollut 308:119606.

Chen, Y., Cheng, Y., Chen, J., Zheng, Z., Hu, C., & Cao, J. (2021). Design and experiment of the buckwheat hill-drop planter hole forming device. *Agriculture, 11*(11), 1085.

Cherian E, Rajan A, Baskar G (2016) Synthesis of manganese dioxide nanoparticles using co-precipitation method and its antimicrobial activity. IJMTST 01:17-22.

Choi, Y., & Lee, S. Y. (2020). Biosynthesis of inorganic nanomaterials using microbial cells and bacteriophages. *Nature Reviews Chemistry*, *4*(12), 638-656.

Coelho, M. C., Rodrigues, A. S., Teixeira, J. A., & Pintado, M. E. (2023). Integral valorisation of tomato by-products towards bioactive compounds recovery: Human health benefits. *Food Chemistry*, *410*, 135319.

Collins, E. J., Bowyer, C., Tsouza, A., & Chopra, M. (2022). Tomatoes: An extensive review of the associated health impacts of tomatoes and factors that can affect their cultivation. *Biology*, *11*(2), 239.

Colvin, J., Nagaraju, N., Moreno-Leguizamon, C., Govindappa, R. M., Reddy, T. M., Padmaja, S. A., ... & Muniyappa, V. (2012). Socio-economic and scientific impact created by whitefly-transmitted, plant-virus disease resistant tomato varieties in Southern India. *Journal of Integrative Agriculture*, *11*(2), 337-345.

Cooke, B. M. (2006). Disease assessment and yield loss. In *The epidemiology of plant diseases* (pp. 43-80). Dordrecht: Springer Netherlands.

Costa, J. M., & Heuvelink, E. (2005). Introduction: the tomato crop and industry. In *Tomatoes* (pp. 1-19). Wallingford UK: CABI Publishing.

Coste S, Baraloto C, Leroy C, Marcon É, Renaud A, Richardson A D, Hérault B (2010) Assessing foliar chlorophyll contents with the SPAD-502 chlorophyll meter: a calibration test with thirteen tree species of tropical rainforest in French Guiana. Ann For Sci 67:607-607.

Cota-Ungson, D., González-García, Y., Cadenas-Pliego, G., Alpuche-Solís, Á. G., Benavides-Mendoza, A., & Juárez-Maldonado, A. (2023). Graphene–Cu nanocomposites induce tolerance against Fusarium oxysporum, increase antioxidant activity, and decrease stress in tomato plants. *Plants*, *12*(12), 2270.

Dao TT, Linthorst HJ, Verpoorte R (2011) Chalcone synthase and its functions in plant resistance. Phytochem Rev 10:397-412

Dawadi, S., Gupta, A., Khatri, M., Budhathoki, B., Lamichhane, G., & Parajuli, N. (2020). Manganese dioxide nanoparticles: synthesis, application and challenges. *Bulletin of Materials Science*, *43*, 1-10.

Dehgahi, R., Subramaniam, S., Zakaria, L., Joniyas, A., Firouzjahi, F. B., Haghnama, K., & Razinataj, M. (2015). Review of research on fungal pathogen attack and plant defense mechanism against pathogen. *Int J Sci Res Agric Sci*, *2*(8), 197-208.

Deplanche K, Caldelari I, Mikheenko IP, Sargent F, Macaskie LE (2010) Involvement of hydrogenases in the formation of highly catalytic Pd (0) nanoparticles by bioreduction of Pd (II) using *Escherichia coli* mutant strains. Microbiology 156:2630-40. DOI: 10.1099/mic.0.036681-0

Deplanche, K., Caldelari, I., Mikheenko, I. P., Sargent, F., & Macaskie, L. E. (2010). Involvement of hydrogenases in the formation of highly catalytic Pd (0) nanoparticles by bioreduction of Pd (II) using Escherichia coli mutant strains. *Microbiology*, *156*(9), 2630-2640.

Dhaliwal, M. S., Jindal, S. K., Sharma, A., & Prasanna, H. C. (2020). Tomato yellow leaf curl virus disease of tomato and its management through resistance breeding: a review. *The Journal of horticultural science and biotechnology*, *95*(4), 425-444.

Díez-Pascual, A. M. (2021). Carbon-based nanomaterials. *International Journal of Molecular Sciences*, *22*(14), 7726.

Dik, A. J., & Wubben, J. P. (2007). Epidemiology of Botrytis cinerea diseases in greenhouses. In *Botrytis: biology, pathology and control* (pp. 319-333). Dordrecht: Springer Netherlands.

Dong, H., & Cohen, Y. (2001). Extracts of killed *Penicillium chrysogenum* induce resistance against *Fusarium* wilt of melon. *Phytoparasitica*, *29*, 421-430.

Donsch, K. H., Gams, W., and Anderson, T. Compendium of Soil Fungi Vols I and II. *Academic Press, London*. (1980) *859*, 405.

Droby, S. Biological control of postharvest diseases of fruits and vegetables: difficulties and challenges. *Phytopathologia Polonica*. *39* (2006)105-117.

Egamberdieva, D., Jabborova, D., & Hashem, A. (2015). *Pseudomonas* induces salinity tolerance in cotton (*Gossypium hirsutum*) and resistance to *Fusarium* root rot through the modulation of indole-3-acetic acid. *Saudi journal of biological sciences*, *22*(6), 773-779.

El-Saadony M T, Desoky E S M, Saad A M, Eid R S, Selem E, Elrys A S (2021) Biological silicon nanoparticles improve Phaseolus vulgaris L. yield and minimize its contaminant contents on a heavy metals-contaminated saline soil. J Environ Sci 106:1-14.

Elsabahy, M., & Wooley, K. L. (2012). Design of polymeric nanoparticles for biomedical delivery applications. *Chemical Society Reviews*, *41*(7), 2545-2561.

Esmaeili, A., Sharafian, S., Safaiyan, S., Rezazadeh, S., & Rustaivan, A. (2009). Biotransformation of one monoterpene by sporulated surface cultures of *Aspergillus niger* and *Penicillium* sp. *Natural Product Research*, *23*(11), 1058-1061.

Ezzouggari, R., Bahhou, J., Taoussi, M., Seddiqi Kallali, N., Aberkani, K., Barka, E. A., & Lahlali, R. (2024). Yeast warriors: Exploring the potential of yeasts for sustainable citrus post-harvest disease management. *Agronomy*, *14*(2), 288.

Fahad, S., Bajwa, A. A., Nazir, U., Anjum, S. A., Farooq, A., Zohaib, A., ... & Huang, J. (2017). Crop production under drought and heat stress: plant responses and management options. *Frontiers in plant science*, *8*, 1147.

Farhana, Farooq, A. B. U., Haroon, U., Saleem, H., Akbar, M., Anar, M., ... & Munis, M. F. H. (2024). Bacillus safensis filtrate-based ZnO nanoparticles control black heart rot disease of apricot fruits by maintaining its soluble sugars and carotenoids. *World Journal of Microbiology and Biotechnology*, *40*(4), 125.

Fatemi H, Esmaiel Pour B, Rizwan M (2021) Foliar application of silicon nanoparticles affected the growth, vitamin C, flavonoid, and antioxidant enzyme activities of coriander (*Coriandrum sativum* L.) plants grown in lead (Pb)-spiked soil. ESPR 28:1417-1425.

Feng, S. H., & Li, G. H. (2017). Hydrothermal and solvothermal syntheses. In *Modern inorganic synthetic chemistry* (pp. 73-104). Elsevier.

Fenta, L., Mekonnen, H., & Kabtimer, N. (2023). The exploitation of microbial antagonists against postharvest plant pathogens. *Microorganisms*, *11*(4), 1044.

Flores, S. S., Cordovez, V., Oyserman, B., Stopnisek, N., Raaijmakers, J. M., & van ‘t Hof, P. (2023). The tomato's tale: Exploring taxonomy, biogeography, domestication, and microbiome for enhanced resilience. *Phytobiomes Journal*, *8*(1), 5-20.

Frusciante, L., Carli, P., Ercolano, M. R., Pernice, R., Di Matteo, A., Fogliano, V., & Pellegrini, N. (2007). Antioxidant nutritional quality of tomato. *Molecular nutrition & food research*, *51*(5), 609-617.

Fu, L., Wang, Z., Dhankher, O. P., & Xing, B. (2020). Nanotechnology as a new sustainable approach for controlling crop diseases and increasing agricultural production. *Journal of Experimental Botany*, *71*(2), 507-519.

Gajewska E, Skłodowska M, Słaba M, Mazur J (2006) Effect of nickel on antioxidative enzyme activities, proline and chlorophyll contents in wheat shoots. Biol Plant 50:653-659.

Gatahi, D. M. (2020). Challenges and opportunities in tomato production chain and sustainable standards. *International Journal of Horticultural Science and Technology*, *7*(3), 235-262.

Geoffrey, S. K., Hillary, N. K., Kibe, M. A., Mariam, M., & Mary, M. C. (2014). Challenges and strategies to improve tomato competitiveness along the tomato value chain in Kenya. *International Journal of Business and Management*, *9*(9), 205.

Ghazy, N., & El-Nahrawy, S. (2021). Siderophore production by *Bacillus subtilis* MF497446 and *Pseudomonas koreensis* MG209738 and their efficacy in controlling *Cephalosporium maydis* in maize plant. *Archives of microbiology*, *203*, 1195-1209. https://doi.org/10.1007/s00203-020-02113-5

Ghori, N. H., Ghori, T., Hayat, M. Q., Imadi, S. R., Gul, A., Altay, V., & Ozturk, M. (2019). Heavy metal stress and responses in plants. *International journal of environmental science and technology*, *16*, 1807-1828.

Ghosh, A. K., Tandon, R. N., Bhargava, S. N., and Srivastava, M. P. Vitamin C content of guava fruits after fungal infection. *Naturwissenschaften*. 16 (1965) 478-478.

Ghosh, S. K., & Pal, T. (2007). Interparticle coupling effect on the surface plasmon resonance of gold nanoparticles: from theory to applications. *Chemical reviews*, *107*(11), 4797-4862.

Ghuffar, S., Ahmad, M. Z., Irshad, G., Zeshan, M. A., Qadir, A., Anwaar, H. A., and Farooq, U. First report of Aspergillus niger causing black rot of grapes in Pakistan. *Plant Disease*. 05 (2021) 1570.

Gil, S. S., Cappellari, L. D. R., Giordano, W., & Banchio, E. (2023). Antifungal Activity and Alleviation of Salt Stress by Volatile Organic Compounds of Native *Pseudomonas* Obtained from *Mentha piperita*. *Plants*, *12*(7), 1488.

González-Estrada, R. R., Blancas-Benitez, F. J., Moreno-Hernández, C. L., Coronado-Partida, L., Ledezma-Delgadillo, A., & Gutiérrez-Martínez, P. (2019). Nanotechnology: A promising alternative for the control of postharvest pathogens in fruits. In *Nanotechnology for Agriculture: Crop Production & Protection* (pp. 323-337). Singapore: Springer Singapore.

Gora, J. S., Verma, A. K., Singh, J., & Choudhary, D. R. (2019). Climate change and production of horticultural crops. In *Agricultural Impacts of Climate Change [Volume 1]* (pp. 45-61). CRC Press La Pena, R. D., & Hughes, J. (2007). Improving vegetable productivity in a variable and changing climate.

Gorin, N., & Heidema, F. T. (1976). Peroxidase activity in Golden Delicious apples as a possible parameter of ripening and senescence. *Journal of agricultural and food chemistry*, *24*(1), 200-201.

Goupil P, Souguir D, Ferjani E, Faure O, Hitmi A, Ledoigt G (2009) Expression of stress-related genes in tomato plants exposed to arsenic and chromium in nutrient solution. J Plant Physio l66(13):1446-52.

Haider, S., Iqbal, J., Naseer, S., Shaukat, M., Abbasi, B. A., Yaseen, T., ... & Mahmood, T. (2022). Unfolding molecular switches in plant heat stress resistance: A comprehensive review. *Plant Cell Reports*, *41*(3), 775-798.

Haneefa, M. M. Green synthesis characterization and antimicrobial activity evaluation of manganese oxide nanoparticles and comparative studies with salicylalchitosan functionalized nanoform. *Asian Journal of Pharmaceutics (AJP)*. *11* (2017) 01

Hano, C., & Abbasi, B. H. (2021). Plant-based green synthesis of nanoparticles: Production, characterization and applications. *Biomolecules*, *12*(1), 31.

Hanson, P. (1996). Cultivation and breeding of tomato. In *Training workshop on vegetable cultivation and seed production technology* (No. AVRDC Staff Publication). AVRDC.

Haroon U, Khizar M, Liaquat F, Ali M, Akbar M, Tahir K, Batool S S, Kamal A, Chaudhary HJ, Munis MFH (2021) Halotolerant plant growth-promoting rhizobacteria induce salinity tolerance in wheat by enhancing the expression of SOS genes. J Plant Growth Regul 1-14.

Haroon, U., Liaquat, F., Khizar, M., Akbar, M., Saleem, H., Arif, S., ... & Munis, M. F. H. (2021). Isolation of halotolerant bacteria from rhizosphere of Khewra salt mine halophytes and their application to induce salt tolerance in wheat. *Geomicrobiology Journal*, *38*(9), 768-775.

Hassanzadeh, M., Ebadi, A., Panahyan-e-Kivi, M., Eshghi, A. G., Jamaati-e-Somarin, S., Saeidi, M., & Zabihi-e-Mahmoodabad, R. (2009). Evaluation of drought stress on relative water content and chlorophyll content of sesame (*Sesamum indicum* L.) genotypes at early flowering stage. *Research Journal of Environmental Sciences*, *3*(3), 345-350.

Heath RL, Packer L (1968) Photoperoxidation in isolated chloroplasts: I. Kinetics and stoichiometry of fatty acid peroxidation. Arch Biochem Biophys 125(1):189-198.

Heaton JW, Lencki RW, Marangoni AG (1996) Kinetic model for chlorophyll degradation in green tissue. J Agric Food Chem 44(2):399-402.

Hernández-Baranda, Y., Rodríguez-Hernández, P., Peña-Icart, M., Meriño-Hernández, Y., & Cartya-Rubio, O. (2019). Toxicity of Cadmium in plants and strategies to reduce its effects. Case study: The tomato. *Cultivos Tropicales*, *40*(3), e10.

Herrera-Téllez, V. I., Cruz-Olmedo, A. K., Plasencia, J., Gavilanes-Ruíz, M., Arce-Cervantes, O., Hernández-León, S., & Saucedo-García, M. (2019). The protective effect of *Trichoderma asperellum* on tomato plants against *Fusarium oxysporum* and *Botrytis cinerea* diseases involves inhibition of reactive oxygen species production. *International journal of molecular sciences*, *20*(8), 2007.

Husain, M., Saber, A. T., Guo, C., Jacobsen, N. R., Jensen, K. A., Yauk, C. L., ... & Halappanavar, S. (2013). Pulmonary instillation of low doses of titanium dioxide nanoparticles in mice leads to particle retention and gene expression changes in the absence of inflammation. *Toxicology and applied pharmacology*, *269*(3), 250-262.

Hussain, I., Alam, S. S., Khan, I., Shah, B., Naeem, A., Khan, N., ... & Iqbal, M. (2016). Study on the biological control of *Fusarium* wilt of tomato. *J Entomol Zool Studies*, *4*(2), 525-8.

Hyder, A., Buledi, J. A., Nawaz, M., Rajpar, D. B., Orooji, Y., Yola, M. L., ... & Solangi, A. R. (2022). Identification of heavy metal ions from aqueous environment through gold, Silver and Copper Nanoparticles: An excellent colorimetric approach. *Environmental research*, *205*, 112475.

Irede, E. L., Awoyemi, R. F., Owolabi, B., Aworinde, O. R., Kajola, R. O., Hazeez, A., ... & Ifijen, I. H. (2024). Cutting-edge developments in zinc oxide nanoparticles: synthesis and applications for enhanced antimicrobial and UV protection in healthcare solutions. *RSC advances*, *14*(29), 20992-21034.

Irshad MK, Chen C, Noman A, Ibrahim M, Adeel M, Shang J (2020) Goethite-modified biochar restricts the mobility and transfer of cadmium in soil-rice system. Chemosphere 242:125152.

Ishfaq, A., Shahid, M., Nawaz, M., Ibrar, D., Hussain, S., Shahzad, T., ... & Khan, S. (2023). Remediation of wastewater by biosynthesized manganese oxide nanoparticles and its effects on development of wheat seedlings. *Frontiers in Plant Science*, *14*, 1263813.

ISLAM, M. R. (2016). *Performance of some tomato varieties against whitefly and fruit borer* (Doctoral dissertation, DEPARTMENT OF ENTOMOLOGY, SHER-E-BANGLA AGRICULTURAL UNIVERSITY, DHAKA.).

Jabbar, K. Q., Barzinjy, A. A., & Hamad, S. M. (2022). Iron oxide nanoparticles: Preparation methods, functions, adsorption and coagulation/flocculation in wastewater treatment. *Environmental Nanotechnology, Monitoring & Management*, *17*, 100661.

Jabeen, H., Haroon, U., Bilal, A., Anjum, L., Kamal, A., Bibi, H., ... & Munis, M. F. H. (2023). Application of phyto-fabricated zinc oxide nanoparticles to diminish brown spot of pear whilst maintaining its quality. *Microscopy Research and Technique*, *86*(7), 834-845.

Jampílek, J., & Kráľová, K. (2019). Beneficial effects of metal-and metalloid-based nanoparticles on crop production. *Nanotechnology for Agriculture: Advances for Sustainable Agriculture*, 161-219.

Jan, A. U., Hadi, F., Midrarullah, A. A., & Rahman, K. (2017). Role of CBF/DREB gene expression in abiotic stress tolerance. A review. *Int. J. Hortic. Agric.*, *2*, 1-12.

Jana S, Choudhuri M A (1981) Glycolate metabolism of three submersed aquatic angiosperms: effect of heavy metals. Aquat Bot 11:67-77.

Janisiewicz, W. J., and Korsten, L. Biological control of postharvest diseases of fruits. *Annual Review of Phytopathology*, *40* (2002) 411-441.

Jayandran, M., Haneefa, M. M., and Balasubramanian, V. Green synthesis and characterization of Manganese nanoparticles using natural plant extracts and its evaluation of antimicrobial activity. *Journal of Applied Pharmaceutical Science*. 12 (2015) 105-110.

Jośko, I., Kusiak, M., Xing, B., & Oleszczuk, P. (2021). Combined effect of nano-CuO and nano-ZnO in plant-related system: From bioavailability in soil to transcriptional regulation of metal homeostasis in barley. *Journal of hazardous materials*, *416*, 126230.

Kamal, A., Haroon, U., Manghwar, H., Alamer, K. H., Alsudays, I. M., Althobaiti, A. T., ... & Munis, M. F. H. (2022). Biological Applications of Ball-Milled Synthesized Biochar-Zinc Oxide Nanocomposite Using Zea mays L. Molecules, 27(16), 5333.

Kamal, A., Saleem, M. H., Alshaya, H., Okla, M. K., Chaudhary, H. J., & Munis, M. F. H. (2022). Ball-milled synthesis of maize biochar-ZnO nanocomposite (MB-ZnO) and estimation of its photocatalytic ability against different organic and inorganic pollutants. *Journal of Saudi Chemical Society*, *26*(3), 101445.

Kasote DM, Lee JH, Jayaprakasha GK, Patil BS (2019) Seed priming with iron oxide nanoparticles modulate antioxidant potential and defense-linked hormones in watermelon seedlings. ACS Sustain Chem Eng 7:5142-5151.

Kasote DM, Lee JH, Jayaprakasha GK, Patil BS (2021) Manganese oxide nanoparticles as safer seed priming agent to improve chlorophyll and antioxidant profiles in watermelon seedlings. Nanomater 11(4):1016.

Kejela, T., Thakkar, V. R., & Patel, R. R. (2017). A novel strain of *Pseudomonas* inhibits *Colletotrichum gloeosporioides* and *Fusarium oxysporum* infections and promotes germination of coffee. *Rhizosphere*, *4*, 9-15. https://doi.org/10.1016/j.rhisph.2017.05.002

Khan, A., Bano, A., Khan, R. A., & Khan, N. (2023). Role of PGPR in suppressing the growth of *Macrophomina phaseolina* by regulating antioxidant enzymes and secondary metabolites in *Vigna radiata* L. Wilczek. *South African Journal of Botany*, *158*, 443-451.

Khan, F., Shahid, A., Zhu, H., Wang, N., Javed, M. R., Ahmad, N., ... & Mehmood, M. A. (2022). Prospects of algae-based green synthesis of nanoparticles for environmental applications. *Chemosphere*, *293*, 133571.

Khan, M. R., & Khan, S. M. (2001). Biomanagement of *Fusarium* wilt of tomato by the soil application of certain phosphatesolubilizing microorganisms. *International journal of pest management*, *47*(3), 227-231.

Khan, S., & Hossain, M. K. (2022). Classification and properties of nanoparticles. In *Nanoparticle-based polymer composites* (pp. 15-54). Woodhead Publishing.

Kistan, A., Mohan, S., Mahalakshmi, S., Jayanthi, A., Ramya, A. J., & Karthik, P. S. (2024). Sol-Gel technique, characterization and photocatalytic degradation activity of Manganese doped ZnO nanoparticles. *Main Group Chemistry*, *23*(1), 17-30.

Knapp, S., & Peralta, I. E. (2016). The tomato (Solanum lycopersicum L., Solanaceae) and its botanical relatives. *The tomato genome*, 7-21.

Kontaxi, N. I., Panoutsopoulou, E., Ofrydopolou, A., & Tsoupras, A. (2024). Anti-Inflammatory Benefits of Grape Pomace and Tomato Bioactives as Ingredients in Sun Oils against UV Radiation for Skin Protection. *Applied Sciences (2076-3417)*, *14*(14).

Kruis, F. E., Fissan, H., & Peled, A. (1998). Synthesis of nanoparticles in the gas phase for electronic, optical and magnetic applications—a review. *Journal of aerosol science*, *29*(5-6), 511-535.

Kulabhusan, P. K., Tripathi, A., & Kant, K. (2022). Gold nanoparticles and plant pathogens: an overview and prospective for biosensing in forestry. *Sensors*, *22*(3), 1259.

Kumar, H., Manisha, S. P., and Sangwan, P. Synthesis and characterization of MnO2 nanoparticles using co-precipitation technique. *International Journal of Chemistry and Chemical Engineering*. 3 (2013) 155-60.

Kumar, K. S., Paswan, S., & Srivastava, S. (2012). Tomato-a natural medicine and its health benefits. *Journal of Pharmacognosy and Phytochemistry*, *1*(1), 33-43.

Kumar, S. P., Srinivasulu, A., & Babu, K. R. (2018). Symptomology of major fungal diseases on tomato and its management. *Journal of Pharmacognosy and Phytochemistry*, *7*(6), 1817-1821.

Kuo, C. H., Li, W., Pahalagedara, L., El-Sawy, A. M., Kriz, D., Genz, N., ... & He, J. (2015). Understanding the role of gold nanoparticles in enhancing the catalytic activity of manganese oxides in water oxidation reactions. *Angewandte Chemie International Edition*, *54*(8), 2345-2350.

La Torre, A., Iovino, V., & Caradonia, F. (2018). Copper in plant protection: Current situation and prospects. *Phytopathologia Mediterranea*, *57*(2), 201-236.

Lamhamdi M, El Galiou O, Bakrim A, Nóvoa-Muñoz JC, Arias-Estevez M, Aarab A, Lafont R (2013) Effect of lead stress on mineral content and growth of wheat (Triticum aestivum) and spinach (*Spinacia oleracea*) seedlings. Saudi J Biol Sci 20(1):29-36.

Lanham-New, S. A. (2008). Importance of calcium, vitamin D and vitamin K for osteoporosis prevention and treatment: symposium on 'diet and bone health'. *Proceedings of the Nutrition Society*, *67*(2), 163-176.

Lau EC, Carvalho LB, Pereira AE, Montanha GS, Corrêa CG, Carvalho HW, Ganin AY, Fraceto LF, Yiu HH (2020) Localization of coated iron oxide (Fe_3O_4) nanoparticles on tomato seeds and their effects on growth. ACS Appl Bio Mater 3(7):4109-4117.

López-Yerena, A., Domínguez-López, I., Abuhabib, M. M., Lamuela-Raventós, R. M., Vallverdú-Queralt, A., & Pérez, M. (2023). Tomato wastes and by-products: upcoming sources of polyphenols and carotenoids for food, nutraceutical, and pharma applications. *Critical Reviews in Food Science and Nutrition*, 1-18.

Loreto, F., & Velikova, V. (2001). Isoprene produced by leaves protects the photosynthetic apparatus against ozone damage, quenches ozone products, and reduces lipid peroxidation of cellular membranes. *Plant Physiology*, *127*(4), 1781-1787.

Luck, H. (1974). Estimation of catalase, methods in enzymatic analysis. *Bergmeyer, HU, & Gawhn, K.(Eds.)*, 885-894.

Ma, M., Taylor, P. W., Chen, D., Vaghefi, N., & He, J. Z. (2023). Major soilborne pathogens of field processing tomatoes and management strategies. *Microorganisms*, *11*(2), 263.

Madeira, A. C., De Varennes, A., Abreu, M. M., Esteves, C., & Magalhães, M. C. F. (2012). Tomato and parsley growth, arsenic uptake and translocation in a contaminated amended soil. *Journal of Geochemical Exploration*, *123*, 114-121.

Mahlambi, M. M., Ngila, C. J., & Mamba, B. B. (2015). Recent developments in environmental photocatalytic degradation of organic pollutants: the case of titanium dioxide nanoparticles—a review. *Journal of Nanomaterials*, *2015*(1), 790173.

Maity, D., Gupta, U., & Saha, S. (2022). Biosynthesized metal oxide nanoparticles for sustainable agriculture: next-generation nanotechnology for crop production, protection and management. *Nanoscale*, *14*(38), 13950-13989.

Majeed, A., & Muhammad, Z. (2019). Salinity: a major agricultural problem—causes, impacts on crop productivity and management strategies. *Plant abiotic stress tolerance: Agronomic, molecular and biotechnological approaches*, 83-99.

Malar S., Shivendra Vikram S, Favas PJC, Perumal V (2016) Lead heavy metal toxicity induced changes on growth and antioxidative enzymes level in water hyacinths [*Eichhornia crassipes* (Mart.)]. Bot Stud 55(1):1-11.

Martí, R., Roselló, S., & Cebolla-Cornejo, J. (2016). Tomato as a source of carotenoids and polyphenols targeted to cancer prevention. *Cancers*, *8*(6), 58.

Meena, M., Pilania, S., Pal, A., Mandhania, S., Bhushan, B., Kumar, S., and Saharan, V. Cu-chitosan nano-net improves keeping quality of tomato by modulating physio-biochemical responses. *Scientific Reports*. *1* (2020) 1-11.

Mohamed, A. H., Abd El-Megeed, F. H., Hassanein, N. M., Youseif, S. H., Farag, P. F., Saleh, S. A., ... & Abdel-Azeem, A. M. (2022). Native rhizospheric and endophytic fungi as sustainable sources of plant growth promoting traits to improve wheat growth under low nitrogen input. *Journal of Fungi*, *8*(2), 94.

Mohamed, H. I., Abd-Elsalam, K. A., Tmam, A. M., & Sofy, M. R. (2021). Silver-based nanomaterials for plant diseases management: Today and future perspectives. In *Silver Nanomaterials for Agri-Food Applications* (pp. 495-526). Elsevier.

Mohiudden, A. S., Mohammed, M. J., & Jassim, M. A. (2023, July). Biosynthesis of Manganese Nanoparticle Mn-NPs by the Fungus Aspergillus niger. In *IOP Conference Series: Earth and Environmental Science* (Vol. 1214, No. 1, p. 012009). IOP Publishing.

Moorthy SK, Ashok CH, Rao KV, Viswanathan C (2015) Synthesis and characterization of MgO nanoparticles by Neem leaves through green method. Mater Today Proc 2(9):4360-4368.

Moradinezhad, F., & Ranjbar, A. (2023). Advances in postharvest diseases management of fruits and vegetables: A review. *Horticulturae*, *9*(10), 1099.

Mordente, A. L. V. A. R. O., Guantario, B., Meucci, E., Silvestrini, A., Lombardi, E., E Martorana, G., ... & Bohm, V. (2011). Lycopene and cardiovascular diseases: an update. *Current medicinal chemistry*, *18*(8), 1146-1163.

Murali, M., Sudisha, J., Amruthesh, K. N., Ito, S. I., & Shetty, H. S. (2013). Rhizosphere fungus *Penicillium chrysogenum* promotes growth and induces defence-related genes and downy mildew disease resistance in pearl millet. *Plant Biology*, *15*(1), 111-118.

Myung, I. S., Kim, D. G., An, S. H., Lee, Y. K., & Kim, W. G. (2008). First report of bacterial canker of tomato caused by Clavibacter michiganensis subsp. michiganensis in Korea. *Plant Disease*, *92*(10), 1472-1472.

Nair PMG, Chung IM (2014) Assessment of silver nanoparticle-induced physiological and molecular changes in *Arabidopsis thaliana*. Environ Sci Pollut Res 21:8858-8869.

Nasrin, L., Podder, S., & Mahmud, M. R. (2018). Investigation of Potential Biological Control of Fusarium Oxysporum f. sp. Lycopersici by Plant Extracts, Antagonistic sp. and Chemical Elicitors.

Natsiopoulos, D., Tziolias, A., Lagogiannis, I., Mantzoukas, S., & Eliopoulos, P. A. (2022). Growth-promoting and protective effect of *Trichoderma atrobrunneum* and *T. simmonsii* on tomato against soil-borne fungal pathogens. *Crops*, *2*(3), 202-217.

Ndondo, J. T. K. (2023). Review of the Food and Agriculture Organisation (FAO) Strategic Priorities on Food Safety 2023. In *Food Safety-New Insights*. IntechOpen.

Nicola, S., Tibaldi, G., Fontana, E., Crops, A. V., & Plants, A. (2009). Tomato production systems and their application to the tropics. *Acta horticulturae*, *821*(821), 27-34.

Noman, M., Ahmed, T., Ijaz, U., Shahid, M., Nazir, M. M., Azizullah, ... & Song, F. (2023). Bio-functionalized manganese nanoparticles suppress Fusarium wilt in watermelon (Citrullus

lanatus L.) by infection disruption, host defense response potentiation, and soil microbial community modulation. *Small*, *19*(2), 2205687.

Ornelas-Paz, J. D. J., Quintana-Gallegos, B. M., Escalante-Minakata, P., Reyes-Hernández, J., Pérez-Martínez, J. D., Rios-Velasco, C., & Ruiz-Cruz, S. (2018). Relationship between the firmness of Golden Delicious apples and the physicochemical characteristics of the fruits and their pectin during development and ripening. *Journal of food science and technology*, *55*, 33-41.

Ortega, S., Ibáñez, M., Liu, Y., Zhang, Y., Kovalenko, M. V., Cadavid, D., & Cabot, A. (2017). Bottom-up engineering of thermoelectric nanomaterials and devices from solution-processed nanoparticle building blocks. *Chemical Society Reviews*, *46*(12), 3510-3528.

Osdaghi, E. (2023). Pectobacterium carotovorum (bacterial soft rot).

Pacios-Michelena, S., González, C. N. A., Herrera, R. R., Alvarez-Perez, O. B., González, M. L. C., Valdés, R. A., ... & Iliná, A. (2023). Biomass from phytopathogens and culture conditions improve Penicillium chrysogenum antimicrobial activity and antifungal compounds production. *Environmental Quality Management*, *33*(1), 349-358.

Paladini, F., & Pollini, M. (2019). Antimicrobial silver nanoparticles for wound healing application: progress and future trends. *Materials*, *12*(16), 2540.

Pandey, R. (2015). Mineral nutrition of plants. *Plant Biology and Biotechnology: Volume I: Plant Diversity, Organization, Function and Improvement*, 499-538.

Panno, S., Davino, S., Caruso, A. G., Bertacca, S., Crnogorac, A., Mandić, A., ... & Matić, S. (2021). A review of the most common and economically important diseases that undermine the cultivation of tomato crop in the mediterranean basin. *Agronomy*, *11*(11), 2188.

Pariona, N., Mtz-Enriquez, A. I., Sánchez-Rangel, D., Carrión, G., Paraguay-Delgado, F., & Rosas-Saito, G. (2019). Green-synthesized copper nanoparticles as a potential antifungal against plant pathogens. *RSC advances*, *9*(33), 18835-18843.

Parveen, A., Rai, G. K., Mushtaq, M., Singh, M., Rai, P. K., Rai, S. K., & Kundoo, A. A. (2019). Deciphering the morphological, physiological and biochemical mechanism associated with drought stress tolerance in tomato genotypes. *Int. J. Curr. Microbiol. Appl. Sci*, *8*, 227-255.

Parveen, S., Wani, A. H., Bhat, M. Y., Pala, S. A., and Ganie, A. A. Biology and management of *Aspergillus niger* Van. Tiegh causing black mold rot of pear (*Pyrus communis* L.) in Kashmir Valley, India. *International Journal of Advanced Research*. 6 (2014) 24-34.

Pasquariello, M. S., Rega, P., Migliozzi, T., Capuano, L. R., Scortichini, M., and Petriccione, M. Effect of cold storage and shelf life on physiological and quality traits of early ripening pear cultivars. *Scientia Horticulturae*. *162* (2013) 341-350.

Patsula, V., Moskvin, M., Dutz, S., & Horák, D. (2016). Size-dependent magnetic properties of iron oxide nanoparticles. *Journal of Physics and Chemistry of Solids*, *88*, 24-30.

Perfileva, A. I., & Krutovsky, K. V. (2024). Manganese Nanoparticles: Synthesis, Mechanisms of Influence on Plant Resistance to Stress, and Prospects for Application in Agricultural Chemistry. *Journal of Agricultural and Food Chemistry*, *72*(14), 7564-7585.

Perfileva, A. I., & Krutovsky, K. V. (2024). Manganese Nanoparticles: Synthesis, Mechanisms of Influence on Plant Resistance to Stress, and Prospects for Application in Agricultural Chemistry. *Journal of Agricultural and Food Chemistry*, *72*(14), 7564-7585.

Perveen, R., Suleria, H. A. R., Anjum, F. M., Butt, M. S., Pasha, I., & Ahmad, S. (2015). Tomato (Solanum lycopersicum) carotenoids and lycopenes chemistry; metabolism, absorption, nutrition, and allied health claims—A comprehensive review. *Critical reviews in food science and nutrition*, *55*(7), 919-929.

Petro-Turza, M. (1986). Flavor of tomato and tomato products. *Food Reviews International*, *2*(3), 309-351.

Pinhero R G, Rao M V, Paliyath G, Murr D P, Fletcher R A (1997) Changes in activities of antioxidant enzymes and their relationship to genetic and paclobutrazol-induced chilling tolerance of maize seedlings. Plant physiol 114(2):695-704.

Pretorius, H. (2009). *The ability of a novel compound to enhance the effect of urea on nitrogen deficient tomatoes* (Doctoral dissertation, University of the Free State).

Przybylska, S., & Tokarczyk, G. (2022). Lycopene in the prevention of cardiovascular diseases. *International Journal of Molecular Sciences*, *23*(4), 1957.

Pucci, A. (2015). Characterization of tomato (Solanum lycopersicum L.) male sterile mutants putatively affected in class B MADS-box transcription factors.

Qadir, M., Sharma, B. R., Bruggeman, A., Choukr-Allah, R., & Karajeh, F. (2007). Non-conventional water resources and opportunities for water augmentation to achieve food security in water scarce countries. *Agricultural water management*, *87*(1), 2-22.

Qadri, R., Azam, M., Khan, I., Yang, Y., Ejaz, S., Akram, M. T., & Khan, M. A. (2020). Conventional and modern technologies for the management of post-harvest diseases. *Plant Disease Management Strategies for Sustainable Agriculture through Traditional and Modern Approaches*, 137-172.

Qi, S., Zhang, S., Islam, M. M., El-Sappah, A. H., Zhang, F., & Liang, Y. (2021). Natural resources resistance to tomato spotted wilt virus (TSWV) in tomato (Solanum lycopersicum). *International Journal of Molecular Sciences*, *22*(20), 10978.

Radhakrishnan, R., Shim, K. B., Lee, B. W., Hwang, C. D., Pae, S. B., Park, C. H., ... & Baek, I. Y. (2013). IAA-producing *Penicillium* sp. NICS01 triggers plant growth and suppresses *Fusarium* sp.-induced oxidative stress in sesame (*Sesamum indicum* L.). *J Microbiol Biotechnol*, *23*(6), 856-63.

Ramasamy, S., & Ravishankar, M. (2018). Integrated pest management strategies for tomato under protected structures. In *Sustainable Management of Arthropod Pests of Tomato* (pp. 313-322). Academic Press.

Ramzan M, Ayub F, Shah A A, Naz G, Shah A N, Malik A, Sardar R, Telesińsk A, Kalaji HM, Dessoky E S, Elgawad H (2022) Synergistic effect of zinc oxide nanoparticles and Moringa oleifera leaf extract alleviates cadmium toxicity in *Linum usitatissimum*: Antioxidants and physiochemical studies. Front Plant Sci 13.

Rao, A. V., & Balachandran, B. (2002). Role of oxidative stress and antioxidants in neurodegenerative diseases. *Nutritional neuroscience*, *5*(5), 291-309.

Rao, N. S., Laxman, R. H., & Shivashankara, K. S. (2016). Physiological and morphological responses of horticultural crops to abiotic stresses. *Abiotic stress physiology of horticultural crops*, 3-17.

Rayner, M. H., & Sadler, P. J. (1990). Precipitation of cadmium in a bacterial culture medium: Luria-Bertani broth. *FEMS Microbiology Letters*, *71*(3), 253-257.

Raza, A., Khandelwal, K., Pandit, S., Singh, M., Kumar, S., Rustagi, S., ... & Prasad, R. (2024). Exploring the potential of metallic and metal oxide nanoparticles for reinforced disease management in agricultural systems: A comprehensive review. *Environmental Nanotechnology, Monitoring & Management*, 100998.

Rizwan M, Ali S, Qayyum M F, Ok Y S, Adrees M, Ibrahim M, Abbas F (2017) Effect of metal and metal oxide nanoparticles on growth and physiology of globally important food crops: A critical review. J Hazard Mater 322:2-16.

Robertson, L. D., & Labate, J. A. (2007). Genetic resources of tomato (Lycopersicon esculentum Mill.) and wild relatives. *Genetic improvement of Solanaceous crops*, *2*, 25-75.

Rodrigues, B. B., & Kakde, U. B. (2019). Post harvest fungi associated with Solanum lycopersicum (Tomato) fruits collected from different markets of Mumbai. *Online International Interdisciplinary Research Journal*, *9*(1), 52-60.

Roșca, M., Mihalache, G., & Stoleru, V. (2023). Tomato responses to salinity stress: From morphological traits to genetic changes. *Frontiers in plant science*, *14*, 1118383.

Rot, B. E. (2021). Tomato: Physiological Disorders and Their Management.

Sachdev, S., Bauddh, K., & Singh, R. P. (2022). Native Rhizospheric Microbes Mediated Management of Biotic Stress and Growth Promotion of Tomato. *Sustainability*, *15*(1), 593.

Sadiq, S. I., & Aliyu, T. I. (2018). Comparative nutritional composition of raw and canned tomatoes Solanum lycopersicum (Lycopersicon esculentum) Dutse Market Jigawa State, Nigeria. *Dutse Journal of Pure and Applied Sciences*, *4*(2), 424-433.

Sáez, V., & Mason, T. J. (2009). Sonoelectrochemical synthesis of nanoparticles. *Molecules*, *14*(10), 4284-4299.

Sakharov I Y, Galaev I Y, Sakharova I V, Pletjushkina O Y (2001) Peroxidase from leaves of royal palm tree *Roystonea regia*: purification and some properties. Plant Sci 161(5):853-860.

Salehi, B., Sharifi-Rad, R., Sharopov, F., Namiesnik, J., Roointan, A., Kamle, M., ... & Sharifi-Rad, J. (2019). Beneficial effects and potential risks of tomato consumption for human health: An overview. *Nutrition*, *62*, 201-208.

Sallam, N. M., AbdElfatah, H. A. S., Dawood, M. F., Hassan, E. A., Mohamed, M. S., & Khalil Bagy, H. M. (2021). Physiological and histopathological assessments of the susceptibility of different tomato (*Solanum lycopersicum*) cultivars to early blight disease. European Journal of Plant Pathology, 160, 541-556.

Sánchez-Sánchez, M., Aispuro-Hernández, E., Quintana-Obregón, E. A., del Carmen Vargas-Arispuro, I., & Martínez-Téllez, M. Á. (2024). Estimating tomato production losses due to plant viruses, a look at the past and new challenges. *Comunicata Scientiae*, *15*, e4247-e4247.

Sanjinés, R., Abad, M. D., Vâju, C., Smajda, R., Mionić, M., & Magrez, A. (2011). Electrical properties and applications of carbon based nanocomposite materials: An overview. *Surface and coatings technology*, *206*(4), 727-733.

Saqib S, Munis M F H, Zaman W, Ullah F, Shah S N, Ayaz A, Bahadur S (2019) Synthesis, characterization and use of iron oxide nano particles for antibacterial activity. Microsc Res Rech 82(4): 415-420.

Saritha, B., Panneerselvam, P., & Ganeshamurthy, A. N. (2015). Antagonistic potential of mycorrhiza associated *Pseudomonas putida* against soil borne fungal pathogens. *Plant Arch*, *15*(2), 763-768.

Schnoor, B., Elhendawy, A., Joseph, S., Putman, M., Chacón-Cerdas, R., Flores-Mora, D., ... & Salvador-Morales, C. (2018). Engineering atrazine loaded poly (lactic-co-glycolic acid) nanoparticles to ameliorate environmental challenges. *Journal of agricultural and food chemistry*, *66*(30), 7889-7898.

Schuster B, Retey J (1995) The mechanism of action of phenylalanine ammonia-lyase: the role of prosthetic dehydroalanine. Proc Natl Acad Sci 92(18):8433-8437

Shah, I. H., Manzoor, M. A., Sabir, I. A., Ashraf, M., Gulzar, S., Chang, L., & Zhang, Y. (2022). A green and environmental sustainable approach to synthesis the Mn oxide nanomaterial from Punica granatum leaf extracts and its in vitro biological applications. *Environmental Monitoring and Assessment*, *194*(12), 921.

Shang, Y., Hasan, M. K., Ahammed, G. J., Li, M., Yin, H., & Zhou, J. (2019). Applications of nanotechnology in plant growth and crop protection: a review. *Molecules*, *24*(14), 2558.

Shao, G., Cheng, X., Liu, N., & Zhang, Z. (2016). Effect of drought pretreatment before anthesis and post-anthesis waterlogging on water relation, photosynthesis, and growth of tomatoes. *Archives of Agronomy and Soil Science*, *62*(7), 935-946.

Sharma, J., Singh, V. K., Kumar, A., Shankarayan, R., & Mallubhotla, S. (2018). Role of silver nanoparticles in treatment of plant diseases. *Microbial Biotechnology: Volume 2. Application in Food and Pharmacology*, 435-454.

Sharma, S., Sharma, J., Soni, V., Kalaji, H. M., & Elsheery, N. I. (2021). Waterlogging tolerance: A review on regulative morpho-physiological homeostasis of crop plants. *Journal of Water and Land Development*, 16-28.

Silva S, Pinto G, Santos C (2017) Low doses of Pb affected *Lactuca sativa* photosynthetic performance. Photosynth 55(1):50-57

Singh, S. (2018). Agrometeorological requirements for sustainable vegetable crops production. *J. Food Prot*, *2*(3), 1-22.

Singh, S. R., Krishnamurthy, N. B., & Mathew, B. B. (2014). A review on recent diseases caused by microbes. *J Appl Environ Microbiol*, *2*(4), 106-115.

Singh, V. K., Singh, A. K., Singh, P. P., & Kumar, A. (2018). Interaction of plant growth promoting bacteria with tomato under abiotic stress: a review. *Agriculture, Ecosystems & Environment*, *267*, 129-140.

Sinha, A., Singh, V. N., Mehta, B. R., & Khare, S. K. (2011). Synthesis and characterization of monodispersed orthorhombic manganese oxide nanoparticles produced by Bacillus sp. cells simultaneous to its bioremediation. *Journal of hazardous materials*, *192*(2), 620-627.

Slimestad, R., & Verheul, M. (2009). Review of flavonoids and other phenolics from fruits of different tomato (Lycopersicon esculentum Mill.) cultivars. *Journal of the Science of Food and Agriculture*, *89*(8), 1255-1270.

Smuleac, V., Varma, R., Sikdar, S., and Bhattacharyya, D. Green synthesis of Fe and Fe/Pd bimetallic nanoparticles in membranes for reductive degradation of chlorinated organics. *Journal of Membrane Science*. *379* (2011) 131-137.

Soliman, G. M. (2017). Nanoparticles as safe and effective delivery systems of antifungal agents: Achievements and challenges. *International journal of pharmaceutics*, *523*(1), 15-32.

Sousa, F., Ferreira, D., Reis, S., & Costa, P. (2020). Current insights on antifungal therapy: Novel nanotechnology approaches for drug delivery systems and new drugs from natural sources. *Pharmaceuticals*, *13*(9), 248.

Spaldon, S., Samnotra, R. K., & Chopra, S. (2015). Climate resilient technologies to meet the challenges in vegetable production. *Int Res Current Acad Review*, *3*(2), 28-47.

Srinivas, C., Devi, D. N., Murthy, K. N., Mohan, C. D., Lakshmeesha, T. R., Singh, B., ... & Srivastava, R. K. (2019). Fusarium oxysporum f. sp. lycopersici causal agent of vascular wilt disease of tomato: Biology to diversity–A review. *Saudi journal of biological sciences*, *26*(7), 1315-1324.

Srivastava, M. P., and Tandon, R. N. Influence of *Botryo diplodia* infection on the ascorbic acid content of two varieties of guava. *Experientia*. 12 (1966) 789-790.

Sudha, A., & Lakshmanan, P. (2009). Integrated disease management of powdery mildew (Leveillula taurica (Lev.) Arn.) of chilli (Capsicum annuum L.). *Archives of Phytopathology and Plant Protection*, *42*(4), 299-317.

Szabo, K., Dulf, F. V., Teleky, B. E., Eleni, P., Boukouvalas, C., Krokida, M., ... & Vodnar, D. C. (2021). Evaluation of the bioactive compounds found in tomato seed oil and tomato peels influenced by industrial heat treatments. *Foods*, *10*(1), 110.

Taylor, M. D., & Locascio, S. J. (2004). Blossom-end rot: a calcium deficiency. *Journal of Plant nutrition*, *27*(1), 123-139.

Thornton B, Basu C (2011) Real-time PCR (qPCR) primer design using free online software. Biochem Mol Biol Educ 39(2):145-54.

Tohill, B. C., & Joint, F. A. O. (2005). *Dietary intake of fruit and vegetables and management of body weight [electronic resource]*. World Health Organization.

Tsedaley, B. (2014). Late blight of potato (Phytophthora infestans) biology, economic importance and its management approaches. *Journal of Biology, Agriculture and Healthcare*, *4*(25), 215-225.

Tumburu, L., Andersen, C. P., Rygiewicz, P. T., & Reichman, J. R. (2017). Molecular and physiological responses to titanium dioxide and cerium oxide nanoparticles in Arabidopsis. *Environmental toxicology and chemistry*, *36*(1), 71-82.

Tutar, L., & Tutar, Y. (2010). Heat shock proteins; an overview. *Current Pharmaceutical Biotechnology*, *11*(2), 216-222.

Tyree, M. T., & Cochard, H. (2003). Vessel contents of leaves after excision: a test of the Scholander assumption. *Journal of Experimental Botany*, *54*(390), 2133-2139. https://doi.org/10.1093/jxb/erg237

Ul Hassan, M., Rasool, T., Iqbal, C., Arshad, A., Abrar, M., Abrar, M. M., ... & Fahad, S. (2021). Linking plants functioning to adaptive responses under heat stress conditions: a mechanistic review. *Journal of Plant Growth Regulation*, 1-18.

Ullah, S., & Ullah, R. (2019). Beneficial effects of several nanoparticles on the growth of different plants species. *Current Nanoscience*, *15*(5), 460-470.

Usman, M., Farooq, M., Wakeel, A., Nawaz, A., Cheema, S. A., ur Rehman, H., ... & Sanaullah, M. (2020). Nanotechnology in agriculture: Current status, challenges and future opportunities. *Science of the total environment*, *721*, 137778.

Vági, P., Preininger, E., Kovács, G. M., Kristóf, Z., Bóka, K., & Böddi, B. (2013). Structure of plants and fungi. *Eötvös Loránd University*, 1-109.

Van Andel, T., Vos, R. A., Michels, E., & Stefanaki, A. (2022). Sixteenth-century tomatoes in Europe: who saw them, what they looked like, and where they came from. *PeerJ*, *10*, e12790.

Venkatachalam P, Jayaraj M, Manikandan R, Geetha N, Rene E R, Sharma N C, Sahi S V (2017) Zinc oxide nanoparticles (ZnONPs) alleviate heavy metal-induced toxicity in *Leucaena leucocephala* seedlings: a physiochemical analysis. Plant Physiol Biochem 110:59-69.

Vetter, J. L., Steinberg, M. P., & Nelson, A. I. (1958). Enzyme assay, quantitative determination of peroxidase in sweet corn. *Journal of agricultural and food chemistry*, 6(1), 39-41.

Wang T, Lin J, Chen Z, Megharaj M, Naidu R (2014) Green synthesized iron nanoparticles by green tea and eucalyptus leaves extracts used for removal of nitrate in aqueous solution. J Clean Prod 83:413–419.

Weatherley, P. (1950). Studies in the water relations of the cotton plant. I. The field measurement of water deficits in leaves. *New Phytologist*, 81-97.

Weisburger, J. H. (1998). Evaluation of the evidence on the role of tomato products in disease prevention. *Proceedings of the Society for Experimental Biology and Medicine*, *218*(2), 140-143.

Wesemael, W., Viaene, N., & Moens, M. (2011). Root-knot nematodes (Meloidogyne spp.) in Europe. *Nematology*, *13*(1), 3-16.

Wheatherley P E (1950) Studies in the water relations of cotton plants. I. The field measurement of water deficit in leaves. New Phytol 49:81-87

White, T. J., Bruns, T., Lee, S. J. W. T., and Taylor, JAmplification and direct sequencing of fungal ribosomal RNA genes for phylogenetics. *PCR Protocols: A guide to methods and applications*. 1 (1990) 315-322.

Wijewardene, I., Shen, G., & Zhang, H. (2021). Enhancing crop yield by using Rubisco activase to improve photosynthesis under elevated temperatures. *Stress Biology*, *1*(1), 2z

Wolf, A. (2024). *The effect of foliar micronutrient applications on nutrient use efficiency in tomatoes* (Doctoral dissertation, Stellenbosch University).

World Health Organization (WHO) (1996) Permissible limits of heavy metals in soil and plants. Geneva, Switzerland, 1996.

Wu, X., Yu, L., & Pehrsson, P. R. (2022). Are processed tomato products as nutritious as fresh tomatoes? Scoping review on the effects of industrial processing on nutrients and bioactive compounds in tomatoes. *Advances in Nutrition*, *13*(1), 138-151.

Xu, H., Zeiger, B. W., & Suslick, K. S. (2013). Sonochemical synthesis of nanomaterials. *Chemical Society Reviews*, *42*(7), 2555-2567.

Yadav, A., Kumar, N., Upadhyay, A., Sethi, S., & Singh, A. (2022). Edible coating as postharvest management strategy for shelf-life extension of fresh tomato (Solanum lycopersicum L.): An overview. *Journal of Food Science*, *87*(6), 2256-2290.

Yadav, P., Bhaduri, A., & Thakur, A. (2023). Manganese oxide nanoparticles: an insight into structure, synthesis and applications. *ChemBioEng Reviews*, *10*(4), 510-528.

Yadav, S., Irfan, M., Ahmad, A., & Hayat, S. (2011). Causes of salinity and plant manifestations to salt stress: a review. *Journal of environmental biology*, *32*(5), 667.

Yadav, T. P., Yadav, R. M., & Singh, D. P. (2012). Mechanical milling: a top down approach for the synthesis of nanomaterials and nanocomposites. *Nanoscience and Nanotechnology*, *2*(3), 22-48.

Ye, H., Song, L., Chen, H., Valliyodan, B., Cheng, P., Ali, L., ... & Nguyen, H. T. (2018). A major natural genetic variation associated with root system architecture and plasticity improves waterlogging tolerance and yield in soybean. *Plant, Cell Environ*, *41*(9), 2169-2182.

Yetisgin, A. A., Cetinel, S., Zuvin, M., Kosar, A., & Kutlu, O. (2020). Therapeutic nanoparticles and their targeted delivery applications. *Molecules*, *25*(9), 2193.

Yin, M. M., Zheng, Y., & Chen, F. L. (2018). Pyraclostrobin-loaded poly (lactic-co-glycolic acid) nanospheres: Preparation and characteristics. *J Integrat Agriculture*, *17*(8), 1822-1832.

Yousaf, Z. (2007). *Taxonomic and biochemical studies of medicinally important species of slanaceae from Pakistan* (Doctoral dissertation, Quaid-i-Azam University Islamabad).

Zhang, H., Gong, H., & Zhou, X. (2009). Molecular characterization and pathogenicity of tomato yellow leaf curl virus in China. *Virus genes*, *39*, 249-255.

Zhang, X., Sathiyaseelan, A., Naveen, K. V., Lu, Y., & Wang, M. H. (2023). Research progress in green synthesis of manganese and manganese oxide nanoparticles in biomedical and environmental applications–A review. *Chemosphere*, *337*, 139312.

Zhang, Z. Q., Chen, T., Li, B. Q., Qin, G. Z., & Tian, S. P. (2021). Molecular basis of pathogenesis of postharvest pathogenic fungi and control strategy in fruits: progress and prospect. *Molecular horticulture*, *1*, 1-10.

Zhou, P., Adeel, M., Shakoor, N., Guo, M., Hao, Y., Azeem, I., ... & Rui, Y. (2020). Application of nanoparticles alleviates heavy metals stress and promotes plant growth: An overview. *Nanomaterials*, *11*(1), 26.

Zhu, T., Fonseca De Lima, C. F., & De Smet, I. (2021). The heat is on: how crop growth, development, and yield respond to high temperature. *Journal of Experimental Botany*, *72*(21), 7359-7373.

Zongzheng, Y., Xin, L., Zhong, L., Jinzhao, P., Jin, Q., and Wenyan, Y. Effect of Bacillus subtilis SY1 on antifungal activity and plant growth. *International Journal of Agricultural and Biological Engineering*. 4 (2010) 55-61.

Zulfiqar, U., Farooq, M., Hussain, S., Maqsood, M., Hussain, M., Ishfaq, M., ... & Anjum, M. Z. (2019). Lead toxicity in plants: Impacts and remediation. *Journal of environmental management*, *250*, 109557.

Physiological and Molecular Plant Pathology 127 (2023) 102126

Contents lists available at ScienceDirect

Physiological and Molecular Plant Pathology

journal homepage: www.elsevier.com/locate/pmpp

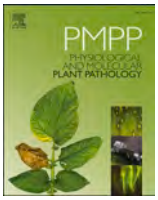

Biosynthesized manganese oxide nanoparticles maintain firmness of tomato fruit by modulating soluble solids and reducing sugars under biotic stress

Maryam Anar, Mahnoor Akbar, Kinza Tahir, Hassan Javed Chaudhary, Muhammad Farooq Hussain Munis *

Department of Plant Sciences, Faculty of Biological Sciences, Quaid-i-Azam University, Islamabad, 45320, Pakistan

ARTICLE INFO

Keywords:
Tomato
MnO NPs
Black rot
SEM
FTIR
Fruit firmness

ABSTRACT

Nanoparticles have been reported to mitigate biotic and abiotic stresses in different fruits and vegetables. In this study, tomato fruit with black rot symptoms were collected and diagnosed. To control this disease, manganese oxide nanoparticles (MnO NPs) were synthesized in bacterial broth-culture. Based on microscopic, morphological, and genetic analyses, the pathogen causing black rot disease was identified as *Aspergillus niger*. MnO NPs were successfully synthesized in broth-culture of *Bacillus subtilis*, following the process of calcination and characterized. Fourier transform infrared (FTIR) spectrum revealed the existence of stabilizing and reducing agents (carboxylic acid, alkenes, and alkyl halides) on the surface of MnO NPs. X-Ray diffraction (XRD) analysis revealed the size (39 nm) and crystal-like nature of synthesized MnO NPs. Energy-dispersive X-ray spectroscopy (EDX) described the mass percentage of manganese (26.4%) and oxygen (23.3%). Scanning electron microscopy (SEM) displayed nearly spherical shape of MnO NPs and confirmed their nano-size. These MnO NPs exhibited significant mycelial growth inhibition of *A. niger* and notable control of tomato black rot disease of tomato. Though, all concentrations exhibited considerable effects, medium concentration of MnO NPs (2.5 mg/mL) performed best in both *in vitro* and *in vivo* analyses. At this concentration, tomato fruit maintained higher percentage of soluble solids, total sugars, reducing sugars and fruit firmness. These results proved very effective application of bacteria supplemented MnO NPs for the control of black rot disease of tomato. To our knowledge, this is the first study of tomato black rot, caused by *A. niger* in Pakistan.

1. Introduction

Tomato is a member of Solanaceae family and it is scientifically described as "*Solanum lycopersicum* L". After potato (*Solanum tuberosum* L.), it is the second most consumed crop in the world. It is used as fresh fruit and processed for long-term usage. Health-promoting substances like carotenoids, vitamins, and phenolic compounds are present in tomato [1]. Fresh tomato fruit contains 1.7–4% sugar content and 0.3–0.6% organic acids (citric acid and malic acid), which are considered as the major quality attributes of tomato. Lycopene is the most common pigment and it gives red color to the tomato fruit [2]. According to Food and Agriculture Organization (FAO), in year 2020, 187 million tonnes (mT) of tomato fruit were produced, worldwide. Major tomato producing countries include China (64.86 mT), India (20.57 mT), Turkey (13.20 mT), USA (12.22 mT), Egypt (6.73 mT), Italy (6.24 mT) and Iran (5.78 mT). In the same reported period, Pakistan produced 0.575 mT of tomato [3].

Tomato is susceptible to a large range of pathogens including fungi, viruses, bacteria, phytoplasma, and viroid [4]. Among variety of diseases, fungal fruit rot is one of the predominant diseases of tomato. Most devastating pathogens of tomato include *Alternaria solani*, *Botrytis cinerea*, the oomycete *Phytophthora infestans* and *Fusarium oxysporum* f. sp. Lycopersici [5]. Grey mold of tomato, caused by *Botrytus cinerea,* has been reported in different parts of the world [6]. Various chemical pesticides have been used to combat fungal diseases. Direct application of chemical fungicides on fruits is hazardous and causes many human health issues. Chemical fungicides also disturb the environment by affecting other living organisms and their residues accumulate in the soil, animals, and plants [7]. These chemicals pesticides persist in the nature due to their non-degradable nature and cause extended destruction. Researchers are working to substitute these chemical pesticides with some environment-friendly bio-pesticides. To prevent and

* Corresponding author.
E-mail address: munis@qau.edu.pk (M.F.H. Munis).

https://doi.org/10.1016/j.pmpp.2023.102126
Received 17 July 2023; Received in revised form 21 August 2023; Accepted 23 August 2023
Available online 23 August 2023

address health issues of living organisms, different types of bio-fungicides are being used in the field. These bio-fungicides provide superior environmental and plant protection, since they are non-toxic. Utilizing readily biodegradable bio-fungicides might help in decreasing the threat posed by ever emerging disease incidences [8].

Nanotechnology is a rapidly developing discipline of research which involves the creation and synthesis of various nanomaterials. Nanotechnology is being used in agriculture and many multinational companies and laboratories are working on the synthesis of nano-fungicides. These fungicides have lessened the environmental challenges due to its biodegradable nature [9]. Small objects with an average size range of 1–100 nm are called nanoparticles [10]. The production of nanoparticles using biological approach has become an important avenue, in the area of agriculture and crop production. A large variety of biological resources (bacteria, fungi, viruses, algae, and plants) is being used for the synthesis of nanoparticles [11,12]. Bacteria are used as promising resource for the synthesis of nanoparticle due to their ease of handling. Moreover, under different kinds of unfavorable conditions, bacteria can usually survive, easily. For instance, at different low or high temperature conditions, in elevated salt concentration and in variable degrees of acidity and alkalinity. Concurrently, uses of biologically formed nanoparticles are numerous and they act as catalysts, in different chemical reactions [13]. Due to their sustainability, non-toxicity, cost effectiveness and biocompatibility, bacterial synthesized nanoparticles can be easily handled [14]. Manganese nanoparticles have been efficiently used for water treatment [15] and controlling plant pathogen [16].

This study was designed to isolate and identify black rot pathogen of tomato. The control of this disease was optimized using bacteria-supplemented MnO NPs. Synthesized nanoparticles were characterized using X-ray Diffraction (XRD), Scanning Electron Microscopy (SEM), Energy Dispersive X-ray (EDX) and Fourier Transform Infrared (FTIR) spectroscopy. These MnO NPs were analyzed for their antifungal activity potential. Additionally, the quality of tomato fruit was also investigated, before and after the application of MnO NPs.

2. Materials and methods

2.1. Collection of diseased fruit samples

Tomato fruit having distinct black rot symptoms were collected from local fruit and vegetable market of Islamabad. These collected samples were brought to the laboratory in sterilized bags for further analyses.

2.2. Identification of pathogen

Collected fruit samples were surface sterilized with 70% ethanol and a small section (3–4 mm) of diseased area was excised and placed in sterile Petri plates, owning potato dextrose agar (PDA) medium. These Petri plates were placed in an incubator at 25 ± 2 °C for 4–6 days. After the appearance of mycelial colonies, the mycelial threads were sub-cultured on PDA medium. Based on characteristic morphological feature of colonies (color, growth pattern etc.), the isolated pathogen was identified [17,18].

For microscopic observation, mycelia were placed on glass slide, dyed with lactophenol cotton blue and observed at 100 × magnification, under light microscope.

2.3. Pathogenicity test

The pathogenicity of isolated pathogen was confirmed, following Koch's postulates [19]. A desired concentration of conidial suspension (10^6 conidia/mL) was achieved by shaking the mycelia of seven days old fungus in Czapek-Dox broth media at 25 ± 2 °C. Sterile needle was used to create a small hole in healthy tomato fruit and 5 μL of conidial suspension was injected. Normal fruits were injected with sterile distilled water. Using muslin cloth, all fruit were covered and incubated at 25 ± 2 °C. After one week, disease symptoms were recorded. From these symptomatic diseased fruit, the pathogen was re-isolated and cultured on PDA media for 5–7 days at 25 ± 2 °C. The colony morphology was compared with that of originally isolated pathogen.

2.4. Molecular identification of isolated fungus

To see the genetic similarity, 18 S ribosomal RNA gene of isolated pathogen was amplified, using universal 18 S rRNA primers [20]. Fungal DNA was isolated using CTAB method and its quality and quantity was assessed with Nanodrop®. Polymerase chain reaction (PCR) was performed to amplify desired 18 S rRNA gene. PCR mixture (20 μL) was comprising of *Taq* DNA polymerase (1 μL), dNTP (1 μL), fungal DNA (0.4 μL), 10 × polymerase buffer (2 μL), and each primer (0.5 μL). At 94 °C, PCR reaction was initiated for 4 min, followed by 35 cycles of 94 °C (30 s), 58 °C (30 s) and 72 °C (40 s). PCR product was sequenced and used for BLAST analysis on NCBI database. MEGA 7 was used for the phylogenetic analysis.

2.5. Synthesis of manganese oxide nanoparticles (MnO NPs)

For the synthesis of NPs, a standard protocol was followed [21], with little modifications. *Bacillus subtilis* was cultured in broth Luria Bertani (LB) media at 35–37 °C, for three days. The culture was centrifuged and clean bacterial biomass (10 g) was transferred to 100 mL distilled water and cultured for a week at 45 °C in an orbital shaking incubator. The bacterial biomass was then sonicated for 40 min at normal room temperature, and the pH of filtrate was determined.

A stock solution of 1000 mg L^{-1} manganese acetate was prepared in Milli Q water and filter sterilized. To synthesize MnO NPs, bacterial filtrate and manganese acetate solution were added in 1:1 ratio, in a beaker and agitated for 24–48 h. The synthesis of NPs was anticipated by observing the difference in color of the solution. After the change of color, the samples were centrifuged and the pellet was washed and kept overnight at 40 °C. For calcination, the nanoparticles were placed for 2 h at 500 °C, in a furnace.

2.6. Characterization of nanoparticles

Following techniques were used to see the size, shape and other characteristics of synthesized MnO NPs.

2.6.1. Fourier transformed infrared (FTIR) spectroscopy

FTIR spectroscopy was performed to see the nature and types of functional groups associated with MnO NPs, FTIR spectroscopy was performed [22]. FTIR spectra was drawn in the array of 400–4000 cm^{-1}. KBr pellet procedure was adopted to prepare samples by enveloping 10 mg of nanoparticles in 100 mg of KBr pellet.

2.6.2. X-ray diffraction (XRD) analysis of MnO NPs

To find out the nature and size of MnO NPs, XRD spectroscopy was performed [23]. Following Scherrer equation was used for size determination of synthesized MnO NPs:

$$D = \frac{K\lambda}{\beta \cos\theta}$$

Where, D = size (diameter), k = shape factor, λ = wavelength of x-ray, ß = full thickness at half-maximum of radians, θ = angle of diffraction.

2.6.3. SEM and EDX analyses

A sonicated double-distilled water solution of MnO NPs was used for SEM and EDX analyses [22]. A drop of sonicated mixture was placed on double carbon coated conductive tape and dried with a lamp. SEM and EDX assessments were carried out using ionic emission SEM apparatus (VEGA3 TESCAN).

2.7. Mycelial growth inhibition analysis of MnO NPs, in vitro

Mycelial growth inhibition potential of MnO NPs was observed in Petri plates. PDA medium was supplemented with MnO NPs in varying doses (0.25 mg/mL, 2.5 mg/mL and 5.0 mg/mL) and solidified in Petri plates. Using a cork-borer, inoculum discs (4 mm) of isolated fungus were placed in the center of each plate. As a positive control, culture media devoid of MnO NPs was used. All inoculated plates were placed in an incubator at 25 ± 2 °C and after one week, growth inhibition was assessed as under:

$$\text{Mycelial growth inhibition } \% = \frac{C - T}{C \times 100}$$

Where, C = mycelial growth in control plates, and T = mycelial growth in treated plates.

2.8. Antifungal activity analysis of MnO NPs, in vivo

To see the effect of MnO NPs in controlling black rot of tomato, a "wound inoculation method" was used. For this purpose, 12 fruit were surface sterilized and 5 μl of fungal conidial suspension (10^6 conidia/mL) was injected into them. Two days after inoculation, MnO NPs were sprayed on these fruit, in three concentrations (0.25 mg/mL, 2.5 mg/mL, and 5.0 mg/mL). Control fruit were inoculated with distilled water, only and placed at 25 °C, in an incubator. The diseased area on each fruit was calculated after 72 h of treatment.

2.9. Organoleptic and biochemical properties

Organoleptic and biochemical properties of control and treated fruit were determined after 10 days of fungal inoculation. A known amount of diluted tomato juice was titrated against a reference N/10 NaOH solution, the titratable acidity (TA) of tomato juice was calculated. Up to the development of a light pink color, phenolphthalein was utilized as an indicator. The soluble solids in all tomato fruits were measured using a numerical refractometer (Pam Abbe, model PA203×, MISCO Refractometer, Solon, OH). The dinitrosalicylic acid, anthrone, and anhydrous sodium sulphate techniques were used to quantify the reducing sugars (%), total sugars (%), and lycopene concentrations (g kg^{-1}), respectively. By diluting a proven volume of filtered juice with 3% metaphosphoric acid and titrating against 2, 6-dichlorophenol indophenol (until a steady light pink color developed), ascorbic acid was measured in mol kg^{-1} [24]. Using TA.XTplus Texture Analyzer (Stable Micro Systems Ltd., Godalming, Surrey, UK), the impact of fungal inoculation on the firmness of tomato was assessed. For this purpose, the probe was inserted into sample, to a depth of 10 mm, with a force of 2 g [25].

2.10. Statistical analysis

All the experiments were performed in three replicates, unless otherwise stated. MS-Excel 2016 (Microsoft Inc., Redmond, Washington, USA) was used to calculate the mean and standard deviation. The acquired data were subjected to an analysis of variance (ANOVA) using Statistix 8.1. Using the HSD value of p0.05, the significant differences between treatment mean values were calculated.

3. Results

3.1. Microscopic and morphological identification of isolated fungus

Tomato fruit with typical black rot symptoms were collected from the market (Fig. 1A) and the disease causing pathogen was isolated on PDA media (Fig. 1B–C). The growth of fungus was rapid and fungal mycelia covered the entire petri plate in 5–7 days. The pathogen appeared black from the center and grey whitish from the edges (Fig. 1 B). Mycelia appeared pale yellow and cracked from the back side of Petri plate (Fig. 1C). Microscopic photograph revealed the presence of clear septate hyphae. Long conidiophores were bearing vesicles that were spherical in shape. Conidia were globose and black in color with rough surface (Fig. 1D). All morphological and cultural features revealed this pathogen as *Aspergillus niger* [26].

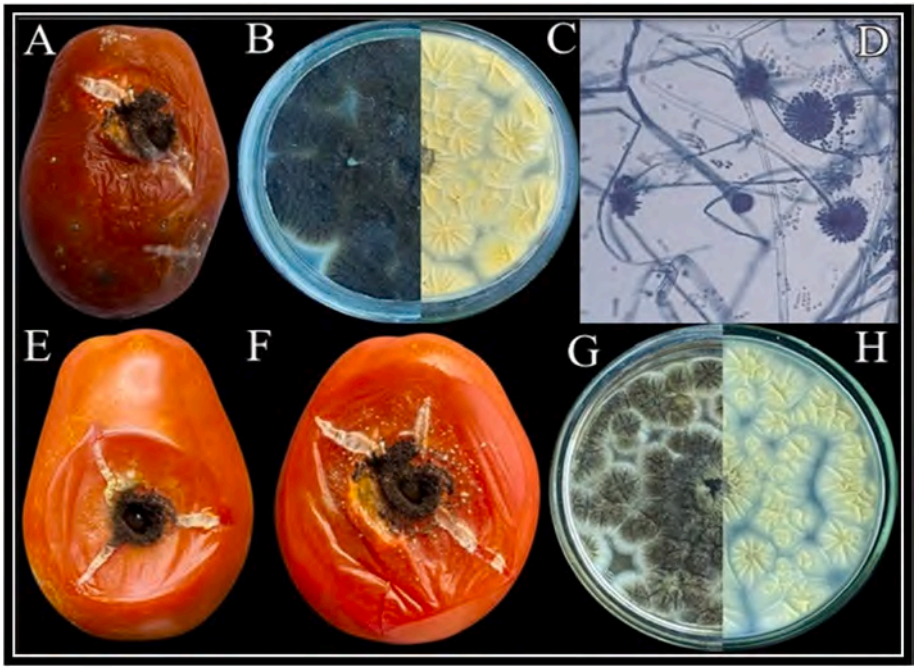

Fig. 1. Black rot symptoms on tomato fruit were examined in the field (A). Infectious pathogen was separated and observed from the front side (B) and back side of Petri plates (C). Microscopy of isolated fungus was performed at 100 × magnification (D). Fungus was re-inoculated on healthy fruit and disease symptoms were observed after 3 days (E), and 5 days of inoculation (F). Pathogen was re-isolated on PDA and viewed from front side (G) and back side (H).

3.2. Pathogenicity test

A pathogenicity test of isolated fungus was brought out efficiently. After 3 days of inoculation, the blackish brown spots could be observed and the surrounding area became soft and pulpy (Fig. 1E). These spots developed quickly after 5 days of inoculation (Fig. 1F). The fungus was isolated on PDA media from these self-inoculated fruit, which displayed similar fungal growth pattern to the previously isolated fungus (Fig. 1G and H).

3.3. Phylogenetic analysis

Obtained 18 S rRNA gene sequence revealed 100% similarity with the strain of *A. niger* (Accession No. MN420840.1). Phylogenetic tree also showed the presence of obtained sequence in the same clade with *A. niger* (Fig. 2).

3.4. Characterization of bacteria supplemented MnO NPs

The following parameters assisted to demonstrate the successful synthesis of MnO NPs.

3.4.1. FTIR analysis

FTIR analysis of MnO NPs revealed characteristic peaks of different functional groups, responsible for the stability and biosynthesis of synthesized MnO NPs (Fig. 3, Table 1). The spectrum of FTIR was brought in the range of 500–4000 cm^{-1} under infrared radiation. One characteristic peak at 2981.04 cm^{-1}, specified the presence of carboxylic acids (O–H stretch), while other significant peak at 999.76 cm^{-1} (=C–H bend) revealed the presence of alkenes. Three other peaks at 608.58 cm^{-1}, 575.14 cm^{-1}, and 555.91 cm^{-1} indicated C–Cl stretch of alkyl halides, while peaks at 547.21 cm^{-1}, 537.01 cm^{-1}, and 522.83 cm^{-1} displayed C–Br stretch of alkyl halides. Previous studies declare that Mn–O bond of manganese nanoparticles can be corresponded by the peaks between 620 and 786 cm^{-1} [27].

3.4.2. XRD analysis

XRD analysis described noticeable peaks at 2θ° around 8.68°, 16.24°, 32.17°, 32.17°, 35.07°, 44.86°, 61.08°, 73.52° and 82.24° planes (Fig. 4). Diffraction peak at 35.07° indexed to [111], indicating cubic structure of MnO [28]. The patterns plane of XRD was in good agreement with standard card JCPDS number 01-076-0874. The average nanoparticle size was determined as 39 nm.

3.4.3. SEM and EDX analysis

Surface of MnO NPs was successfully observed by scanning electron microscope (Fig. 5). The uniform spreading of grains was monitored in micrographs. The particles were nearly spherical in shape with uniform size. EDX analysis determined the elemental makeup of MnO NPs (Fig. 6). Oxygen (23.3%) and manganese (26.4%) were the most dominant elements. Sharp manganese and oxygen peaks proved the synthesis of MnO NPs, in the studied materials.

3.5. Fungal growth inhibition assay, in vitro

The growth of *A. niger* on PDA media containing MnO NPs was significantly lower than that of control (Fig. 7). Though all concentrations of MnO NPs exhibited mycelial growth inhibition, the maximum growth inhibition (86.25%) was displayed by 2.5 mg/mL concentration of MnO NPs (Fig. 8.).

3.6. Disease control assay of MnO NPs

A variable effect of different treatments on the development of black rot disease was observed (Fig. 9, Fig. 10). MnO NPs significantly suppressed black rot disease and the greatest control was displayed by 2.5 mg/mL concentration of MnO.

3.7. Biochemical and organoleptic properties

The quality of tomato fruit was significantly impacted by the fungal inoculation. Application of MnO NPs helped tomato fruit to maintain organoleptic and biochemical attributes and resist fruit decay under fungal stress conditions (Table 2). All MnO NPs treated fruit maintained high soluble solids and total sugars than diseased control fruit. The highest soluble solids and total sugar contents were maintained at 2.5

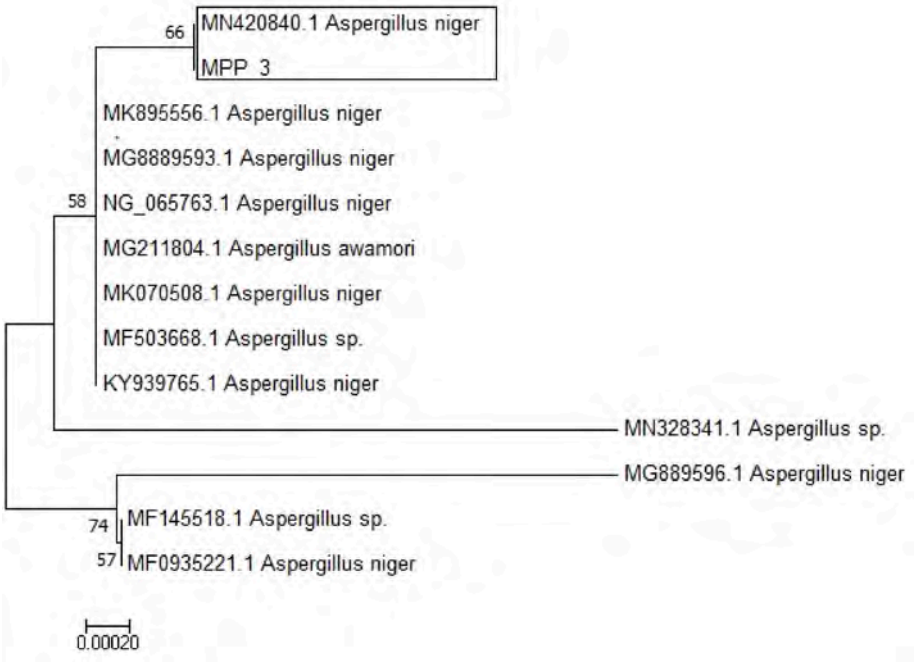

Fig. 2. Phylogenetic tree depicting the evolutionary relationship of 18 S sequence of isolated fungus with 12 related sequences on NCBI.

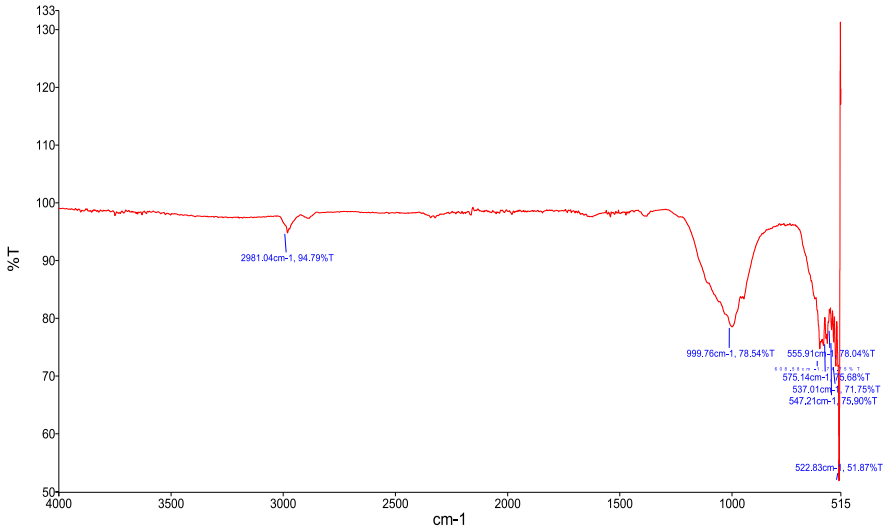

Fig. 3. FTIR spectrum showing standard peaks of important functional groups.

Table 1
FTIR analysis revealing characteristic peak numbers, functional groups, appearance and class of compound on MnO NPs.

Sample No	Sample Peak	Standard Table Absorption (cm^{-1})	Functional group	Bounding	Class Compound
1	2981.04 cm^{-1}	3300–2500 (m)	O–H	O–H stretch	carboxylic acids
2	999.76 cm^{-1}	1000–650 (s)	= C–H	= C–H bend	Alkenes
3	608.58 cm^{-1}	850–550 (m)	C–Cl	C–Cl stretch	alkyl halides
4	575.14 cm^{-1}	850–550 (m)	C–Cl	C–Cl stretch	alkyl halides
5	555.91 cm^{-1}	850–550 (m)	C–Cl	C–Cl stretch	alkyl halides
6	547.21 cm^{-1}	690–515 (m)	C–Br	C–Br stretch	alkyl halides
7	537.01 cm^{-1}	690–515 (m)	C–Br	C–Br stretch	alkyl halides
8	522.83 cm^{-1}	690–515 (m)	C–Br	C–Br stretch	alkyl halides

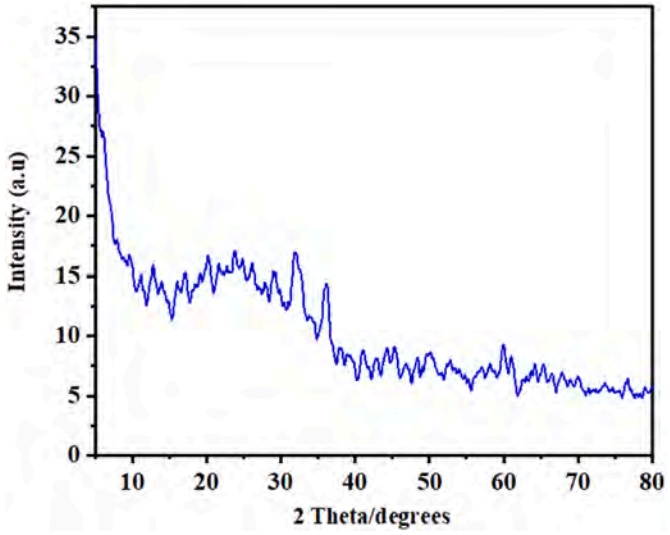

Fig. 4. XRD analysis of MnO NPs.

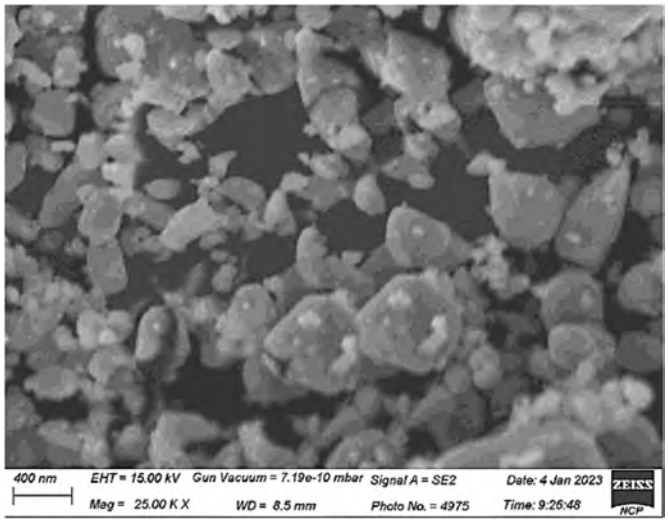

Fig. 5. Scanning electron microscopic photograph of *B. subtilis* supplemented manganese NPs.

mg/mL concentration of MnO NPs. Diseased fruit also displayed less reducing sugar, ascorbic acid, and total sugar contents in un-treated control fruit. Findings of this study proved that the application of MnO NPs helps diseased fruit to conserve higher contents of these useful compounds. Fruits treated with MnO NPs were noticeably firmer than control fruits. Tomato fruit exposed to 2.5 mg/mL concentration of NPs had a harder texture than that of other treatments.

4. Discussion

Fruits have long been considered as a commercially and nutritionally important commodity. Postharvest decays of fruit have been a matter of consideration for decades. Even the common consumer is aware of the ongoing issue of postharvest degradation [29]. Microbes and non-technical post-harvest handling adversely affect the quality of harvested fruit, worldwide [30].

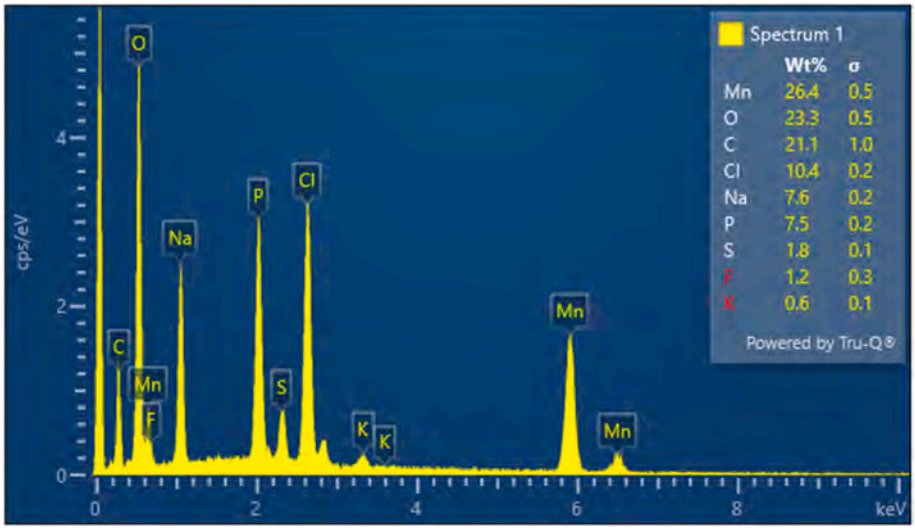

Fig. 6. EDX analysis of *B. subtilis* supplemented MnO NPs.

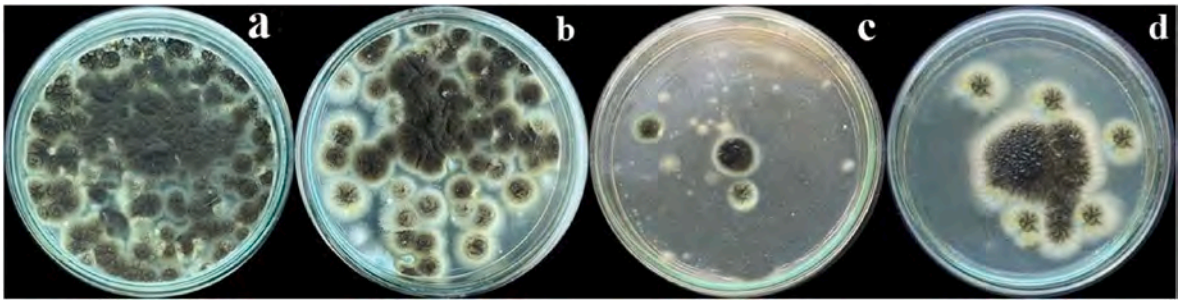

Fig. 7. Mycelial growth inhibition of *A. niger* in control (A), at 0.25 mg/mL concentration (B), at 2.5 mg/mL concentration (C), and at 5.0 mg/mL concentration of MnO NPs (D).

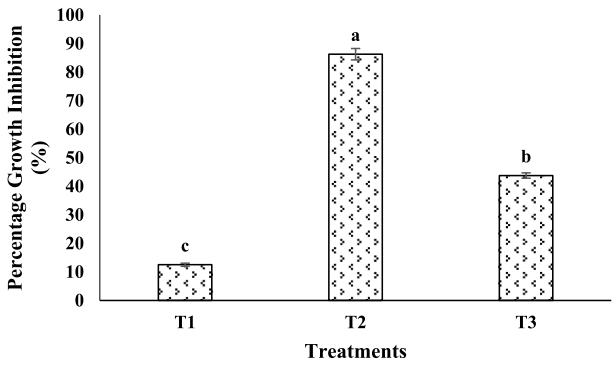

Fig. 8. Growth inhibition of *A. niger* at 0.25 mg/mL concentration (T1), 2.5 mg/mL concentration (T2), and 5.0 mg/mL concentration (T3) of MnO NPs. Capped bars above mean values represent ± SE of three replicates.

In this study, the infected tomato fruit were diagnosed and *A. niger* was recognized as its black rot pathogen. To our knowledge, this is the first report of black rot of tomato, caused by *A. niger*, in Pakistan, Previously, this fungus has reportedly caused black rot of grapes in Pakistan [31]. In India, *A. niger* has been proved as the causative agent of black rot mold of pear [32]. In this research, black rot fruit disease of tomato has been controlled by using biodegradable MnO NPs. These MnO NPs were manufactured in the cultural extract *B. subtilis*. Many earlier studies have described the antifungal potential of *B. subtilis* [33,34]. Moreover, green MnO NPs have been documented to successfully control the growth of *Candida albicans*, *Curvularia lunata*, *A. niger* and *Trichophyton simii* [35].

Characterization of prepared MnO NPs with FTIR spectroscopy confirmed the presence of different enzymes as predominant capping and stabilizing biomolecules on the surface of MnO NPs [36,37]. Absorbance, in the range of 500 cm^{-1} is a characteristic feature of MnO NPs [38]. The presence of alkyl halides on the surface of MnO NPs depicts their antifungal potential [39]. FTIR spectrum analysis assured the presence of organic compounds in all samples, which indicates successful stabilization and reduction of MnO NPs [40]. XRD pattern verified the crystalline nature of MnO NPs by displaying characteristic diffraction peaks at 2θ degree. These plane dimensions further demonstrate the face-centered cubic crystal structure of MnO NPs (de França et al., 2020) [41]. XRD results depicted >100 nm size of synthesized MnO NPs, which suggest their antimicrobial potential that enormously depends upon the size and crystal-like nature of NPs [42]. Crystalline nature of NPs helps them to damage fungal cell wall [43]. SEM analysis displayed nearly spherical shape of NPs, which is coherent with previous results [39].

In this study, different concentrations of MnO NPs (0.25, 2.5 and 5 mg/mL) successfully inhibited mycelial growth in Petri plates (*in vitro*) and controlled fruit diseases (*in vivo*). The antifungal activities of MnO NPs have been earlier reported against different fungi [44]. Use of MnO NPs helped tomato fruit to maintain their good quality under biotic stress conditions. Fruits with a more percentage of sugars and soluble solids has better taste and have higher food property [23]. In the present study, ascorbic acid contents were severely decreased in infected fruit,

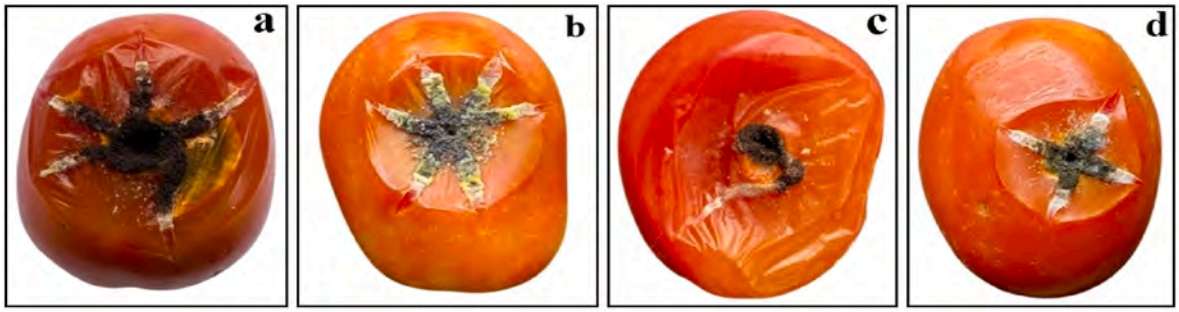

Fig. 9. Disease control assay in tomato fruit. Disease area was observed in control (A), and at different concentrations of MnO NPs including 0.25 mg/mL concentration (B), 2.5 mg/mL concentration (C), and 5.0 mg/mL concentration (D).

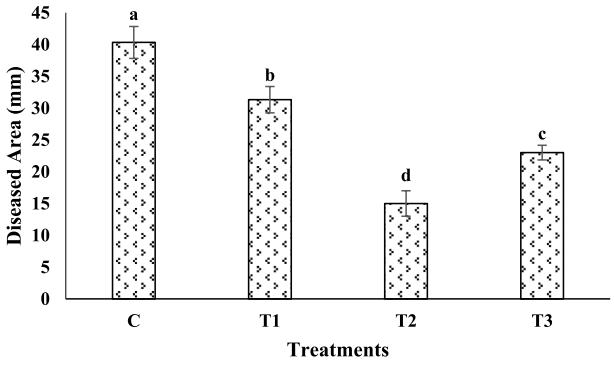

Fig. 10. Effect of different concentrations of MnO NPs on the development of black rot disease in tomato fruit. Control (C), 0.25 mg/mL concentration of MnO NPs (T1), 2.5 mg/mL concentration of MnO NPs (T2), 5.0 mg/mL concentration of MnO NPs (T3). Capped bars above mean values represent ± SE of three replicates.

Table 2
Biochemical and organoleptic changes in diseased fruit.

Treatments	Soluble solids (%)	Total sugars (%)	Reducing sugars (%)	Ascorbic acid (µmol/kg)	Firmness (%)
Control	6.0 ± 0.52	7.9 ± 0.9	2.1 ± 0.09	7.5 ± 1.1	14.7 ± 1.5
0.25 mg/mL NPs	6.5 ± 0.77	8.7 ± 1.2	2.9 ± 0.02	8.1 ± 0.9	20.2 ± 2.1
2.5 mg/mL NPs	8 ± 0.61	12.5 ± 0.7	4 ± 0.05	14 ± 1	30.5 ± 3.2
5.0 mg/mL NPs	7.5 ± 0.67	9.8 ± 0.8	3.7 ± 0.01	10.2 ± 1.5	22.4 ± 1.8

Values are described as mean and ± denotes standard error. Dissimilar alphabets represent significantly different values from each other.

while the application of MnO NPs helped to maintain it. According to previous studies, ascorbic acid content is decreased in rotten fruits [45]. Firmness is one of the most crucial physical factors to assess the quality of fruits. In this study, application of MnO NPs helped tomato fruit to retain firmness which may be attributed to the selective permeability of NPs to gas and water transfer, which lowers the respiration ratio, enzyme activities, and the most metabolic changes while delaying fruit ripening and over-softening [46].

5. Conclusion

This is the first study to reveal the black rot of tomato in Pakistan, caused by *A. niger*. Finding of this study has also described an environment-friendly way to control this disease. Successful synthesis of MnO NPs in the filtrate of *B. subtilis* has proposed a cost-effective way to limit fruit rot diseases of perishable fruits and vegetable. The outcomes demonstrated that black rot in tomato fruit can be effectively controlled by using MnO NPs at their optimal concentration (2.5 mg/mL).

Declaration of competing interest

Authors declare no conflict of interest.

Data availability

Data will be made available on request.

Acknowledgement

This study was financially supported by the university research fund (URF-20-21) of Quaid-i-Azam University, Islamabad.

References

[1] M. Quinet, T. Angosto, F.J. Yuste-Lisbona, R. Blanchard-Gros, S. Bigot, J. P. Martinez, S. Luttus, Tomato fruit development and metabolism, Front. Plant Sci. 10 (2019) 1554, https://doi.org/10.3389/fpls.2019.01554.
[2] L. Helyes, A. Lugasi, Formation of certain compounds having technological and nutritional importance in tomato fruits during maturation, Acta Aliment. 2 (2006) 183–193, https://doi.org/10.1556/aalim.35.2006.2.5.
[3] FAOSTAT, FAO Statistics, Food and Agriculture Organization of the United Nations, Rome, 2020. http://faostat.fao.org/. (Accessed 15 May 2023).
[4] S. Panno, S. Davino, A.G. Caruso, S. Bertacca, A. Crnogorac, A. Mandić, E. Noris, S. Matic, A review of the most common and economically important diseases that undermine the cultivation of tomato crop in the Mediterranean basin, Agron. 11 (2021) 2188, https://doi.org/10.3390/agronomy11112188.
[5] A.H. Wani, An overview of the fungal rot of tomato, Mycopathologia 1 (2012) 33–38.
[6] R. Dean, J.A.L. Van Kan, Z.A. Pretorius, K.E. Hammond-Kosack, A. Di Pietro, P. D. Spanu, J.J. Rudd, M. Dickman, R. Kahmann, J. Ellis, G.D. Foster, The Top 10 fungal pathogens in molecular plant pathology, Mol. Plant Pathol. 4 (2012) 414–430, https://doi.org/10.1111/j.1364-3703.2011.00783.x.
[7] L. Rani, K. Thapa, N. Kanojia, N. Sharma, S. Singh, A.S. Grewal, A.L. Srivastav, J. Kaushal, An extensive review on the consequences of chemical pesticides on human health and environment, J. Clean. Prod. 283 (2021), 124657, https://doi.org/10.1016/j.jclepro.2020.124657.
[8] M.S. Zubair, M.F.H. Munis, I.M. Alsudays, K.H. Alamer, U. Haroon, A. Kamal, M. Ali, J. Ahmed, Z. Ahmad, H. Attia, First report of fruit rot of cherry and its control using Fe_2O_3 nanoparticles synthesized in *Calotropis procera*, Molecules 14 (2022) 4461, https://doi.org/10.3390/molecules27144461.
[9] W. Elmer, J.C. White, The future of nanotechnology in plant pathology, Annu. Rev. Phytopathol. 56 (2018) 111–133, https://doi.org/10.1146/annurev-phyto-080417-050108.
[10] M. Hasan, J. Iqbal, U. Awan, Y. Saeed, Y. Ranran, Y. Liang, R. Dai, Y. Deng, Mechanistic study of silver nanoparticle's synthesis by dragon's blood resin ethanol extract and antiradiation activity, J. Nanosci. Nanotechnol. 2 (2015) 1320–1326, https://doi.org/10.1166/jnn.2015.9090.
[11] K.N. Thakkar, S.S. Mhatre, R.Y. Parikh, Biological synthesis of metallic nanoparticles, Nanomed. Nanotechnol. Biol. Med. 2 (2010) 257–262, https://doi.org/10.1016/j.nano.2009.07.002.
[12] B. Malaikozhundan, B. Vaseeharan, S. Vijayakumar, M.P. Thangaraj, *Bacillus thuringiensis* coated zinc oxide nanoparticle and its biopesticidal effects on the pulse

beetle, *Callosobruchus maculatus*, J. Photochem. Photobiol. B Biol. 174 (2017) 306–314, https://doi.org/10.1016/j.jphotobiol.2017.08.014.
[13] K.I. Alsamhary, Eco-friendly synthesis of silver nanoparticles by Bacillus subtilis and their antibacterial activity, Saudi J. Biol. Sci. 8 (2020) 2185–2191, https://doi.org/10.1016/j.sjbs.2020.04.026.
[14] A. Javaid, S.F. Oloketuyi, M.M. Khan, F. Khan, Diversity of bacterial synthesis of silver nanoparticles, BioNanoScience 8 (2018) 43–59, https://doi.org/10.1007/s12668-017-0496-x.
[15] N.T. Nguyen, G.T. Tran, N.T. Nguyen, T.T. Nguyen, D.T. Nguyen, T. Van Tran, A critical review on the biosynthesis, properties, applications and future outlook of green MnO2 nanoparticles, Environ. Res. 27 (2023), 116262, https://doi.org/10.1016/j.envres.2023.116262.
[16] N.T. Nguyen, L.M. Nguyen, T.T. Nguyen, D.H. Nguyen, D.T. Nguyen, T. Van Tran T, Recent advances on biogenic nanoparticles for detection and control of plant pathogens in sustainable agriculture: a review, Ind. Crops Prod. 198 (2023), 116700, https://doi.org/10.1016/j.indcrop.2023.116700.
[17] K.H. Donsch, W. Gams, T. Anderson, Compendium of Soil Fungi Vols I and II, vol. 859, Academic Press, London, 1980, p. 405.
[18] H.L. Barnett, B.B. Hunter, Illustrated Genera of Imperfect Fungi, fourth ed., 1998. St. Paul, MN.
[19] M. Ali, U. Haroon, M. Khizar, H.J. Chaudhary, M.F.H. Munis, Facile single step preparations of phyto-nanoparticles of iron in Calotropis procera leaf extract to evaluate their antifungal potential against Alternaria alternata, Curr. Plant Biol. 23 (2020), 100157, https://doi.org/10.1016/j.cpb.2020.100157.
[20] T.J. White, T. Bruns, S.J.W.T. Lee, J. Taylor, Amplification and direct sequencing of fungal ribosomal RNA genes for phylogenetics, PCR Protoc.: A guide to methods and appl. 1 (1990) 315–322.
[21] A. Sinha, V.N. Singh, B.R. Mehta, S.K. Khare, Synthesis and characterization of monodispersed orthorhombic manganese oxide nanoparticles produced by Bacillus sp. cells simultaneous to its bioremediation, J. Hazard Mater. 192 (2011) 620–627, https://doi.org/10.1016/j.jhazmat.2011.05.103.
[22] A. Kamal, M.A. Saleem, H. Alshaya, M.K. Okla, H.J. Chaudhary, M.F.H. Munis, Ball-milled synthesis of maize biochar-ZnO nanocomposite (MB-ZnO) and estimation of its photocatalytic ability against different organic and inorganic pollutants, J. Saudi Chem. Soc. 26 (2022), 101445, https://doi.org/10.1016/j.jscs.2022.101445.
[23] M. Akbar, U. Haroon, M. Ali, K. Tahir, H.J. Chaudhary, M.F.H. Munis, Mycosynthesized Fe2O3 nanoparticles diminish brown rot of apple whilst maintaining composition and pertinent organoleptic properties, J. Appl. Microbiol. 132 (2022) 3735–3745, https://doi.org/10.1111/jam.15483.
[24] M. Meena, S. Pilania, A. Pal, S. Mandhania, B. Bhushan, S. Kumar, G. Gohri, V. Saharan, Cu-chitosan nano-net improves keeping quality of tomato by modulating physio-biochemical responses, Sci. Rep. 1 (2020) 1–11, https://doi.org/10.1038/s41598-020-78924-9.
[25] J.D.J. Ornelas-Paz, B.M. Quintana-Gallegos, P. Escalante-Minakata, J. Reyes-Hernández, J.D. Pérez-Martínez, C. Rios-Velasco, S. Ruiz-Cruz, Relationship between the firmness of Golden Delicious apples and the physicochemical characteristics of the fruits and their pectin during development and ripening, J. Food Sci. Technol. 1 (2018) 33–41, https://doi.org/10.1007/s13197-017-2758-6.
[26] K. Diba, P. Kordbacheh, S.H. Mirhendi, S. Rezaie, M. Mahmoudi, Identification of Aspergillus species using morphological characteristics, Pakistan J. Med. Sci. 1 (2007) 867.
[27] T. Van Tran, D.T. Nguyen, P.S. Kumar, A.T. Din, A.S. Qazaq, D.V. Vo, Green synthesis of Mn3O4 nanoparticles using Costus woodsonii flowers extract for effective removal of malachite green dye, Environ. Res. 214 (2022), 113925, https://doi.org/10.1016/j.envres.2022.113925.
[28] W.M. Saod, L. L Hamid, N.J. Alaallah, A. Ramizy, Biosynthesis and antibacterial activity of manganese oxide nanoparticles prepared by green tea extract, Biotechnol. Rep. 134 (2022), e00729, https://doi.org/10.1007/s12033-023-00799-8.
[29] W.J. Janisiewicz, L. Korsten, Biological control of postharvest diseases of fruits, Annu. Rev. Phytopathol. 40 (2002) 411–441, https://doi.org/10.1146/annurev.phyto.40.120401.130158.
[30] S. Droby, Biological control of postharvest diseases of fruits and vegetables: difficulties and challenges, Phytopathol. Pol. 39 (2006) 105–117.
[31] S. Ghuffar, M.Z. Ahmad, G. Irshad, M.A. Zeshan, A. Qadir, H.A. Anwaar, M. Z. Mansha, H.M. Asadullah, A. Abdullah, U. Farooq, First report of Aspergillus Niger causing black rot of grapes in Pakistan, Plant Dis. 5 (2021) 1570, https://doi.org/10.1094/PDIS-06-20-1390-PDN.
[32] S. Parveen, A.H. Wani, M.Y. Bhat, S.A. Pala, A.A. Ganie, Biology and management of Aspergillus Niger Van. Tiegh causing black mold rot of pear (Pyrus communis L.) in Kashmir Valley, India, Int. J. Adv. Res. 6 (2014) 24–34.
[33] Y. Zongzheng, L. Xin, L. Zhong, P. Jinzhao, Q. Jin, Y. Wenyan, Effect of Bacillus subtilis SY1 on antifungal activity and plant growth, Int. J. Agric. Biol. Eng. 4 (2010) 55–61, https://doi.org/10.3965/j.issn.1934-6344.2009.04.055-061.
[34] A.O. Oyedele, T.S. Ogunbanwo, Antifungal activities of Bacillus subtilis isolated from some condiments and soil. Afr. J. Microbiol. Res. 181 92014) 841-1849. http://www.academicjournals.org/AJMR.
[35] M. Jayandran, M.M. Haneefa, V. Balasubramanian, Green synthesis and characterization of Manganese nanoparticles using natural plant extracts and its evaluation of antimicrobial activity, J. Appl. Pharmaceut. Sci. 12 (2015) 105–110, https://doi.org/10.7324/JAPS.2015.501218.
[36] V. Smuleac, R. Varma, S. Sikdar, D. Bhattacharyya, Green synthesis of Fe and Fe/Pd bimetallic nanoparticles in membranes for reductive degradation of chlorinated organics, J. Membr. Sci. 379 (2011) 131–137, https://doi.org/10.1016/j.memsci.2011.05.054.
[37] T. Wang, J. Lin, Z. Chen, M. Megharaj, R. Naidu, Green synthesized iron nanoparticles by green tea and eucalyptus leaves extracts used for removal of nitrate in aqueous solution, J. Clean. Prod. 83 (2014) 413–419, https://doi.org/10.1016/j.jclepro.2014.07.006.
[38] S. Kumar, A.K. Sharma, S.S. Rawat, D.K. Jain, S. Ghosh, Use of pesticides in agriculture and livestock animals and its impact on environment of India, Asian J. Environ. Sci. 1 (2013) 51–57.
[39] J. Ahmed, M. Ali, H.M. Sheikh, M.O. Al-Kattan, U. Haroon, M. Safaeishakib, M. Akbar, A. Kamal, M.S. Zubair, M.F.H. Munis, Biocontrol of fruit rot of Litchi chinensis using zinc oxide nanoparticles synthesized in Azadirachta indica, Micromachines 13 (2022) 1461, https://doi.org/10.3390/mi13091461.
[40] W. Pei, Y. Liu, J. Deng, K. Zhang, Z. Hou, X. Zhao, H. Dai, Partially embedding Pt nanoparticles in the skeleton of 3DOM Mn2O3: an effective strategy for enhancing catalytic stability in toluene combustion, Appl. Catal., B 256 (2019), 117814, https://doi.org/10.1016/j.apcatb.2019.117814.
[41] G.M. de França Bettencourt, J. Degenhardt, L.A.Z. Torres, V.O. de Andrade Tanobe, C.R. Soccol, Green biosynthesis of single and bimetallic nanoparticles of iron and manganese using bacterial auxin complex to act as plant bio-fertilizer, Biocatal. Agric. Biotechnol. 30 (2020), 101822, https://doi.org/10.1016/j.bcab.2020.101822.
[42] S. Saqib, M.F.H. Munis, W. Zaman, F. Ullah, S.N. Shah, A. Ayaz, M. Farooq, S. Bahadur, Synthesis, characterization and use of iron oxide nano particles for antibacterial activity, Microsc. Res. Tech. 4 (2019) 415–420, https://doi.org/10.1002/jemt.23182.
[43] A.F. Oussou-Azo, T. Nakama, M. Nakamura, T. Futagami, M.D.C.M. Vestergaard, Antifungal potential of nanostructured crystalline copper and its oxide forms, Nanomaterials 5 (2020) 1003, https://doi.org/10.3390/nano10051003.
[44] R. Ahuja, A. Sidhu, A. Bala, Manganese sulfide nanospheres as mycocidal material and priming agent for fungi-infested rice seeds, J. Phytopathol. 168 (2020) 678–687, https://doi.org/10.1111/jph.12948.
[45] X. Zheng, M. Gong, Q. Zhang, H. Tan, L. Li, Y. Tang, Z. Li, M. Peng, W. Deng, Metabolism and regulation of ascorbic acid in fruits, Plants 18 (2022) 1602, https://doi.org/10.3390/plants11121602.
[46] M.S. Pasquariello, P. Rega, T. Migliozzi, L.R. Capuano, M. Scortichini, M. Petriccione, Effect of cold storage and shelf life on physiological and quality traits of early ripening pear cultivars, Sci. Hortic. 162 (2013) 341–350, https://doi.org/10.1016/j.scienta.2013.08.034.

Journal of Plant Growth Regulation (2024) 43:2280–2293
https://doi.org/10.1007/s00344-024-11262-6

Bacteria-Based MnO Nanoparticles Alleviate Lead Toxicity in Tomato Seedling Through Improving Growth Attributes and Enhanced Gene Expression of Candidate Genes

Maryam Anar[1] · Urooj Haroon[1] · Asif Kamal[1] · Kinza Tahir[1] · Mahnoor Akbar[1] · Farhana[1] · Hira Saleem[1] · Abdul Rehman[1] · Hassan Javed Chaudhary[1] · Muhammad Farooq Hussain Munis[1]

Received: 18 August 2023 / Accepted: 3 February 2024 / Published online: 18 March 2024

Abstract

Lead (Pb) is a well-recognized toxic trace element that is harmful for both plants and humans. In this study, the research work strived to fabricate nanoparticles (NPs) incorporating 'features' of *Bacillus subtilis* and manganese oxide (MnO). MnO-NPs were synthesized in the filtrate of *B. subtilis* and used for the seed priming of tomato, to mitigate lead (Pb) toxicity. Fourier transform infrared spectrum (FTIR) described the presence of carboxylic acid, alkenes, and alkyl halides on the surface of MnO-NPs, that serve as stabilizing and reducing agents. X-ray diffraction revealed MnONPs as 22 nm crystalline structures while scanning electron microscopy (SEM) displayed nano-flower structure of MnO-NPs. The energy dispersive X-ray (EDX) analysis determined the mass percentage of manganese (38.27%) and oxygen (36.91%). Before sowing under Pb stress conditions, tomato seeds were primed with three different concentrations (0.25 mg/mL, 2.5 mg/mL and 5.0 mg/mL) of MnO-NPs. In comparison to control, different concentrations of MnO-NPs displayed variable improvement in growth attributes of tomato seedlings including shoot and root lengths, plants fresh and dry weights, chlorophyll and carotenoid contents, relative water content, and proline and sugar accumulation. Nano-priming also decreased relative electrolyte leakage and the production of malondialdehyde and hydrogen peroxide. Seed priming positively influenced tomato seedling and enhanced the gene expression of chalcone synthase and phenylalanine ammonia lyase enzymes, while the expression of chlorophyllase was reduced. These findings suggested that MnO-NPs help tomato seedlings to resist the absorption and accumulation of Pb in the roots and leaves.

Keywords Pb toxicity · *Bacillus subtilis* · Malondialdehyde · SEM · Seed priming

Introduction

Rapid and uncontrolled urbanization, industrialization, and intensive agriculture exert remarkable pressure on the environment. Anthropogenic activities lead to the release of various toxic pollutants into the atmosphere. Among these pollutants, heavy metals (HMs) pose a substantial threat to the environment, due to their non-biodegradable nature and potential cytotoxic, genotoxic, and mutagenic properties. Certain HMs, such as chromium (Cr), arsenic (As), lead (Pb), aluminum (Al) and cadmium (Cd), are particularly concerning as they do not serve any known physiological function in plants (Rascio et al. 2011). Pb is among one of the most toxic heavy metals, that have detrimental effects on plants. These effects include growth inhibition, altered nutrient assimilation, reduced biomass accumulation, and senescence, which can ultimately lead to plant death (Singh et al. 2016).

Plants typically do not require Pb for growth and development and its absorption in plants occurs through surrounding environment, particularly in zones with high levels of automotive exhaust such as rural areas. Additionally, plants can absorb lead through fertilizers that contain heavy metal impurities (Lamhamdi et al. 2013). The United States Environmental Protection Agency reported Pb as a major prevalent heavy metal in both terrestrial ecosystems and water.

Handling Author: Puneet Singh Chauhan.

✉ Muhammad Farooq Hussain Munis
munis@qau.edu.pk

[1] Department of Plant Sciences, Faculty of Biological Sciences, Quaid-i-Azam University, Islamabad 45320, Pakistan

This widespread presence of lead in the ecosystem poses a significant risk to plants as it can be directly released into the atmosphere, making it a hazardous metal. Plants uptake Pb from the soil through their roots, as it is often present in soil in significant quantities. According to Kopittke et al. (2007), Pb^{2+} is often present in an insoluble form within the roots of plants. Pb toxicity has been found to impact photosynthetic pathways by causing disorders in the assembly of chloroplasts and hindering the synthesis of vital pigments such as chlorophyll and carotenoids. Furthermore, it interferes with the Calvin cycle and the electron transport chain, leading to a limited supply of CO_2 (Sharma and Dubey 2005).

Food is a necessary human need that plays a necessary role in the well-being and progress of civilizations. However, the increasing environmental impairment and growing global population pose significant encounters to the production of sufficient food for everyone. The rise in population has developed in the deprivation of agricultural land, and increased demand for better production per unit area. In the past, various methods have been employed to reduce heavy metal concentrations in farming soils (Etesami and Maheshwari 2018). Researchers have recently shown interest in nanotechnology, due to its widespread application in sectors like agriculture (Rizwan et al. 2017). Nanoparticles (NPs) can work as an effective source of nutrients, particularly micronutrients, for plants. These nano-fertilizers hold promise as plants require only trace amounts of chemical fertilizers, applied to the soil (Hussain et al. 2018). Metal oxide NPs have been identified for their potential role in enhancing agricultural productivity in an environmentally friendly manner (Kah et al. 2013). These NPs are characterized by their small size (typically ranging from 1 to 100 nm), diverse concentration, composition, and chemical and physical properties. These characteristics have been found to impact the growth and development of different plant species, leading to both beneficial and detrimental effects (Ahmed et al. 2022). Synthesis of NPs using plant extracts and microorganisms (particularly fungi and bacteria) has been well optimized and described in past few years. These biosynthesized nanoparticles have been successfully used in agriculture to control different biotic diseases (Akbar et al. 2024) and abiotic stresses (Etesami 2018).

Manganese is a crucial element for various physiological processes in plants, such as respiration and photosynthesis. Over 30 different manganese oxides and hydroxides can be easily produced by the oxidation of several naturally occurring manganese elements in the earth's crust. Associated to predictable bulk or compounds of ionic manganese, nanoscale manganese has been shown to be effective in mitigating abiotic stress in plants. Several studies have utilized phyto-extracts to produce manganese oxide nanoparticles (MnO-NPs), which are naturally generated by the environmental bacteria (Kasote et al. 2021). Manganese-based nanoparticles have been reported to have a great potential of biomedical applications (Haque et al. 2021). Successful application of MnO-NPs has been described, around the world. These NPs act as plant biofertilizer to improve plant growth in an environment friendly way (de França et al. 2020). MnO-NPs and they have also been reported to control different fungal diseases including Fusarium wilt in watermelon (Noman et al. 2023) and bacterial leaf blight (Ogunyemi et al. 2020). MnO-NPs have been reported to control black rot disease of tomato fruit by modulating its soluble solids (Anar et al. 2023). For last one decade, manganese-based magnetic nanoparticles have been used for the detection and environmental remediation of heavy metals (Kong et al. 2013).

Nano-priming is useful to improve the storage and longevity of seeds, promote plant growth, improve germination and synchronization, and enhance the resistance of crops to various abiotic and biotic stressors. This approach can hypothetically reduce the dependence on pesticides and fertilizers (Ahmed et al. 2022). Seed priming can activate specific germination-related genes under stress condition (Ye et al. 2020). Previous studies have described the usefulness of priming (Kasote et al. 2019).

In this study, MnO-NPs were utilized to mitigate Pb toxicity in tomatoes. Effect of MnO-NPs was studied to improve biochemical and physiological processes of tomato seedlings under Pb stress conditions. Findings of this study can help farmers to improve crop productivity in Pb contaminated soil by modulating antioxidant performance (Ayyaz et al. 2022) and improving photosynthetic activity (Ayyaz et al. 2021).

Materials and Methods

Synthesis of MnO-NPs

Bacteria-based nanoparticles were synthesized using the protocol of Deplanche et al. (2010). *B. subtilis* was acquired from the culture bank (Accession No. FCBP-SF-1277) of the Punjab University, Lahore and cultured in broth Luria Bertani (LB) media at 25–27 °C, for three days. The culture was centrifuged, and clean bacterial biomass (10 g approx.) was transferred to 100 mL distilled water and cultured for a week at 45 °C in an orbital shaking incubator. The bacterial biomass was then sonicated for 40 min at normal room temperature, and the pH of filtrate was determined.

A stock solution (1000 mg L^{-1}) of manganese acetate was prepared in Milli Q water and filter sterilized. To synthesize MnO-NPs, bacterial filtrate and manganese acetate solution were added in 1:1 ratio, in a beaker and agitated for 24–48 h. The synthesis of NPs was anticipated by observing the difference in color of the solution. After the change of color from yellowish to brownish, the samples were centrifuged,

and the pellet was washed and kept overnight at 40 °C. For calcination, the nanoparticles were placed for two hours at 500 °C, in a furnace. At this temperature, nanoparticles with the best degree of crystallinity and particle size are obtained (Ahmed et al. 2022).

Characterization of Nanoparticles

Synthesized MnO-NPs were assessed for size determination and analyses of other characteristic features using the following techniques.

Fourier Transformed Infrared (FTIR) Spectroscopy

FTIR spectroscopy was accomplished to verify the nature and forms of functional groups linked with MnO-NPs. FTIR spectra was drawn in the array of 400 to 4000 cm^{-1}. KBr pellet procedure was used to prepare sample by covering 10 mg of nanoparticles in 100 mg pellet of KBr.

X-ray Diffraction (XRD) Analysis of MnO-NPs

To find out the nature and size of MnO-NPs, XRD spectroscopy was performed using Bruker's X-ray Diffraction (D8-Discover) instrument. Following Scherrer equation was used for size determination of synthesized MnO-NPs:

$$D = K\lambda / \approx \cos\theta,$$

where D = size (diameter), k = shape factor, λ = wavelength of X-ray, β = full thickness at half-maximum of radians, θ = angle of diffraction.

SEM and EDX Analysis

For SEM and EDX analyses, a sonicated double-distilled water solution of MnO-NPs was produced. A dew drop of the sonicated mixture was placed to double carbon coated conductive tape and dried up with a lamp. SEM and EDX analyses were carried out using ionic emission SEM equipment (VEGA3 TESCAN).

Pot Experiment

Soil Preparation

Uncontaminated soil samples were obtained from Quaid-i-Azam University-Islamabad, (33° 44′ N, 73° 09′ E) Pakistan, at a depth of 5–25 cm. To remove gravel and larger debris, the collected soil was filtered through a 2-mm mesh and subsequently air-dried for a period of 1 week at a temperature of 22–24 °C. The sieved soil was analyzed (Table 1) and completely mixed with peat moss in 2:1 ratio, before adding Pb to soil. In a container, soil of 50 ppm concentration was prepared by adding 50 mg Pb in one kg soil, mixed together and left for 2 weeks. Soil was mixed thoroughly at regular intervals for proper metal stabilization. After 2 weeks, each pot was filled with this soil and Pb mixture. The concentration of Pb applied was more than the acceptable limit for heavy metal in soil, as stipulated by WHO (1996). Before planting, the containers were stored in a chamber at a temperature range of 18–22 °C for 2 weeks, and they were moisturized to 70% of their maximum water-holding capacity, using tap water.

Table 1 Key properties of the soil used in experiments

Parameter	Value
Texture	Clay loam
Sand (%)	35
Silt (%)	36
Clay (%)	29
Organic matter (%)	1.42
Organic C (%)	0.55
Total N (% wt)	0.51
Phosphorus (mg/kg)	8.2
Electrical conductivity (dS/m)	1.85
pH	7.7

Seeds Sterilization and Nano-priming

Tomato seeds were taken from National Agricultural Research Centre (NARC) Islamabad and sterilized by drenching in 70% ethanol for 5 mins, and $HgCl_2$ (0.1%) for 1 min. Seeds were rinsed with autoclaved water for 5–6 times. Following an already established protocol, three different concentrations of MnO-NPs (0.25 mg/mL, 2.5 mg/mL and 5.0 mg/mL) were used for seed priming (Lau et al. 2020). To make a solution, MnO-NPs were dispersed in deionized water by ultra-sonication, for around 30 min. At room temperature, tomato seeds were soaked in these solutions for 20 h and placed in dark conditions with continuous aeration. Seeds were imbibed until phase II, dried and placed again for imbibition in the germination plates. Control seeds were soaked in deionized water for the same amount of time. Seeds were dried to their original moisture levels, before sowing (Rizwan et al. 2017). Following the protocol of Fatemi et al. (2021), 500 ppm soil was prepared by adding 500 mg Pb in one kg soil to induce Pb stress.

Seeds were sown in 8 different treatments including; C (un-primed seeds sown in control soil), N1 (seeds primed with 0.25 mg/mL concentration of MnO-NPs and sown in control soil), N2 (seeds primed with 2.5 mg/mL concentration of MnO-NPs and sown in control soil), N3 (seeds primed with 5.0 mg/mL concentration of MnO-NPs and

sown in control soil), Pb (Un-primed seeds sown in metal stressed soil), Pb + N1 (seeds primed with 0.25 mg/mL concentration of MnO-NPs and sown in metal stressed soil), Pb + N2 (seeds primed with 2.5 mg/mL concentration of MnO-NPs and sown in metal stressed soil) and Pb + N3 (seeds primed with 5.0 mg/mL concentration of MnO-NPs and sown in metal stressed soil). The treatments were designed in triplicate, in completely randomized design (CRD).

Harvesting of Plants for Experimental Analysis

All cultivated tomato seedlings were harvested after 21 days of sowing and following physiological, biochemical and antioxidant parameters were measured**.**

Measurement of Growth Features of Plants

The growth attributes of all the harvested experimental plants such as shoot length, root length, dry weight and fresh weight of plants were noted, carefully. These plant parts were calculated using a common scale while fresh and dry weights were measured using electrical weighing balance (Haroon et al. 2021).

Measurement of Osmolytes

Sugar Content

The quantification of soluble sugars was accomplished using "phenol sulfuric acid method". Specifically, 0.01 g of dried leaves was completely mixed with deionized water. The resulting extract was filtered and subsequently treated with a solution of 5% phenol and 98% sulfuric acid. After letting the mixture to stand for 1 h, the absorbance was measured at 485 nm, using a spectrophotometer (Abbasi et al. 2020).

Proline Contents

Following a standard protocol, measurement of proline content was performed (Bates et al. 1973). Fresh leaf (1 g) was completely grinded in 4 mL of a 3% sulpho-salicylic acid solution and left at room temperature for 24 h. After centrifugation, the supernatant was completely mixed with ninhydrin and glacial acetic acid. The resulting mixture was heated in a water bath at 100 °C for 1 h, and cooled in an ice bath. Mixture extraction was performed using toluene, and the absorbance at 520 nm was measured.

Measurement of Physiological Traits of Plants

Following the methodology of Coste et al. (2010), chlorophyll content in the treated plants was assessed using a SPAD-502 meter (Konica-Minolta, Osaka, Japan). Fresh leaf weighing 0.1 g were grinded in 80% acetone and kept in the dark for 24 h. To determine the absorbance of carotenoids in the extracts, measurements were taken at 480 nm (Haroon et al. 2021).

To calculate RWC, initially fresh weight (FW) of leaves was measured. The leaves were soaked in water for 24 h and after its turgid weight (TW) was measured. Leaves were dried out in a hot air oven till consistent dry weight (DW). Relative water content (RWC) was derived by the following formula (Wheatherley 1950).

$$\mathrm{RWC}\ (\%) = \left[(\mathrm{FW} - \mathrm{DW})/(\mathrm{TW} - \mathrm{DW})\right] \times 100$$

Oxidative Stress Biomarkers Determination

Relative Electrolyte Leakage (REL)

Leaves were collected to find out their REL (Irshad et al. 2020). The leaf samples were placed in test tubes containing 8 mL of distilled water. The test tubes ware placed in a water bath at 32 °C for 2 h, and an early electrical conductivity (EC1) was determined. The samples were then autoclaved at 121 °C for 20 min and the closing electrical conductivity (EC2) was determined. Electrolyte leakage was determined by the following formula:

$$\text{Electrolyte leakage}\ (\%) = (\mathrm{EC1}/\mathrm{EC2}) \times 100$$

Malondialdehyde (MDA)

For the quantification of malondialdehyde (MDA), protocol of Heath and Packer (1968) was followed. For this purpose, 0.2 g of leaves were crushed in 5 mL solution of thiobarbituric acid. The mixture was centrifuged at 12,000 rpm for 10 minutes and 1 mL of supernatant was mixed with 20% trichloroacetic acid (CCl_3COOH). The solution was subsequently heated to 90 °C, boiled for 30 min, and allowed to cool in an ice bath. Absorbance was measured at 450 nm, 532 nm, and 600 nm, using a spectrophotometer (AA240FS, USA).

Hydrogen Peroxide (H_2O_2)

The quantification of H_2O_2 content was performed using methodology of Jana and Choudhuri (1981). To determine the concentration of H_2O_2, 3 mL of extract was mixed with 1 mL of 0.1% titanium sulfate (dissolve in 20% H_2SO_4). The absorbance of resulted mixture was recorded using a spectrophotometer at a wavelength of 410 nm (AA240FS, USA).

Appraisal of Antioxidant Enzymes Activities

Fresh leaves (0.25 g) were grinded and added to 5 mL of sodium phosphate buffer (pH 7). The mixture was centrifuged at 12,000 rpm, and the supernatant was placed at − 20 °C. To verify the activity of superoxide dismutase (SOD) enzyme, a solution covering 100 µL of enzyme extract, 50 mM sodium phosphate buffer solution, 10 mM methionine, 1.1 mM riboflavin, and 56 mM nitro blue tetrazolium was prepared (Pinhero et al. 1997). The absorbance of the samples was measured using a spectrophotometer (AA240FS, USA). For measuring peroxidase (POD) activity, a mixture comprising 2.75 mL sodium phosphate buffer solution (pH 7), 0.05 mL enzyme extract, 0.1 mL of 4% guaiacol, and 0.1 mL of 1% H_2O_2 was prepared (Sakharov et al. 2001).

Lead Measurements in Plant Tissues

The plant stuff was collected and divided into roots and leaves. Following a thorough wash with tap water and deionized (DI) water, the plant parts were dried in an oven at 65 °C. In order to determine the levels of Pb in various sections of tomato seedlings, 0.5 g of plant samples were digested with HNO_3 and analyzed using an atomic absorption spectrophotometer (Varian FAAS-240, Triad Scientific, USA), following the methodology of Irshad et al. (2020).

Gene Expression Analysis of Stress-Related Enzymes

Expression of defense-related genes was observed in four treatments viz. C (un-primed seeds sown in control soil), N_2 (seeds primed with 2.5 mg/mL concentration of MnO-NPs and sown in control soil), Pb (Un-primed seeds sown in metal stressed soil), Pb + N_2 (seeds primed with 2.5 mg/mL concentration of MnO-NPs and sown in metal stressed soil)

For the isolation of total RNA and synthesis of cDNA from tomato seedlings of these treatments, the protocol of Goupil et al. (2009) was followed. For quantitative real-time PCR (qPCR), Primer3 software was used to design primers (Thornton and Basu 2011) from the partial gene sequences of three defense-related genes (Table 2) available on NCBI database. In this analysis, Ubiquitin was used as housekeeping (internal control) gene for normalization. Complete information of studied genes has been provided in Table. 2.

Data Analysis

The data were subjected to one-way analysis of variance (ANOVA). Fisher's LSD (least significant difference) test was used to calculate errors of means with a significance level of 5%. Correlation analysis and principal component analysis (PCA) were conducted using R-studio.

Results

Characterization of MnO Nanoparticles

FTIR Analysis of Synthesized MnO-NPs

FTIR analysis of MnO-NPs revealed characteristic peaks of different functional groups (Fig. 1, Table 3). Several functional groups and proteins involved in stability and biosynthesis of NPs were identified. The spectrum of FTIR was brought in the range 500–4000 cm^{-1} under infrared radiation. Characteristic peak at 3384.72 cm^{-1}, specified the presence of alcohols and phenols (O–H stretch). Another significant peak at 1630.52 cm^{-1} (N–H bend) revealed the presence of 1° amines. Four other peaks at 602.98 cm^{-1}, 590.56 cm^{-1}, 578.87 cm^{-1} and 572.31 cm^{-1} indicated C–Cl stretch of alkyl halides, while peaks at 543.32 cm^{-1}, 534.95 cm^{-1}, 527.50 $cm^{-1}$and 517.12 cm^{-1} displayed C–Br stretch of alkyl halides.

X-ray Diffraction (XRD) Analysis of Synthesized MnO-NPs

XRD analysis described noticeable peaks pattern of MnO-NPs at 8.68, 16.24, 32.17, 44.86, 61.08 and 82.24, which corresponded to peaks values (110), (200), (310), (521), (730) and (301), respectively (Fig. 2). Clear peaks, displayed by XRD spectra, were comparable to Orthorhombic space group, revealing magnetite manganese oxide (Fig. 4). The

Table 2 Primers used for qRT-PCR

Gene Name	NCBI GenBank ID	Primer sequence
Chlorophyllase	XM_010328388	Forward primer 5′ GGGGTAAGAGGAAAGGCAAC 3′ Reverse primer 5′ CCACATCTCGAAGCTCAACA 3′
Chalcone synthase	HQ008773	Forward primer 5′ GCCAAAACTTGGCAAAGAAG 3′ Reverse primer 5′ CAGCAAAGCAACCTTGTTGA 3′
Phenylalanine ammonia lyase	M90692	Forward primer 5′ CTCACTGGCAGGCCTAACTC 3′ Reverse primer 5′ CGTTCATCACTTCAGCGAAA 3′
Ubiquitin	NM_001366381	Forward primer 5′ GGAGGACGGACGTACTCTAGC 3′ Reverse primer 5′ TTCGACCTCAAGGGTAATCG 3′

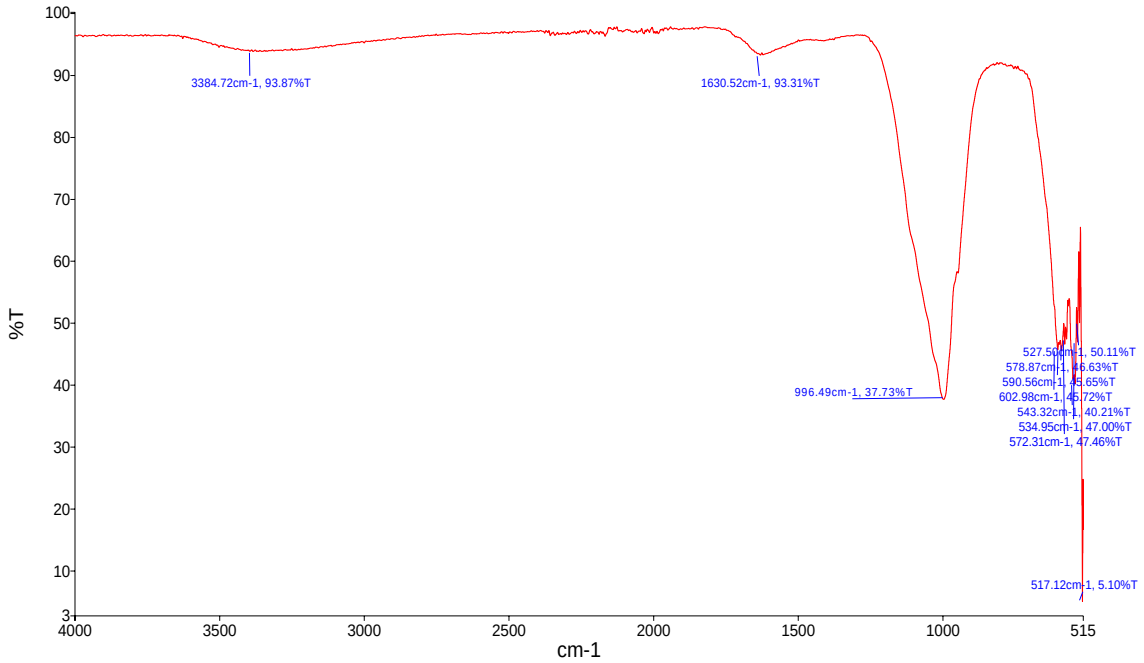

Fig. 1 FTIR spectra of MnO-NPs showing peaks at different wavelengths

Table 3 FTIR analysis revealed characteristic peak numbers, functional groups, appearance and class of compound on MnO-NPs

Sample No.	Sample peak (cm^{-1})	Standard table absorption (cm^{-1})	Functional group	Bounding	Class compound
1	3384.72	3500–3200 (s, b)	O–H	O–H stretch, H–bonded	Alcohols, phenols
2	1630.52	1650–1580 (m)	N–H	N–H bend	1° amines
3	996.49	1000–650 (s)	=C–H	=C–H bend	Alkenes
4	602.98	850–550 (m)	C–Cl	C–Cl stretch	Alkyl halides
5	590.56	850–550 (m)	C–Cl	C–Cl stretch	Alkyl halides
6	578.87	850–550 (m)	C-Cl	C-Cl stretch	Alkyl halides
7	572.31	850–550 (m)	C–Cl	C–Cl stretch	Alkyl halides
8	543.32	690–515 (m)	C–Br	C–Br stretch	Alkyl halides
9	534.95	690–515 (m)	C–Br	C–Br stretch	Alkyl halides
10	527.50	690–515 (m)	C–Br	C–Br stretch	Alkyl halides
11	517.12	690–515 (m)	C–Br	C–Br stretch	Alkyl halides

patterns plane of XRD was in decent deal with JSCPD having number 01076–0958. The usual nanoparticle size was determined as 22.2 nm (Table 4).

Scanning Electron Microscopy and EDX Analysis

The surface morphology of MnO-NPs was studied by scanning electron microscopy which exhibited highly monodispersed flower-like nanostructure (Fig. 3). This nano-flower structure reflected large specific surface area. The elemental makeup of the prepared nanoparticle is shown in Fig. 4. Manganese and oxygen peaks were detected, confirming the synthesis of MnO-NPs. EDX depicted high weight percentages of oxygen (36.91%) and manganese (38.27%) and low signals for C (20.97%), F (1.23%), Na (2.15%), Mg (0.07%), Al (0.15%), Si (0.11%) and Ca (0.14%).

Growth Attributes of Tomato Seedlings

A remarkable reduction in growth attributes of tomato seedlings was observed under Pb stress. Different concentrations of MnO-NPs variably influenced root and shoot lengths (Fig. 5A), and fresh and dry weights of tomato seedlings (Fig. 5B), in response to different treatments of MnO-NPs.

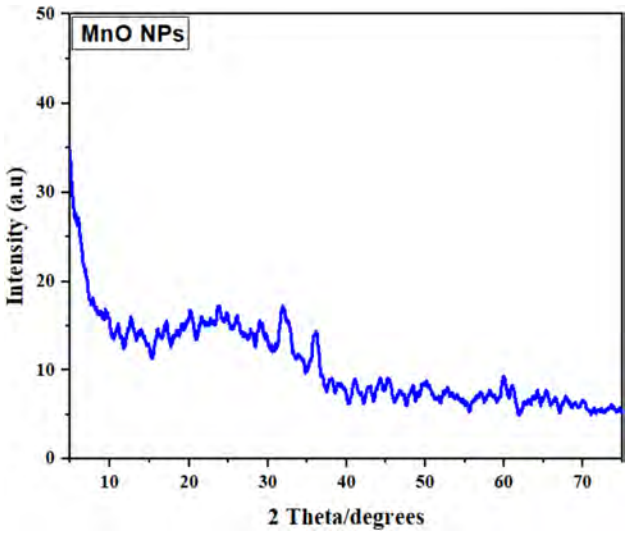

Fig. 2 XRD spectra of MnO-NPs showing peaks at different wavelengths

Table 4 Size of MnO-NPs synthesized in *B. subtilis.*

Peak number	2 Theta	FWHM	Crystallite size *D* (nm)	Average size (nm)
1	8.683	0.416	190.264	22.22319
2	16.241	2.297	34.212	
3	32.170	0.0689	1106.32	
4	61.028	92.138	0.7425	
5	82.275	223.589	0.2674	
6	44.8519	46.3216	12.5847	

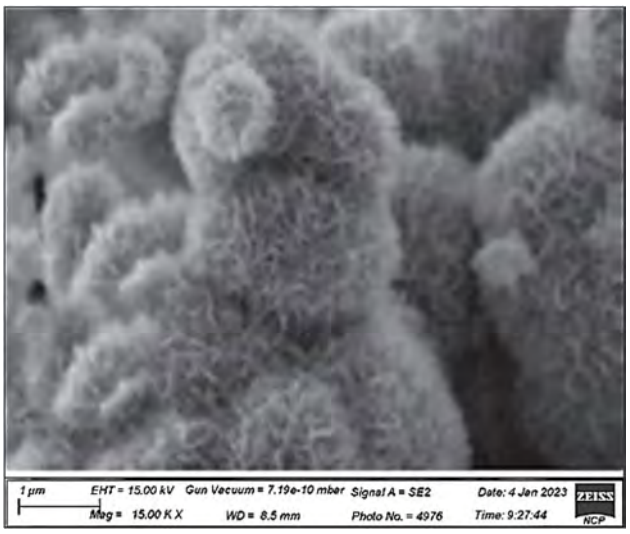

Fig. 3 Scanning electron microscopic photograph of MnO-NPs prepared in *B. subtilis*

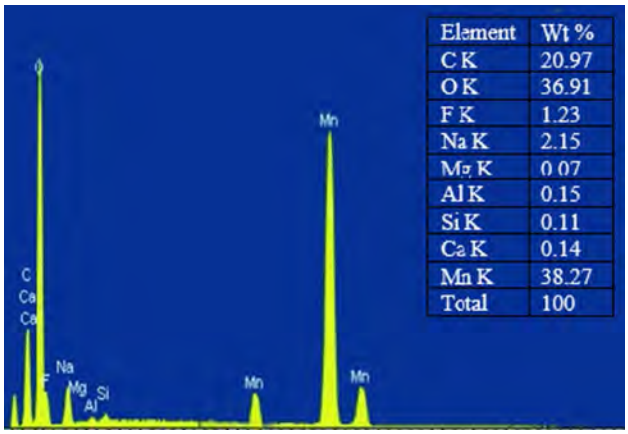

Fig. 4 EDX analysis of MnO-NPs prepared in in *B. subtilis*

Interestingly, medium concentration of MnO-NPs (2.5 mg/mL) performed best under Pb stress conditions.

Measurement of Osmolytes

Proline and sugar contents were significantly increased in the leaves of nano-primed and lead-stressed seedlings of tomato, as compared to control. Various concentrations of MnO-NPs influenced the level of osmolytes in lead-alone treatment. The maximum increase in proline (69%) and sugar content (36%) was observed upon nano-priming with 2.5 mg/mL concentration of MnO-NPs (Fig. 6).

Measurement of Physiological Traits of Plants

Different concentrations of MnO-NPs increased photosynthetic pigments (chlorophyll and carotenoid) in the seedlings of both control and Pb-stressed plants. In comparison to control seedlings, the presence of Pb lowered the levels of chlorophyll and carotenoid. However, the nono-priming of MnO-NPs proved effective in mitigating Pb toxicity by maintaining higher levels of chlorophyll and carotenoid. Notably, the highest concentrations of chlorophyll and carotenoid were observed in plants treated with 2.5 mg/mL concentration of MnO-NPs (Fig. 7).

Leaf RWC was significantly influenced by MnO-NPs treatments and lead stress conditions. All MnO-NPs treatments increased RWC in tomato seedling under normal as well as Pb stress conditions. Among all treatments of MnO-NPs, the maximum RWC were observed at 2.5 mg/mL concentration of MnO-NPs (Fig. 8)

Determination of Oxidative Stress Biomarkers

Seed priming with MnO-NPs significantly impacted the relative electrolytic leakage (REL) in the leaves of tomato

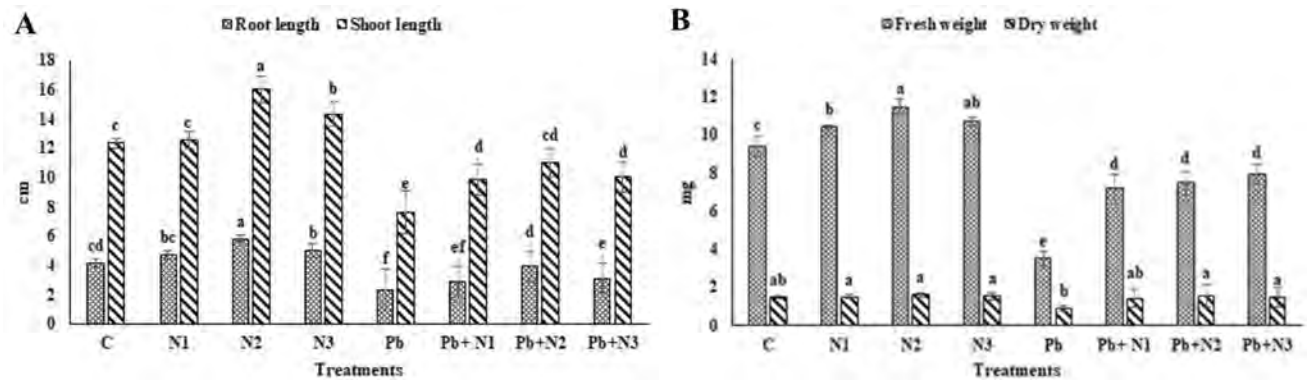

Fig. 5 Effect of seed nano-priming on growth attributes of tomato seedlings, grown in control and lead-stressed conditions. The bars with caps above them indicate the standard error (SE) of means. Different letters indicate significant variation in means

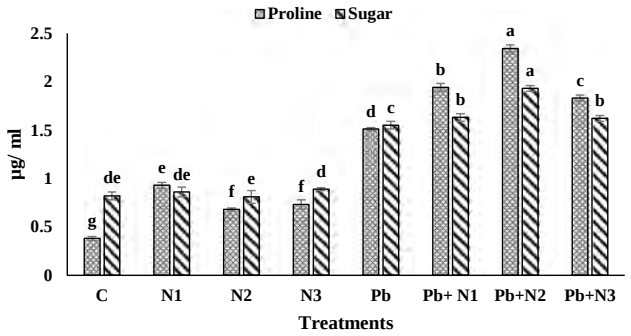

Fig. 6 Effect of seed nano-priming on proline and sugar content of tomato seedlings, grown in control and lead-stressed conditions. The bars with caps above them indicate the standard error (SE) of means. Different letters indicate significant variation in means

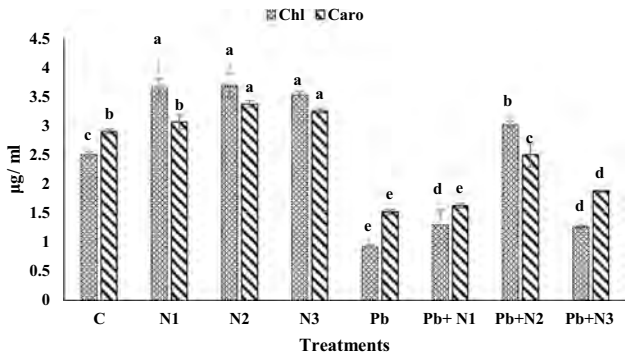

Fig. 7 Effect of seed nano-priming on photosynthetic contents of tomato seedlings, grown in control and lead-stressed conditions. The bars with caps above them indicate the standard error (SE) of means. Different letters indicate significant variation in means

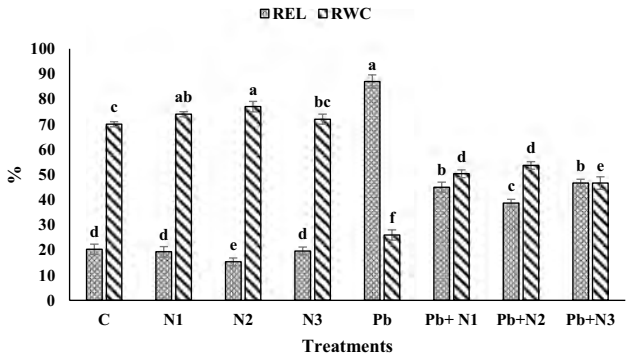

Fig. 8 Effect of seed nano-priming on relative water content and relative electrolytic leakage of tomato seedlings, grown in control and lead-stressed conditions. The bars with caps above them indicate the standard error (SE) of means. Different letters indicate significant variation in means

seedlings. The above average value for REL was detected in the plants under lead stress, while the minimal value of REL was discovered under the influence of the seed priming with different doses of NPs. The least REL was observed in the plants primed with 2.5 mg/mL concentration of MnO-NPs (Fig. 8).

Current findings revealed that MDA and H_2O_2 contents were enhanced in leaves of lead-stressed plants, as compared to control (C). Under Pb stress, the MDA contents in leaves were decreased in MnO-NPs treated plants. Variable decrease was observed in MDA content of plants treated with different concentration of NPs and the maximum decrease in MDA and H_2O_2 content was observed in plants treated with 2.5 mg/mL concentration of MnO-NPs (Fig. 9).

Antioxidant Enzymes Activities

The presence of Pb increased superoxide dismutase (SOD) and peroxidase (POD) enzymes activities in tomato seedlings. Interestingly, priming of seeds with MnO-NPs further enhanced this activity and the greatest activity of antioxidant enzymes was observed in plants treated with 2.5 mg/mL concentration of MnO-NPs (Fig. 10)

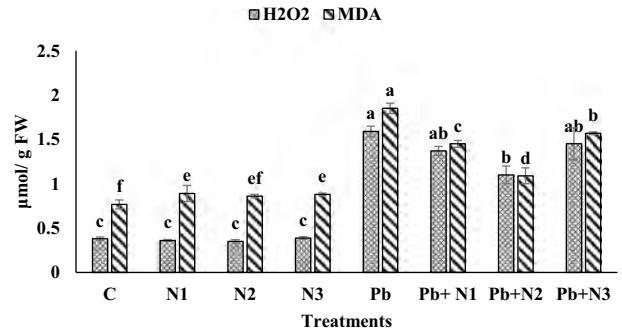

Fig. 9 Effect of seed nano-priming on MDA and H_2O_2 content of tomato seedlings, grown in control and lead-stressed conditions. The bars with caps above them indicate the standard error (SE) of means. Different letters indicate significant variation in means

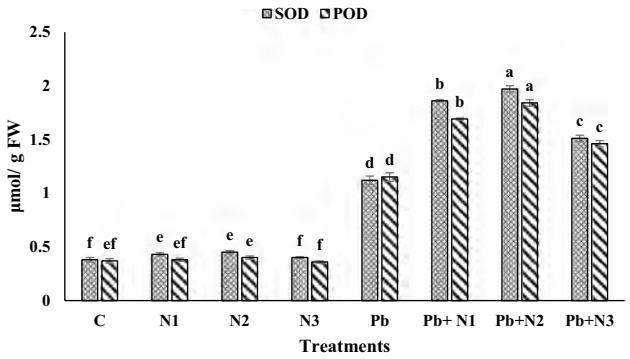

Fig. 10 Effect of seed nano-priming on antioxidant activities of tomato seedlings, grown in control and lead-stressed conditions. The bars with caps above them indicate the standard error (SE) of means. Different letters indicate significant variation in means

Pb measurements in Plant Tissues

Different treatments of NPs decreased the accumulation of Pb in the roots and leaves of tomato seedlings (Fig. 11). These results indicated the importance of the seed priming of tomato seeds with MnO-NPs. Roots accumulated more Pb in roots than shoots. Least accumulation of Pb was observed in plants treated 2.5 mg/mL concentration of MnO-NPs.

Principal Component Analysis and Correlation Matrix

Principal component analysis (PCA) analyzed the relationship between various attributes in tomato plants, subjected to Pb stress and different concentrations of MnO-NPs (Fig. 12). In PCA, two dimensions (Dim-1 and Dim-2) collectively accounted for approximately 97.4% of the inconsistency in the dataset with 0.6 (r^2) value. Dim-1 contributed 88.9% of the total variation, while Dim-2 accounted for 8.5%. Notably, all treatments

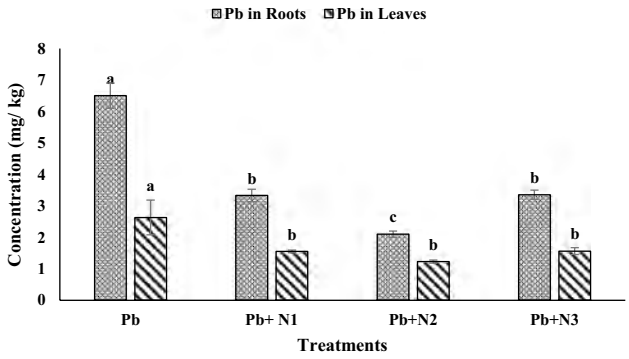

Fig. 11 Effect of seed nano-priming on roots and leaves of tomato seedlings, grown in control and lead-stressed conditions. The bars with caps above them indicate the standard error (SE) of means. Different letters indicate significant variation in means

exhibited distinct and evident impact patterns on tomato seedlings. Specifically, MDA, REL, sugar, H_2O_2, proline, and Pb played a significant role in shaping Dim-1, while other plant traits were more closely associated with Dim-2. To validate the findings of PCA-biplot, a correlation matrix was constructed (Fig. 13). Dark red color bar in the correlation matrices indicated strong negative correlations, whereas the dark blue indicated strong positive correlation. The Pearson's correlation matrix showed a compelling positive correlation between REL, proline, sugar, H_2O_2, MDA and Pb contents. Simultaneously, they showed a robust adverse correlation with growth attributes of plants, photosynthetic attributes and antioxidant enzymatic assay.

Gene Expression Analysis of Stress-Related Enzymes

Gene expression studies revealed higher expression of chlorophyllase under metal stress environment, indicating the catalysis of chlorophyl to chlorophyllide (Heaton et al. 1996). Application of MnO-NPs reduced the expression of the gene, responsible for the production of chlorophyllase and rescued tomato seedlings from stress conditions (Fig. 14A). Expression profiling of chalcone synthase and phenylalanine ammonia lyase genes indicated enhanced production of these enzymes under stress conditions. Application of MnO-NPs further enhanced the expression of both chalcone synthase (Fig. 14B) and phenylalanine ammonia lyase (Fig. 14C) genes under Pb stress conditions. Chalcone synthase is a key enzyme of flavonoid biosynthesis pathway. This enzyme has been reported to be produced under biotic and abiotic stress conditions and it also plays role in salicylic acid defense pathway (Dao et al. 2011). Phenylalanine ammonia lyase is a famous protective plant enzyme that converts L-phenylalanine to the precursors of major

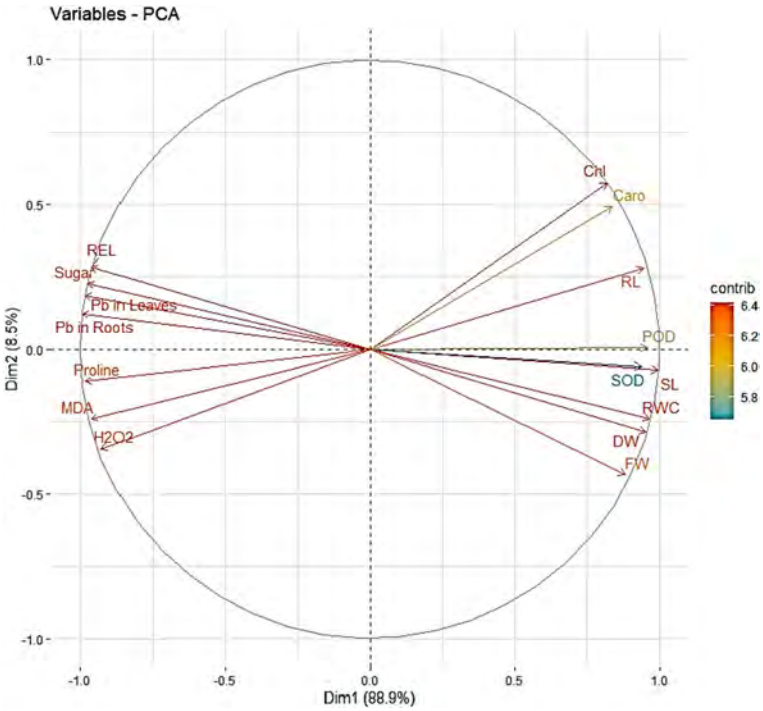

Fig. 12 Principal component analysis expressed the relationship between different studied attributes. Root length (RL); shoot length (SL); fresh weight (FW); dry weight (DW); chlorophyll (Chl); carotenoid (Caro); relative water content (RWC); relative electrolytic leakage (REL); malondialdehyde (MDA); superoxide dismutase (SOD); peroxidase (POD); hydrogen peroxide (H_2O_2)

defense-related compounds like lignin, flavonoids, and coumarins, under stress conditions (Schuster and Retey 1995). Production of these two enzymes indicates the positive influence of MnO-NPs on tomato.

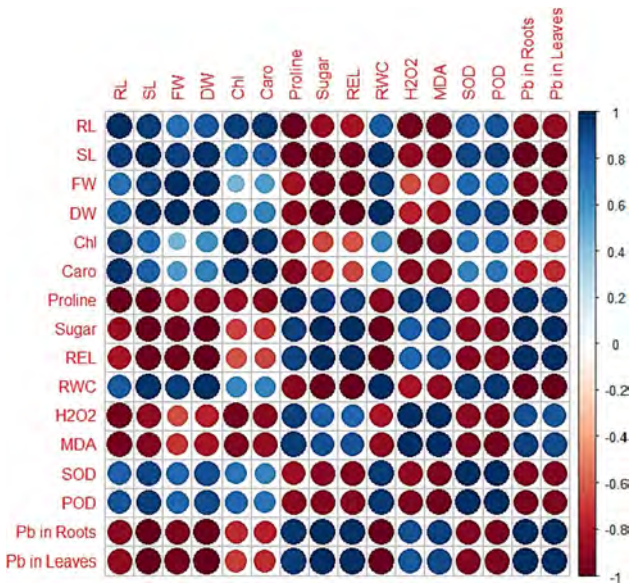

Fig. 13 Pearson's correlation analysis between physiological, antioxidant, and biochemical parameters of tomato seedlings under Pb stress condition after their priming with MnO-NPs. Root length (RL); shoot length (SL); fresh weight (FW); dry weight (DW) chlorophyll (Chl); carotenoid (Caro); relative water content (RWC); relative electrolytic leakage (REL); malondialdehyde (MDA); superoxide dismutase (SOD); peroxidase (POD); hydrogen peroxide (H_2O_2)

Discussion

Heavy metals (HMs) are known for their high density and high toxicity to humans, plants, and animals, and they pose diverse harmful environmental concerns. Among these heavy metals, lead (Pb) contaminates the air, water, and agricultural soil, and impacts both human health and the environment badly (Malar et al. 2016). Although Pb is not an essential element for plants, plants can absorb this metal when it is present in their environment (Lamhamdi et al. 2013). The accumulation of Pb in soils due to human activities poses a thoughtful threat to agriculture (Silva et al. 2017).

In this study, the effect of seed priming with MnO-NPs under Pb stress conditions was observed. *B. subtilis* was used to prepare MnO-NPs and FTIR spectroscopy was used to depict the presence of reducing agents, on the surface of MnO-NPs. Bactria produce diverse enzymes that act as predominant capping and stabilizing biomolecules on the surface of NPs (Wang et al. 2014). MnO-NPs exhibit absorbance in the range of 500 cm^{-1}, which is their characteristic feature (Kumar et al. 2013). The presence of alkyl halides on the surface of MnO-NPs suggests their antifungal potential (Ahmed et al. 2022). FTIR spectrum analysis confirmed the presence of organic compounds in all experiments, indicating successful stabilization and reduction of MnO-NPs (Kasote et al. 2021). XRD analysis displayed the stable crystalline nature and smaller size (22.2 nm) of the produced MnO-NPs. These results indicated the antimicrobial potential of MnO-NPs, which is heavily dependent on their

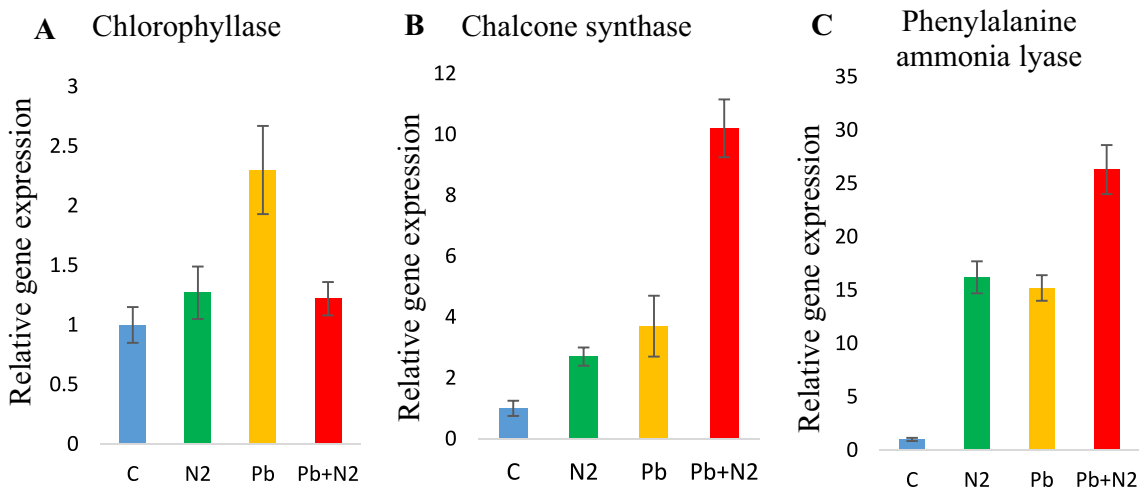

Fig. 14 Effect of seed priming on the expression of chlorophyllase, chalcone synthase and phenylalanine ammonia lyase in tomato seedling after three weeks of sowing. C = un-primed seeds sown in control soil, N_2 = seeds primed with 2.5 mg/mL concentration of MnO-NPs and sown in control soil, Pb = Un-primed seeds sown in metal stressed soil, Pb + N_2 = seeds primed with 2.5 mg/mL concentration of MnO-NPs and sown in metal stressed soil

size and crystalline nature (Saqib et al. 2019). Like previous findings, SEM micrographs exposed a high monodispersed flower-like nanostructure of MnO-NPs (Cherian et al. (2016). EDX study proved the elemental composition of the MnO-NPs, confirming their crystalline structure through the narrow peaks observed in the EDX spectrum (Moorthy et al. 2015).

In the present study, the detrimental effects of Pb on plant biomass were pronounced. However, the application of MnO-NPs synthesized in bacterial filtrate exhibited a significant improvement in growth characteristics of Pb-stressed plants. Earlier research has reported the enhanced biomass of Pb-stressed *Coriandrum sativum* L. (Fatemi et al. 2021). Pb stress was found to reduce the levels of essential osmolytes, particularly proline and sugar, in this study. Nonetheless, the supplementation of MnO-NPs to Pb-stressed seedlings increased proline and sugar contents. These conclusions align with the results presented by Ramzan et al. (2022), who emphasized the significance of osmolytes in alleviating stress-induced damage. Proline, as a non-enzymatic antioxidant, tends to increase under stress conditions, thereby enhancing the antioxidant systems and energy compensation in plants. It plays a vital role in the osmotic adjustment of plant cells during stress, reducing damage caused by reactive oxygen species (ROS) and enhancing plant tolerance to salinity stress. Additionally, the accumulation of sugar content helps to maintain osmotic balance between the cytosol and vacuole (El-Saadony et al. 2021).

Chlorophyll plays a vital role in photosynthesis and is closely associated with the photosynthetic activity of plants. Metal toxicity in plants can significantly affect the levels of chlorophyll in leaves (Rizwan et al. 2017). Consequently, changes in chlorophyll content directly reflect the health of plants and their response to environmental variations. Our study revealed an increase in chlorophyll content and photosynthetic parameters in leaves treated with MnO-NPs. This enhancement in chlorophyll content may be linked to the beneficial effects of NPs on chlorophyll fluorescence parameters under metal stress conditions (Fatemi et al. 2021). Carotenoids, which act as non-enzymatic scavengers of reactive oxygen species (ROS), are abundant in plants (El-Saadony et al. 2021). In our investigation, we observed a noticeable increase in carotenoid content due to the application of NPs, both under stressed and non-stressed conditions. Conversely, high concentrations of Pb stress reduced chlorophyll and carotenoid content in seedlings, indicating a specific response to metal stress that resulted in chlorophyll deprivation and inhibition of photosynthesis (Gajewska et al. 2006).

Furthermore, our research demonstrated a decrease in relative electrolyte leakage (REL) and an increase in leaf water content in Pb-stressed plants, after the priming of MnO-NPs. This response could be attributed to the enhanced absorption of water and mineral elements, facilitated by the presence of MnO-NPs (Kumar et al. 2013). Increasing severity of Pb stress in tomato plants resulted in higher levels of malondialdehyde (MDA) and hydrogen peroxide (H_2O_2). However, nano-priming with MnO-NPs, in our study, effectively reduced the accumulation of MDA and H_2O_2, which aligns with the findings of previous reports involving different plant species (Venkatachalam et al. 2017). Metal stress leads to the invention of reactive oxygen species (ROS), causing oxidative damage to plants. The resistance to oxidative stress is closely linked to the activities of ROS scavenging enzymes

such as SOD and POD (Nair et al. 2014). In this study, the activities of antioxidant enzymes (SOD and POD) were found to be significantly increased in tomato plants treated with MnO-NPs compared to stressed plants. Plants employ various defense mechanisms to adapt to stressful conditions and scavenging ROS through antioxidant enzyme techniques for maintaining normal plant development under salt stress (Haroon et al. 2021).

The results showed that the presence of MnO-NPs lowered the uptake of Pb in the roots and leaves of tomato plants compared to plants grown in Pb-stressed soil. The reduced bioaccumulation of Pb in tomato tissues can be credited to the changes in the mobile fractions of Pb in the soil, caused by NPs. This observation is uniform with previous study that also informed higher Pb accumulation in the roots, compared to the leaves (Malar et al. 2016). This accumulation in the root serves as a defense mechanism in plants and is influenced by genotypic and environmental factors. The concentration of Pb in the culture medium also affects the accumulation of Pb in seedlings (Fatemi et al. 2021).

Principal component analysis evaluated the association between treatments and plant traits under Pb stress conditions and under different concentrations of MnO-NPs. The PCA results and correlation matrix of this study align with the results of Chen et al. (2022), who observed severe impacts of Pb application on plant growth and antioxidant contents. Previous studies describe that the metal substances expose a strong positive collaboration with MDA and other antioxidants but a considerably negative relationship between biomass and photosynthetic characteristics (Venkatachalam et al. 2017).

Conclusion

This study has described the significance of seed priming with MnO-NPs in mitigating Pb toxicity in tomato. This study has described the production of MnO-NPs in the powder form, which can be easily transferred to the field and used for the priming of seeds (pre-sowing seed soaking). Priming of seeds with MnO-NPs has the ability to enhance growth, promote synthesis of photosynthetic pigments, regulate osmoregulation, and mitigate Pb stress in tomato plants. This study represents the first investigation of nano-priming with *B. subtilis* supplemented MnO-NPs for the purpose of enhancing growth and mitigating Pb stress in tomato plants. Enhanced production of chalcone synthase and phenylalanine ammonia lyase enzymes helped us to comprehend underlying defense mechanism of tomato.

Acknowledgements This work was financially supported by university research fund (Grant No. URF-2022), Quaid-i-Azam University, Islamabad.

Author Contributions MAn designed study, conducted experiments, interpreted data and wrote the original draft. UH contributed to conceptualization and data analysis. AK performed statistical analysis. KT and MAk did quantitative analysis and developed methodology. F validated data. HS and AR contributed in pot experiments and analyzed physiological data, HJC supervised microbial experiments and reviewed the manuscript. MFHM contributed to conceptualization, data analysis, manuscript editing and overall supervision. All authors have read and approved the final paper.

Funding Funding was provided by Quaid-i-Azam University (Grant No. URF-2022).

Data Availability The authors confirm that the data supporting the original study results are included in the article.

Declarations

Conflict of interest Authors declare no conflict of interest.

References

Abbasi S, Sadeghi A, Safaie N (2020) Streptomyces alleviate drought stress in tomato plants and modulate the expression of transcription factors ERF1 and WRKY70 genes. Sci Hortic 265:109206. https://doi.org/10.1016/j.scienta.2020.109206

Ahmed J, Ali M, Sheikh HM, Al-Kattan MO, Haroon U, Safaeishakib M, Munis MFH (2022) Biocontrol of fruit rot of *Litchi chinensis* using zinc oxide nanoparticles synthesized in *Azadirachta indica*. Micromachines 13(9):1461. https://doi.org/10.3390/mi13091461

Akbar M, Ali N, Imran M, Hussain A, Hassan SW, Haroon U, Kamal A, Chaudhary HJ, Munis MFH (2024) Spherical Fe_2O_3 nanoparticles inhibit the production of aflatoxins (B_1 and B_2) and regulate total soluble solids and titratable acidity of peach fruit. Int J Food Microbiol 410:110508. https://doi.org/10.1016/j.ijfoodmicro.2023.110508

Anar M, Akbar M, Tahir K, Chaudhary HJ, Munis MF (2023) Biosynthesized manganese oxide nanoparticles maintain firmness of tomato fruit by modulating soluble solids and reducing sugars under biotic stress. Physiol Mol Plant Pathol 127:102126. https://doi.org/10.1016/j.pmpp.2023.102126

Ayyaz A, Farooq MA, Dawood M, Majid A, Javed M, Athar HU, Bano H, Zafar ZU (2021) Exogenous melatonin regulates chromium stress-induced feedback inhibition of photosynthesis and antioxidative protection in *Brassica napus* cultivars. Plant Cell Rep 40:2063–80. https://doi.org/10.1007/s00299-021-02769-3

Ayyaz A, Fang R, Ma J, Hannan F, Huang Q, Sun Y, Javed M, Ali S, Zhou W, Farooq MA (2022) Calcium nanoparticles (Ca-NPs) improve drought stress tolerance in *Brassica napus* by modulating the photosystem II, nutrient acquisition and antioxidant performance. NanoImpact 1:100423. https://doi.org/10.1016/j.impact.2022.100423

Bates LS, Waldren RA, Teare ID (1973) Rapid determination of free proline for water-stress studies. Plant Soil 39:205–207

Chen F, Aqeel M, Maqsood MF, Khalid N, Irshad MK, Ibrahim M, Akhter N, Afzaal M, Ma J, Hashem M, Almari S, Noman A, Lam SS (2022) Mitigation of lead toxicity in *Vigna radiata* genotypes by silver nanoparticles. Environ Pollut 308:119606. https://doi.org/10.1016/j.envpol.2022.119606

Cherian E, Rajan A, Baskar G (2016) Synthesis of manganese dioxide nanoparticles using co-precipitation method and its antimicrobial activity. IJMTST 01:17–22

Coste S, Baraloto C, Leroy C, Marcon É, Renaud A, Richardson AD, Hérault B (2010) Assessing foliar chlorophyll contents with the SPAD-502 chlorophyll meter: a calibration test with thirteen tree species of tropical rainforest in French Guiana. Ann For Sci 67:607–607. https://doi.org/10.1051/forest/2010020

Dao TT, Linthorst HJ, Verpoorte R (2011) Chalcone synthase and its functions in plant resistance. Phytochem Rev 10:397–412

de França Bettencourt GM, Degenhardt J, Torres LA, de Andrade Tanobe VO, Soccol CR (2020) Green biosynthesis of single and bimetallic nanoparticles of iron and manganese using bacterial auxin complex to act as plant bio-fertilizer. Biocatal Agric Biotechnol 1:101822. https://doi.org/10.1016/j.bcab.2020.101822

Deplanche K, Caldelari I, Mikheenko IP, Sargent F, Macaskie LE (2010) Involvement of hydrogenases in the formation of highly catalytic Pd(0) nanoparticles by bioreduction of Pd(II) using *Escherichia coli* mutant strains. Microbiology 156:2630–40. https://doi.org/10.1099/mic.0.036681-0

El-Saadony MT, Desoky ESM, Saad AM, Eid RS, Selem E, Elrys AS (2021) Biological silicon nanoparticles improve *Phaseolus vulgaris* L. yield and minimize its contaminant contents on a heavy metals-contaminated saline soil. J Environ Sci 106:1–14. https://doi.org/10.1016/j.jes.2021.01.012

Etesami H (2018) Bacterial mediated alleviation of heavy metal stress and decreased accumulation of metals in plant tissues: mechanisms and future prospects. Ecotoxicol Environ Saf 147:175–191. https://doi.org/10.1016/j.ecoenv.2017.08.032

Fatemi H, Esmaiel Pour B, Rizwan M (2021) Foliar application of silicon nanoparticles affected the growth, vitamin C, flavonoid, and antioxidant enzyme activities of coriander (*Coriandrum sativum* L.) plants grown in lead (Pb)-spiked soil. ESPR 28:1417–1425. https://doi.org/10.1007/s11356-020-10549-x

Gajewska E, Skłodowska M, Słaba M, Mazur J (2006) Effect of nickel on antioxidative enzyme activities, proline and chlorophyll contents in wheat shoots. Biol Plant 50:653–659

Goupil P, Souguir D, Ferjani E, Faure O, Hitmi A, Ledoigt G (2009) Expression of stress-related genes in tomato plants exposed to arsenic and chromium in nutrient solution. J Plant Physiol 166(13):1446–52

Haque S, Tripathy S, Patra CR (2021) Manganese-based advanced nanoparticles for biomedical applications: future opportunity and challenges. Nanoscale 13:16405–26. https://doi.org/10.1039/D1NR04964J

Haroon U, Khizar M, Liaquat F, Ali M, Akbar M, Tahir K, Batool SS, Kamal A, Chaudhary HJ, Munis MFH (2021) Halotolerant plant growth-promoting rhizobacteria induce salinity tolerance in wheat by enhancing the expression of SOS genes. J Plant Growth Regul. https://doi.org/10.1007/s00344-021-10457-5

Heath RL, Packer L (1968) Photoperoxidation in isolated chloroplasts: I. Kinetics and stoichiometry of fatty acid peroxidation. Arch Biochem Biophys 125(1):189–198. https://doi.org/10.1016/0003-9861(68)90654-1

Heaton JW, Lencki RW, Marangoni AG (1996) Kinetic model for chlorophyll degradation in green tissue. J Agric Food Chem 44(2):399–402

Hussain A, Ali S, Rizwan M, ur Rehman MZ, Javed MR, Imran M, Chatha SAS, Nazir R (2018) Zinc oxide nanoparticles alter the wheat physiological response and reduce the cadmium uptake by plants. Environ Pollut 242:1518–1526. https://doi.org/10.1016/j.envpol.2018.08.036

Irshad MK, Chen C, Noman A, Ibrahim M, Adeel M, Shang J (2020) Goethite-modified biochar restricts the mobility and transfer of cadmium in soil-rice system. Chemosphere 242:125152. https://doi.org/10.1016/j.chemosphere.2019.125152

Jana S, Choudhuri MA (1981) Glycolate metabolism of three submersed aquatic angiosperms: effect of heavy metals. Aquat Bot 11:67–77. https://doi.org/10.1016/0304-3770(81)90047-4

Kah M, Beulke S, Tiede K, Hofmann T (2013) Nanopesticides: state of knowledge, environmental fate, and exposure modeling. Crit Rev Environ Sci. https://doi.org/10.1080/10643389.2012.671750

Kasote DM, Lee JH, Jayaprakasha GK, Patil BS (2019) Seed priming with iron oxide nanoparticles modulate antioxidant potential and defense-linked hormones in watermelon seedlings. ACS Sustain Chem Eng 7:5142–5151. https://doi.org/10.1021/acssuschemeng.8b06013

Kasote DM, Lee JH, Jayaprakasha GK, Patil BS (2021) Manganese oxide nanoparticles as safer seed priming agent to improve chlorophyll and antioxidant profiles in watermelon seedlings. Nanomater 11(4):1016. https://doi.org/10.3390/nano11041016

Kong J, Coolahan K, Mugweru A (2013) Manganese based magnetic nanoparticles for heavy metal detection and environmental remediation. Anal Methods 5:5128–33. https://doi.org/10.1039/C3AY40359A

Kopittke PM, Asher CJ, Kopittke RA, Menzies NW (2007) Toxic effects of Pb^{2+} on growth of cowpea (*Vigna unguiculata*). Environ Pollut 150(2):280–287. https://doi.org/10.1016/j.envpol.2007.01.011

Kumar H, Manisha SP, Sangwan P (2013) Synthesis and characterization of MnO_2 nanoparticles using co-precipitation technique. Inter J Chem Chem Eng 3(3):155–60

Lamhamdi M, El Galiou O, Bakrim A, Nóvoa-Muñoz JC, Arias-Estevez M, Aarab A, Lafont R (2013) Effect of lead stress on mineral content and growth of wheat (*Triticum aestivum*) and spinach (*Spinacia oleracea*) seedlings. Saudi J Biol Sci 20(1):29–36. https://doi.org/10.1016/j.sjbs.2012.09.001

Lau EC, Carvalho LB, Pereira AE, Montanha GS, Corrêa CG, Carvalho HW, Ganin AY, Fraceto LF, Yiu HH (2020) Localization of coated iron oxide (Fe_3O_4) nanoparticles on tomato seeds and their effects on growth. ACS Appl Biol Mater 3(7):4109–4117. https://doi.org/10.1021/acsabm.0c00216

Malar S, Shivendra Vikram S, Favas PJC, Perumal V (2016) Lead heavy metal toxicity induced changes on growth and antioxidative enzymes level in water hyacinths [*Eichhornia crassipes* (Mart.)]. Bot Stud 55(1):1–11

Moorthy SK, Ashok CH, Rao KV, Viswanathan C (2015) Synthesis and characterization of MgO nanoparticles by Neem leaves through green method. Mater Today Proc 2(9):4360–4368. https://doi.org/10.1016/j.matpr.2015.10.027

Nair PMG, Chung IM (2014) Assessment of silver nanoparticle-induced physiological and molecular changes in *Arabidopsis thaliana*. Environ Sci Pollut Res 21:8858–8869. https://doi.org/10.1007/s11356-014-2822-y

Noman M, Ahmed T, Ijaz U, Shahid M, Nazir MM, Azizullah JC, Li D, Song F (2023) Bio-functionalized manganese nanoparticles suppress Fusarium wilt in watermelon (*Citrullus lanatus* L.) by infection disruption, host defense response potentiation, and soil microbial community modulation. Small 19:2205687. https://doi.org/10.1002/smll.202205687

Ogunyemi SO, Zhang M, Abdallah Y, Ahmed T, Qiu W, Ali MA, Yan C, Yang Y, Chen J, Li B (2020) The bio-synthesis of three metal oxide nanoparticles (ZnO, MnO_2, and MgO) and their antibacterial activity against the bacterial leaf blight pathogen. Front Microbiol 4:588326. https://doi.org/10.3389/fmicb.2020.588326

Pinhero RG, Rao MV, Paliyath G, Murr DP, Fletcher RA (1997) Changes in activities of antioxidant enzymes and their relationship to genetic and paclobutrazol-induced chilling tolerance of maize seedlings. Plant Physiol 114(2):695–704. https://doi.org/10.1104/pp.114.2.695

Ramzan M, Ayub F, Shah AA, Naz G, Shah AN, Malik A, Sardar R, Telesińsk A, Kalaji HM, Dessoky ES, Elgawad H (2022) Synergistic effect of zinc oxide nanoparticles and *Moringa oleifera* leaf extract alleviates cadmium toxicity in *Linum usitatissimum*:

antioxidants and physiochemical studies. Front Plant Sci. https://doi.org/10.3389/fpls.2022.900347
Rascio N, Navari-Izzo F (2011) Heavy metal hyperaccumulating plants: how and why do they do it? And what makes them so interesting? Plant sci 180(2):169–181. https://doi.org/10.1016/j.plantsci.2010.08.016
Rizwan M, Ali S, Qayyum MF, Ok YS, Adrees M, Ibrahim M, Abbas F (2017) Effect of metal and metal oxide nanoparticles on growth and physiology of globally important food crops: a critical review. J Hazard Mater 322:2–16. https://doi.org/10.1016/j.jhazmat.2016.05.061
Sakharov IY, Galaev IY, Sakharova IV, Pletjushkina OY (2001) Peroxidase from leaves of royal palm tree *Roystonea regia*: purification and some properties. Plant Sci 161(5):853–860. https://doi.org/10.1016/S0168-9452(01)00466-6
Saqib S, Munis MFH, Zaman W, Ullah F, Shah SN, Ayaz A, Bahadur S (2019) Synthesis, characterization and use of iron oxide nano particles for antibacterial activity. Microsc Res Rech 82(4):415–420. https://doi.org/10.1002/jemt.23182
Schuster B, Retey J (1995) The mechanism of action of phenylalanine ammonia-lyase: the role of prosthetic dehydroalanine. Proc Natl Acad Sci USA 92(18):8433–8437
Sharma P, Dubey RS (2005) Lead toxicity in plants. Braz J Plant Physiol 17:35–52. https://doi.org/10.1590/S1677-04202005000100004
Silva S, Pinto G, Santos C (2017) Low doses of Pb affected *Lactuca sativa* photosynthetic performance. Photosynthetica 55(1):50–57
Singh S, Parihar P, Singh R, Singh VP, Prasad SM (2016) Heavy metal tolerance in plants: role of transcriptomics, proteomics, metabolomics, and ionomics. Front Plant Sci 6:1143. https://doi.org/10.3389/fpls.2015.01143
Thornton B, Basu C (2011) Real-time PCR (qPCR) primer design using free online software. Biochem Mol Biol Educ 39(2):145–54
Venkatachalam P, Jayaraj M, Manikandan R, Geetha N, Rene ER, Sharma NC, Sahi SV (2017) Zinc oxide nanoparticles (ZnONPs) alleviate heavy metal-induced toxicity in *Leucaena leucocephala* seedlings: a physiochemical analysis. Plant Physiol Biochem 110:59–69. https://doi.org/10.1016/j.plaphy.2016.08.022
Wang T, Lin J, Chen Z, Megharaj M, Naidu R (2014) Green synthesized iron nanoparticles by green tea and eucalyptus leaves extracts used for removal of nitrate in aqueous solution. J Clean Prod 83:413–419. https://doi.org/10.1016/j.jclepro.2014.07.006
Wheatherley PE (1950) Studies in the water relations of cotton plants. I. The field measurement of water deficit in leaves. New Phytol 49:81–87
World Health Organization (WHO) (1996) Permissible limits of heavy metals in soil and plants. WHO, Geneva, p 1996
Ye Y, Cota-Ruiz K, Hernandez-Viezcas JA, Valdes C, Medina-Velo IA, Turley RS, Peralta-Videa JR, Gardea-Torresdey JL (2020) Manganese nanoparticles control salinity-modulated molecular responses in *Capsicum annuum* L. through priming: a sustainable approach for agriculture. ACS Sustain Chem Eng 8(3):1427–1436

Turnitin Originality Report

Implementation of Bacteriogenic Manganese Oxide Nanoparticles to Manage Biotic and Abiotic Stresses by Maryam Anar .

From Quick Submit (Quick Submit)

- Processed on 09-Oct-2024 10:16 PKT
- ID: 2479869999
- Word Count: 26473

Similarity Index
15%
Similarity by Source

Internet Sources:
8%
Publications:
13%
Student Papers:
3%

Dr. M. Farooq H. Munis
Professor
Department of Plant Sciences
Quaid-i-Azam University
Islamabad, PAKISTAN

sources:

1 2% match ("Nanobiotechnology", Springer Science and Business Media LLC, 2021)
"Nanobiotechnology", Springer Science and Business Media LLC, 2021

2 1% match (student papers from 30-Apr-2022)
Submitted to Nottingham Trent University on 2022-04-30

3 1% match (Kinza Tahir, Urooj Haroon, Mahnoor Akbar, Minhas Elahi, Umar Masood Quraishi. "Tetragonal crystalline MnO nanoparticles alleviate Pb stress in wheat by modulating antioxidant enzymes in leaves", Physiology and Molecular Biology of Plants, 2024)
Kinza Tahir, Urooj Haroon, Mahnoor Akbar, Minhas Elahi, Umar Masood Quraishi. "Tetragonal crystalline MnO nanoparticles alleviate Pb stress in wheat by modulating antioxidant enzymes in leaves", Physiology and Molecular Biology of Plants, 2024

4 1% match (Faryal Niazi, Musrat Ali, Urooj Haroon, Farhana et al. "Effect of green Fe2O3 nanoparticles in controlling Fusarium fruit rot disease of loquat in Pakistan", Brazilian Journal of Microbiology, 2023)
Faryal Niazi, Musrat Ali, Urooj Haroon, Farhana et al. "Effect of green Fe2O3 nanoparticles in controlling Fusarium fruit rot disease of loquat in Pakistan", Brazilian Journal of Microbiology, 2023

5 < 1% match (Internet from 24-Jan-2024)
https://WWW.MDPI.COM/1422-0067/24/2/1381

6 < 1% match (Internet from 14-Dec-2022)
https://www.mdpi.com/1420-3049/27/14/4461

7 < 1% match (Internet from 19-Oct-2022)
https://www.mdpi.com/2073-4395/11/9/1820/htm

8 < 1% match (Internet from 29-Mar-2023)
https://www.mdpi.com/2223-7747/12/6/1210

9 < 1% match (Internet from 01-May-2024)
https://WWW.MDPI.COM/1996-1944/17/7/1472

10 < 1% match (Internet from 25-Apr-2024)
https://WWW.MDPI.COM/2073-4395/12/12/3053

11 < 1% match (Internet from 19-Aug-2023)
https://www.mdpi.com/1999-4923/15/1/264/htm

12 < 1% match (Internet from 15-Dec-2023)
https://www.mdpi.com/2036-7481/14/3/81

13 < 1% match (Internet from 21-Mar-2023)
https://www.mdpi.com/2073-4395/13/3/902

14 < 1% match (Internet from 10-Jul-2023)